Pathophysiology of Vascular Calcification:

Mechanisms and Therapeutic Options

(Pathophysiologie der vaskulären Kalzifizierung:
Mechanismen und Therapieoptionen)

Inaugural-Dissertation
to obtain the academic degree
Doctor rerum naturalium (Dr. rer. nat.)

submitted to the Department of Biology, Chemistry, Pharmacy
of Freie Universität Berlin

By

Jaqueline Nicolé Herrmann

2022

The work was carried out between June 2016 and November 2021
under the supervision of Priv.-Doz. Dr. Markus Tölle
at the
Department of Nephrology and Medical Intensive Care,
Charité – Universitätsmedizin Berlin

1st Reviewer: Priv.-Doz. Dr. Markus Tölle

2nd Reviewer: Prof. Dr. Maria Kristina Parr

Date of disputation 24.06.2022

Acknowledgements

To sum up the gratitude for many years of professional support, team spirit and personal assistance seems like an impossible task to me. This selection of words can therefore only indicate the depth of gratitude I feel towards the great number of people that supported me in the last years.

To begin with I am grateful towards my reviewers and supervisors Priv.-Doz. Dr. med. Markus Tölle, Prof. Dr. Maria Kristina Parr, Prof. Dr. Günther Weindl and Prof. Prof. h.c. Dr. med. Markus van der Giet. Their support enabled me to pursue this project.

Without the support of our head of lab Dr. Mirjam Tölle-Schuchardt I would have been lost on my way. I deeply appreciate her personal and professional support under all circumstances.

Being able to solve problems, manage obstacles and celebrate achievements in a fantastic team is a wonderful fortune. Without the support and experience of my colleagues plus a lot of shared laughter I never would have made it to the end. I want to thank Katharina Kuschfeldt, Brigitte Egbers, Anna Marta Schulz, Nadine Neitzel, Milen Babic, Manasa Gummi, Mengdi Xia, Anna Greco, Janis Hoffer and Annika Schacke for our time together.

I am grateful to friends and family, who encouraged me in good times and restored me in bad times. Without them, I would not be writing these lines. Thank you dear Christa, Elke, Werner, Dagmar, Oli, Nico, Jule, Adrian and Alina for your reliable assistance and backup. Thanks to my wonderful friends Maria, Johannes, Kerstin and Benni for their warm friendship, sympathy and support.

Dear Mama, dear Papa, thank you for always loving, believing and supporting me. Dear Jonathan, thank you for your smile, remembering me every day of what is really important in life. Dear Manu, thank you for being with me every day, in good times and in bad times. I am blessed to be able to follow my path together with you.

Selbstständigkeitserklärung

Hierdurch versichere ich, dass ich meine Dissertation selbstständig verfasst und keine anderen als die von mir angegeben Quellen und Hilfsmittel verwendet habe.

Contents

List of Tables

List of Figures

List of Abbreviations

6-MP	-	6-Mercaptopurine
ALP	-	Alkaline Phosphatase
ASC	-	Apoptosis Associated Speck-like Protein Containing a Caspase Recruitment Domain
ATM	-	Ataxia Telangiectasia Mutated
AZA	-	Azathioprine
BMP2	-	Bone Morphogenetic Protein 2
CANTOS	-	Canakinumab Anti-Inflammatory Thrombosis Outcome Study
CBFA1	-	Core Binding Factor Alpha 1
CKD	-	Chronic Kidney Disease
CNN1	-	Calponin 1
CVD	-	Cardiovascular Disease
DAMP	-	Damage Associated Molecular Pattern
DDR	-	DNA Damage Response
DM	-	Diabetes Mellitus
DOX	-	Doxorubicin
FISH	-	Fluorescence *in situ* Hybridization
HGPS	-	Hutchinson-Gilford Progeria Syndrome
IL-18	-	Interleukin-18
IL-1ß	-	Interleukin-1ß
IL-1R	-	Interleukin 1 Receptor
IL-6	-	Interleukin-6
IVC	-	Intimal Vascular Calcification
LDL	-	Low Density Lipoprotein
MCP-1	-	Monocyte Chemoattractant Protein-1
MGP	-	Matrix Gla Protein
MI	-	Myocardial Infarction
MSC	-	Mesenchymal Stem Cell
MSX2	-	Msh Homeobox 2
mTOR	-	Mammalian Target of Rapamycin
MVC	-	Media Vascular Calcification
MYH11	-	Myosin Heavy Chain 11
NADPH	-	Nicotinamide Adenine Dinucleotide Phosphate
NF-κB	-	Nuclear Factor 'kappa-light-chain-enhancer' of Activated B-Cells

NLRP3	-	Nucleotide-Binding Oligomerization Domain-like Receptor family pyrin domain containing 3
NLRs	-	Nucleotide-binding Oligomerization Domain-like Receptors
NO	-	Nitric Oxide
NOS	-	Nitric Oxide Synthase
NOX	-	NADPH Oxidase
OPG	-	Osteoprotegerin
OPN	-	Osteopontin
OxDNA	-	Oxidized DNA
PAMP	-	Pathogen Associated Molecular Pattern
PCR	-	Polymerase Chain Reaction
PRR	-	Pattern Recognition Receptor
RAC1	-	Ras-related C3 Botulinum Toxin Substrate 1
ROS	-	Reactive Oxygen Species
RUNX2	-	Runt Related Transcription Factor 2
SAA	-	Serum Amyloid A
SA-ß-Gal	-	Senescence Associated ß-Galactosidase
SAHF	-	Senescence Associated Heterochromatin Foci
SASP	-	Senescence Associated Secretory Phenotype
scq PCR	-	Single Cell Quantitative PCR
sc-RNA-seq	-	Single Cell RNA Sequencing
SIPS	-	Stress Induced Premature Senescence
SM22	-	Smooth Muscle 22alpha
SMA	-	Smooth Muscle Actin
SOD	-	Superoxide Dismutase
TGF-ß	-	Transforming Growth Factor ß
TLR	-	Toll Like Receptor
TNFα	-	Tumour Necrosis Factor alpha
VC	-	Vascular Calcification
VSMCs	-	Vascular Smooth Muscle
WT	-	Wild Type
XO	-	Xanthine Oxidase

Zusammenfassung

Kardiovaskuläre Erkrankungen stellen sowohl in Deutschland als auch weltweit die häufigste Todesursache dar. Es ist davon auszugehen, dass aufgrund von sich verändernden Lebensgewohnheiten und einer Zunahme der Lebenserwartung die kardiovaskulär bedingte Morbidität und Mortalität zukünftig noch weiter ansteigen wird. Viele Risikofaktoren, wie zum Beispiel Übergewicht, Bluthochdruck und Dyslipidämie, sind medikamentös und nicht-medikamentös behandelbar. Vaskuläre Kalzifizierungen hingegen sind ein wichtiger Bestandteil der Pathophysiologie kardiovaskulärer Erkrankungen, zugleich sind sie aber momentan nicht ursächlich behandelbar. Hier besteht dringender Forschungsbedarf, um die therapeutische Lücke zu schließen und betroffenen Patienten eine Behandlungsmöglichkeit bieten zu können.

Vaskuläre Kalzifizierung ist ein aktiver, zellulärer Prozess, der der Knochenbildung ähnelt. Im Zentrum dieses Prozesses stehen insbesondere glatte Gefäßmuskelzellen, die unter Einfluss verschiedener Stimuli ihr Transkriptom hin zu einem Osteoblasten-ähnlichen Phänotyp verändern und als Folge kalzifizieren können. Die bisher entdeckten Induktoren dieser osteoblastischen Transdifferenzierung und Kalzifizierung sind fast unüberschaubar vielfältig. Allerdings zeigt sich, dass insbesondere Alterungsprozesse, verstärkter oxidativer Stress sowie Inflammation eine Modifikation des Transkriptoms von glatten Gefäßmuskelzellen induzieren können. Dabei weisen neue Forschungsarbeiten darauf hin, dass Seneszenz, oxidativer Stress und Inflammation physiologisch eng verknüpfte Prozesse sind.

Ziel dieser Arbeit ist es, zum einen verschiedene Modelle vaskulärer Kalzifizierung zusammenzufassen und zu bewerten und zum anderen den Effekt zellulärer Stressoren auf die Induktion von oxidativem Stress, zellulärer Seneszenz, Inflammation sowie osteoblastischer Transdifferenzierung und Kalzifizierung zu untersuchen. Als zelluläre Stressoren wurden dabei zum einen das Immunsuppressivum Azathioprin untersucht, welches als Substrat der Xanthinoxidase oxidativen Stress induziert. Zum anderen wurde das Zytostatikum Doxorubicin getestet, ein potenter Induktor von genotoxischem Stress und reaktiven Sauerstoffspezies. Im Ergebnis induzieren insbesondere Doxorubicin (*in vitro*) wie auch Azathioprin (*in vivo*) oxidativen Stress, zelluläre Seneszenz sowie eine Sekretion von pro-inflammatorischen Zytokinen. Glatte Gefäßmuskelzellen unter Stimulation mit Azathioprin und Doxorubicin transdifferenzieren zu Osteoblasten-ähnlichen Zellen und kalzifizieren. Insbesondere die Expression bzw. Sekretion der pro-inflammatorischen Zytokine Interleukin-1ß und Interleukin-6 sowie von Komponenten des NLRP3 Inflammasomes steigt unter Stimulation mit Azathioprin und Doxorubicin an. Die Stressor-induzierte Kalzifizierung konnte durch Inhibition des NLRP3 Inflammasomes reduziert

werden. Während Interleukin-6 in diesen Versuchen keine induzierende Wirkung auf Seneszenz und Kalzifizierung zeigte, führte eine Stimulation mit Interleukin-1ß zur Induktion eines pro-inflammatorischen Auto-Loops mit verstärkter Expression pro-inflammatorischer Zytokine, von Mustererkennungsrezeptoren wie TLR2 und TLR4 sowie von Komponenten des NLRP3-Inflammasomes. Des Weiteren führt eine Stimulation mit Interleukin-1ß zur Induktion von osteoblastischer Transdifferenzierung von glatten Gefäßmuskelzellen und Kalzifizierung, die durch die Inhibition von NLRP3 gehemmt werden kann.

In meinen Arbeiten zeige ich, dass die von Stressoren induzierte zelluläre Antwort aus oxidativem Stress, Seneszenz und Inflammation besteht und zu einer Kalzifizierung von glatten Gefäßmuskeln führt. Diese Ergebnisse stehen im Einklang mit weiteren Forschungsarbeiten, in denen sich für den Zusammenhang der Begriff „Entzündungsaltern“ (Engl. *Inflammaging*) durchgesetzt hat. Für die Prävention und Behandlung vaskulärer Kalzifizierung ergeben sich durch die Erkenntnis, dass *Inflammaging* an der Pathophysiologie beteiligt ist, neue therapeutische Angriffspunkte: Neben dem therapeutischen Potential von Antioxidantien rücken insbesondere Senotherapeutika in den Fokus der wissenschaftlichen Forschung: Unter Senotherapeutika kann man dabei zum einen Senolytika erfassen, welche die Apoptose seneszenter Zellen induzieren können, zum anderen Senomorphika, welche im Rahmen dieser Arbeit insbesondere als Therapeutika, die den pro-inflammatorischen Seneszenz Assoziierten Sekretorischen Phänotyp modulieren, verstanden werden. Viele potentielle Senomorphika sind bereits als anti-inflammatorische Therapien in anderen Indikationen zugelassen oder in Erforschung: In meiner Arbeit zeige ich, dass MCC950, ein selektiver Inhibitor des NLRP3 Inflammasomes und damit mechanistisch ein Senomorphikum, *in vitro* die Doxorubicin und Interleukin-1ß induzierte Kalzifizierung von VSMCs hemmen kann.

Auch wenn es bis zur klinischen Verwendbarkeit entsprechender Therapeutika noch ein weiter Weg sein wird, könnten diese neuen Therapieansätze dabei helfen, die therapeutische Lücke bei der Behandlung von vaskulären Kalzifizierungen zu schließen und insbesondere auch die Prognose von Patienten mit hohen chronologischem oder biologischem Alter zu verbessern.

Zusammenfassung in leichter Sprache

Kalziumablagerungen in menschlichen Blutgefäßen stellen schon seit langer Zeit ein gesundheitliches Problem dar: Sie wurden schon bei ägyptischen Mumien und dem Eismann „Ötzi“ gefunden. Ging man früher davon aus, dass diese Ablagerung rein passiv entstehen, ähnlich wie Kesselstein-Bildung in einer Rohrleitung, so weiß man heute, dass menschliche Blutgefäße durch Zellveränderungen „verkalken“: Hierbei verändern sich die Zellen der Gefäßwand so, dass sie Kalziumablagerungen auf eine Art bilden können, die dem Knochen sehr ähnlich ist. Vor allem Muskelzellen der Blutgefäße, deren eigentliche Aufgabe die Kontrolle der Gefäßspannung ist, können sich durch unterschiedliche Einflüsse so verändern, dass sie Kalziumablagerungen bilden und Blutgefäße dadurch schädigen können. Als Folge können Blutgefäße verengt oder steif werden und dadurch nicht mehr flexibel auf unterschiedlich starke Blutströme reagieren. Bei Patienten erhöhen diese Kalziumablagerungen das Risiko für Herz-Kreislauf-Erkrankungen. Sie können zu einer Belastung für das Herz und zu einer Unterversorgung von Gewebe führen, was der Patient unter anderem als Kurzatmigkeit, Brustenge oder mangelnde Belastbarkeit wahrnimmt.

Ziel meiner Arbeiten ist es, die vielen verschiedenen Einflüsse, die Gefäßmuskelzellen zum „Verkalken“ bringen, zu erfassen und zu zeigen, dass viele dieser Einflussfaktoren miteinander zusammenhängen: Entzündungsprozesse, Alterungsprozesse und die Bildung zellschädigender Sauerstoffverbindungen sind eng miteinander verbunden und verstärken sich gegenseitig. Um diese enge Verknüpfung zu betonen hat sich hierfür auch der Begriff „Entzündungsaltern“ (Engl. *Inflammaging*) durchgesetzt. In der vorliegenden Forschungsarbeit wurden verschiedene Auslöser von Entzündungsaltern untersucht: Zum einen Azathioprin, ein Wirkstoff zur Unterdrückung der Immunabwehr, bei dessen Abbau im Körper zellschädigende Sauerstoffverbindungen entstehen können. Daneben wurde Doxorubicin, ein Wirkstoff, der auf verschiedenen Wegen zellschädigend wirken kann und zur Behandlung von Krebserkrankungen eingesetzt wird, untersucht. Außerdem wurden die Effekte verschiedener Entzündungsbotenstoffe analysiert. Werden Gefäßmuskelzellen mit diesen Substanzen behandelt, dann verändern die Zellen das Ablesen ihrer Gene und den Zusammenbau von Proteinen so, dass sie eher knochenaufbauenden Zellen ähnlich werden und vermehrt Kalzium ablagern. Auch wenn dies vermutlich über mehrere Signalwege läuft, konnte in diesen Versuchen gezeigt werden, dass durch Hemmung eines „Hauptschalters“ für Entzündungsreaktionen, dem so genannten NLRP3-Inflammasome, die Kalziumablagerungen und die Bildung von Entzündungsstoffen vermindert werden können.

Diese Ergebnisse fügen sich in eine Reihe weiterer Forschungsergebnisse ein, die darauf hinweisen, dass Kalziumablagerungen in den Blutgefäßen und das damit verbundene Risiko

für Herz-Kreislauf-Erkrankungen in Zukunft durch neue Therapieansätze reduziert werden könnten: Diese neuen Therapien könnten daran ansetzen, Zellschäden zu verhindern, indem zum Beispiel spezielle Entzündungsvorgänge unterbunden werden, oder Zellen, bei denen Schäden aufgetreten sind, aus dem Körper entfernt werden. Da Medikamente hier aber in ganz grundlegende körpereigene Prozesse eingreifen würden, etwa dem körpereigenen Krebsschutz und der Abwehr gegen körperfremde Krankheitserreger, sind solche Behandlungsansätze auch mit besonderer Vorsicht zu betrachten. Erste Studien zeigen zwar positive Effekte, aber es wird noch viel Forschungsarbeit nötig sein, bis auch Patienten von solchen Behandlungen profitieren können.

Abstract

Cardiovascular diseases are a leading cause of morbidity and mortality in western societies. One main risk factor for the development and progression of cardiovascular diseases is vessel calcification. Although the occurrence of vascular calcifications increases in our societies, due to changed lifestyle, including over-nutrition and lack of movement as well as increasing life expectancy, vascular calcifications are by no means a “new” disease: Vascular calcifications were detectable in ancient Egyptian mummies and in Ötzi, the ice men. Yet, although vascular calcification has been of interest in research for centuries, the lack of effective treatment and prevention strategies still reveals a huge therapeutic gap for affected patients. Our knowledge of the underlying pathophysiological processes has evolved when new concepts of vascular calcification as active, cell-driven processes replaced the theory of passive calcium deposition as main driver of ectopic calcification. At present, consent exists that vascular calcification results from active cellular processes that resemble bone formation and that vascular cells, for example *Vascular Smooth Muscle Cells* (VSMCs), can transdifferentiate in response to a variety of stimuli, thus assuming an osteoblastic phenotype and transcriptome. Among the numerous stimuli inducing osteoblastic transdifferentiation of VSMCs are cellular aging processes, oxidative stress, and inflammation. These inducers can be linked via formation of damage associated molecular patterns, persistent DNA damage and formation of a senescence associated secretory phenotype with respective pro-inflammatory signalling, connecting senescence, oxidative stress and inflammation in a concept termed *inflammaging*.

The objective of this work was to further analyse the effects of different cellular stressors and pro-inflammatory cytokines on vascular calcification and osteoblastic transdifferentiation of VSMCs. As inducers of cellular stress, the immunosuppressive azathioprine and the cytostatic drug doxorubicin were used. Azathioprine as a substrate of xanthine oxidase induces cellular stress by formation of reactive oxygen species, while doxorubicin, next to induction of reactive oxygen species, also exerts direct genotoxicity. Both azathioprine and doxorubicin induce cellular senescence, osteoblastic transdifferentiation and calcification of VSMCs. After treatment, also the pro-inflammatory cytokines interleukin-1ß and interleukin-6 as well as NLRP3 inflammasome components are upregulated. In our experiments, while interleukin-6 stimulation did not upregulate senescence and calcification in VSMCs, we found interleukin-1ß to induce a pro-inflammatory auto-loop with increased expression of pro-inflammatory cytokines, toll like receptors 2 and 4 as well as components of the NLRP3 inflammasome. Stimulation with interleukin-1ß induced osteoblastic transdifferentiation and calcification, but only few markers of cellular senescence in VSMCs. The relevance of the

NLRP3 inflammasome in vascular calcification is further emphasized by the fact that both, cellular stressors and interleukin-1ß induced calcification, is diminished by NLRP3 inhibition.

This work is in line with recent research that emphasizes the involvement of *inflammaging* in vascular calcification. The contribution of oxidative stress, inflammation and senescence in the pathophysiology of VSMC calcification reveals several therapeutic options for the treatment and prevention of vascular calcification: Next to the potential of the application of anti-oxidative agents, also senotherapeutics can provide therapeutic options. Senotherapeutics can encompass senolytics, which can induce apoptosis in senescent cells, and senomorphics, which can modulate the pro-inflammatory signalling induced in senescent cells by modulation of the senescence associated secretory phenotype. The selective NLRP3 inhibitor MCC950, which in my work is effective in inhibiting doxorubicin and interleukin-1ß induced calcification of VSMCs, can be considered a senomorphic drug.

Although the transfer of these approaches from bench to bedside will require extensive further research, new therapies might help to close the therapeutic gap and provide urgently needed therapeutic options for the treatment of vascular calcification.

1. Introduction

In the last decades, although success in the medical care of patients with C*hronic Kidney Disease* (CKD) and dialysis has improved patient morbidity and mortality rates, both remain particularly increased for these patients [1]. Globally, approximately 1.2 million deaths were attributed to CKD in 2017 and additional 1.4 million deaths were attributed to *Cardiovascular Disease* (CVD) resulting from impaired kidney function [1]. Individually, a patient aged 30 years who becomes diagnosed with CKD statistically loses 34.3 years of lifetime in comparison to a life without CKD [2]. Even though treatment options for CKD patients have improved significantly, this gap in life expectancy increased in the last decades [2]. As the medical options for treatment of CKD have progressed, both in the field of transplantation and in dialysis techniques, the reasons for patient mortality have shifted: CVD are now the leading cause of death in patients with CKD [3]. CVD are a leading cause of death worldwide (32% of all global deaths in 2019) [4]. In patients with CKD the risk for the occurrence of CVD is even higher than in the general population and the disease prognosis is worse [3]. In addition to patients suffering from CKD, also patients with rare genetic disorders, such as for example *Hutchinson-Gilford Progeria Syndrome* (HGPS, a genetic disease with accelerated aging) or Pseudoxanthoma Elasticum and patients with *Diabetes Mellitus* (DM) or patients at a high age have a risk for CVD that is surpassing that of the general population [5-8]. These patient populations especially suffer from increased *Vascular Calcification* (VC) [5-8]. VC is an underlying cause of CVD, often referred to as “the killer”[9] in patients with CKD and has been established both as risk factor and as prognostic marker of morbidity and mortality in CVD [9,10].

Calcification can occur in a physiologic context, thus being decisive in the formation of bone in vertebrates [11]. Yet, calcification can also be a pathophysiological process leading to the formation of ectopic calcification [12,13]. Several tissues can calcify, including vessels [13]. VC can occur in different vessels and in different layers of the vessel [12]. The nomenclature of the calcification of different layers of the vessels is slightly inconsistent, with *Intimal Vascular Calcification* (IVC) often referred to as atherosclerosis and *Media Vascular Calcification* (MVC) often referred to as Mönckeberg’s Medial Sclerosis, Mönckeberg Arteriosclerosis or arteriosclerosis [13-15]. Nevertheless, particularly atherosclerosis and arteriosclerosis are often used synonymously, especially in a colloquial context. The relevance of VC, both intimal and medial, for morbidity and mortality has long been recognized by medical research: VC, especially IVC, was a well-known pathological condition as early as in Virchow’s time [16-18]. MVC, although already known earlier, came into focus of scientific research when Mönckeberg systematically assessed MVC in his autopsies, both isolated and occurring jointly with IVC [19,20]. The pathophysiologic process

was considered physicochemical: VC was considered a passive formation of calcium phosphate particles due to trespassing the calcium phosphate solubility in the blood [16-18]. Although these thermodynamics are decisive in the formation of calcium precipitates and the development and progression of VC [21], the formation of VC involves several additional mechanisms: Research from the last 30 years found that the process of VC is cell mediated, resembles bone formation and involves several cell types and signalling pathways [12,22].

Both IVC and MVC influence hemodynamic parameters [10]. In IVC, plaque formation can reduce the blood flow by decreasing the vessel lumen diameter and plaque rupture can cause thrombosis with stenosis of vessels [23]. MVC reduces elasticity of the vessel, causing stiffening of the vessel wall [7,10,12]. As hemodynamic consequence, vessel stiffness can lead to an impaired *Windkessel* function of the aorta, thus increasing the afterload of the left ventricle and decreasing the perfusion of the coronary artery [7]. Stiffening of the vessels also leads to increased blood flow versatility [7]. These hemodynamic impairments caused by MVC explain the association between MVC and CVD that has been established in several patient populations [7]. Different patient populations share some risk factors for the development of MVC: Patients with CKD, DM and high biological age have increased levels of cellular stress, including *Reactive Oxygen Species* (ROS), which can result in the formation of DNA damage and reinforced inflammation [24,25]. Among other mechanisms, the formation of cellular stress can induce the osteogenic transformation of *Vascular Smooth Muscle Cells* (VSMCs) and calcification [25]. Notwithstanding that several diseases can cause VC, this work mainly focusses on mechanisms behind CKD associated vessel calcifications. Although several therapy options for the treatment of CKD and CVD are available, therapeutic options for the prevention or treatment of VC and especially MVC are scarce, even though there is high clinical need [7,22]. In order to find new therapeutic targets for the development of treatment options, research into the underlying pathophysiological mechanisms of VC is urgently needed.

2. Cellular Mechanisms of Vascular Smooth Muscle Cell Calcification

The formation of bone is a tightly regulated process, involving the interplay and balance of osteoblasts, osteoclasts and chondrocytes, while the main cell type involved in bone formation are osteoblasts [11]. Already Virchow noted, that in calcified arteries, mineral components resemble rather ossification than mere calcification [16,18,26]. Yet, the switch from a theory of passive calcium-phosphate precipitation to an active cellular process of vascular calcification, resembling the process of bone formation, was more recently fuelled by the discovery of Boström et al. that *Bone Morphogenetic Protein 2* (BMP2), an osteoblast related protein, is expressed in calcified human atherosclerotic lesions [26]. In addition, it was found that cultured human and bovine aortic smooth muscle cells form calcifying nodules after prolonged culturing, thus putting VSMCs into the spotlight of research [26].

Osteoblasts and myocytes (including VSMCs) both derive from *Mesenchymal Stem Cells* (MSC) [27]. VSMCs normally have a contractile phenotype to serve the adaption of vessel tonus as their physiologic function [28]. Yet, VSMCs also have a wide plasticity, enabling them to transdifferentiate into a multitude of different phenotypes: They can display an osteoblastic or chondrogenic phenotype as well as features of adipocytes or macrophage foam cells [25]. Several stimuli with multifactorial underlying mechanisms can result in phenotype changing of VSMCs (figure 1). Stimuli modifying VSMCs transcriptome towards an osteoblastic phenotype include (1) altered physiologic homeostasis, including altered phosphate and calcium as well as glucose and insulin homeostasis, (2) the absence of calcification inhibitors, (3) senescence, (4) excessive ROS, and (5) inflammation [29,30].

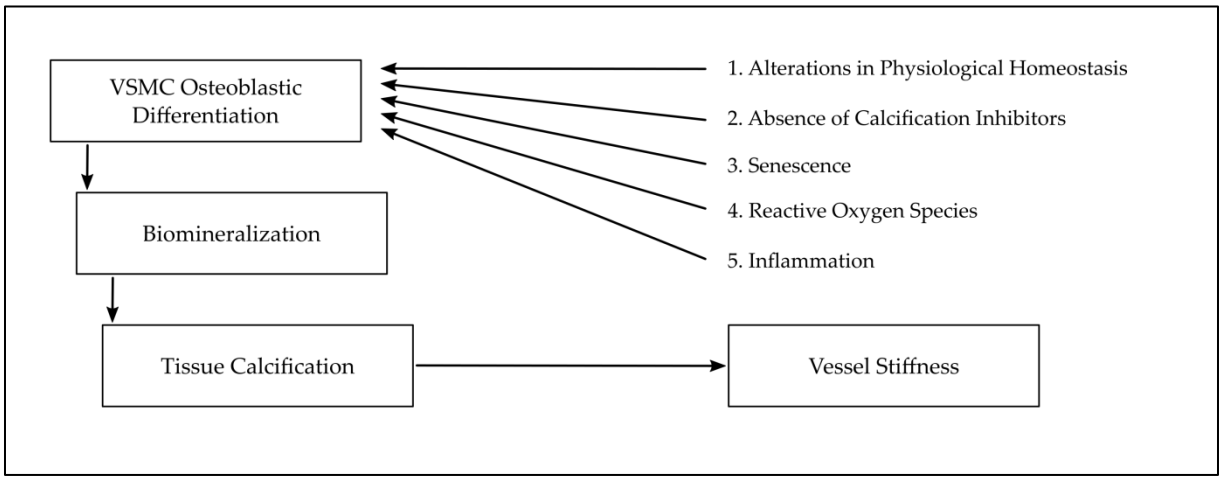

Fig. 1: Overview over the Inducers of VSMC Osteoblastic Transdifferentiation and the Process of Vessel Calcification

(Source: Own Illustration, based upon [29,30])
Abbreviation: *VSMC* - Vascular Smooth Muscle Cell

Several signalling pathways are involved and interconnected in the differentiation of MSC into osteoblasts, with *Transforming Growth Factor ß* (TGF-ß) / BMP signalling being one

decisive pathway in VSMCs osteoblastic transdifferentiation [27,31,32]: The superfamily of TGF-ß consists, among others, of TGF-ß and BMP [32]. In the TGF-ß signalling pathway (canonical and non-canonical) activation of the TGF-ß receptor results in a modulation of gene expression, inducing the expression and activation of transcription factors such as *Runt Related Transcription Factor 2* (RUNX2, synonymously known as *Core Binding Factor Alpha 1* (CBFA1)), *Msh Homeobox 2* (MSX2) and osterix [32]. Especially RUNX2 was identified as master transcription regulator, governing the phenotype transition of VSMCs to an osteoblastic phenotype [33]. The osteogenic transcriptome is then further driven by these transcription factors to express osteogenic proteins, including e.g., non-tissue specific *Alkaline Phosphatase* (ALP), BMP2, Osteocalcin as well as type 1 collagen and to suppress the expression of smooth muscle lineage markers [34].

Although in the process of osteoblastic transdifferentiation VSMCs resume an osteoblastic phenotype, transdifferentiated VSMCs and osteoblasts remain distinctly different cell populations [35]. VSMCs do not reach a full osteoblast transcriptome, but rather express genes of the extracellular matrix and tissue mineralization that osteoblasts use for osteogenesis, resulting in biomineralization [35]. Yet, while osteoblastic transdifferentiation of VSMCs is clearly a decisive aspect in pathophysiologic calcification, several other mechanisms are involved in VSMC calcification, including: (1) matrix remodelling as consequence of increased matrix metalloproteinase production, (2) increased collagen synthesis and deposition and (3) induction of VSMC apoptosis, resulting in apoptotic bodies that can become nidi for calcification [34].

VC follows the process of biomineralization, that to date is incompletely understood [36]. Biomineralization comprises both intracellular osteogenic processes and extracellular crystallization processes, which remain more elusive [37]. Even under physiologic conditions the concentration of both calcium and phosphate is sufficient for mineralization, yet natural inhibiting mechanisms prevent mineralization [36]. Biomineralization requires initialisation by crystallization nucleators [36]. These crystallization nucleators induce mineralization by (1) formation of a primary crystallization nucleus or (2) the removal of endogenous inhibitors of mineralization [36]. Physiologically, several endogenous inhibitors exist to prevent formation of calcium precipitates, including *Matrix Gla Protein* (MGP), Fetuin A and pyrophosphate [12]. MGP is a gamma-carboxylated protein capable of binding both BMP-2 and calcium crystals [38-40]. Availability of functional MGP can be diminished by inhibition of gamma-carboxylation, for example as a consequence of decreased Vitamin K availability or treatment with Warfarin [39]. Fetuin A can prevent the formation of calcium precipitations by binding of calcium phosphate [38]. Pyrophosphate inhibits calcium phosphate nucleation and is inactivated upon degradation by ALP, making expression of ALP decisive both in formation

of bone and VC [38]. The Co-expression of ALP and collagen 1 was found sufficient for the induction of (ectopic) calcification [41]. Hyperphosphatemia was found to induce both, the expression of ALP and extracellular matrix remodelling, inducing the synthesis of collagen and creating a collagen enriched extracellular matrix [34]. Extracellular matrix vesicles may serve as primary crystallization nuclei, as under pathophysiological conditions their loading is altered: they are loaded with ALP and contain high calcium as well as phosphate [37]. Also, apoptotic bodies serve as site of primary crystallization [42]. Calcium-phosphate-lipid complexes are formed in the membranes of vesicles and become nucleators for further accumulation of calcium and phosphate [36].

Although the process of VSMC calcification is in general considered harmful for the organism, calcification is also likely a protective repair mechanism [43]. For example, calcification of a plaque can result in increased stability, reducing the risk of plaque rupture compared to plaques that are not or only slightly (spotty) calcified [43].

2.1. Altered Physiologic Homeostasis as Inducer of Vascular Smooth Muscle Cell Calcification

VSMCs react with transcriptome modulation to several alterations of physiologic homeostasis. Osteoblastic transdifferentiation and calcification was found e.g., as consequence of hyperphosphatemia, hypercalcemia and hyperglycemia [44]. Phosphate is of special interest, as several clinical studies found a strong link between elevated blood phosphate levels and ectopic calcification [45].

In *in vitro* research, hyperphosphatemia, hypercalcemia and hyperglycemia can be resembled by the application of culture medium supplemented with phosphate, calcium, increased glucose content or insulin [44]. Selected studies and the effects of respective supplementation on VSMCs are summarized in table 1.

Tbl. 1: Alterations in Culture Conditions and Resulting Modification in Vascular Smooth Muscle Cell Transcriptome and Calcification

Components in Osteogenic Medium	Assessed Marker of Osteoblastic Transdifferentiation / Calcification	Source
ß-Glycerophosphate	Calcium↑	[46]
Inorganic Phosphate	RUNX2↑, BMP2↑, SM22↓,	[47]
Ascorbic Acid	Calcium↑	[46]
$CaCl_2$	Calcium↑	[46]
ß-Glycerophosphate Insulin Ascorbic Acid	Calcium↑, ALP↑, SMA↓	[48]
Inorganic Phosphate Fetal Calf Serum $CaCl_2$	RUNX2↑, BMP2↑, ALP↑, SMA↓, OPN↑	[49,50]
Glucose (25mM) (in Addition to ß-Glycerophosphate and Ascorbic Acid)	Calcium↑, RUNX2↑, BMP2↑, ALP↑	[51]

Abbreviations: *ALP* - Alkaline Phosphatase; *BMP2* - Bone Morphogenetic Protein 2; *OPN* – Osteopontin; *RUNX2* - Runt Related Transcription Factor 2; *SMA* – Smooth Muscle Actin; *SM22* - Smooth Muscle 22alpha

In vitro, application of phosphate, both organic and inorganic, increases VSMCs calcification and induces changes in VSMCs transcriptome towards an osteoblastic phenotype [46-49]. Stimulation with phosphate results in an upregulated expression of several osteo-chondrogenic markers, including MSX, RUNX2, BMP2 and ALP and in downregulation of smooth muscle cell markers, such as *Smooth Muscle Actin* (SMA, synonymously known as Actin Alpha 2), *Myosin Heavy Chain 11* (MYH11) and *Smooth Muscle 22alpha* (SM22) [48,49,51-54]. The effect of phosphate is dose dependent: for example, human VSMC cultured in medium containing 1.4 mM phosphate do not calcify, while human VSMC cultured in medium containing higher phosphate concentration calcify dose and time dependent [55]. Calcium supplementation can also increase calcification of VSMCs in a dose dependent effect, but in comparison to phosphate supplementation, the effect of calcium without additional co-stimulants is weaker [46,49]. Calcification can be further enhanced by supplementation with high (4.5 g/l) glucose, high concentration of fetal calf serum as well as by application of insulin [44,49].

Current research revealed that stimulation with phosphate does not only induce osteoblastic transdifferentiation of VSMCs, but also results in upregulation of (1) oxidative stress (2) inflammatory markers and (3) senescence markers [47,50,56]. Wei et al. detected next to an increase in RUNX2, BMP2 and *Osteopontin* (OPN) an induction of ROS in VSMCs stimulated with phosphate [50]. Zhang et al. showed upregulation of both osteoblastic (BMP2, RUNX2) and inflammatory markers (*Interleukin-6* (IL-6), *Interleukin-1ß* (IL-1ß) and *Tumour Necrosis Factor alpha* (TNFα)) upon stimulation with phosphate [47]. Troyano et al. showed upon treatment of VSMCs with ß-glycerophosphate that markers of senescence (p53, p16, p21) increase [56].

2.2. Reactive Oxygen Species as Inducer of Vascular Smooth Muscle Cell Calcification

ROS are partially reduced oxygen metabolites with oxidizing capacities [57]. Although ROS as decisive elements of several signal transduction pathways and components of immune responses against pathogens have crucial physiologic effects, especially sustained release of ROS is associated with detrimental effects, including pathophysiological effects on the vasculature [58]. Oxidative stress is the condition, where deleterious effects of ROS outbalance their beneficial effects [59]. Oxidative stress can either result from increased production of ROS, from endogenous sources as well as due to environmental stressors, can be a consequence of reduced anti-oxidant capacities or can derive from a combination of both [57,59-61]. Increased ROS can cause oxidative damage to a variety of different biomolecules, including peroxidation of lipids, oxidation of proteins and DNA damage formation [61].

ROS include for example the radical superoxide, hydroxyl radicals as well as hydrogen peroxide (H_2O_2) and derive in the vasculature from different sources, mainly from endothelial cells and VSMCs [59,60]. These sources include, among others, uncoupled endothelial *Nitric Oxide Synthase* (NOS), inducible NOS, *Xanthine Oxidase* (XO), *Nicotinamide Adenine Dinucleotide Phosphate* (NADPH) *Oxidase* (NOX) and the mitochondria [57]. Selected sources and forms of ROS are summarized in figure 2.

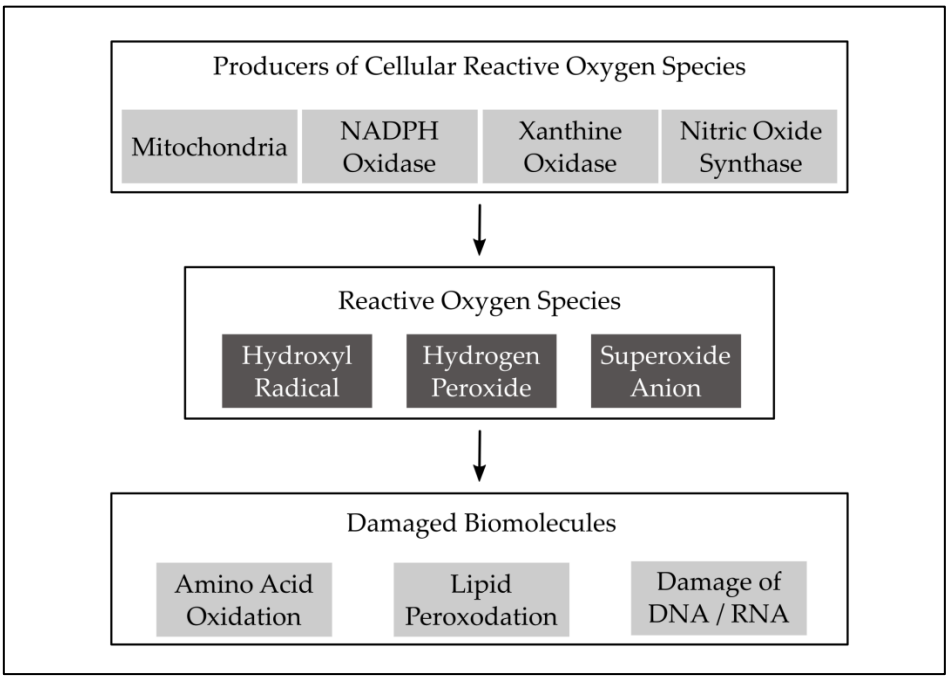

Fig. 2: Reactive Oxygen Species in the Vasculature: Selected Sources, Forms and Damage to Biomolecules

(Source: Own Illustration, based on [57,59-61])

Abbreviation: *NADPH* - Nicotinamide Adenine Dinucleotide Phosphate

NOX are considered the most important source of ROS in the vasculature, with continuous, slow but sustained release of superoxide [60,62]. The isoforms NOX1 and NOX4 are of special relevance in the vasculature [63]. NOX1 is mainly situated at the cell membrane and comprises of the p22phox at the catalytic core and two further subunits required for activation: p47phox and *Ras-related C3 botulinum toxin substrate 1* (Rac1) [64]. NOX1 activity, resulting in increased superoxide production, can be upregulated in VSMCs as a response to several stimuli, including for example oxidized *Low Density Lipoprotein* (LDL), thrombin, lipopolysaccharide and pro-inflammatory stimuli like TNFα [64]. NOX1 activity can be enhanced by increased transcriptional expression, post-translational modification and complex activation [64]. After generation of superoxide, *Superoxide Dismutases* (SOD) can further convert superoxide into H_2O_2, which in turn can be further modified to hydroxyl radicals [60]. In contrast to NOX1, the constitutional active isoform NOX4 preferentially produces H_2O_2 and is situated in the plasma membrane as well as intracellularly [65]. NOX4 activity is independent of both, Rac1 and p47phox, and is mainly regulated at the expression level, for example by pro-inflammatory stimuli like TGF-ß [65].

Several studies associate oxidative stress resulting from augmented ROS with increased osteoblastic differentiation of VSMC and link excess ROS to vascular calcification [60,66]. Selected studies are summarized in table 2.

Tbl. 2: Sources of Oxidative Stress and Resulting Modification in Vascular Smooth Muscle Cell Transcriptome and Calcification

Exemplary Stimulus for / Source of ROS	Assessed Marker of Oxidative Stress	Assessed Marker of Osteoblastic Transdifferentiation / Calcification	Source
H_2O_2	-	RUNX2↑, ALP↑, Calcium↑, SMA↓, SM22↓	[67]
XO (Application of 6-MP as Substrate)	Superoxide ↑	ALP↑, Calcium↑, RUNX2↑	[68]
NOX activity (Upregulated by ß-Glycerophosphate or Uremic Serum)	p22phox↑, H_2O_2↑	ALP↑, Calcium↑, RUNX2↑,	[69]
Mitochondrial ROS (Upregulated by ß-Glycerophosphate)	Mitochondrial Membrane Potential↑, Superoxide ↑	RUNX2↑, MSX↑, Calcium↑, SMA↓, SM22↓	[70]

Abbreviations: *6-MP* – 6-Mercaptopurine; *ALP* - Alkaline Phosphatase; *BMP2* - Bone Morphogenetic Protein 2; *MSX* - Msh Homeobox 2; *NOX* - NADPH Oxidase; *ROS* - Reactive Oxygen Species; *RUNX2* - Runt Related Transcription Factor 2; *SMA* – Smooth Muscle Actin; *SM22* - Smooth Muscle 22alpha; *XO* – Xanthine Oxidase

H_2O_2 is produced by several enzymes in vascular cells [67]. Application of H_2O_2 to a cell culture of VSMCs promoted the phenotype modification towards an osteoblastic phenotype with upregulation in RUNX2 and calcification [67]. H_2O_2 induced calcification could be inhibited by blocking of RUNX2 and AKT signalling [67]. Prüfer et al. applied a substrate of XO (*6-Mercaptopurine* (6-MP), the cleavage product of A*zathioprine* (AZA)) to VSMCs and

showed increased production of superoxide and induction of osteoblastic markers upon treatment [68]. The induction of superoxide and osteoblastic markers was reduced upon co-treatment with ROS scavenger tiron and XO inhibitor allopurinol [68]. Phosphate has been demonstrated by several studies to induce the formation of ROS: Sutra et al. found treatment with both ß-glycerophosphate and uremic serum to induce the expression of the NADPH subunit p22phox and increase the production of H_2O_2 as well as markers of osteoblastic transdifferentiation and calcification in VSMCs [69]. These effects were at least in part diminished by treatment with a NADPH inhibitor [69]. Zhao et al. detected increased mitochondrial membrane potential and increased mitochondrial derived superoxide formation in VSMCs after treatment with ß-glycerophosphate, accompanied by a pro-osteoblastic modulation of VSMC transcriptome and increased calcification [70]. An inhibition of the mitochondrial ROS generation by either inhibiting the respiratory chain or application of a SOD mimic reduced the phosphate induced transdifferentiation and calcification of VSMCs [70].

ROS are involved in in numerous physiological and pathophysiological processes, including for example acute and chronic inflammation as well as induction of cellular senescence [57,71]. As a link between oxidative stress and inflammation, oxidative specific epitopes, like for example oxidized cholesteryl esters, can be recognized as *Damage Associated Molecular Patterns* (DAMPs) by the innate immune system, resulting in a host derived activation of the immune system [72]. In addition, as response to oxidative damage, for example persistent DNA damage, cellular senescence as one stress response can be induced [71].

2.3. Cellular Senescence as Inducer of Vascular Smooth Muscle Cell Calcification

Organism age has long been a well-known risk factor for the development of vascular calcification [73]. Organism and biological age are closely related to cellular senescence [74]. The concept of senescence at a cellular level was first published by Hayflick and Moorhead in 1961 [75]. They found that cultured cells do not expand indefinite, but have a limited life span for replication, finally reaching growth arrest [75]. This concept is considered dependent on telomere shortening and termed replicative senescence [76]. Since then, further research showed, that cells do not only undergo senescence because of replication and telomere shortening but can also stay in a temporary or persistent growth arrest due to cellular damage; a concept termed S*tress Induced Premature Senescence* (SIPS) [77]. The term “premature” emphasizes that chronological and biological age of organisms and cells are not necessarily synonymous, but that e.g., stressors can accelerate aging [73].

An important connection between elevated oxidative stress and senescence is the formation of DNA damage as consequence of elevated ROS, inducing a protein cascade termed the

DNA Damage Response (DDR) [24]. One central aspect in this pathway is the formation of γH2AX, a histone modification created through phosphorylation by *Ataxia Telangiectasia Mutated* (ATM) in reaction to DNA double strand breaks [78]. γH2AX is both a marker of double strand DNA breaks and a component of the *Senescence Associated Heterochromatin Foci* (SAHF) [79]. γH2AX functionally acts as a recruiter and modulator for DNA repair mechanisms and modulates the induction of senescence and apoptosis, thus connecting ROS and senescence via the ATM pathway [24].

Senescent cells are arrested and can no longer proceed through the cell cycle [74,80]. This growth arrest can be both beneficial, as tumour suppressive and repair mechanisms are provided with time for execution, or detrimental, due to reduced regenerative capacity and altered signalling [81]. Senescent cells, independent of their cell type, share some characteristics: They remain metabolically active, with altered gene and protein expression [76]. These changes include the expression of tumor suppressor p53 and the cyclin dependent kinases and cell cycle inhibitors p21 and p16 [80]. These cyclin dependent kinase inhibitors are essential in tumour suppression pathways, leading to the establishment of senescence growth arrest [76]. In addition, changes in gene and protein expression include the secretion of proteins, especially pro-inflammatory cytokines, due to an acquired *Senescence Associated Secretory Phenotype* (SASP), by which senescent cells can alter their microenvironment [82]. Other senescence markers include DNA damage foci like γH2AX and other SAHF, *Senescence Associated ß-Gal* (SA-ß-Gal) and a flattened, enlarged, granulated morphology [71]. Selected inducers and markers of cellular senescence are summarized in figure 3.

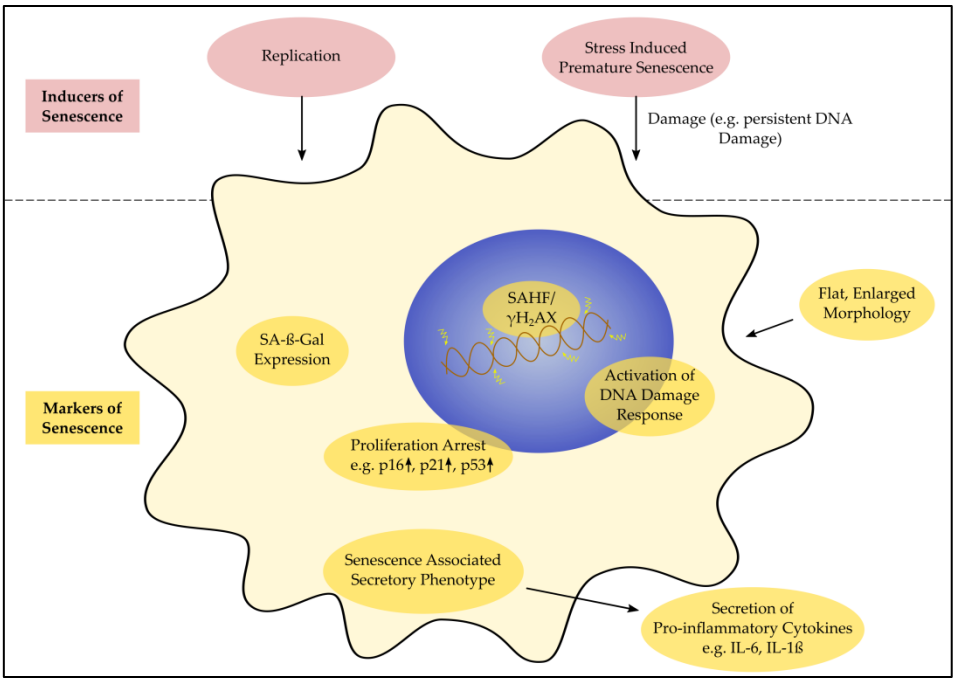

Fig. 3: Inducers and Markers of Cellular Senescence

(Source: Own Illustration, based on [24,71,74,76,77,80-82])

Abbreviations: *IL-6* - Interleukin-6; *IL-1ß* - Interleukin-1ß; *SA-ß-Gal* - Senescence Associated ß-Galactosidase; *SAHF* – Senescence Associated Heterochromatin Foci

As age and diseases leading to stress induced premature biological aging, such as DM, CKD and inflammatory disorders, are known risk factors for the development of VC, there is strong indication that senescence and calcification are interconnected [73]. Nakano-Kurimoto et al. found that replicative senescence triggered by extended cell passaging induces calcification and expression of calcification markers in VSMCs [83]. Since then, several markers of VSMC osteoblastic transdifferentiation and calcification were found to increase upon induction of senescence. A selection of respective studies is summarized in table 3. Among others, Bielak-Zmijewska et al. confirmed that extended cell passaging leads to induction of senescence and increased ALP activity in VSMCs [84]. VSMCs suffering from SIPS, induced e.g., by treatment with Prelamin A, were found to express, next to senescence markers, also markers of osteoblastic cell differentiation and increased calcification [85]. Similar results were obtained by Sanchis et al., who found CKD and dialysis to function as inducers of SIPS [86]. They found that VSMCs from children on dialysis exhibited increased DNA damage, accelerated senescence, increased calcification and osteogenic differentiation [86].

Tbl. 3: Induction of Senescence and Resulting Modification in Vascular Smooth Muscle Cell Transcriptome and Calcification

Exemplary Stimulus for Senescence Induction		Marker of Senescence	Marker of Osteoblastic Transdifferentiation / Calcification	Source
Replicative Senescence / Extended Cell Passaging		SA-ß-Gal↑, p21↑, p16↑	ALP↑, MGP↓, Calcium ↑	[83]
		SA-ß-Gal↑, p21↑, p53↑, p16↑, Granularity↑, γH2AX↑, SASP↑	ALP↑	[84]
Stress Induced Premature Senescence	CKD / Dialysis	SA-ß-Gal↑, p21↑, p16↑, γH2AX↑, ATM↑ SASP↑	RUNX2↑, BMP2↑, Calcium↑, SMA↓	[86]
	Prelamin A	p16↑, γH2AX↑, ATM↑	RUNX2↑, BMP2↑, Calcium↑, ALP↑	[85]

Abbreviations: *ALP* - Alkaline Phosphatase; *ATM* - Ataxia Telangiectasia Mutated; *BMP2* - Bone Morphogenetic Protein 2; *CKD* - Chronic Kidney Disease; *MGP* - Matrix Gla Protein; *RUNX2* - Runt Related Transcription Factor 2; *SA-ß-Gal* - Senescence Associated ß-Galactosidase; *SASP* - Senescence Associated Secretory Phenotype; *SMA* - Smooth Muscle Actin

Research on the concurrent induction of SIPS and increased calcification in VSMCs also indicates that the DDR, mentioned earlier as one link between elevated ROS and senescence, can also link senescence and VC: In studies inducing SIPS and calcification, inhibition of ATM with the inhibitor Ku55933 reduced both osteoblastic transdifferentiation and calcification [85,86]. More recently, the work by Cobb et al. detected a direct link between the ATM pathway and RUNX2: They found RUNX2 to locate at sites of DNA damage and to be poly-ADP-ribosylated upon DNA damage, resulting in enhanced expression of osteogenes [87]. In addition, the induction of the SASP and cellular senescence results in secretion of pro-inflammatory cytokines, thus directly linking senescence to inflammation [86,88].

2.4. Inflammation as Inducer of Vascular Smooth Muscle Cell Calcification

Inflammation is a physiological defence mechanism against several harmful stimuli [89]. These stimuli can derive both exogenously, for example from bacteria, and endogenously, e.g., from cancer cells [89,90]. The physiological objective is the elimination of these potentially harmful stimuli and the facilitation of tissue repair [89].

Next to inflammation in response to harmful stimuli, inflammatory disorders, including autoinflammatory diseases and chronic low-grade inflammation, can have detrimental effects [89]. In patients suffering from CKD, inflammatory markers, including cytokines TNFα, IL-6 and IL-1ß, markedly increase and contribute to chronic inflammation [91]. These cytokines are, among others, retained as uremic toxins in CKD patients, can influence VSMCs physiologic functions and are induced in VSMCs upon treatment with ß-glycerophosphate (table 4) [92-95]. As especially IL-6 and IL-1ß are also considered essential components of the SASP, their secretion is directly linked to cellular senescence [86,88]. Table 4 and figure 4 summarize pro-inflammatory stimuli and cytokines involved in VSMCs transdifferentiation.

Tbl. 4: Induction of Inflammation and Resulting Modification in Vascular Smooth Muscle Cell Transcriptome and Calcification

Exemplary Inflammatory Stimulus	Marker of Inflammation	Marker of Osteoblastic Transdifferentiation / Calcification	Source
ß-Glycerophosphate	TNFα↑, IL-1ß↑, IL-6↑	BMP2↑, MSX2↑, RUNX2↑, Calcium↑	[92]
	ASC↑, NLRP3↑, Caspase 1↑, IL-1ß↑	Calcium↑	[93]
TNFα	-	RUNX2↑, MSX2↑, ALP↑, SMA↓, Calcium↑	[96,97]
IL-1ß	-	BMP2↑, RUNX2↑, Calcium↑	[98]
IL-6	-	BMP2↑, RUNX2↑, OPN↑, Calcium↑,	[99,100]

Abbreviations: *ALP* - Alkaline Phosphatase; *ASC* - Apoptosis Associated Speck-like Protein Containing a Caspase Recruitment Domain; *BMP2* - Bone Morphogenetic Protein 2; *IL-6* - Interleukin-6; *IL-1ß* - Interleukin-1ß; *MSX2* - Msh Homeobox 2; *NLRP3* - NOD-, LRR- and Pyrin Domain-containing Protein 3; *RUNX2* - Runt Related Transcription Factor 2; *OPN* - Osteopontin; *SMA* - Smooth Muscle Actin; *TNFα* - Tumour Necrosis Factor alpha

To assess stimuli as dangerous, the immune system can detect DAMPs [101]. DAMPs can either derive from pathogens and are then also termed *Pathogen Associated Molecular Patterns* (PAMPs), which include for example highly conserved bacterial structures such as lipopolysaccharide [102]. Endogenously, DAMPs can derive from cells that are damaged or dying, including for example histones, ATP, uric acid and interleukins [101]. Also, oxidative damage of biomolecules can result in the formation of DAMPs [72]. DAMPs can be detected by *Pattern Recognition Receptors* (PRRs), which can then activate inflammatory signalling [101]. Several receptors can sense PAMPs and DAMPs, among others *Toll Like Receptors* (TLRs) and *Nucleotide-binding Oligomerization Domain-like Receptors* (NLRs) [101].

TLRs are type 1 transmembrane proteins and comprise of an extracellular leucine rich repeat, which recognizes DAMPs and PAMPs, an intracellular *Interleukin 1 Receptor* (IL-1R) domain, which is activating the downstream signal, and a connecting transmembrane domain [102]. To date, several subtypes of TLRs have been described, residing either on the cell surface or intracellularly, of which TLR2 and TLR4 are of special significance in the vascular system [103].

Another signalling pathway of PRR is the formation of inflammasomes [101]. Among others PRRs, NLR family member *Nucleotide-Binding Oligomerization Domain-like Receptor family pyrin domain containing 3* (NLRP3) can form an inflammasome [104]. In the process of NLRP3 inflammasome formation, NLRP3 as the sensor PRR oligomerizes with the adaptor *Apoptosis associated Speck-like protein containing a Caspase recruitment domain* (ASC) and the effector pro-caspase 1, which is activated to caspase 1 [104]. Pro-IL-1ß and pro-interleukin 18 are then cleaved by caspase 1 into the biological active forms IL-1ß and *Interleukin-18* (IL-18) [104]. Involvement of NLRP3 has been implicated in a variety of different disease pathologies, including for example CKD and CVD [105,106]. The currently proposed mechanism of NLRP3 activation comprises 2 steps [107]. The first step is referred

to as “priming”: A signal activating for example IL-1R or TLR results in an upregulation of gene expression of NLRP3 inflammasome components (e.g., NLRP3, ASC, caspase 1 and IL-1ß) and their posttranslational stabilisation via the NF-κB pathway [107]. In the second step, a variety of different signals induce the “activation” of NLRP3, which comprises of association of NLRP3 with ASC, oligomerization of the NLRP3-ASC complexes and recruitment of caspase 1 to the oligomer [107]. As effector mechanism, NLRP3 inflammasome activation can then result in the release of pro-inflammatory cytokines (IL1-ß and IL-18) or via cleavage of gasdermin in pyroptosis [107]. A decisive feature of the NLRP3 inflammasome is the activation in response to several different stimuli and versatile triggers, including for example detection of extracellular ATP, lipopolysaccharide, oxidized mitochondrial DNA, uric acid and calcium crystals [104]. For NLRP3 to successfully react to this multitude of signals with diverse chemical structures, there has to be a mechanism integrating the variety of stimuli towards few, universally occurring signals [104]. The most likely explanation to date is the integration of diverse signals into signals of cellular stress, including for example mitochondrial dysfunction and ROS, although the specific signals remain elusive to date [104].

Figure 4 summarizes the involvement and integration of several pro-inflammatory stimuli and pathways into the process of VSMC calcification and shows the link to oxidative stress via induction of DAMPs and senescence via induction of SASP. The involvement of NLRP3 in calcification of VSMCs shown in figure 4 has been demonstrated by several studies, including the work of Wen et al. who demonstrated that treatment of VSMCs with ß-glycerophosphate upregulates expression of NLRP3 inflammasome components and showed that inhibition of NLRP3 reduced ß-glycerophosphate induced calcification [93]. In line with these results, Han et al. found IL-1ß to induce calcification and osteoblastic transdifferentiation in VSMCs [98]. Also, other cytokines like IL-6 and TNFα are upregulated in response to treatment with ß-glycerophosphate and induce osteoblastic transdifferentiation and calcification in VSMCs [96,97,99,100].

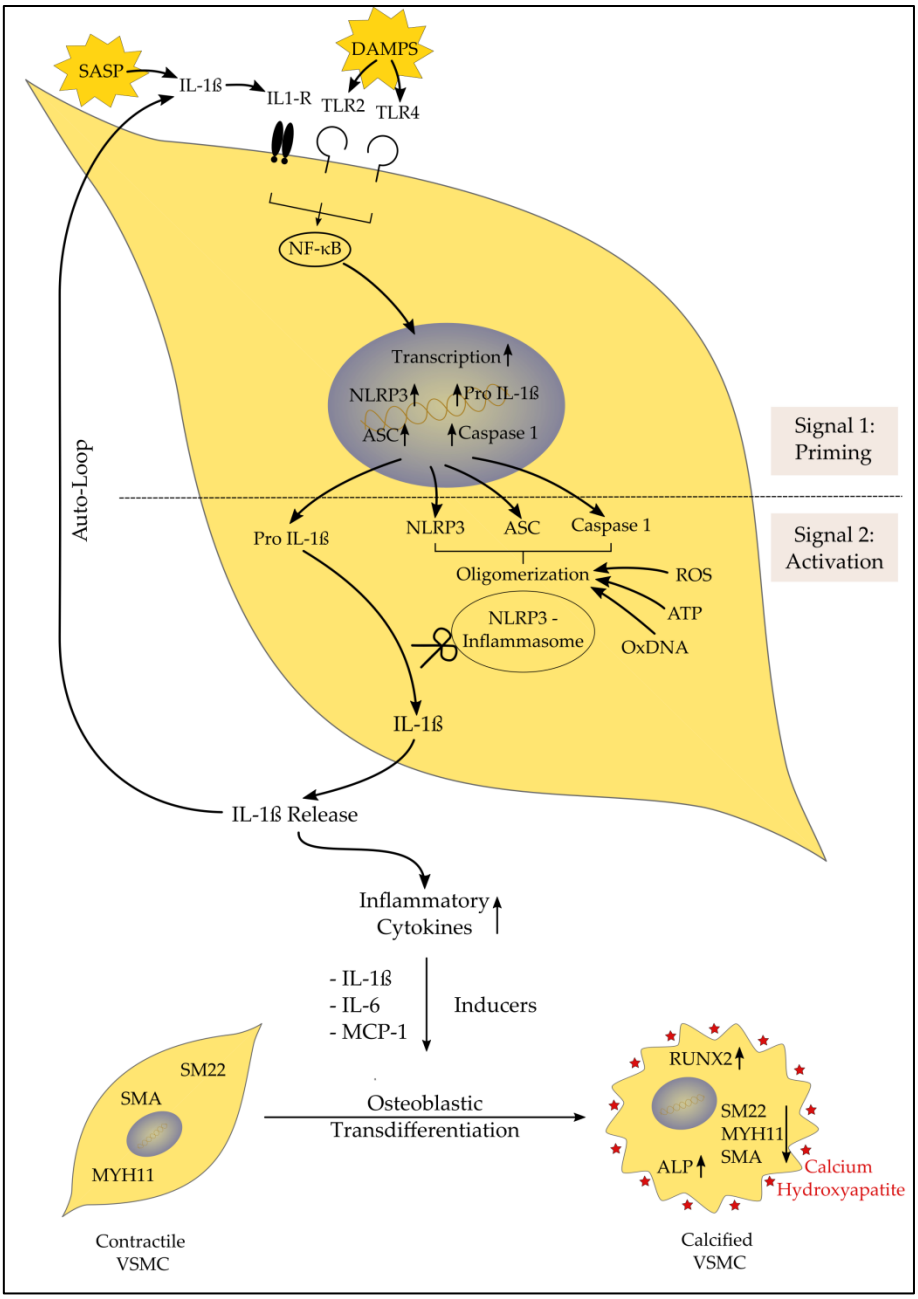

Fig. 4: Involvement of Inflammatory Pathways, Especially NLRP3 Activation, in VSMC Calcification

(Source: Own Illustration, based on [93,98,104,105,107,108])

Activation of PRRs (e.g., IL1-R, TLR2, TLR4) results in priming of the NLRP3 inflammasome. Upon activation and oligomerization of the NLRP3 inflammasome (e.g., by ROS, ATP, *oxidized DNA* (OxDNA)), IL-1ß is cleaved from Pro-IL-1ß and released from the cell. IL-1ß can induce the release of inflammatory cytokines, including in the context of an auto-loop IL-1ß itself. Pro-inflammatory cytokines can then induce osteoblastic transdifferentiation of VSMC (including downregulation of VSMCs lineage markers (SM22, SMA, MYH11) and upregulation of osteoblastic markers (RUNX2, ALP)) and VSMC calcification.

Abbreviations: *ALP* - Alkaline Phosphatase; *ASC* – Apoptosis Associated Speck-like Protein Containing a Caspase Recruitment Domain; *DAMP* - Damage Associated Molecular Pattern; *IL-6* - Interleukin-6; *IL-1ß* - Interleukin-1ß; *IL-1R* - Interleukin 1 Receptor; *MCP-1* - Monocyte Chemoattractant Protein; *Myh11* - Myosin Heavy Chain 11; *NF-κB* - Nuclear Factor 'kappa-light-chain-enhancer' of Activated B-Cells; *NLRP3* - Nucleotide-Binding Oligomerization Domain-like Receptor family pyrin domain containing 3; *ROS* - Reactive Oxygen Species; *RUNX2* - Runt Related Transcription Factor 2; *SASP* - Senescence Associated Secretory Phenotype; *SMA* - Smooth Muscle Actin; *SM22* - Smooth Muscle 22alpha; *TLR* - Toll Like Receptor; *VSMC* - Vascular Smooth Muscle Cell

3. Aims of Research

Due to a lack of therapy options for treatment of VC and a huge patient population concerned, there is an unmet clinical need for pharmaceutical drugs that prevent, slow or even reverse the formation of VC. The objective of this dissertation is to provide deeper insight into the mechanisms of stress induced VSMC calcification and to unravel underlying signalling pathways that could be targeted by therapeutics, especially concerning the involvement of inflammaging in VC. In order to meet these goals, the effects of cellular stressors in eligible models for VC were analysed.

For the purpose of selection of an eligible experimental setting (1) the status quo of currently available experimental models of VC induction was reviewed (Manuscript 1).

Because the assessment of VSMCs transdifferentiation required an analysis on single cell level, (2) a protocol for the conjoint detection of markers of cellular senescence and VSMCs osteoblastic transdifferentiation via *in situ* hybridization and immunofluorescence in a VSMC *in vitro* model was established (Manuscript 2).

By adaption of eligible models and detection methods for induction and assessment of VC, oxidative stress and inflammation-associated signal transduction pathways in VC were analysed. The purpose was to identify key targets in the signalling pathways that permit assessment of applicable antagonists for stressor induced calcification and thereby support the development of therapeutic options.

Therefore (3) cellular stressors, including *Doxorubicin* (DOX), AZA and IL-1ß, were investigated to unravel the pathophysiological setting and interaction of reactive oxygen stress, pro-inflammatory conditions and senescence in VSMC during calcification (Manuscripts 3 and 4). In order to (4) test the potential of inhibition of stressor induced calcification, several targets in the supposed signalling pathways were inhibited, either by employment of a knock down animal model or by application of respective antagonists (Manuscripts 3 and 4).

4. Publications

*authors contributed equally

Manuscript 1:

Herrmann J, Babic M, Tolle M, van der Giet M, Schuchardt M. Research Models for Studying Vascular Calcification. Int J Mol Sci. 2020;21(6):2204.

Manuscript 2:

Herrmann J*, Babic M*, Tolle M, Eckardt KU, van der Giet M, Schuchardt M. A Novel Protocol for Detection of Senescence and Calcification Markers by Fluorescence Microscopy. *Int J Mol Sci.* 2020;21(10):3475.

Manuscript 3:

Herrmann J, Xia M, Gummi MR, Greco A, Schacke A, van der Giet M, Tolle M, Schuchardt M. Stressor-Induced "Inflammaging" of Vascular Smooth Muscle Cells via Nlrp3-Mediated Pro-inflammatory Auto-Loop. *Front Cardiovasc Med.* 2021;8(1932):752305.

Manuscript 4:

Schuchardt M, **Herrmann J**, Henkel C, Babic M, van der Giet M, Tolle M. Long-Term Treatment of Azathioprine in Rats Induces Vessel Mineralization. *Biomedicines.* 2021;9(3):327.

Manuscript 1: Research Models for Studying Vascular Calcification

The manuscript has been published in *International Journal of Molecular Science (*IF: 5.923):

Herrmann J, Babic M, Tolle M, van der Giet M, Schuchardt M. Research Models for Studying Vascular Calcification. Int J Mol Sci. 2020;21(6):2204.

DOI: 10.3390/ijms21062204

The authors' contributions are stated in the publication on page 13/23. My personal contribution to this article encompasses:

Manuscript preparation:

- Conceptualization of the review
- Preparation of figures and tables
- Literature research
- Writing of the original draft, adaption after revision and final editing

International Journal of
Molecular Sciences

MDPI

Review

Research Models for Studying Vascular Calcification

Jaqueline Herrmann [1,2], Milen Babic [1], Markus Tölle [1], Markus van der Giet [1] and Mirjam Schuchardt [1,*]

1 Campus Benjamin Franklin, Department of Nephrology, Charité-Universitätsmedizin Berlin, Corporate Member of Freie Universität Berlin, Humboldt-Universtität zu Berlin, and Berlin Institute of Health, Hindenburgdamm 30, 12203 Berlin, Germany; Jaqueline.Herrmann@charite.de (J.H.); Milen.Babic@charite.de (M.B.); Markus.Toelle@charite.de (M.T.); Markus.vanderGiet@charite.de (M.v.d.G.)

2 Department of Chemistry, Biochemistry and Pharmacy, Freie Universität Berlin, Königin-Luise-Straße 2+4, 14195 Berlin, Germany

* Correspondence: Mirjam.Schuchardt@charite.de

Received: 2 March 2020; Accepted: 18 March 2020; Published: 23 March 2020

check for updates

Abstract: Calcification of the vessel wall contributes to high cardiovascular morbidity and mortality. Vascular calcification (VC) is a systemic disease with multifaceted contributing and inhibiting factors in an actively regulated process. The exact underlying mechanisms are not fully elucidated and reliable treatment options are lacking. Due to the complex pathophysiology, various research models exist evaluating different aspects of VC. This review aims to give an overview of the cell and animal models used so far to study the molecular processes of VC. Here, in vitro cell culture models of different origins, ex vivo settings using aortic tissue and various in vivo disease-induced animal models are summarized. They reflect different aspects and depict the (patho)physiologic mechanisms within the VC process.

Keywords: vascular calcification; in vitro; ex vivo; in vivo

1. Introduction

Cardiovascular disease plays a pivotal role in global morbidity and mortality. One main cause is alterations of the vessel structure, such as atherosclerosis and arteriosclerosis. Arteriosclerosis describes the literal calcification of the media vessel wall of arteries, and atherosclerosis is mainly caused by lipid accumulation and formation of atheromatous plaques in the intima of arteries, with secondary calcification occurring. The calcification in both entities is believed to share underlying mechanisms. Until now, the treatment of vascular calcification (VC) has been limited to management of risk factors with attempts at regulating the impaired calcium–phosphate metabolism. However, VC is an active process which the mechanisms of bone formation, inhibitors of mineralization and local alterations of the vessel wall take part in [1]. One pivotal point of VC is probably the vascular smooth muscle cell (VSMC) with its phenotype changes ending in vessel mineralization [2]. The phenotype shift of VSMC seems to be induced by a variety of conditions such as inflammation [3], reactive oxygen species (ROS) [4,5] and senescence [6]. Aside from differentiated VSMC, other cell types are associated with VC. Mesenchymal osteoprogenitor cells, hematopoietic progenitor cells, endothelial progenitor cells and myeloid cells are circulating cells that bear osteogenic and calcifying potential [7,8]. Not only circulating cells, but also abnormal metabolic conditions such as uremia in the context of chronic kidney disease (CKD) [9], impaired bone metabolism with hyperphosphatemia [10], hypercalcemia and diabetes mellitus type 2 [11,12] lead to medial located calcification, depicting the idea of a systemic disease. The idea of a systemic disease is further supported by decreasing levels of endogenous inhibitors of ectopic calcification like fetuin-a, matrix gla protein (MGP) and inorganic pyrophosphate (PPi) being part of the pathogenesis [13,14]. Under calcifying conditions

with high levels of phosphate and calcium in blood, not only cells but also their deposits act as a nidus for the process of mineralization. In order to reduce the intracellular calcium–phosphate burden, VSMC, for example, can form matrix vesicles or apoptotic bodies. Both of these extracellular deposits serve as a nucleation site for hydroxyapatite and therefore promote calcification [15–17]. Aside from this, degradation of the extracellular matrix (ECM) by matrix metalloproteinases (MMP) facilitates hydroxyapatite deposition and even osteoblastic transdifferentiation of VSMC [18]. This vast variety of probably influencing factors and different components in the development of VC reflect, at least in part, the variety of research models and vice versa. As long as the underlying mechanisms of VC are not fully understood and treatment options are lacking, evaluation methods and research models will emerge. This review summarizes currently available cell and animal models to study the molecular processes of VC. The assessment and research methods for VC in humans are summarized elsewhere [19].

2. In Vitro Models

Our comprehension of processes that underlie VC expands and unravels an intriguing and complex interaction of different cell types and mechanistic signaling. In vitro models are very successful in reducing this complexity and therefore enable scientists to gain insights into the multitude of mechanisms that lead to VC.

2.1. Cell Types

Various models allow studying the processes of VC in vitro. Table 1 summarizes the cell types employed to study the mineralization processes of the vasculature with an emphasis on the arterial tree.

Table 1. Selected cell types for researching vascular calcification in vitro.

Origin	Cell Type	Source
Tunica Externa	Myofibroblasts	[20]
Tunica Media	Primary VSMC	[21–25]
	MOVAS	[26–28]
	A7r5	[29,30]
	A10	[31,32]
Tunica Intima	Pericytes	[33]
	Endothelial Cells	[34]
Circulating	Mesenchymal origin	[35,36]
	Hematopoietic origin	[37–39]
Heart	Valvular Interstitial Cells	[40]

VSMC are of particular importance in the calcification of the vessel media: by changing their phenotype from a contractile into an osteoblast-like phenotype, they actively promote VC via different pathways [41]. Therefore VSMC of different origins, including human, rat, mouse and bovine, are by far the most widely studied in vitro model for medial VC [21–25,42]. Next to them, cell lines of murine (MOVAS) and embryonic rat (A7r5 and A10) origin are utilized [28–32].

Myofibroblasts from the adventitia can transdifferentiate bone morphogenic protein-(BMP2)-Msx2 dependently into an osteoblast lineage and contribute to medial calcification [43].

Pericytes as progenitor cells have osteogenic potential and can differentiate, among others, into osteoblasts and chondrocytes [44,45]. In pericyte in vitro culture, calcification does not require hyperphospatemia, but takes place in physiological calcium concentration [33].

Endothelial cells (EC) form a monolayer barrier in the intimal layer of the vessel lumen. During development, but also upon vascular injury or several stress factors, EC lose EC-specific markers

(e.g., CD31, PECAM-1) and gain expression of mesenchymal progenitor cells—a process referred to as endothelial-to-mesenchymal transition (EndMT) [46,47]. A variety of signaling cascades trigger the EndMT program including, but not limited to, inflammatory conditions and oxidative stress [47]. The transition is characterized by a switch from a fully differentiated phenotype into a pluripotent-like state, where the cell is able to de-differentiate to other mesenchymal-derived lineages. Because of their switch in phenotype, they can accelerate VC progression by secretion of ECM vesicles, expression of adhesion molecules and enhanced proliferation and migration [48]. In addition, they can contribute to ectopic calcification by undergoing osteogenic differentiation and mineralization [49].

Although this review focuses on calcification of the arteries, cardiovascular calcification can also affect the heart e.g., in aortic valve sclerosis. Here, mineralization is mediated mainly by valve interstitial cells (VIC) that form calcified aggregates when cultured in calcifying medium [40]. VIC can either transform into myofibroblasts or osteoblast-like cells, a process that is triggered by several factors, including calcifying medium and inflammatory stimuli, but also mechanical stress and culture conditions [40,50].

Various circulating cells of mesenchymal or hematopoietic origin can contribute to VC, in particular to intimal calcification, although the underlying mechanisms are not fully understood. In recent years, several contributing cell types were identified and reviewed in detail by Albiero et al. [7] and Cianciolo et al. [8]. The isolation and stimulation procedures of those cells differ. Endothelial progenitor cells derived from rat bone marrow calcify and express markers of osteogenic transdifferentiation after stimulation with oxidized LDL or β-glycerophosphate [51]. In human mesenchymal stem cells, calcification could be induced by dexamethasone or β-glycerophosphate [52]. The contribution of those circulating cells to VC, the driving forces for their shift to calcification and the underlying mechanisms need additional elaboration in functional models.

2.2. *Stimuli for Calcification In Vitro*

Although spontaneous calcification within 6 days of cell culture was shown, for example, for VSMC isolated from spontaneously hypertensive rats [53] and for pericytes [33], most cells studied in in vitro experiments do not calcify spontaneously, but instead require stimuli for calcification. The calcification media used so far vary in the essential components as well as the additional factors (Table 2). Frequently, the medium is supplemented with 5%–20% fetal bovine serum (FBS) in low (1 g/L) or high (4.5 g/L) glucose. Supplementation with phosphate in inorganic (sodium phosphates, 1–5 mM) or organic (β-glycerophosphate e.g., 10 mM) form has a dose- and time-dependent stimulatory effect on calcification and additional supplementation with calcium has an additive effect. Ascorbic acid (AA), a cofactor for a variety of enzymes, is also often added. AA influences mesenchymal differentiation and promotes a phenotype switch of cells [54,55]. By the stimulation of, e.g., type I and IV collagens and MMP-2 activity, AA promotes ECM remodeling [56–58]. In addition, the ALP activity increases in the presence of AA and ALP-enriched matrix vesicles contains more apatite-like minerals [58]. Furthermore, sodium pyruvate, insulin or calciferol are frequently used supplements in calcification media. A recent work compared the influence of different factors such as phosphate, calcium and FBS on in vitro calcification yield and reproducibility [59].

Table 2. Selected supplements and representative dosage for in vitro induction of calcification.

Supplement	Common Concentration	Source
Serum/FBS	0%–20%	[21,24,25,33]
Glucose	5–25 mM	[21,60]
Inorganic Phosphate: Sodium hydrogen phosphate	1.6 mM	[32]
Organic Phosphate: β-glycerophosphate	1.25–10 mM	[21,27,52]
Calcium	2.5 mM CaCl	[43]
Ascorbic Acid	10 µg/mL–50 µg/mL	[24,25,27,40]
Sodium pyruvate	10 mM	[21]
Insulin	10^{-7} M	[21]

2.3. Limitations of In Vitro Models

In vitro cell culture experiments are helpful to analyze several research questions e.g., screening substances for inducing/inhibitory effects and/or studying the signaling pathways involved. Nevertheless, one must consider that in cell culture models tissue organization of cells is lost and processes involving cooperative interaction with the ECM cannot be investigated. Research in the field of calcific aortic valve disease gives a striking impression of the effects that non-physiologic environments can have on cell behavior: VIC cultured on a more compliant matrix in calcifying media acquired osteoblast-like properties, while cells cultured on a stiff matrix differentiate into contractile myofibroblasts [40]. Calcification occurred in both cases: on the compliant matrix, calcification was found in aggregates of viable cells that expressed osteoblast-like transcription factors, while on the stiff matrix calcification was found in aggregates containing apoptotic bodies [40]. Alternative models include 3D cell culture models. 3D models mimic the direct physiologic environment and can therefore support physiologic cell behavior, but their implementation is complex. To overcome the problem of myofibroblast differentiation, Hjortnaes et al. developed a 3D model for the research of calcific aortic valve disease that comes closer to the human situation and seems to be a better drug-screening tool than 2D cell culture [61].

3. Ex Vivo Models

Beside stimulation of VSMC, ex vivo experiments using vessel tissue are an alternative for studying calcification pathways [62]. Compared to isolated VSMC, the intact vascular cell structure during stimulation procedure is one advantage. Currently, aortic rings from rats and mice are commonly used for studying vessel calcification under various conditions. The stimulation time varies from 3–14 days [6,24,25,28,59,62–65]. Although the utilization of aortic rings comes closer to the physiologic setting, a multitude of influencing factors is still lost. The luminal side of the aortic ring is not exposed to a flow resembling the blood flow, while the media and adventitia are in direct contact with the calcifying medium or other substances used for stimulation. Endocrine signaling is also missing. To overcome some of these limitations, our group recently developed a modified ex vivo setting of rat artery perfusion in a more physiological way. Here, an increase of mRNA expression in the aortic tissue comparable to in vitro settings and medial-located VC could be induced upon stimulation with high-phosphate medium for 14 days [66]. This model is usable for mouse aortas as well.

4. In Vivo Models

In vitro and ex vivo experiments offer a variety of feasible research models for the analysis of VC by providing a detailed insight into one aspect of the broad physiological picture. Nevertheless, an analysis of the whole organism is often required, as in vitro and ex vivo experiments cannot reflect the whole physiological context, but rather individual aspects. In calcification research, rat and mice models have been well established as they offer certain advantages. As calcification is an age-dependent process, rat and mice models enable monitoring of the calcification progression in a reasonable time. The large homology of their genes with humans and the ease of genetic manipulation in addition to their rapid reproduction allow the development of a variety of genetically modified mouse models.

The following chapter will focus on rat and especially mouse models of VC (Table 3). Of course, the application of rat and mice in vivo models also has several disadvantages that will be discussed at the end of this chapter.

Table 3. In vivo research models inducing vascular calcification in mice and rats.

Model Type	Predominant Localization of Calcification	
	Intimal	Medial
Naturally Occurring		DBA2 mice CY^+ rat with autosomal dominant polycystic kidney disease Lewis polycystic kidney disease rat
Operation		Kidney reduction (electrocautery, nephrectomy)
Feeding/Substance Application	Cholesterol Rich Chow PCSK9-AAV	Adenine Vitamin D Phosphate Streptozotocin
Genetic Modification	Lipoprotein System *ApoE*$^{-/-}$ *Lldlr*$^{-/-}$ *ApoE3 Leiden* *PCSK9-AAV*	Phosphate Metabolism *Klotho*$^{-/-}$ *FGF23*$^{-/-}$ *Galnt*$^{-/-}$ *Tcal/Tcal* Pyrophosphate Metabolism *Abcc*$^{-/-}$ *Enpp1*$^{-/-}$ *Lmna*$^{-/-}$ Osteogenic Signaling *Fetuin A*$^{-/-}$ *Opg*$^{-/-}$ *Mgp*$^{-/-}$ *Opn*$^{-/-}$ *Madh6*$^{-/-}$

Abbreviations: AAV: adeno-associated virus vector; Abcc6: ATP binding cassette subfamily C member 6; ApoE: apolipoprotein E; Enpp: ectonucleotide pyrophosphatase phosphodiesterase; FGF23: fibroblast growth factor 23; Galnt3: GalNAc transferase 3; MGP: matrix gla protein, OPN: osteopontin; OPG: osteoprotegerin; PCSK9: proprotein Convertase subtilisin/kexin type 9.

4.1. Naturally Occuring

Spontaneous and age-dependent mineralization of the vessel wall were found in some animal models. The animals develop sex-specific, mild to moderate medially located VC.

The heterozygous Han:SPRD Cy rat (Cy/+) exhibits a slowly developing and progressive polycystic kidney disease [67] and develops a mild medial-located VC when fed a high phosphate (0.7%) diet [68]. The severity of the kidney damage is sex-specific and progresses predominantly in male rats [67]. In the calcification study, male animals were used [68]. Another rat model suffering from renal failure is the Lewis polycystic kidney disease rat. These animals develop increased arterial stiffness and aortic calcium content compared to Lewis rats with normal kidney function [69].

An age-dependent increase in the severity of soft tissue calcification was also observed in DBA/2 mice [70]. Specifically, cardiac tissue calcification was observed in 6-week-old mice followed by mineralization of the soft tissues in 39–52-week-old mice [70]. The severity of calcification was higher in female than in male animals [70]. Limitations of these models may include the long experimental duration as well as the less progressive medial calcification. However, the mild severity might be a benefit for intervention studies.

4.2. Induction of a Disease State by Chirurgic Intervention and Substance Application

Beside the models described above, rodents are not prone to VC, so several intervention procedures are necessary for induction of a certain degree of disease. In line with the calcification progression under uremic conditions in humans, rats and mice develop comparable vessel calcification upon

uremic conditions. For induction of chronic renal failure, several protocols exist, mainly by surgical reduction of kidney mass and ureter obstruction or dietary intake of nephrotoxic adenine diet. The most common surgical method is the 5/6 to 7/8 reduction of functional kidney mass in rats and mice [71,72]. Various techniques and procedures have been used in the past: electrocautery or dissection of renal arteries combined with full nephrectomy on the contralateral side in a one-step or two-step surgical procedure [73]. The major limitations of these models are the high effort required for the surgical preparation, the surgery-dependent variation in the CKD (mild to severe) and post-operative complications. Furthermore, comparable vessel calcification occurs after an extended observation period [73].

A dietary component that causes kidney failure is a high dietary intake of adenine [74]. The precipitation of adenine causes nephrotoxicity along the renal tubules and urinary tract [74], which induces severe kidney damage representative of uremic features of the human condition [40,74,75]. The disease progression is associated with moderate to severe aortic calcification localized primarily in the media of the vessel wall [40,75–83]. In contrast to the high effort required for the surgically-induced CKD rodent models, the experimental process of generating adenine-induced CKD is relatively easy. However, a limitation of the older treatment protocols is weight loss and the high biological variability in calcification progression. Furthermore, the original model with a 0.75% adenine diet has many confounding factors in researching VC e.g., high blood pressure, lipid disorder, rapid malnutrition and high fatality at 4–6 weeks [84]. Therefore, the administration protocols in various VC studies with rats have been optimized for adenine content, dietary supplements (vitamins, grain/casein), time course of treatment (2–12 weeks) and intervals of standard chow to control food intake and weight loss. Shobeiri et al. reduced the adenine content to 0.25% and characterized the calcification of different vascular beds after 5 to 11 weeks of treatment [76]. In this dosing protocol, extreme weight loss was not an issue (9%–12% reduction of the initial weight) [76]. Furthermore, a progression of increased calcification of various vessel types was found [76]. The adenine-dosing schemes vary between different treatment protocols. Some provided the same adenine content throughout the whole course of the experiment [40,76,85], whereas others changed the adenine content e.g., by dose reduction from 0.75% to 0.5% adenine after one week [86] or an interval period with standard chow [77,81,86]. Between those models, blood parameters such as blood urea nitrogen (BUN), calcium and PTH seem to be comparable. However, weight loss of the animals varies between the studies. Interestingly, the severity of the vascular medial calcification is exceptionally variable. One study found moderate to severe mineralization in different vascular beds of Wistar rats upon feeding a chow with a constant 0.25% adenine content for 5 to 11 weeks [76]. In contrast, no VC was found in Wistar rats using a dose-reduction adenine regime (0.75% adenine diet for 2 weeks, followed by 2 weeks of 0.5% adenine chow and subsequent standard chow for 5 weeks) [86]. Inferentially, the extent of VC depends on the duration and dose of adenine administration. Until recently, the adenine-feeding model has only been used in mineralization studies with rats, because a high adenine content in mice causes acute kidney failure with a mortality rate of nearly 100% within 6 days [87]. Recently, Santana et al. characterized a mouse model for CKD using a 0.2% adenine diet for up to 6 weeks [85].

To answer the question if potential differences in CKD conditions using surgical or adenine-diet protocols exists, one laboratory compared the 5/6 nephrectomy rat model with the adenine-diet-induced CKD, while animal and housing conditions were consistent. The authors observed no differences in the blood parameters including serum phosphate, calcium, PTH and fibroblast growth factor 23 (FGF23). However, the adenine-fed rats had a higher rate of bone turnover [86].

In addition to kidney failure, diabetes mellitus is also associated with VC. To study diabetic artery calcification, a model with rats combining streptozotocin-induced diabetes (SD) with high-fat diet and vitamin D3 treatment was established [88].

Additionally to disease induction in rodents, special dietary supplements are necessary to enhance the effects. For example, the SD rat strain was resistant to VC when fed a diet without increased phosphorus content [89]. Other authors have used various phosphorus concentrations (0.6% to 1.8%)

combined with dietary calcium contents ranging from 0.6% to 4% as well as supplementation with various amounts of vitamin D [86,89–103]. The extent of arterial mineralization depends on duration of treatment and the diet used. Depending on the genetic background of the animal, the dietary regime and degree of kidney damage, the severity and location of VC varies. Most of the studies involved increased dietary calcium and phosphorus content. Moreover, supplementation with dietary vitamin D [104–107] and cholesterol [105] has been found to enhance arterial VC in various rodent studies. However, vitamin D administration influences physical impairment and promotes weight loss [105,107]. The cholesterol-enriched diet was primarily used in models studying intimal calcification. Furthermore, nicotine [88,108–110] has been administrated to animals to induce or promote mineralization of the vessel wall.

In addition to the diet-induced effects on VC, a recent study in uremic rats investigated the influence of electromagnetic fields on promoting VC [111]. However, no effects of electromagnetic fields were found in rats without kidney damage [111].

4.3. Genetically Modified Mouse Models

In genetically modified mouse models, atherosclerotic plaque formation and calcification can be reinforced by manipulation of cholesterol metabolism. Calcification of the media can be amplified by interruption of vascular protective mechanisms, which physiologically inhibit calcification or increase serum phosphate concentration by uncoupling of physiological phosphate metabolism.

4.3.1. Phosphate Metabolism

Elevated phosphate can be a consequence of increased phosphate absorption, decreased phosphate excretion or a shift from intracellular to extracellular phosphate. Hormonal regulation of phosphate involves the intestine, kidneys and bones and several signaling pathways, including, but not limited to, vitamin D, FGF23 and α-Klotho. Disturbance in vitamin D and calcium–phosphate metabolism was shown to play a role in the progression of ectopic mineralization [112,113]. Reduction in active vitamin D, by either vitamin D deficient diet, disruption of the vitamin D receptor, or its gene reduced ectopic calcification. However, these interventions likewise reduce phosphate blood concentration, whereas phosphate reduction, even when increasing active vitamin D and calcium concentration, is effective in reducing VC [112,114–121]. Therefore, the following models are summarized as altered phosphate metabolism (Figure 1).

FGF23: Hyperphosphatemia often succeeds CKD, hypoparathyreoidism and vitamin D intoxication, but can also result from rare genetic disorders like hyperphosphatemic tumoral familial calcinosis (hFTC). In hFTC, the FGF23 receptor cannot be activated due to a mutation of either the FGF23, the α-Klotho or the GalNAc transferase 3 (GALNT3) gene [122]. FGF23 is an essential regulator of phosphate homeostasis and vitamin D metabolism promoting phosphaturia. FGF23 decreases the surface expression of sodium-dependent phosphate co-transporters type IIa (NPT2a) and IIc (NPT2c) in the proximal renal tubules. Furthermore, it reduces vitamin D availability by downregulation of the expression of the Cyp27b1 gene, encoding 1α-hydroxylase, an enzyme required for active vitamin D synthesis. Furthermore, the expression of the Cyp24a1 gene is upregulated, which encodes vitamin D degrading 24α-hydrolase [120,123–126]. Thus, FGF23 suppresses synthesis and promotes degradation of vitamin D. Mice lacking FGF23 exhibit increased plasma levels of phosphate and calcium [115,127] as well as VC [115,117]. Interestingly, whereas a phosphate-deficient diet prevented vessel calcification in the $FGF23^{-/-}$ mice, a vitamin D deficient diet did not indicate a significant role for hyperphosphatemia in that calcification model [115]. In addition, the mice lacking FGF23 exhibit a premature aging process similar to $Klotho^{-/-}$ [117]. The aging process seems to be partly exerted through effects on vitamin D metabolism because a genetic ablation of the 1α-hydroxylase reduced the aging phenotype in the $FGF23^{-/-}$ mice [117]. O-glycosylation of FGF23 through Galnt3 reduces the susceptibility of FGF23 to proteolysis and therefore permits the secretion of intact FGF23 [128].

Galnt3: Patients with mutations in Galnt3 suffer from hyperphosphatemia and extensive calcium depositions [129]. Results from mice models are contradicting: Galnt3$^{-/-}$ mice have hyperphosphatemia and increased FGF23 expression, although secretion of intact FGF23 is impaired, but show no sign of abnormal calcification [128]. In contrast, Tcal/Tcal mice, which feature a missense mutation in the Galnt3 gene, feature hyperphosphatemia and extensive ectopic calcification [130]. In Galnt3$^{-/-}$ mice, breeding with FGF23 transgenic mice can increase the amount of intact FGF23 and reduce hyperphosphatemia [131].

Mechanistic Overview	Model	Source
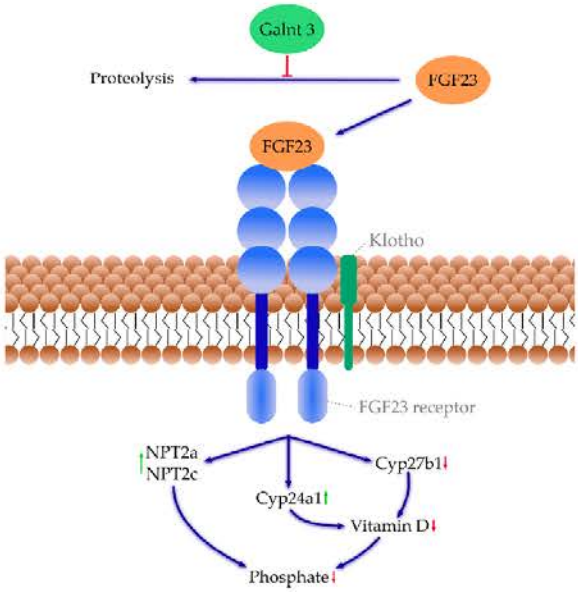	FGF23$^{-/-}$	[117,127]
	Klotho$^{-/-}$	[132,133]
	Galnt$^{-/-}$	[128]
	Tcal/Tcal	[130]

Figure 1. Selected mice models of altered phosphate metabolism and their mechanisms. Green arrows: activation, red arrows: down regulation, blue arrows: pathway. References: [117,127,128,130,132,133]. Cyp24a1: 24-hydroxyvitamin D-1α-hydroxylase; Cyp27b1: 25-hydroxyvitamin D-1α-hydroxylase; FGF23: fibroblast growth factor 23; Galnt3: N-acetylgalactosaminyltransferase 3; NPT2a: renal sodium-dependent phosphate co-transporter type IIa; NPT2c: renal sodium-dependent phosphate co-transporter type IIc.

Klotho: Klotho is a necessary co-factor required for FGF23 binding to its receptor. Because most tissues and cells express FGF receptors, the target organs of endocrine FGF are determined by tissue-specific expression of Klotho [134]. Klotho deficiency results in high FGF23 levels [112,135]. Similarly to the FGF23$^{-/-}$ mice, mice deficient in the Klotho gene show ectopic soft-tissue and vessel mineralization and premature aging [132]. In Klotho/1α-hydroxylase double knockout mice, VC and soft tissue calcification were eliminated [118]. In the absence of membrane-bound Klotho, delivery of circulating soluble Klotho reduced serum phosphate levels and aorta mineral content in alpha Klotho null mice [133].

4.3.2. Absence or Dysfuntion of Calcification Inhibitor Proteins

Mineralization is a tightly controlled process and several mechanisms serve as inhibitors of ectopic mineralization (Figure 2). Body fluids tend for mineralization as they are supersaturated in phosphate and calcium. Several endogenous circulating calcification inhibitors help to prevent pathophysiological mineralization. In addition, promotors and inhibitors of calcification could also

serve as biomarkers for onset and progression of VC [136]. Mouse models with disrupted protective mechanisms partially feature extensive ectopic calcification. Circulating inhibitors prevent calcification by different mechanisms and include MGP, Fetuin-A, osteoprotegerin (OPG), osteopontin (OPN) and PPi, which as a non-peptide inhibitor of VC is considered later. The consensus statement of Bäck et al. [137] offers an excellent overview of the endogenous calcification inhibitors and their therapeutic potential.

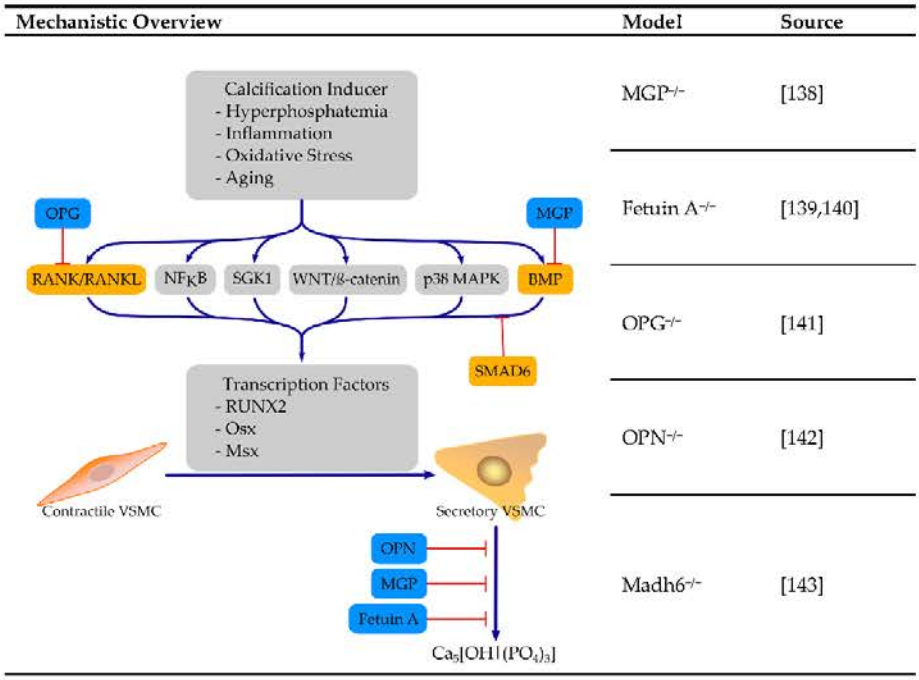

Figure 2. Selected mice models with absent or dysfunctional calcification inhibiting peptides and their mechanisms. Red T-arrows: inhibition, blue arrows: pathway. References: [138–143]. MGP: matrix-gla protein; OPG: osteoprotegerin; OPN: osteopontin; Madh6: gene coding for smad family member 6.

MGP: In mice, deletion of the MGP gene is lethal, due to extensive VC [138]. Death occurs within two months of age because of thoracic or abdominal aortic rupture [138]. In these mice, VSMC undergo chondrocyte differentiation and form cartilage in blood vessels [144]. The arterial phenotype of MGP-deficient mice can be restored in a transgenic animal, where MGP is reintroduced in VSMC [145]. The molecular mechanisms by which MGP prevents ectopic calcification include prevention of mineralization by binding of calcium ions as well as inhibition of the pro-osteogenic effects of BMP2 (reviewed in detail by Proudfoot and Shanahan [146]). MGP requires vitamin K dependent γ-carboxylation to exert its calcification inhibitory functions. Therefore, models of vitamin K inhibition e.g., by application of warfarin, exhibit similar calcification of the arteries [147].

Fetuin A: Fetuin A, also known as α_2-Heremans-Schmidt glycoprotein (ahsg), inhibits ectopic mineralization through the formation of fetuin-mineral complexes, which are also termed calciprotein particles [148,149]. Mice on a C57BL/6-129sv background deficient for fetuin show no general ectopic calcification, although serum inhibition of apatite formation is diminished and some homozygous animals develop soft tissue calcification after breeding [139]. Feeding these animals with a chow rich in minerals and vitamin D resulted in an increase in calcification and backcrossing these mice to the more calcification-prone DBA/2 background resulted in severe systematic calcification [140].

OPG: OPG is a soluble decoy receptor for the receptor-activated nuclear factor κB ligand (RANKL), also known as tumor necrosis factor receptor superfamily member 11B (TNFRSF11B). As one of its

mechanisms, it prevents interaction of RANKL and RANK, thus inhibiting downstream signaling such as osteoclastic cell differentiation, survival and function [150]. Mice deficient for OPG exhibit calcification of the aortic media and renal arteries [141]. When mice deficient for OPG were treated with injected recombinant OPG, the incidence of aortic calcification was not reduced, whereas transgene animals showed no calcification of major arteries [151].

OPN: OPN, also known as secreted phosphoprotein 1 (SPP1), is a multifunctional protein that also serves as a mineralization inhibitor and is found in abundance at sites of mineral calcification, but the precise mechanisms of action remain unclear to date [152]. Deficiency in OPN alone is not sufficient to induce spontaneous VC, but the deficiency in OPN combined with other inducers of VC e.g., deficiency in MGP, reinforces mineralization [142].

SMAD6: Smad6 is an inhibitor of tumor growth factor β (TGFβ) signaling and a negative regulator in BMP signaling [153,154]. Targeted deletion of Madh6, the gene that encodes Smad6, results in a mice model that experiences cardiovascular mortality, including aortic ossification, which is restricted to areas with VSMC and increases lethality [143].

Taken together, these mice models exhibit particular conditions for calcification. They have been very critical in the identification of pathophysiological mechanisms resulting in ectopic calcification and have helped to move the perspective of VC as a tightly controlled active process.

4.3.3. Pyrophosphate System

PPi is a crucial circulating inhibitor of VC preventing calcium apatite precipitation [155]. Serum PPi can have several sources (Figure 3).

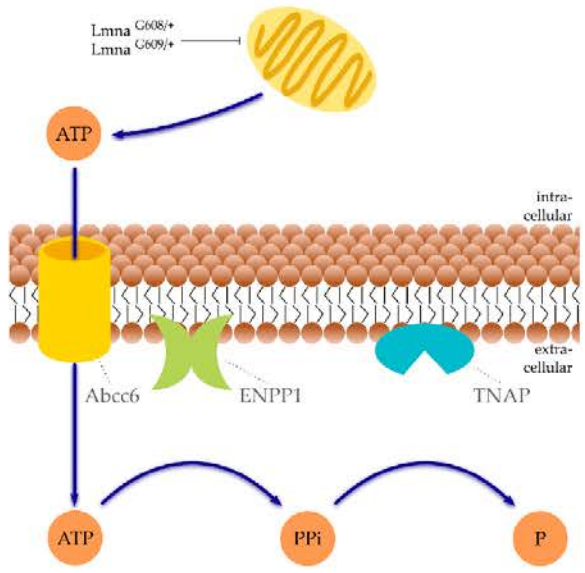

Mechanistic Overview	Model	Source
	ENPP$^{-/-}$	[156]
	ENPP$^{ttw/ttw}$	[157]
	ENPP1^{asj}	[158]
	Abcc$^{-/-}$	[159]
	Lmna$^{G608G/+}$	[160]
	Lmna$^{G609G/+}$	[161]

Figure 3. Selected mice models of reduced serum pyrophosphate concentration and their mechanisms. Blue arrows: pathway. References: [156–161]. Abcc: adenosinte tetraphosphate-binding cassette subfamily C; ATP: adenosine tetraphosphate; ENPP1: ectonucleotide pyrophosphatase phosphodiesterase; Lmna: lamin A/C gene; P: phosphate; PPi: inorganic pyrophosphate; TNAP: tissue-nonspecific alkaline phosphatase.

The hydrolysis of ATP by ectonucleotide pyrophosphatase phosphodiesterase (ENPP1) forms the majority of PPi [14]. A significant part of ATP is provided by the release from hepatocytes via ATP binding cassette subfamily C member 6 (Abbc6) [162]. Next to that, PPi can be directly transported from the intracellular to the extracellular environment via ANK [163]. The major sources for ATP are the mitochondria. Therefore, mitochondrial dysfunction can reduce the available amount of ATP, as, for example, in the rare genetic human disorder Hutchinson–Gilford progeria syndrome. A number of other orphan diseases in humans feature reduced circulating PPi levels, resulting in ectopic calcification, including generalized arterial calcification of infancy and pseudoxanthoma elasticum.

ENPP1: The enzyme ENPP1 generates extracellular PPi from ATP. Mice lacking ENPP1 are prone to the development of VC. Different mice models for ENPP1 deficiency currently exist, including the genetically engineered ENPP1$^{-/-}$ mice, the tip-toe walking mice (ENPP$^{ttw/ttw}$) and the mutant ENPP1^{asj} mice [156–158]. All three mice models suffer from VC of the aorta. From these models, ENPP$^{-/-}$ mice are best studied. In ENPP1$^{-/-}$ mice, aortic calcification was developed within 2 months of age. Calcification is accelerated by phosphate diet [14]. However, under the same chow, aortas transplanted from ENPP1$^{-/-}$ mice into WT mice did not calcify, which indicates that the systemic availability of sufficient amounts of PPi is sufficient to prevent calcification [14]. On a high phosphate diet, ENPP$^{ttw/ttw}$ mice exhibit ectopic aortic calcification associated with increased aortic Runx2 expression [157]. ENPP^{asj} mice also demonstrate an early onset of extensive arterial calcification upon being fed a high phosphate diet [158].

Abcc6: In Abcc6$^{-/-}$ mice, arterial calcium accumulates at the age of 16 months and was around 2-fold higher than in wild type mice [159]. Administration of PPi and etidronate inhibited calcification, but was unable to reverse already existing calcification [164]. Similar results were found in a study where early intravenous administration of a wild type human Abcc6 expressing adenovirus into Abcc6$^{-/-}$ mouse reduced mineral deposition, but late administration failed to reduce mineralization [165].

Lamin A/C (LMNA): Mutations in the LMNA gene result in the synthesis of progerin, a splicing isoform of the precursor protein prelamin A [166]. Alternatively, a mutation in ZMPSTE24 (farnesylated protein-converting enzyme 1) can result in an abnormal accumulation of prelamin A [166]. In G608G transgenic mice (Lmna$^{G608G/+}$), pathological changes in the media layer of large vessels e.g., VSMC loss and calcification [160] have been reported. In heterozygous Lmna$^{G609G/+}$ mice, increased medial calcification of the aortic arch and thoracic aorta, as well as reduced PPi levels, were found, resulting from impaired mitochondrial ATP synthesis [161].

4.3.4. Lipoprotein System

Hyperlipidemia in one of the main triggering factors in the pathophysiology of human atherosclerosis. In mice, the lipoprotein profile significantly differs from humans [167,168]. Mice are lacking the cholesteryl ester transfer protein, an enzyme that transfers cholesterol from high-density lipoprotein (HDL) to apolipoprotein B-containing lipoproteins as low-density lipoprotein (LDL) and very low-density particles (VLDL) [169]. In addition, mice also have bile acid compositions that differ from humans [168,170], affecting the enterohepatic cycle of cholesterol [170]. Several models for the disruption of lipid metabolism exist e.g., including LDL receptor (LDLR)$^{-/-}$, apolipoprotein E (ApoE)$^{-/-}$, LDLR and ApoE double knockout, ApoE3 Leiden transgenic mice and proprotein convertase subtilisin/kexin type 9 (PCSK9) gain of function models (Figure 4). Additional existing models are reviewed in detail elsewhere [167].

LDLR and PCSK9: LDLR dysfunction results in the accumulation of LDL in patients with familial hypercholesterolemia. Mice homozygous for LDLR deficiency have a delayed clearance of VLDL and LDL from plasma and calcifications of the aorta [171,172]. Overexpression of PCSK9 results in an increased degradation of LDLR [173]. When mice are injected a gain of function PCSK9 adeno-associated virus vector (AAV), they develop increased cholesterol levels, atherosclerotic lesions and aortic calcification [174].

ApoE: Clearance of remnants of chylomicrons and VLDL require ApoE as a receptor ligand. Knockout of ApoE results in atherogenic accumulation of cholesterol-rich remnants [175] and development of calcification of advanced lesions [176]. ApoE and LDLR double knockout mice developed calcifications along the aortic arch [177]. Inducing uremia by partial kidney ablation in ApoE$^{-/-}$ mice resulted in an acceleration of arterial calcification [178]. A mutation in the ApoE gene can result in a defective protein, which has reduced capacity for remnant clearance [179]. In transgenic Apo3 Leiden mice, a high fat/cholesterol diet induces hyperlipidemia and calcification of aortic lesions [179,180].

Mechanistic Overview	Model	Source
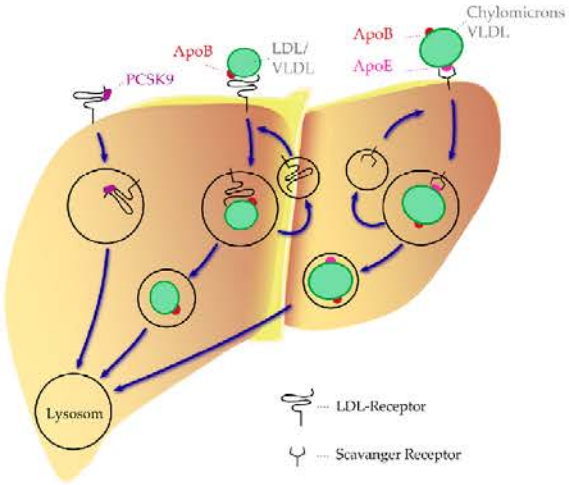	ApoE$^{-/-}$	[175,176]
	LDLR$^{-/-}$	[171,172]
	Apo$^{-/-}$/LDLR$^{-/-}$	[177]
	Apo3 Leiden	[179,180]
	PCSK9-AAV	[174]

Figure 4. Mice models of atherosclerotic hyperlipidemia and their mechanisms. Blue arrows: pathway. References: [171,172,174–177,179,180]. AAV: adeno-associated virus vector; Apo: Apolipoprotein; LDL: low-density lipoprotein; PCSK9: pro-protein convertase subtilisin/kexin type 9; VLDL: very low-density lipoprotein.

4.4. Limitation of In Vivo Models

The optimal choice of the animal model depends on the target to be assessed. A general limitation is that mice and rats are less prone to calcification than humans. In addition, a timespan of decades in humans where the disease progression occurs has to be limited for a study period of several weeks in animal models. Therefore, hard stimuli for induction might hamper the comparability to the human situation. However, animal models allow the study of signaling pathways under controllable conditions.

5. Conclusions

The variety of influencing factors and different components in the development of VC reflect, at least in part, the variety of research models and vice versa. Therefore, studying VC entails the challenge of utilizing a manageable experimental setting depicting the complexity of its pathophysiologic interrelations. In vitro models employ a variety of vascular cells and inducers of calcification for studying pathways and screening inhibitors and inducers; however, they provide a non-physiological

environment. Ex vivo settings using vessel tissue meet this drawback at least partly and might bridge the gap to in vivo models. Animal models with rodents involve the induction of VC by establishing uremic conditions, genetically modified calcium–phosphate and lipid metabolism as well as impairment of calcification inhibitors. While offering a natural environment, immense interventions are needed to achieve the VC condition. The current data show that VSMC appear to be a central cell type within the mineralization process in the media of the vessel wall. Further research is required to understand the detailed mechanisms, contributors and inhibitors in the process of VC and to establish working treatment options to reduce and/or inhibit calcification and stiffening of the vessel wall leading to increased mortality. An ongoing effort should be taken to improve the experimental models studying VC by improving the identification and diagnostic tools for quantification of VC to achieve maximized comparability of the results. This might not only help to reduce animal numbers for primary cell isolation and in vivo settings in case of the 3R (Replacement, Reduction and Refinement) thought of Russel and Burch [181], but also identify the most promising therapeutic strategies to reduce the cardiovascular morbidity and mortality of the patients.

Author Contributions: Conceptualization and figure/table preparation, M.S. and J.H.; literature search, J.H., M.S., M.T., and M.B.; writing—original draft preparation, J.H., M.S., M.T., and M.B.; writing—review and editing, J.H., M.S., M.T., M.v.d.G.; funding acquisition, M.S. and M.T. All authors have read and agreed to the published version of the manuscript.

Funding: The experimental work in the laboratory of the authors was funded by a grant from the Berlin Institute of Health (to M.S.), a grant of Charité3R (to M.T. and M.S) and a grant by the Sonnenfeld Stiftung (to M.S. and M.T.). The authors acknowledge support from the German Research Foundation (DFG) and the Open Access Publication Fund of Charité – Universitätsmedizin Berlin.

Acknowledgments: The authors thank Manuel Herrmann-Fiechtner for his kind help in preparing the figures.

Conflicts of Interest: The authors declare no conflict of interest. The funders had no role in the design of and writing of the manuscript, or in the decision to publish it.

Abbreviations

AA	Ascorbic Acid
ahsg	α_2-Heremans-Schmidt Glycoprotein
AAV	Adeno-Associated Virus Vector
ALP	Alkaline Phosphatase
ApoE	Apolipoprotein E
Abcc6	ATP Binding Cassette Subfamily C Member 6
BUN	Blood Urea Nitrogen
BMP	Bone Morphogenic Protein
CKD	Chronic Kidney Disease
EC	Endothelial Cell
EndMT	Endothelial-to-Mesenchymal Transition
Enpp	Ectonucleotide Pyrophosphatase Phosphodiesterase
ECM	Extracellular Matrix
FBS	Fetal Bovine Serum
FGF23	Fibroblast Growth Factor 23
Galnt3	GalNAc trans-ferase 3
HDL	High Density Lipoprotein
hFTC	Hyperphosphatemic Tumoral Familial Calcinosis
Ppi	Inorganic Pyrophosphate
LDL	Low Density Lipoprotein
LDLR	Low Density Lipoprotein Receptor
LMNA	Gene encoding the Lamin A/C protein
MGP	Matrix Gla Protein
MMP	Matrix Metalloproteinases
Opn	Osteopontin

Opg	oPsteoprotegerin
PTH	Parathyroid Hormone
PCSK9	Proprotein Convertase Subtilisin/Kexin Type 9
ROS	Reactive Oxygen Species
RANK	Receptor Activated Nuclear Factor κB
RANKL	Receptor Activated Nuclear Factor κB Ligand
SPP1	Secreted Phosphoprotein 1
NPT2a	Sodium-Dependent Phosphate Co-Transporters Type IIa
NPT2c	Sodium-Dependent Phosphate Co-Transporters Type IIc
SD	Streptozotocin-induced Diabetes
TNFRSF11B	Tumor Necrosis Factor Receptor Superfamily Member 11B
VC	Vascular Calcification
VSMC	Vascular Smooth Muscle Cell
VLDL	Very Low Density Lipoprotein

References

1. Demer, L.L.; Watson, K.E.; Bostrom, K. Mechanism of calcification in atherosclerosis. *Trends Cardiovasc. Med.* **1994**, *4*, 45–49. [CrossRef]
2. Jiang, Z.M.; Wu, X.J.; Liu, Y.; Du, X.H.; Shen, S.J.; Xu, L.Y.; Sun, W.X. Changes of gene expression profiles across different phases of vascular calcification in rats. *Genet. Mol. Res. GMR* **2013**, *12*, 5945–5957. [CrossRef] [PubMed]
3. Moe, S.M.; Chen, N.X. Inflammation and vascular calcification. *Blood Purif.* **2005**, *23*, 64–71. [CrossRef] [PubMed]
4. Mody, N.; Parhami, F.; Sarafian, T.A.; Demer, L.L. Oxidative stress modulates osteoblastic differentiation of vascular and bone cells. *Free Radic. Biol. Med.* **2001**, *31*, 509–519. [CrossRef]
5. Byon, C.H.; Javed, A.; Dai, Q.; Kappes, J.C.; Clemens, T.L.; Darley-Usmar, V.M.; McDonald, J.M.; Chen, Y. Oxidative stress induces vascular calcification through modulation of the osteogenic transcription factor Runx2 by AKT signaling. *J. Biol. Chem.* **2008**, *283*, 15319–15327. [CrossRef]
6. Sanchis, P.; Ho, C.Y.; Liu, Y.; Beltran, L.E.; Ahmad, S.; Jacob, A.P.; Furmanik, M.; Laycock, J.; Long, D.A.; Shroff, R.; et al. Arterial "inflammaging" drives vascular calcification in children on dialysis. *Kidney Int.* **2019**, *95*, 958–972. [CrossRef]
7. Albiero, M.; Avogaro, A.; Fadini, G.P. Circulating cellular players in vascular calcification. *Curr. Pharm. Des.* **2014**, *20*, 5889–5896. [CrossRef]
8. Cianciolo, G.; Capelli, I.; Cappuccilli, M.; Schillaci, R.; Cozzolino, M.; La Manna, G. Calcifying circulating cells: An uncharted area in the setting of vascular calcification in CKD patients. *Clin. Kidney J.* **2016**, *9*, 280–286. [CrossRef]
9. Shanahan, C.M.; Crouthamel, M.H.; Kapustin, A.; Giachelli, C.M. Arterial calcification in chronic kidney disease: Key roles for calcium and phosphate. *Circ. Res.* **2011**, *109*, 697–711. [CrossRef]
10. Lu, K.C.; Wu, C.C.; Yen, J.F.; Liu, W.C. Vascular calcification and renal bone disorders. *Sci. World J.* **2014**, *2014*, 637065. [CrossRef]
11. Lehto, S.; Niskanen, L.; Suhonen, M.; Ronnemaa, T.; Laakso, M. Medial artery calcification. A neglected harbinger of cardiovascular complications in non-insulin-dependent diabetes mellitus. *Arterioscler. Thromb. Vasc. Biol.* **1996**, *16*, 978–983. [CrossRef] [PubMed]
12. Niskanen, L.; Siitonen, O.; Suhonen, M.; Uusitupa, M.I. Medial artery calcification predicts cardiovascular mortality in patients with NIDDM. *Diabetes Care* **1994**, *17*, 1252–1256. [CrossRef] [PubMed]
13. Moe, S.M.; Neal, C.X.; O'Neill, K.D.; Brown, K.; Westenfeld, R.; Jahnen-Dechent, W.; Ketteler, M. Fetuin-A and matrix gla protein (MGP) are important inhibitors of vascular calcification in CKD. *J. Am. Soc. Nephrol.* **2003**, *14*, 692A.
14. Lomashvili, K.A.; Narisawa, S.; Millan, J.L.; O'Neill, W.C. Vascular calcification is dependent on plasma levels of pyrophosphate. *Kidney Int.* **2014**, *85*, 1351–1356. [CrossRef] [PubMed]
15. Proudfoot, D.; Skepper, J.N.; Hegyi, L.; Farzaneh-Far, A.; Shanahan, C.M.; Weissberg, P.L. The role of apoptosis in the initiation of vascular calcification. *Z. Fur Kardiol.* **2001**, *90* (Suppl. 3), 43–46. [CrossRef]

16. Proudfoot, D.; Skepper, J.N.; Hegyi, L.; Bennett, M.R.; Shanahan, C.M.; Weissberg, P.L. Apoptosis regulates human vascular calcification in vitro: Evidence for initiation of vascular calcification by apoptotic bodies. *Circ. Res.* **2000**, *87*, 1055–1062. [CrossRef]
17. New, S.E.; Aikawa, E. Role of extracellular vesicles in de novo mineralization: An additional novel mechanism of cardiovascular calcification. *Arterioscler. Thromb. Vasc. Biol.* **2013**, *33*, 1753–1758. [CrossRef]
18. Lei, Y.; Sinha, A.; Nosoudi, N.; Grover, A.; Vyavahare, N. Hydroxyapatite and calcified elastin induce osteoblast-like differentiation in rat aortic smooth muscle cells. *Exp. Cell Res.* **2014**, *323*, 198–208. [CrossRef]
19. Tolle, M.; Reshetnik, A.; Schuchardt, M.; Hohne, M.; van der Giet, M. Arteriosclerosis and vascular calcification: Causes, clinical assessment and therapy. *Eur. J. Clin. Investig.* **2015**, *45*, 976–985. [CrossRef]
20. Li, Q.; Sundberg, J.P.; Levine, M.A.; Terry, S.F.; Uitto, J. The effects of bisphosphonates on ectopic soft tissue mineralization caused by mutations in the ABCC6 gene. *Cell Cycle* **2015**, *14*, 1082–1089. [CrossRef]
21. Shioi, A.; Nishizawa, Y.; Jono, S.; Koyama, H.; Hosoi, M.; Morii, H. Beta-glycerophosphate accelerates calcification in cultured bovine vascular smooth muscle cells. *Arterioscler. Thromb. Vasc. Biol.* **1995**, *15*, 2003–2009. [CrossRef]
22. Alesutan, I.; Musculus, K.; Castor, T.; Alzoubi, K.; Voelkl, J.; Lang, F. Inhibition of Phosphate-Induced Vascular Smooth Muscle Cell Osteo-/Chondrogenic Signaling and Calcification by Bafilomycin A1 and Methylamine. *Kidney Blood Press. Res.* **2015**, *40*, 490–499. [CrossRef] [PubMed]
23. Luong, T.T.D.; Estepa, M.; Boehme, B.; Pieske, B.; Lang, F.; Eckardt, K.U.; Voelkl, J.; Alesutan, I. Inhibition of vascular smooth muscle cell calcification by vasorin through interference with TGFbeta1 signaling. *Cell. Signal.* **2019**, *64*, 109414. [CrossRef] [PubMed]
24. Schuchardt, M.; Tolle, M.; Prufer, J.; Prufer, N.; Huang, T.; Jankowski, V.; Jankowski, J.; Zidek, W.; van der Giet, M. Uridine adenosine tetraphosphate activation of the purinergic receptor P2Y enhances in vitro vascular calcification. *Kidney Int.* **2012**, *81*, 256–265. [CrossRef] [PubMed]
25. Prufer, J.; Schuchardt, M.; Tolle, M.; Prufer, N.; Hohne, M.; Zidek, W.; van der Giet, M. Harmful effects of the azathioprine metabolite 6-mercaptopurine in vascular cells: Induction of mineralization. *PLoS ONE* **2014**, *9*, e101709. [CrossRef]
26. Mackenzie, N.C.; Zhu, D.; Longley, L.; Patterson, C.S.; Kommareddy, S.; MacRae, V.E. MOVAS-1 cell line: A new in vitro model of vascular calcification. *Int. J. Mol. Med.* **2011**, *27*, 663–668.
27. Frauscher, B.; Kirsch, A.H.; Schabhuttl, C.; Schweighofer, K.; Ketszeri, M.; Pollheimer, M.; Dragun, D.; Schroder, K.; Rosenkranz, A.R.; Eller, K.; et al. Autophagy Protects from Uremic Vascular Media Calcification. *Front Immunol* **2018**, *9*, 1866. [CrossRef]
28. Skafi, N.; Abdallah, D.; Soulage, C.; Reibel, S.; Vitale, N.; Hamade, E.; Faour, W.; Magne, D.; Badran, B.; Hussein, N.; et al. Phospholipase D: A new mediator during high phosphate-induced vascular calcification associated with chronic kidney disease. *J. Cell. Physiol.* **2019**, *234*, 4825–4839. [CrossRef]
29. Firulli, A.B.; Han, D.; Kelly-Roloff, L.; Koteliansky, V.E.; Schwartz, S.M.; Olson, E.N.; Miano, J.M. A comparative molecular analysis of four rat smooth muscle cell lines. In *In Vitro Cellular & Developmental Biology-Animal*; Springer: Berlin/Heidelberg, Germany, 1998; Volume 34, pp. 217–226.
30. Sutra, T.; Morena, M.; Bargnoux, A.S.; Caporiccio, B.; Canaud, B.; Cristol, J.P. Superoxide production: A procalcifying cell signalling event in osteoblastic differentiation of vascular smooth muscle cells exposed to calcification media. *Free Radic. Res.* **2008**, *42*, 789–797. [CrossRef]
31. Rao, R.S.; Miano, J.M.; Olson, E.N.; Seidel, C.L. The A10 cell line: A model for neonatal, neointimal, or differentiated vascular smooth muscle cells? *Cardiovasc. Res.* **1997**, *36*, 118–126. [CrossRef]
32. Beazley, K.E.; Deasey, S.; Lima, F.; Nurminskaya, M.V. Transglutaminase 2-mediated activation of beta-catenin signaling has a critical role in warfarin-induced vascular calcification. *Arterioscler. Thromb. Vasc. Biol.* **2012**, *32*, 123–130. [CrossRef] [PubMed]
33. Schor, A.M.; Allen, T.D.; Canfield, A.E.; Sloan, P.; Schor, S.L. Pericytes derived from the retinal microvasculature undergo calcification in vitro. *J. Cell Sci.* **1990**, *97 Pt 3*, 449–461. [PubMed]
34. Wu, M.; Zhang, J.D.; Tang, R.N.; Crowley, S.D.; Liu, H.; Lv, L.L.; Ma, K.L.; Liu, B.C. Elevated PTH induces endothelial-to-chondrogenic transition in aortic endothelial cells. *Am. J. Physiol. Ren. Physiol.* **2017**, *312*, F436–F444. [CrossRef] [PubMed]
35. Eghbali-Fatourechi, G.Z.; Lamsam, J.; Fraser, D.; Nagel, D.; Riggs, B.L.; Khosla, S. Circulating osteoblast-lineage cells in humans. *N. Engl. J. Med.* **2005**, *352*, 1959–1966. [CrossRef] [PubMed]

36. Otsuru, S.; Tamai, K.; Yamazaki, T.; Yoshikawa, H.; Kaneda, Y. Bone marrow-derived osteoblast progenitor cells in circulating blood contribute to ectopic bone formation in mice. *Biochem. Biophys. Res. Commun.* **2007**, *354*, 453–458. [CrossRef]
37. Gossl, M.; Modder, U.I.; Atkinson, E.J.; Lerman, A.; Khosla, S. Osteocalcin expression by circulating endothelial progenitor cells in patients with coronary atherosclerosis. *J. Am. Coll. Cardiol.* **2008**, *52*, 1314–1325. [CrossRef]
38. Chen, J.L.; Hunt, P.; McElvain, M.; Black, T.; Kaufman, S.; Choi, E.S. Osteoblast precursor cells are found in CD34+ cells from human bone marrow. *Stem Cells* **1997**, *15*, 368–377. [CrossRef]
39. Fadini, G.P.; Albiero, M.; Menegazzo, L.; Boscaro, E.; Vigili de Kreutzenberg, S.; Agostini, C.; Cabrelle, A.; Binotto, G.; Rattazzi, M.; Bertacco, E.; et al. Widespread increase in myeloid calcifying cells contributes to ectopic vascular calcification in type 2 diabetes. *Circ. Res.* **2011**, *108*, 1112–1121. [CrossRef]
40. Yip, C.Y.; Chen, J.H.; Zhao, R.; Simmons, C.A. Calcification by valve interstitial cells is regulated by the stiffness of the extracellular matrix. *Arterioscler. Thromb. Vasc. Biol.* **2009**, *29*, 936–942. [CrossRef]
41. Voelkl, J.; Lang, F.; Eckardt, K.U.; Amann, K.; Kuro, O.M.; Pasch, A.; Pieske, B.; Alesutan, I. Signaling pathways involved in vascular smooth muscle cell calcification during hyperphosphatemia. *Cell. Mol. Life Sci. CMLS* **2019**, *76*, 2077–2091. [CrossRef]
42. Henze, L.A.; Luong, T.T.D.; Boehme, B.; Masyout, J.; Schneider, M.P.; Brachs, S.; Lang, F.; Pieske, B.; Pasch, A.; Eckardt, K.U.; et al. Impact of C-reactive protein on osteo-/chondrogenic transdifferentiation and calcification of vascular smooth muscle cells. *Aging* **2019**, *11*, 5445–5462. [CrossRef] [PubMed]
43. Li, N.; Cheng, W.; Huang, T.; Yuan, J.; Wang, X.; Song, M. Vascular Adventitia Calcification and Its Underlying Mechanism. *PLoS ONE* **2015**, *10*, e0132506. [CrossRef] [PubMed]
44. Doherty, M.J.; Ashton, B.A.; Walsh, S.; Beresford, J.N.; Grant, M.E.; Canfield, A.E. Vascular pericytes express osteogenic potential in vitro and in vivo. *J. Bone Min. Res.* **1998**, *13*, 828–838. [CrossRef] [PubMed]
45. Canfield, A.E.; Doherty, M.J.; Wood, A.C.; Farrington, C.; Ashton, B.; Begum, N.; Harvey, B.; Poole, A.; Grant, M.E.; Boot-Handford, R.P. Role of pericytes in vascular calcification: A review. *Z. Fur Kardiol.* **2000**, *89* (Suppl 2), 20–27. [CrossRef]
46. Yao, Y.; Jumabay, M.; Ly, A.; Radparvar, M.; Cubberly, M.R.; Bostrom, K.I. A role for the endothelium in vascular calcification. *Circ. Res.* **2013**, *113*, 495–504. [CrossRef]
47. Sánchez-Duffhues, G.; García de Vinuesa, A.; ten Dijke, P. Endothelial-to-mesenchymal transition in cardiovascular diseases: Developmental signaling pathways gone awry. *Dev. Dyn.* **2018**, *247*, 492–508. [CrossRef]
48. Chen, P.Y.; Qin, L.; Baeyens, N.; Li, G.; Afolabi, T.; Budatha, M.; Tellides, G.; Schwartz, M.A.; Simons, M. Endothelial-to-mesenchymal transition drives atherosclerosis progression. *J. Clin. Investig.* **2015**, *125*, 4514–4528. [CrossRef]
49. Sánchez-Duffhues, G.; García de Vinuesa, A.; van de Pol, V.; Geerts, M.E.; de Vries, M.R.; Janson, S.G.; van Dam, H.; Lindeman, J.H.; Goumans, M.-J.; Ten Dijke, P. Inflammation induces endothelial-to-mesenchymal transition and promotes vascular calcification through downregulation of BMPR2. *J. Pathol.* **2019**, *247*, 333–346. [CrossRef]
50. Bogdanova, M.; Kostina, A.; Zihlavnikova Enayati, K.; Zabirnyk, A.; Malashicheva, A.; Stenslokken, K.O.; Sullivan, G.J.; Kaljusto, M.L.; Kvitting, J.P.; Kostareva, A.; et al. Inflammation and Mechanical Stress Stimulate Osteogenic Differentiation of Human Aortic Valve Interstitial Cells. *Front. Physiol.* **2018**, *9*, 1635. [CrossRef]
51. Liu, L.; Liu, Z.Z.; Chen, H.; Zhang, G.J.; Kong, Y.H.; Kang, X.X. Oxidized low-density lipoprotein and beta-glycerophosphate synergistically induce endothelial progenitor cell ossification. *Acta Pharmacol. Sin.* **2011**, *32*, 1491–1497. [CrossRef]
52. Jaiswal, N.; Haynesworth, S.E.; Caplan, A.I.; Bruder, S.P. Osteogenic differentiation of purified, culture-expanded human mesenchymal stem cells in vitro. *J. Cell. Biochem.* **1997**, *64*, 295–312. [CrossRef]
53. Kanemaru, K.; Seya, K.; Miki, I.; Motomura, S.; Furukawa, K. Calcification of aortic smooth muscle cells isolated from spontaneously hypertensive rats. *J. Pharmacol. Sci.* **2008**, *106*, 280–286. [CrossRef] [PubMed]
54. Franceschi, R.T. The role of ascorbic acid in mesenchymal differentiation. *Nutr. Rev.* **1992**, *50*, 65–70. [CrossRef] [PubMed]
55. Piersma, B.; Wouters, O.Y.; de Rond, S.; Boersema, M.; Gjaltema, R.A.F.; Bank, R.A. Ascorbic acid promotes a TGFβ1-induced myofibroblast phenotype switch. *Physiol. Rep.* **2017**, *5*, e13324. [CrossRef] [PubMed]

56. Ivanov, V.; Ivanova, S.; Roomi, M.W.; Kalinovsky, T.; Niedzwiecki, A.; Rath, M. Extracellular Matrix-Mediated Control of Aortic Smooth Muscle Cell Growth and Migration by a Combination of Ascorbic Acid, Lysine, Proline, and Catechins. *J. Cardiovasc. Pharmacol.* **2007**, *50*, 541–547. [CrossRef] [PubMed]
57. Qiao, H.; Bell, J.; Juliao, S.; Li, L.; May, J.M. Ascorbic acid uptake and regulation of type I collagen synthesis in cultured vascular smooth muscle cells. *J. Vasc. Res.* **2009**, *46*, 15–24. [CrossRef]
58. Roszkowska, M.; Strzelecka-Kiliszek, A.; Bessueille, L.; Buchet, R.; Magne, D.; Pikula, S. Collagen promotes matrix vesicle-mediated mineralization by vascular smooth muscle cells. *J. Inorg. Biochem.* **2018**, *186*, 1–9. [CrossRef]
59. Gayrard, N.; Muyor, K.; Notarnicola, C.; Duranton, F.; Jover, B.; Argilés, À. Optimisation of cell and ex vivo culture conditions to study vascular calcification. *PLoS ONE* **2020**, *15*, e0230201. [CrossRef]
60. Chen, N.X.; Duan, D.; O'Neill, K.D.; Moe, S.M. High glucose increases the expression of Cbfa1 and BMP-2 and enhances the calcification of vascular smooth muscle cells. *Nephrol. Dial. Transplant. Off. Publ. Eur. Dial. Transpl. Assoc.-Eur. Ren. Assoc.* **2006**, *21*, 3435–3442. [CrossRef]
61. Hjortnaes, J.; Goettsch, C.; Hutcheson, J.D.; Camci-Unal, G.; Lax, L.; Scherer, K.; Body, S.; Schoen, F.J.; Kluin, J.; Khademhosseini, A.; et al. Simulation of early calcific aortic valve disease in a 3D platform: A role for myofibroblast differentiation. *J. Mol. Cell. Cardiol.* **2016**, *94*, 13–20. [CrossRef]
62. Akiyoshi, T.; Ota, H.; Iijima, K.; Son, B.K.; Kahyo, T.; Setou, M.; Ogawa, S.; Ouchi, Y.; Akishita, M. A novel organ culture model of aorta for vascular calcification. *Atherosclerosis* **2016**, *244*, 51–58. [CrossRef] [PubMed]
63. Tuffaha, R.; Voelkl, J.; Pieske, B.; Lang, F.; Alesutan, I. Role of PKB/SGK-dependent phosphorylation of GSK-3alpha/beta in vascular calcification during cholecalciferol overload in mice. *Biochem. Biophys. Res. Commun.* **2018**, *503*, 2068–2074. [CrossRef] [PubMed]
64. Villa-Bellosta, R.; Hernandez-Martinez, E.; Merida-Herrero, E.; Gonzalez-Parra, E. Impact of acetate- or citrate-acidified bicarbonate dialysate on ex vivo aorta wall calcification. *Sci. Rep.* **2019**, *9*, 11374. [CrossRef] [PubMed]
65. Wang, P.; Quan, Z.; Luo, D.; Chen, W.; Peng, D. Spironolactone dosedependently alleviates the calcification of aortic rings cultured in hyperphosphatemic medium with or without hyperglycemia by suppressing phenotypic transition of VSMCs through downregulation of Pit1. *Mol. Med. Rep.* **2019**, *19*, 3622–3632. [PubMed]
66. Schuchardt, M.; Siegel, N.V.; Babic, M.; Reshetnik, A.; Lutzenberg, R.; Zidek, W.; van der Giet, M.; Tolle, M. A Novel Long-Term ex vivo Model for Studying Vascular Calcification Pathogenesis: The Rat Isolated-Perfused Aorta. *J. Vasc. Res.* **2020**, *57*, 46–52. [CrossRef] [PubMed]
67. Kaspareit-Rittinghausen, J.; Rapp, K.; Deerberg, F.; Wcislo, A.; Messow, C. Hereditary polycystic kidney disease associated with osteorenal syndrome in rats. *Vet. Pathol.* **1989**, *26*, 195–201. [CrossRef]
68. Moe, S.M.; Chen, N.X.; Seifert, M.F.; Sinders, R.M.; Duan, D.; Chen, X.; Liang, Y.; Radcliff, J.S.; White, K.E.; Gattone, V.H., 2nd. A rat model of chronic kidney disease-mineral bone disorder. *Kidney Int.* **2009**, *75*, 176–184. [CrossRef]
69. Ng, K.; Hildreth, C.M.; Phillips, J.K.; Avolio, A.P. Aortic stiffness is associated with vascular calcification and remodeling in a chronic kidney disease rat model. *Am. J. Physiol.-Renal Physiol.* **2011**, *300*, F1431–F1436. [CrossRef]
70. Rings, R.W.; Wagner, J.E. Incidence of cardiac and other soft tissue mineralized lesions in DBA-2 mice. *Lab. Anim. Sci.* **1972**, *22*, 344–352.
71. Chauntin, A.; Ferris, E. Experimental renal insufficiency produced by partial nephrectomy. *Arch. Intern. Med.* **1932**, *49*, 767–787. [CrossRef]
72. Gagnon, R.F.; Duguid, W.P. A reproducible model for chronic renal failure in the mouse. *Urol. Res.* **1983**, *11*, 11–14. [CrossRef] [PubMed]
73. Shobeiri, N.; Adams, M.A.; Holden, R.M. Vascular calcification in animal models of CKD: A review. *Am. J. Nephrol.* **2010**, *31*, 471–481. [CrossRef] [PubMed]
74. Yokozawa, T.; Oura, H.; Okada, T. Metabolic effects of dietary purine in rats. *J. Nutr. Sci. Vitaminol.* **1982**, *28*, 519–526. [CrossRef] [PubMed]
75. Matsui, I.; Hamano, T.; Mikami, S.; Fujii, N.; Takabatake, Y.; Nagasawa, Y.; Kawada, N.; Ito, T.; Rakugi, H.; Imai, E.; et al. Fully phosphorylated fetuin-A forms a mineral complex in the serum of rats with adenine-induced renal failure. *Kidney Int.* **2009**, *75*, 915–928. [CrossRef]

76. Shobeiri, N.; Pang, J.; Adams, M.A.; Holden, R.M. Cardiovascular disease in an adenine-induced model of chronic kidney disease: The temporal link between vascular calcification and haemodynamic consequences. *J. Hypertens.* **2013**, *31*, 160–168. [CrossRef]
77. Katsumata, K.; Kusano, K.; Hirata, M.; Tsunemi, K.; Nagano, N.; Burke, S.K.; Fukushima, N. Sevelamer hydrochloride prevents ectopic calcification and renal osteodystrophy in chronic renal failure rats. *Kidney Int.* **2003**, *64*, 441–450. [CrossRef] [PubMed]
78. Price, P.A.; Roublick, A.M.; Williamson, M.K. Artery calcification in uremic rats is increased by a low protein diet and prevented by treatment with ibandronate. *Kidney Int.* **2006**, *70*, 1577–1583. [CrossRef] [PubMed]
79. Neven, E.; Dauwe, S.; De Broe, M.E.; D'Haese, P.C.; Persy, V. Endochondral bone formation is involved in media calcification in rats and in men. *Kidney Int.* **2007**, *72*, 574–581. [CrossRef] [PubMed]
80. Henley, C.; Davis, J.; Miller, G.; Shatzen, E.; Cattley, R.; Li, X.; Martin, D.; Yao, W.; Lane, N.; Shalhoub, V. The calcimimetic AMG 641 abrogates parathyroid hyperplasia, bone and vascular calcification abnormalities in uremic rats. *Eur. J. Pharmacol.* **2009**, *616*, 306–313. [CrossRef]
81. Neven, E.; Dams, G.; Postnov, A.; Chen, B.; De Clerck, N.; De Broe, M.E.; D'Haese, P.C.; Persy, V. Adequate phosphate binding with lanthanum carbonate attenuates arterial calcification in chronic renal failure rats. *Nephrol. Dial. Transplant. Off. Publ. Eur. Dial. Transpl. Assoc.-Eur. Ren. Assoc.* **2009**, *24*, 1790–1799. [CrossRef]
82. Lomashvili, K.A.; Monier-Faugere, M.C.; Wang, X.; Malluche, H.H.; O'Neill, W.C. Effect of bisphosphonates on vascular calcification and bone metabolism in experimental renal failure. *Kidney Int.* **2009**, *75*, 617–625. [CrossRef] [PubMed]
83. Persy, V.; Postnov, A.; Neven, E.; Dams, G.; De Broe, M.; D'Haese, P.; De Clerck, N. High-resolution X-ray microtomography is a sensitive method to detect vascular calcification in living rats with chronic renal failure. *Arterioscler. Thromb. Vasc. Biol.* **2006**, *26*, 2110–2116. [CrossRef] [PubMed]
84. Tamagaki, K.; Yuan, Q.; Ohkawa, H.; Imazeki, I.; Moriguchi, Y.; Imai, N.; Sasaki, S.; Takeda, K.; Fukagawa, M. Severe hyperparathyroidism with bone abnormalities and metastatic calcification in rats with adenine-induced uraemia. *Nephrol. Dial. Transplant. Off. Publ. Eur. Dial. Transpl. Assoc.-Eur. Ren. Assoc.* **2006**, *21*, 651–659. [CrossRef] [PubMed]
85. Santana, A.C.; Degaspari, S.; Catanozi, S.; Delle, H.; de Sa Lima, L.; Silva, C.; Blanco, P.; Solez, K.; Scavone, C.; Noronha, I.L. Thalidomide suppresses inflammation in adenine-induced CKD with uraemia in mice. *Nephrol. Dial. Transplant. Off. Publ. Eur. Dial. Transpl. Assoc.-Eur. Ren. Assoc.* **2013**, *28*, 1140–1149. [CrossRef]
86. Ferrari, G.O.; Ferreira, J.C.; Cavallari, R.T.; Neves, K.R.; dos Reis, L.M.; Dominguez, W.V.; Oliveira, E.C.; Graciolli, F.G.; Passlick-Deetjen, J.; Jorgetti, V.; et al. Mineral bone disorder in chronic kidney disease: Head-to-head comparison of the 5/6 nephrectomy and adenine models. *BMC Nephrol.* **2014**, *15*, 69. [CrossRef] [PubMed]
87. Morishita, Y.; Ohnishi, A.; Watanabe, M.; Ishibashi, K.; Kusano, E. Establishment of acute kidney injury mouse model by 0.75% adenine ingestion. *Ren. Fail.* **2011**, *33*, 1013–1018. [CrossRef] [PubMed]
88. Ren, X.; Wei, Q.; Shao, H.; Sun, Z.; Liu, N. A rat model of diabetic artery calcification. *J. Endocrinol. Investig.* **2012**, *35*, 497–503.
89. Ejerblad, S.; Eriksson, I.; Johansson, H. Uraemic arterial disease. An experimental study with special reference to the effect of parathyroidectomy. *Scand. J. Urol. Nephrol.* **1979**, *13*, 161–169. [CrossRef]
90. Krog, M.; Ejerblad, S.; Eriksson, I.; Johansson, H. Arterial calcifications in uraemic rats treated with 1-alpha-hydroxycholecalciferol and parathyroidectomy. *Scand. J. Urol. Nephrol.* **1984**, *18*, 227–239. [CrossRef]
91. Hirata, M.; Katsumata, K.; Endo, K.; Fukushima, N.; Ohkawa, H.; Fukagawa, M. In subtotally nephrectomized rats 22-oxacalcitriol suppresses parathyroid hormone with less risk of cardiovascular calcification or deterioration of residual renal function than 1,25(OH)2 vitamin D3. *Nephrol. Dial. Transplant. Off. Publ. Eur. Dial. Transpl. Assoc.-Eur. Ren. Assoc.* **2003**, *18*, 1770–1776. [CrossRef]
92. Henley, C.; Colloton, M.; Cattley, R.C.; Shatzen, E.; Towler, D.A.; Lacey, D.; Martin, D. 1,25-Dihydroxyvitamin D3 but not cinacalcet HCl (Sensipar/Mimpara) treatment mediates aortic calcification in a rat model of secondary hyperparathyroidism. *Nephrol. Dial. Transplant. Off. Publ. Eur. Dial. Transpl. Assoc.-Eur. Ren. Assoc.* **2005**, *20*, 1370–1377. [CrossRef] [PubMed]
93. Lopez, I.; Aguilera-Tejero, E.; Mendoza, F.J.; Almaden, Y.; Perez, J.; Martin, D.; Rodriguez, M. Calcimimetic R-568 decreases extraosseous calcifications in uremic rats treated with calcitriol. *J. Am. Soc. Nephrol. Jasn* **2006**, *17*, 795–804. [CrossRef] [PubMed]

94. Wu-Wong, J.R.; Noonan, W.; Ma, J.; Dixon, D.; Nakane, M.; Bolin, A.L.; Koch, K.A.; Postl, S.; Morgan, S.J.; Reinhart, G.A. Role of phosphorus and vitamin D analogs in the pathogenesis of vascular calcification. *J. Pharmacol. Exp. Ther.* **2006**, *318*, 90–98. [CrossRef] [PubMed]
95. Tamura, K.; Suzuki, Y.; Matsushita, M.; Fujii, H.; Miyaura, C.; Aizawa, S.; Kogo, H. Prevention of aortic calcification by etidronate in the renal failure rat model. *Eur. J. Pharmacol.* **2007**, *558*, 159–166. [CrossRef] [PubMed]
96. Cardus, A.; Panizo, S.; Parisi, E.; Fernandez, E.; Valdivielso, J.M. Differential effects of vitamin D analogs on vascular calcification. *J. Bone Min. Res.* **2007**, *22*, 860–866. [CrossRef]
97. Mendoza, F.J.; Lopez, I.; Montes de Oca, A.; Perez, J.; Rodriguez, M.; Aguilera-Tejero, E. Metabolic acidosis inhibits soft tissue calcification in uremic rats. *Kidney Int.* **2008**, *73*, 407–414. [CrossRef]
98. Lopez, I.; Mendoza, F.J.; Aguilera-Tejero, E.; Perez, J.; Guerrero, F.; Martin, D.; Rodriguez, M. The effect of calcitriol, paricalcitol, and a calcimimetic on extraosseous calcifications in uremic rats. *Kidney Int.* **2008**, *73*, 300–307. [CrossRef]
99. Haut, L.L.; Alfrey, A.C.; Guggenheim, S.; Buddington, B.; Schrier, N. Renal toxicity of phosphate in rats. *Kidney Int.* **1980**, *17*, 722–731. [CrossRef]
100. Cozzolino, M.; Staniforth, M.E.; Liapis, H.; Finch, J.; Burke, S.K.; Dusso, A.S.; Slatopolsky, E. Sevelamer hydrochloride attenuates kidney and cardiovascular calcifications in long-term experimental uremia. *Kidney Int.* **2003**, *64*, 1653–1661. [CrossRef] [PubMed]
101. Mizobuchi, M.; Ogata, H.; Hatamura, I.; Koiwa, F.; Saji, F.; Shiizaki, K.; Negi, S.; Kinugasa, E.; Ooshima, A.; Koshikawa, S.; et al. Up-regulation of Cbfa1 and Pit-1 in calcified artery of uraemic rats with severe hyperphosphataemia and secondary hyperparathyroidism. *Nephrol. Dial. Transplant. Off. Publ. Eur. Dial. Transpl. Assoc.-Eur. Ren. Assoc.* **2006**, *21*, 911–916. [CrossRef] [PubMed]
102. Graciolli, F.G.; Neves, K.R.; dos Reis, L.M.; Graciolli, R.G.; Noronha, I.L.; Moyses, R.M.; Jorgetti, V. Phosphorus overload and PTH induce aortic expression of Runx2 in experimental uraemia. *Nephrol. Dial. Transplant. Off. Publ. Eur. Dial. Transpl. Assoc.-Eur. Ren. Assoc.* **2009**, *24*, 1416–1421. [CrossRef] [PubMed]
103. El-Abbadi, M.M.; Pai, A.S.; Leaf, E.M.; Yang, H.Y.; Bartley, B.A.; Quan, K.K.; Ingalls, C.M.; Liao, H.W.; Giachelli, C.M. Phosphate feeding induces arterial medial calcification in uremic mice: Role of serum phosphorus, fibroblast growth factor-23, and osteopontin. *Kidney Int.* **2009**, *75*, 1297–1307. [CrossRef] [PubMed]
104. Qin, X.; Corriere, M.A.; Matrisian, L.M.; Guzman, R.J. Matrix metalloproteinase inhibition attenuates aortic calcification. *Arterioscler. Thromb. Vasc. Biol.* **2006**, *26*, 1510–1516. [CrossRef] [PubMed]
105. Assmann, A.; Zwirnmann, K.; Heidelberg, F.; Schiffer, F.; Horstkotter, K.; Munakata, H.; Gremse, F.; Barth, M.; Lichtenberg, A.; Akhyari, P. The degeneration of biological cardiovascular prostheses under pro-calcific metabolic conditions in a small animal model. *Biomaterials* **2014**, *35*, 7416–7428. [CrossRef] [PubMed]
106. Bas, A.; Lopez, I.; Perez, J.; Rodriguez, M.; Aguilera-Tejero, E. Reversibility of calcitriol-induced medial artery calcification in rats with intact renal function. *J. Bone Min. Res.* **2006**, *21*, 484–490. [CrossRef]
107. Tang, F.T.; Chen, S.R.; Wu, X.Q.; Wang, T.Q.; Chen, J.W.; Li, J.; Bao, L.P.; Huang, H.Q.; Liu, P.Q. Hypercholesterolemia accelerates vascular calcification induced by excessive vitamin D via oxidative stress. *Calcif. Tissue Int.* **2006**, *79*, 326–339. [CrossRef]
108. Atkinson, J.; Poitevin, P.; Chillon, J.M.; Lartaud, I.; Levy, B. Vascular Ca overload produced by vitamin D3 plus nicotine diminishes arterial distensibility in rats. *Am. J. Physiol.* **1994**, *266 Pt 2*, H540–H547. [CrossRef]
109. Wang, Q.Q.; Zhao, X.; Pu, X.P. Proteome analysis of the left ventricle in the vitamin D(3) and nicotine-induced rat vascular calcification model. *J. Proteom.* **2011**, *74*, 480–489. [CrossRef]
110. Niederhoffer, N.; Bobryshev, Y.V.; Lartaud-Idjouadiene, I.; Giummelly, P.; Atkinson, J. Aortic calcification produced by vitamin D3 plus nicotine. *J. Vasc. Res.* **1997**, *34*, 386–398. [CrossRef]
111. Shuvy, M.; Abedat, S.; Beeri, R.; Valitzki, M.; Stein, Y.; Meir, K.; Lotan, C. Electromagnetic fields promote severe and unique vascular calcification in an animal model of ectopic calcification. *Exp. Toxicol. Pathol. Off. J. Ges. Fur Toxikol. Pathol.* **2014**, *66*, 345–350. [CrossRef]
112. Hu, M.C.; Shiizaki, K.; Kuro-o, M.; Moe, O.W. Fibroblast growth factor 23 and Klotho: Physiology and pathophysiology of an endocrine network of mineral metabolism. *Annu. Rev. Physiol.* **2013**, *75*, 503–533. [CrossRef]
113. Mizobuchi, M.; Towler, D.; Slatopolsky, E. Vascular calcification: The killer of patients with chronic kidney disease. *J. Am. Soc. Nephrol. JASN* **2009**, *20*, 1453–1464. [CrossRef] [PubMed]

114. Tsujikawa, H.; Kurotaki, Y.; Fujimori, T.; Fukuda, K.; Nabeshima, Y. Klotho, a gene related to a syndrome resembling human premature aging, functions in a negative regulatory circuit of vitamin D endocrine system. *Mol. Endocrinol.* **2003**, *17*, 2393–2403. [CrossRef] [PubMed]
115. Stubbs, J.R.; Liu, S.; Tang, W.; Zhou, J.; Wang, Y.; Yao, X.; Quarles, L.D. Role of hyperphosphatemia and 1,25-dihydroxyvitamin D in vascular calcification and mortality in fibroblastic growth factor 23 null mice. *J. Am. Soc. Nephrol. JASN* **2007**, *18*, 2116–2124. [CrossRef] [PubMed]
116. Hesse, M.; Frohlich, L.F.; Zeitz, U.; Lanske, B.; Erben, R.G. Ablation of vitamin D signaling rescues bone, mineral, and glucose homeostasis in Fgf-23 deficient mice. *Matrix Biol. J. Int. Soc. Matrix Biol.* **2007**, *26*, 75–84. [CrossRef]
117. Razzaque, M.S.; Sitara, D.; Taguchi, T.; St-Arnaud, R.; Lanske, B. Premature aging-like phenotype in fibroblast growth factor 23 null mice is a vitamin D-mediated process. *Faseb J. Off. Publ. Fed. Am. Soc. Exp. Biol.* **2006**, *20*, 720–722. [CrossRef]
118. Ohnishi, M.; Nakatani, T.; Lanske, B.; Razzaque, M.S. Reversal of mineral ion homeostasis and soft-tissue calcification of klotho knockout mice by deletion of vitamin D 1alpha-hydroxylase. *Kidney Int.* **2009**, *75*, 1166–1172. [CrossRef]
119. Ohnishi, M.; Razzaque, M.S. Dietary and genetic evidence for phosphate toxicity accelerating mammalian aging. *Faseb J. Off. Publ. Fed. Am. Soc. Exp. Biol.* **2010**, *24*, 3562–3571. [CrossRef]
120. Kuro, O.M. Molecular Mechanisms Underlying Accelerated Aging by Defects in the FGF23-Klotho System. *Int. J. Nephrol.* **2018**, *2018*, 9679841. [CrossRef]
121. Scialla, J.J.; Lau, W.L.; Reilly, M.P.; Isakova, T.; Yang, H.Y.; Crouthamel, M.H.; Chavkin, N.W.; Rahman, M.; Wahl, P.; Amaral, A.P.; et al. Fibroblast growth factor 23 is not associated with and does not induce arterial calcification. *Kidney Int.* **2013**, *83*, 1159–1168. [CrossRef]
122. Folsom, L.J.; Imel, E.A. Hyperphosphatemic familial tumoral calcinosis: Genetic models of deficient FGF23 action. *Curr. Osteoporos. Rep.* **2015**, *13*, 78–87. [CrossRef] [PubMed]
123. Gattineni, J.; Baum, M. Regulation of phosphate transport by fibroblast growth factor 23 (FGF23): Implications for disorders of phosphate metabolism. *Pediatr. Nephrol.* **2010**, *25*, 591–601. [CrossRef] [PubMed]
124. Dusso, A.S.; Brown, A.J.; Slatopolsky, E. Vitamin D. *Am. J. Physiol. Ren. Physiol.* **2005**, *289*, F8–F28. [CrossRef] [PubMed]
125. Liu, S.; Tang, W.; Zhou, J.; Stubbs, J.R.; Luo, Q.; Pi, M.; Quarles, L.D. Fibroblast growth factor 23 is a counter-regulatory phosphaturic hormone for vitamin D. *J. Am. Soc. Nephrol. JASN* **2006**, *17*, 1305–1315. [CrossRef]
126. Meyer, M.B.; Pike, J.W. Mechanistic homeostasis of vitamin D metabolism in the kidney through reciprocal modulation of Cyp27b1 and Cyp24a1 expression. *J. Steroid Biochem. Mol. Biol.* **2020**, *196*, 105500. [CrossRef]
127. Shimada, T.; Kakitani, M.; Yamazaki, Y.; Hasegawa, H.; Takeuchi, Y.; Fujita, T.; Fukumoto, S.; Tomizuka, K.; Yamashita, T. Targeted ablation of Fgf23 demonstrates an essential physiological role of FGF23 in phosphate and vitamin D metabolism. *J. Clin. Investig.* **2004**, *113*, 561–568. [CrossRef]
128. Ichikawa, S.; Sorenson, A.H.; Austin, A.M.; Mackenzie, D.S.; Fritz, T.A.; Moh, A.; Hui, S.L.; Econs, M.J. Ablation of the Galnt3 gene leads to low-circulating intact fibroblast growth factor 23 (Fgf23) concentrations and hyperphosphatemia despite increased Fgf23 expression. *Endocrinology* **2009**, *150*, 2543–2550. [CrossRef]
129. Topaz, O.; Shurman, D.L.; Bergman, R.; Indelman, M.; Ratajczak, P.; Mizrachi, M.; Khamaysi, Z.; Behar, D.; Petronius, D.; Friedman, V.; et al. Mutations in GALNT3, encoding a protein involved in O-linked glycosylation, cause familial tumoral calcinosis. *Nat. Genet.* **2004**, *36*, 579–581. [CrossRef]
130. Esapa, C.T.; Head, R.A.; Jeyabalan, J.; Evans, H.; Hough, T.A.; Cheeseman, M.T.; McNally, E.G.; Carr, A.J.; Thomas, G.P.; Brown, M.A.; et al. A mouse with an N-Ethyl-N-nitrosourea (ENU) Induced Trp589Arg Galnt3 mutation represents a model for hyperphosphataemic familial tumoural calcinosis. *PLoS ONE* **2012**, *7*, e43205. [CrossRef]
131. Ichikawa, S.; Gray, A.K.; Padgett, L.R.; Allen, M.R.; Clinkenbeard, E.L.; Sarpa, N.M.; White, K.E.; Econs, M.J. Genetic rescue of glycosylation-deficient Fgf23 in the Galnt3 knockout mouse. *Endocrinology* **2014**, *155*, 3891–3898. [CrossRef]
132. Kuro-o, M.; Matsumura, Y.; Aizawa, H.; Kawaguchi, H.; Suga, T.; Utsugi, T.; Ohyama, Y.; Kurabayashi, M.; Kaname, T.; Kume, E.; et al. Mutation of the mouse klotho gene leads to a syndrome resembling ageing. *Nature* **1997**, *390*, 45–51. [CrossRef] [PubMed]

133. Hum, J.M.; O'Bryan, L.M.; Tatiparthi, A.K.; Cass, T.A.; Clinkenbeard, E.L.; Cramer, M.S.; Bhaskaran, M.; Johnson, R.L.; Wilson, J.M.; Smith, R.C.; et al. Chronic Hyperphosphatemia and Vascular Calcification Are Reduced by Stable Delivery of Soluble Klotho. *J. Am. Soc. Nephrol. JASN* **2017**, *28*, 1162–1174. [CrossRef] [PubMed]
134. Kuro-o, M. Klotho in health and disease. *Curr. Opin. Nephrol. Hypertens.* **2012**, *21*, 362–368. [CrossRef] [PubMed]
135. Ichikawa, S.; Imel, E.A.; Kreiter, M.L.; Yu, X.; Mackenzie, D.S.; Sorenson, A.H.; Goetz, R.; Mohammadi, M.; White, K.E.; Econs, M.J. A homozygous missense mutation in human KLOTHO causes severe tumoral calcinosis. *J. Clin. Investig.* **2007**, *117*, 2684–2691. [CrossRef] [PubMed]
136. Clemente, A.; Traghella, I.; Mazzone, A.; Sbrana, S.; Vassalle, C. Chapter Two—Vascular and valvular calcification biomarkers. In *Advances in Clinical Chemistry*; Makowski, G.S., Ed.; Elsevier: Amsterdam, The Netherlands, 2020; Volume 95, pp. 73–103.
137. Back, M.; Aranyi, T.; Cancela, M.L.; Carracedo, M.; Conceicao, N.; Leftheriotis, G.; Macrae, V.; Martin, L.; Nitschke, Y.; Pasch, A.; et al. Endogenous Calcification Inhibitors in the Prevention of Vascular Calcification: A Consensus Statement from the COST Action EuroSoftCalcNet. *Front. Cardiovasc. Med.* **2018**, *5*, 196. [CrossRef] [PubMed]
138. Luo, G.; Ducy, P.; McKee, M.D.; Pinero, G.J.; Loyer, E.; Behringer, R.R.; Karsenty, G. Spontaneous calcification of arteries and cartilage in mice lacking matrix GLA protein. *Nature* **1997**, *386*, 78–81. [CrossRef] [PubMed]
139. Jahnen-Dechent, W.; Schinke, T.; Trindl, A.; Muller-Esterl, W.; Sablitzky, F.; Kaiser, S.; Blessing, M. Cloning and targeted deletion of the mouse fetuin gene. *J. Biol. Chem.* **1997**, *272*, 31496–31503. [CrossRef]
140. Schafer, C.; Heiss, A.; Schwarz, A.; Westenfeld, R.; Ketteler, M.; Floege, J.; Muller-Esterl, W.; Schinke, T.; Jahnen-Dechent, W. The serum protein alpha 2-Heremans-Schmid glycoprotein/fetuin-A is a systemically acting inhibitor of ectopic calcification. *J. Clin. Investig.* **2003**, *112*, 357–366. [CrossRef]
141. Bucay, N.; Sarosi, I.; Dunstan, C.R.; Morony, S.; Tarpley, J.; Capparelli, C.; Scully, S.; Tan, H.L.; Xu, W.; Lacey, D.L.; et al. Osteoprotegerin-deficient mice develop early onset osteoporosis and arterial calcification. *Genes Dev.* **1998**, *12*, 1260–1268. [CrossRef]
142. Speer, M.Y.; McKee, M.D.; Guldberg, R.E.; Liaw, L.; Yang, H.Y.; Tung, E.; Karsenty, G.; Giachelli, C.M. Inactivation of the osteopontin gene enhances vascular calcification of matrix Gla protein-deficient mice: Evidence for osteopontin as an inducible inhibitor of vascular calcification in vivo. *J. Exp. Med.* **2002**, *196*, 1047–1055. [CrossRef]
143. Galvin, K.M.; Donovan, M.J.; Lynch, C.A.; Meyer, R.I.; Paul, R.J.; Lorenz, J.N.; Fairchild-Huntress, V.; Dixon, K.L.; Dunmore, J.H.; Gimbrone, M.A., Jr.; et al. A role for smad6 in development and homeostasis of the cardiovascular system. *Nat. Genet.* **2000**, *24*, 171–174. [CrossRef] [PubMed]
144. El-Maadawy, S.; Kaartinen, M.T.; Schinke, T.; Murshed, M.; Karsenty, G.; McKee, M.D. Cartilage formation and calcification in arteries of mice lacking matrix Gla protein. *Connect. Tissue Res.* **2003**, *44* (Suppl. 1), 272–278. [CrossRef] [PubMed]
145. Murshed, M.; Schinke, T.; McKee, M.D.; Karsenty, G. Extracellular matrix mineralization is regulated locally; different roles of two gla-containing proteins. *J. Cell Biol.* **2004**, *165*, 625–630. [CrossRef] [PubMed]
146. Proudfoot, D.; Shanahan, C.M. Molecular mechanisms mediating vascular calcification: Role of matrix Gla protein. *Nephrology* **2006**, *11*, 455–461. [CrossRef] [PubMed]
147. Price, P.A.; Faus, S.A.; Williamson, M.K. Warfarin causes rapid calcification of the elastic lamellae in rat arteries and heart valves. *Arterioscler. Thromb. Vasc. Biol.* **1998**, *18*, 1400–1407. [CrossRef] [PubMed]
148. Heiss, A.; DuChesne, A.; Denecke, B.; Grotzinger, J.; Yamamoto, K.; Renne, T.; Jahnen-Dechent, W. Structural basis of calcification inhibition by alpha 2-HS glycoprotein/fetuin-A. Formation of colloidal calciprotein particles. *J. Biol. Chem.* **2003**, *278*, 13333–13341. [CrossRef] [PubMed]
149. Price, P.A.; Nguyen, T.M.; Williamson, M.K. Biochemical characterization of the serum fetuin-mineral complex. *J. Biol. Chem.* **2003**, *278*, 22153–22160. [CrossRef]
150. Collin-Osdoby, P. Regulation of vascular calcification by osteoclast regulatory factors RANKL and osteoprotegerin. *Circ. Res.* **2004**, *95*, 1046–1057. [CrossRef]
151. Min, H.; Moronyb, S.; Sarosib, I.; Dunstanb, C.; Capparellib, C.; Scullyb, S.; Vanb, G.; Kaufmanb, S.; Kostenuikb, P.; Laceyb, D. Osteoprotegerin reverses osteoporosis by inhibiting endosteal osteoclasts and prevents vascular calcification by blocking a process resembling osteoclastogenesis. *J. Exp. Med.* **2000**, *192*, 463–474. [CrossRef]

152. Lok, Z.S.Y.; Lyle, A.N. Osteopontin in Vascular Disease. *Arterioscler. Thromb. Vasc. Biol.* **2019**, *39*, 613–622. [CrossRef]
153. Ishida, W.; Hamamoto, T.; Kusanagi, K.; Yagi, K.; Kawabata, M.; Takehara, K.; Sampath, T.K.; Kato, M.; Miyazono, K. Smad6 is a Smad1/5-induced smad inhibitor. Characterization of bone morphogenetic protein-responsive element in the mouse Smad6 promoter. *J. Biol. Chem.* **2000**, *275*, 6075–6079. [CrossRef] [PubMed]
154. Goto, K.; Kamiya, Y.; Imamura, T.; Miyazono, K.; Miyazawa, K. Selective inhibitory effects of Smad6 on bone morphogenetic protein type I receptors. *J. Biol. Chem.* **2007**, *282*, 20603–20611. [CrossRef] [PubMed]
155. Fleisch, H.; Bisaz, S. Mechanism of calcification: Inhibitory role of pyrophosphate. *Nature* **1962**, *195*, 911. [CrossRef] [PubMed]
156. Mackenzie, N.C.; Zhu, D.; Milne, E.M.; van 't Hof, R.; Martin, A.; Darryl Quarles, L.; Millan, J.L.; Farquharson, C.; MacRae, V.E. Altered bone development and an increase in FGF-23 expression in Enpp1(-/-) mice. *PLoS ONE* **2012**, *7*, e32177. [CrossRef]
157. Watanabe, R.; Fujita, N.; Sato, Y.; Kobayashi, T.; Morita, M.; Oike, T.; Miyamoto, K.; Kuro, O.M.; Michigami, T.; Fukumoto, S.; et al. Enpp1 is an anti-aging factor that regulates Klotho under phosphate overload conditions. *Sci. Rep.* **2017**, *7*, 7786. [CrossRef] [PubMed]
158. Li, Q.; Guo, H.; Chou, D.W.; Berndt, A.; Sundberg, J.P.; Uitto, J. Mutant Enpp1asj mice as a model for generalized arterial calcification of infancy. *Dis. Models Mech.* **2013**, *6*, 1227–1235. [CrossRef]
159. Kauffenstein, G.; Pizard, A.; Le Corre, Y.; Vessieres, E.; Grimaud, L.; Toutain, B.; Labat, C.; Mauras, Y.; Gorgels, T.G.; Bergen, A.A.; et al. Disseminated arterial calcification and enhanced myogenic response are associated with abcc6 deficiency in a mouse model of pseudoxanthoma elasticum. *Arterioscler. Thromb. Vasc. Biol.* **2014**, *34*, 1045–1056. [CrossRef]
160. Varga, R.; Eriksson, M.; Erdos, M.R.; Olive, M.; Harten, I.; Kolodgie, F.; Capell, B.C.; Cheng, J.; Faddah, D.; Perkins, S.; et al. Progressive vascular smooth muscle cell defects in a mouse model of Hutchinson-Gilford progeria syndrome. *Proc. Natl. Acad. Sci. USA* **2006**, *103*, 3250–3255. [CrossRef]
161. Villa-Bellosta, R.; Rivera-Torres, J.; Osorio, F.G.; Acin-Perez, R.; Enriquez, J.A.; Lopez-Otin, C.; Andres, V. Defective extracellular pyrophosphate metabolism promotes vascular calcification in a mouse model of Hutchinson-Gilford progeria syndrome that is ameliorated on pyrophosphate treatment. *Circulation* **2013**, *127*, 2442–2451. [CrossRef]
162. Jansen, R.S.; Duijst, S.; Mahakena, S.; Sommer, D.; Szeri, F.; Varadi, A.; Plomp, A.; Bergen, A.A.; Oude Elferink, R.P.; Borst, P.; et al. ABCC6-mediated ATP secretion by the liver is the main source of the mineralization inhibitor inorganic pyrophosphate in the systemic circulation-brief report. *Arterioscler. Thromb. Vasc. Biol.* **2014**, *34*, 1985–1989. [CrossRef]
163. Ho, A.M.; Johnson, M.D.; Kingsley, D.M. Role of the mouse ank gene in control of tissue calcification and arthritis. *Science* **2000**, *289*, 265–270. [CrossRef] [PubMed]
164. Pomozi, V.; Brampton, C.; van de Wetering, K.; Zoll, J.; Calio, B.; Pham, K.; Owens, J.B.; Marh, J.; Moisyadi, S.; Varadi, A.; et al. Pyrophosphate Supplementation Prevents Chronic and Acute Calcification in ABCC6-Deficient Mice. *Am. J. Pathol.* **2017**, *187*, 1258–1272. [CrossRef] [PubMed]
165. Huang, J.; Snook, A.E.; Uitto, J.; Li, Q. Adenovirus-Mediated ABCC6 Gene Therapy for Heritable Ectopic Mineralization Disorders. *J. Investig. Derm.* **2019**, *139*, 1254–1263. [CrossRef] [PubMed]
166. Hamczyk, M.R.; Villa-Bellosta, R.; Gonzalo, P.; Andres-Manzano, M.J.; Nogales, P.; Bentzon, J.F.; Lopez-Otin, C.; Andres, V. Vascular Smooth Muscle-Specific Progerin Expression Accelerates Atherosclerosis and Death in a Mouse Model of Hutchinson-Gilford Progeria Syndrome. *Circulation* **2018**, *138*, 266–282. [CrossRef]
167. Emini Veseli, B.; Perrotta, P.; De Meyer, G.R.A.; Roth, L.; Van der Donckt, C.; Martinet, W.; De Meyer, G.R.Y. Animal models of atherosclerosis. *Eur. J. Pharm.* **2017**, *816*, 3–13. [CrossRef]
168. Oppi, S.; Lüscher, T.F.; Stein, S. Mouse Models for Atherosclerosis Research—Which Is My Line? *Front. Cardiovasc. Med.* **2019**, *6*, 46. [CrossRef]
169. Barter, P.J.; Brewer, H.B.; Chapman, M.J.; Hennekens, C.H.; Rader, D.J.; Tall, A.R. Cholesteryl Ester Transfer Protein. *Arterioscler. Thromb. Vasc. Biol.* **2003**, *23*, 160–167. [CrossRef]
170. Takahashi, S.; Fukami, T.; Masuo, Y.; Brocker, C.N.; Xie, C.; Krausz, K.W.; Wolf, C.R.; Henderson, C.J.; Gonzalez, F.J. Cyp2c70 is responsible for the species difference in bile acid metabolism between mice and humans. *J. Lipid Res.* **2016**, *57*, 2130–2137. [CrossRef]

171. Ishibashi, S.; Goldstein, J.L.; Brown, M.S.; Herz, J.; Burns, D.K. Massive xanthomatosis and atherosclerosis in cholesterol-fed low density lipoprotein receptor-negative mice. *J. Clin. Investig.* **1994**, *93*, 1885–1893. [CrossRef]
172. Awan, Z.; Denis, M.; Bailey, D.; Giaid, A.; Prat, A.; Goltzman, D.; Seidah, N.G.; Genest, J. The LDLR deficient mouse as a model for aortic calcification and quantification by micro-computed tomography. *Atherosclerosis* **2011**, *219*, 455–462. [CrossRef]
173. Maxwell, K.N.; Fisher, E.A.; Breslow, J.L. Overexpression of PCSK9 accelerates the degradation of the LDLR in a post-endoplasmic reticulum compartment. *Proc. Natl. Acad. Sci. USA* **2005**, *102*, 2069–2074. [CrossRef] [PubMed]
174. Goettsch, C.; Hutcheson, J.D.; Hagita, S.; Rogers, M.A.; Creager, M.D.; Pham, T.; Choi, J.; Mlynarchik, A.K.; Pieper, B.; Kjolby, M.; et al. A single injection of gain-of-function mutant PCSK9 adeno-associated virus vector induces cardiovascular calcification in mice with no genetic modification. *Atherosclerosis* **2016**, *251*, 109–118. [CrossRef] [PubMed]
175. Zhang, S.H.; Reddick, R.L.; Piedrahita, J.A.; Maeda, N. Spontaneous hypercholesterolemia and arterial lesions in mice lacking apolipoprotein E. *Science* **1992**, *258*, 468–471. [CrossRef] [PubMed]
176. Rattazzi, M.; Bennett, B.J.; Bea, F.; Kirk, E.A.; Ricks, J.L.; Speer, M.; Schwartz, S.M.; Giachelli, C.M.; Rosenfeld, M.E. Calcification of advanced atherosclerotic lesions in the innominate arteries of ApoE-deficient mice: Potential role of chondrocyte-like cells. *Arter. Thromb. Vasc. Biol.* **2005**, *25*, 1420–1425. [CrossRef]
177. Langheinrich, A.C.; Michniewicz, A.; Sedding, D.G.; Walker, G.; Beighley, P.E.; Rau, W.S.; Bohle, R.M.; Ritman, E.L. Correlation of vasa vasorum neovascularization and plaque progression in aortas of apolipoprotein E(−/−)/low-density lipoprotein(−/−) double knockout mice. *Arter. Thromb. Vasc. Biol.* **2006**, *26*, 347–352. [CrossRef]
178. Massy, Z.A.; Ivanovski, O.; Nguyen-Khoa, T.; Angulo, J.; Szumilak, D.; Mothu, N.; Phan, O.; Daudon, M.; Lacour, B.; Drueke, T.B.; et al. Uremia accelerates both atherosclerosis and arterial calcification in apolipoprotein E knockout mice. *J. Am. Soc. Nephrol. JASN* **2005**, *16*, 109–116. [CrossRef]
179. van Vlijmen, B.J.; van den Maagdenberg, A.M.; Gijbels, M.J.; van der Boom, H.; HogenEsch, H.; Frants, R.R.; Hofker, M.H.; Havekes, L.M. Diet-induced hyperlipoproteinemia and atherosclerosis in apolipoprotein E3-Leiden transgenic mice. *J. Clin. Investig.* **1994**, *93*, 1403–1410. [CrossRef]
180. Lutgens, E.; Daemen, M.; Kockx, M.; Doevendans, P.; Hofker, M.; Havekes, L.; Wellens, H.; de Muinck, E.D. Atherosclerosis in APOE*3-Leiden transgenic mice: From proliferative to atheromatous stage. *Circulation* **1999**, *99*, 276–283. [CrossRef]
181. Russell, W.M.S.; Burch, R.L. *The Principles of Humane Experimental Technique*; Methuen & Co Ltd.: London UK, 1959.

Manuscript 2: A Novel Protocol for Detection of Senescence and Calcification Markers by Fluorescence Microscopy

This manuscript has been published in *International Journal of Molecular Science (IF:5.923)*:

Herrmann J*, Babic M*, Tolle M, Eckardt KU, van der Giet M, Schuchardt M. A Novel Protocol for Detection of Senescence and Calcification Markers by Fluorescence Microscopy. *Int J Mol Sci.* 2020;21(10):3475.

DOI: 10.3390/ijms21103475

*authors contributed equally

The authors' contributions are stated in the publication on page 10/12. My personal contribution to this article encompasses:

Laboratory work:

- Conceptualization of the protocols
- Execution of *in vitro* experiments:
  - Primary cell isolation, culture and stimulation
  - RNA *in situ* staining and immunhistological staining & SA-ß-Gal staining
  - Microscopic imaging, data analysis and quantification

Manuscript preparation:

- Conceptualization of article
- Preparation of figures and tables
- Literature research
- Writing of the original draft

International Journal of
Molecular Sciences

MDPI

Technical Note

A Novel Protocol for Detection of Senescence and Calcification Markers by Fluorescence Microscopy

Jaqueline Herrmann [1,2,†], Milen Babic [1,†], Markus Tölle [1], Kai-Uwe Eckardt [1], Markus van der Giet [1,*] and Mirjam Schuchardt [1]

[1] Department of Nephrology and Medical Intensive Care, Charité—Universitätsmedizin Berlin, Corporate Member of Freie Universität Berlin, Humboldt-Universtität zu Berlin, and Berlin Institute of Health, Hindenburgdamm 30, 12203 Berlin, Germany; Jaqueline.Herrmann@charite.de (J.H.); Milen.Babic@charite.de (M.B.); Markus.Toelle@charite.de (M.T.); Kai-Uwe.Eckardt@charite.de (K.-U.E.); Mirjam.Schuchardt@charite.de (M.S.)

[2] Department of Chemistry, Biochemistry and Pharmacy, Freie Universität Berlin, Königin-Luise Straße 2+4, 14195 Berlin, Germany

* Correspondence: Markus.vanderGiet@charite.de

† These authors contribute equally to this work.

Received: 14 April 2020; Accepted: 11 May 2020; Published: 14 May 2020

check for updates

Abstract: Vascular calcification and stiffening of the arterial wall is a systemic phenomenon that is associated with aging and it can be increased by several risk factors. The underlying mechanisms, especially the pathways of cellular senescence, are under current investigation. Easily manageable in vitro settings help to study the signaling pathways. The experimental setting presented here is based on an in vitro model using rat vascular smooth muscle cells and the detection of senescence and osteoblastic markers via immunofluorescence and RNAscope™. Co-staining of the senescence marker p21, the osteoblastic marker osteopontin, detection of senescence-associated heterochromatin foci, and senescence-associated β-galactosidase is possible within one test approach requiring fewer cells. The protocol is a fast and reliable evaluation method for multiplexing of calcifying and senescence markers with fluorescence microscopy detection. The experimental setting enables analysis on single cell basis and allows detection of intra-individual variances of cultured cells.

Keywords: calcification; senescence; smooth muscle cell; SA-β-galactosidase; senescence-associated heterochromatin foci

1. Introduction

Aging is associated with a variety of characteristic changes of the vessel wall [1]. There are several disorders, in which patients show signs of premature aging of vessels that appear much older than their biological age e.g., in chronic kidney disease [2–4]. A hallmark of vascular aging is a stiffening of the arterial wall with increasing pulse-wave velocity and the mineralization of vascular smooth muscle cells (VSMC) in the media layer of the vessel wall [1,5]. Treatment options are currently not available [5].

Resulting from clinical and basic research, there is strong evidence that vascular calcification and aging occur jointly [4,6,7]. Several underlying mechanisms are discussed for vessel mineralization, including, but not limited to, oxidative stress from various sources and resulting DNA damage, continuous inflammation, and activation of pro-osteogenic signaling pathways [3,7,8]. However, the underlying pathophysiological mechanisms need further clarification. Currently, several hypotheses exist regarding joint or consecutive appearance of calcification and senescence in a vicious cycle in smooth muscle cells e.g., induced by uremic toxins [4,9]. In addition, the senescence level can vary within and between cells and the tissue of the same individual [10]. It has to be illuminated whether,

in one cell population, cells experience senescence and calcification jointly or consecutively, or whether aged vessels contain distinctly different cell populations of aged and calcified cells.

A better understanding of the underlying mechanisms inducing and linking calcification and senescence of VSMC in the vessel wall will be necessary for establishing promising treatment options.

Detecting cellular senescence is hampered by the heterogeneity of senescence markers. For the reliable identification of DNA damage and cell senescence, the detection of several known markers is necessary. Here, the increased messenger-ribonucleic acid (mRNA) and protein expression of the cell cycle protein and cyclin inhibitor p21 as well as the formation of senescence-associated heterochromatin foci (SAHF) and the accumulation of senescence-associated β-galactosidase (SA-β-Gal) are typically used [10–12]. Additionally, the cells often undergo morphological changes that are detectable by light microscopy. Cell mineralization is accompanied by a shift in expression of a wide array of different markers e.g., osteopontin (OPN) [3,13].

The study aims to develop a fast, robust, and easy to handle protocol by detection of SA-β-Gal, SAHF, p21, OPN, and control of cell morphology, on single cell basis in vitro in order to facilitate jointly and/or consecutively activation of senescence and calcification markers within the cells in a parallel experimental setting. Therefore, the described method combines ultrasensitive RNAscope™ in situ hybridization and immunohistochemistry in a multiplex approach requiring few cells. Other currently available experimental settings with their advantages and disadvantages are summarized in the supplementary Table S1. Briefly, the in situ hybridization technique enables the detection of various nucleotide sequences in cells and tissue by radioactive, fluorescence, or immunohistochemistry labeling and it permits a multiplex approach in the right experimental setting [14]. The protocol presented here utilizes RNAscope™, a technology that applies oligonucleotide probes and immunohistochemical or fluorescence-based detection [15]. The utilized RNAscope™ kit allows for the analysis of three targets of interest in one experimental setting by fluorescence-based detection.

For the establishment and optimization of the protocol steps, the known inductor of cell senescence, doxorubicin (Dox) [16], as well as a known inducer of cell mineralization, the uremic toxin uridine-adenosine tetraphosphate (Up_4A) [17], were used. The established protocol provides reliable data while requiring fewer primary cell numbers and, therefore, fewer animals per experiment by multiplexing several markers of interest.

2. Results and Discussion

Currently, several senescence markers for cells and tissue are known [10,11]. Often, the detection of more than one marker is used for reliable detection and the senescence levels can vary between cells and tissue, respectively, within the same animal [10].

Here, we provided a staining protocol for four markers of interest to detect senescence and osteoblastic differentiation in cells. Besides, the protocol can be expanded for the detection of other markers by using a laser-scanning microscope for image acquisition. The detection via fluorescence staining allows not only the visualization in individual cells, but also quantification for statistical analysis of the results.

2.1. Detection of SA-β-Gal

SA-β-Gal was selected as marker accumulating in cells during aging, according to previous studies [6,10]. The staining of the cells with SPiDER-SA-ß-Gal upon stimulation with Dox, as a known inductor of cell senescence [16], results in the accumulation of SA-β-Gal within the cytoplasm of the cell, as shown in Figure 1. In contrast, while Up_4A induces cell calcification [17], no accumulation of SA-β-Gal could be detected upon stimulation of VSMC for 72 h. For counterstaining of the nucleus, Hoechst stain was used. The quantification of the pixel sum intensity (Figure 2) confirmed the findings of the representative images that are shown in Figure 1.

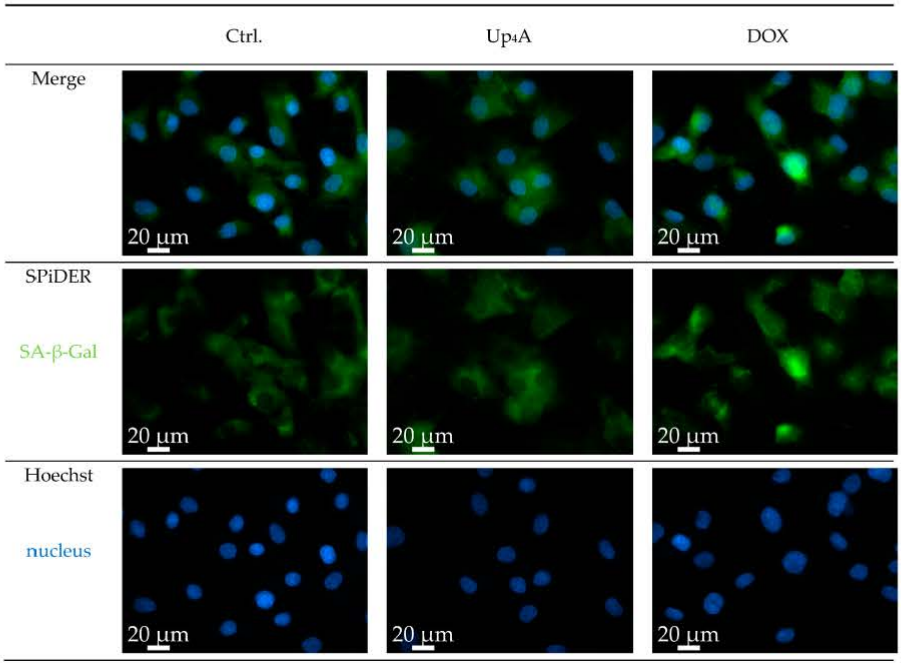

Figure 1. Detection of senescence-associated β-galactosidase (SA-β-Gal) in primary rat smooth muscle cells upon stimulation with doxorubicin (Dox, 500 nmol/L) and uridine-adenosine tetraphosphate (Up_4A, 100 µmol/L) for 72 h. 40× objective. Representative images out of three independent experiments. Ctrl.: control.

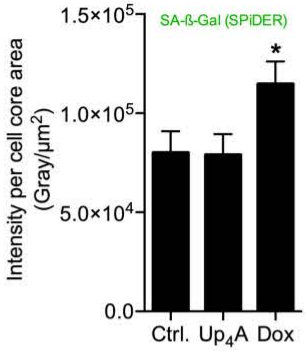

Figure 2. Quantification of senescence-associated β-galactosidase (SA-β-Gal) in primary rat smooth muscle cells upon stimulation with doxorubicin (Dox, 500 nmol/L) and uridine-adenosine tetraphosphate (Up_4A, 100 µmol/L) for 72 h. For analysis, intensity pixel sum per channel was normalized to cell core area. Bar graph represents mean ± SEM of three independent experiments. Ctrl.: control.

The results suggest that accumulation of SA-β-Gal in rat vascular smooth muscle cells (rVSMC) depends on the inductor and may be dependent on time for different inductors. This underlines the fact that the detection of more than one senescence marker often seems necessary [10].

2.2. OPN and p21 mRNA Detection and Detection of SAHF

OPN was selected as a calcification marker, because its gene expression was increased by stimulation with different calcification inducers in previous experiments [17]. The gene expression of the cyclin inhibitor p21 is one typical marker used for the detection of cellular senescence [6,10].

Several experimental protocols currently exist for the detection of calcification or senescence markers in vascular cells (summarized in Table S1). However, the current goal was to use a single cell-based identification of a senescence and osteoblastic marker while using RNA in situ hybridization via RNAscope™ technology. The significant advantage is the multiplexing possibility of several target genes of interest in a cell and tissue sample in a robust way with high sensitivity [15]. Dox strongly induced SAHF and mRNA expression of p21, but only slightly induced OPN mRNA expression upon 48 h of stimulation, as shown in Figure 3. In contrast, upon Up_4A stimulation, OPN mRNA expression is induced profoundly, but no SAHF could be detected and p21 mRNA expression is not induced in VSMC.

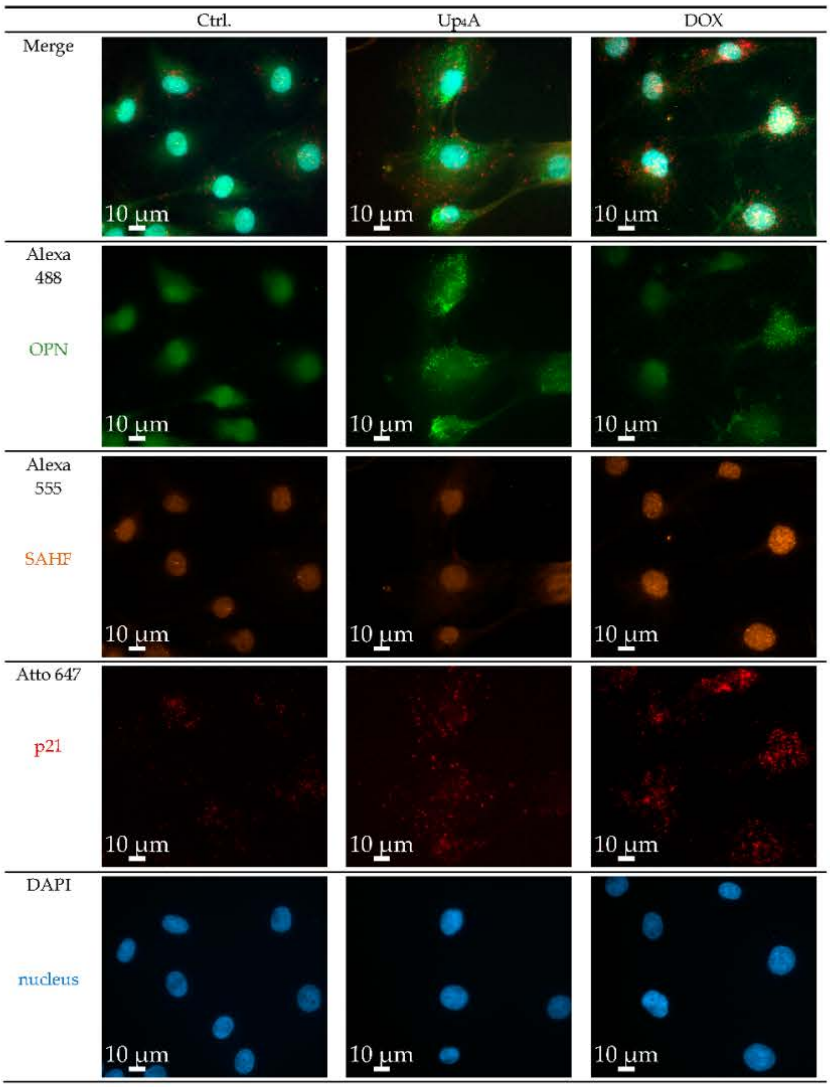

Figure 3. Detection of osteopontin (OPN), senescence-associated heterochromatin foci (SAHF), and p21 in primary rat smooth muscle cells upon stimulation with doxorubicin (Dox, 500 nmol/L) and uridine-adenosine tetraphosphate (Up_4A, 100 µmol/L) for 48 h. 40× objective. Representative images out of three independent experiments. Ctrl.: control.

The quantification of the pixel sum intensity confirmed the findings for channel Atto 647 (Figure 4). The crosstalk between the channels Alexa 488 and Alexa 555 and the resulting background impedes the quantification of OPN mRNA expression and SAHF formation with a standardized, automated, and reproducible ZEN protocol in this experimental setting. Several options exist to overcome this issue: next to the application of alternative software permitting manual identification of targets and subsequent quantification, which can be prone to researcher bias and, therefore, is not presented here, imaging with a confocal microscope could facilitate quantification by reducing cross talk and background.

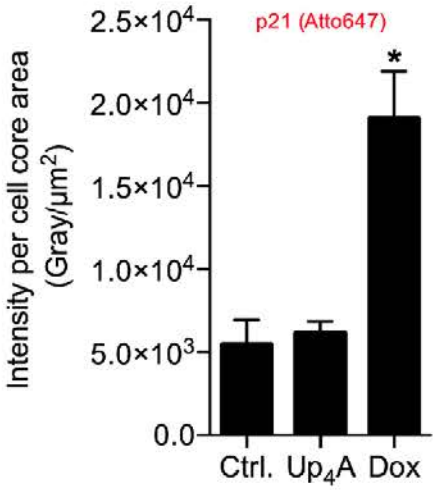

Figure 4. Quantification of p21 in primary rat smooth muscle cells upon stimulation with doxorubicin (Dox, 500 nmol/L) and uridine-adenosine tetraphosphate (Up_4A, 100 µmol/L) for 48 h. For analysis, intensity pixel sum per channel was normalized to cell core area. Bar graph represents mean ± SEM of three independent experiments. Ctrl.: control.

Stimulation with different inducers as Dox and Up_4A varies in the markers analyzed for calcification and senescence. This underlines that, often, the detection of more than one senescence and calcification marker seems to be necessary for reliable and comparable results. In addition, in our experimental setting, we observed a certain level of cell batch specific variances in the expression levels of markers that are comparable to alternative protocols, like Western Blot and polymerase chain reaction (PCR). However, representative images also illustrate differences in marker expression between individual cells, especially for the investigated calcification marker OPN. This information is critical in order to understand the mechanisms and pathways within one cell during the calcification process. This information is lost in protocols that jointly analyze cell bulks. The current protocol can allow for the analysis of co-localization analysis within one cell and differences between cells of the same cell batch.

2.3. Limitations

The experimental design that is presented here is established for an in vitro experiment. Nevertheless, a transfer from cells to tissue should be possible. The development of appropriate pre-treatment and imaging of tissue section will require further optimization steps. In the case of SA-β-Gal staining in tissue, we recommend using freshly frozen tissue and process the material immediately, as storage even at −80°C reduces enzyme activity. In a proof of concept experiment, we tested RNAscope™ staining in frozen and paraffin-embedded aortic sections (unpublished data). We found a similar background in both materials and better results in paraffin-embedded tissue, which we attribute to easier handling. Alternative targets might be of interest, according to the focus of research. Here, our protocol provides some opportunities for variation: alternative target genes can be analyzed with the RNA in situ hybridization technique. The utilized protocol allows up to three different target

genes. We used one of the available channels for immune-histological staining to make use of the optimal capacity of our microscope. If equipped with alternative hardware, combination with another secondary antibody for immune histological staining is possible, thus enriching the opportunities for multiplexing.

We are aware that there is a variety of alternative protocols. Alternative research models, such as primary cells from mouse or human, cell lines, as well as tissue sections from clinical or laboratory origin, are suitable alternatives. Next to that, a huge variety of different methods for the detection and quantification of our selected targets are possible. Each comes with its advantages and disadvantages that are shortly summarized in Table S1. In comparison to 5-bromo-4-chloro-3-indolyl-β-D-galactopyranoside (X-Gal/BCIG) staining, we found fluorescence staining of SA-β-Gal to be more robust, faster, and easier to image.

3. Materials and Methods

Figure 5 summarizes the complete and stepwise workflow of the experimental procedures. Primary VSMC from rat thoracic aorta was selected for experiments. Further special ordering information for kits with its components and antibodies can be found in the Supplementary Material (Tables S2 and S3).

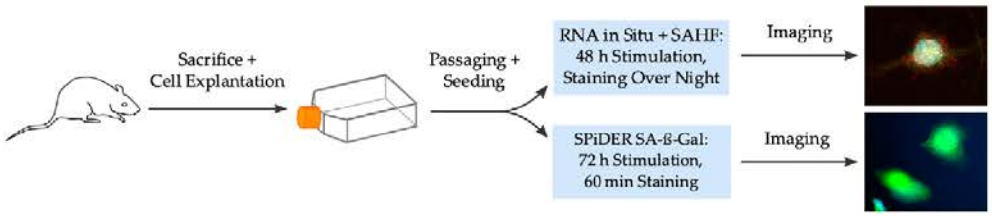

Figure 5. Scheme of the complete experimental workflow. SAHF: senescence-associated heterochromatin foci, SA-ß Gal: senescence-associated ß-galactosidase.

3.1. Cell Isolation and Culturing

The study was in accordance with the EU Directive 2010/63/EU for animal experiments and it was approved by the Landesamt für Gesundheit und Soziales Berlin, Germany (T0211/02) and the animal facility of the Charité—Universitätsmedizin Berlin, Germany. The aorta of Wistar rats was prepared after euthanasia with sodium pentobarbital (400 mg/kg body weight) per intraperitoneal injection. After removal of the adventitia of rat thoracic aorta, primary rat VSMC were isolated by explant outgrowth, as described previously [17]. VSMC were cultured in Dulbecco Modified Eagle Medium (DMEM, Biochrom AG) containing 1 g/L glucose, supplemented with 10% fetal calf serum (FCS, Biochrom AG), penicillin (100 U/mL, Biochrom AG), and streptomycin (0.1 mg/mL, Biochrom AG). The cells were cultured in a humidified incubator at 37°C with 5% carbon dioxide. Cells at passages 4 were used for experiments. The cells were seeded in IBIDI 8 Well µ- Slides (ibidi GmbH) for SA-ß-Gal staining and 8-well LabTec Chamber Slides (Thermo Scientific) for RNA in situ hybridization. Cells were cultured for 24 h to a confluence of 70–80%. It is essential to ensure subconfluence of cells prior stimulation, because confluence itself was described as an inducer of SA-β-Gal activity [18]. The cells were serum starved for 24 h prior stimulation in DMEM containing 4.5 g/L glucose, supplemented with 1% glutamin and antibiotics (penicillin 100 U/mL, streptomycin 0.1 mg/mL). This medium was also used for stimulation. For SA-β-Gal staining, the cells were stimulated for 72 h, whereas for mRNA and SAHF detection a stimulation time of 48 h was used.

3.2. Experimental Setting for Detection of SA-β-Galactosidase

Information regarding the kit components and ordering information are summarized in the Supplementary Material (Table S3).

3.2.1. Preparations

- Heat incubator to 37 °C (no humidity and carbon dioxide control).
- Warm 4% formalin and PBS to 37 °C.
- Prepare McIlvaine buffer: Mix 7.4 mL 0.1 mol/L citric acid solution and 12.6 mL 0.2 mol/L sodium phosphate solution and set pH to 6.0.
- Solve 20 µg SPiDER-SA-β-Gal (Gerbu Biotechnologie) in 35 µL dimethylsulfoxide (DMSO). Store aliquots at −20°C.
- Dilute McIlvaine buffer 1:5 in ultrapure water and warm dilution to 37 °C. Dilute SPiDER-SA-ß-Gal 1:500 in McIlvaine buffer in order to obtain the working solution. Protect working solution from light.
- Prepare Hoechst working solution by dissolving Hoechst 33342 (Thermo Fisher) in the appropriate amount of water to obtain a stock concentration of 10 mg/mL. The stock concentration can be aliquoted and stored at −20°C. To obtain the working solution, dilute Hoechst 1:2000 in PBS. Protect working solution from light.

3.2.2. Staining Procedure

The step-by-step staining procedure according to the manufacturer's (Dojindo) recommendations is given below. Figure 6 summarizes the main steps with an incubation time less than 40 min for the whole procedure.

1. After stimulation, aspirate medium and wash cells once with PBS.
2. Add 300 µL of 4% buffered formalin to each well and fix cells for 3 min at room temperature, ensure the exact fixation time.
3. Aspirate formalin and wash three times with warm PBS.
4. Add 300 µL of working solution per well and incubate for 30 min in the incubator under light protection. Caution: Ensure the right fixation times and pH conditions—this is critical for the β-Gal staining.
5. Aspirate working solution and wash cells twice with PBS.
6. Counterstain with Hoechst working solution for 5 min under light protection.
7. Aspirate solution and wash once with PBS.
8. Add 300 µL of PBS and image within 24 h.

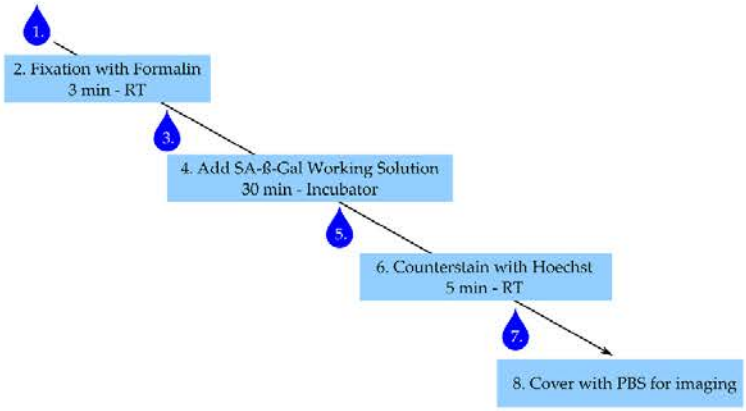

Figure 6. Staining procedure for senescence-associated-β-galactosidase (SA-ß-Gal). Numbering represents steps in staining procedure. Drop corresponds to wash step. RT: room temperature.

3.3. Experimental Setting for Detection of OPN, p21 and SAHF

All kit components for staining with the ordering information are summarized in the Supplementary Material (Table S3).

3.3.1. Preparations

- Add purified water to the humidity control tray and heat oven to 40 °C.
- Thaw ProLong™ diamond antifade medium (Thermo Scientific) at room temperature.
- Prepare wash buffer (ACD Bio) according to manufacturer's instructions.
- Heat mRNA probes (ACD Bio) gently at 40 °C for 10 min in a water bath, centrifuge probes and mix according to manufacturer's instructions.
- Dilute Protease III (ACD Bio) 1:15 with PBS.
- Prepare washing dishes for PBS and wash buffer.
- Prepare 10% Roti™ImmunoBlock (Carl Roth) by diluting in PBS.
- Prepare 1:500 dilution of primary antibody anti-histone H2A.X (phosphoS139) antibody [EP854(2)Y] (abcam) in 1% Roti™ImmunoBlock/PBS.
- Prepare 1:1,000 dilution of secondary goat anti-Rabbit IgG (H+L) highly cross-adsorbed antibody, Alexa Fluor 555 (Invitrogen) in 1% Roti™ImmunoBlock/PBS.
- If applicable: Prepare Hoechst stain, as explained above.

3.3.2. Staining Procedure

The step-by-step staining procedure according to the manufactures' recommendations (ACD Bio) is given below. Figure 7 summarizes the main points with several incubation steps, including one overnight incubation time.

1. After stimulation aspirate medium and wash cells once with PBS.
2. Add 300 µL of 4% buffered formalin to each well and fix cells for 30 min at room temperature.
3. Aspirate formalin and wash twice with PBS.
4. Carefully detach the chamber from the slide according to the manufacturer's instruction and place the slide in a PBS filled washing dish. Caution: The glue is strong. Make sure to remove the glue of the chamber properly, otherwise the slide–coverslip combination becomes too thick.
5. Remove slide from the washing dish and thoroughly apply a barrier around each well with the ImmEdge™ hydrophobic barrier pen (ACD Bio) and place slide again in PBS.
6. Remove the slide from PBS, remove attaching PBS by gently inverting the slide and add 50 µL of diluted Protease III to each well. Place slide in the humidity control tray, close humidity control tray, and incubate in the oven for 15 min.
7. Remove slides from tray; remove protease from slide by inverting the slide and place slide in fresh PBS. Caution: The movement should be gently, but still removing the majority of liquid.
8. Remove slide from PBS, remove PBS by gently inverting the slide, and add 50 µL of diluted target probes or one drop of positive or negative control to the according wells, place slides in the humidity control tray, and incubate in the oven for 120 min.
9. Take slides out of the tray, inverse, and wash twice for 2 min each in wash buffer.
10. Remove attached liquid by gentle inversion and add one drop of amplifier 1-fluid (Amp 1-FL) to each well. Put slides in the humidity control tray in the oven for 30 min.
11. Take slides out of the tray, inverse, and wash twice for 2 min each in wash buffer.
12. Remove attached liquid by gentle inversion and add 1 drop of Amp 2-FL to each well, place in the humidity control tray in the oven for 15 min.
13. After 15 min take slides out of the tray, inverse and wash twice for 2 min each in wash buffer.

14. Remove attached liquid by gentle inversion and add 1 drop of Amp 3-FL to each well, place in the humidity control tray in the oven for 30 min.
15. Take slides out of the tray, inverse and wash twice for 2 min each in wash buffer.
16. Remove attached liquid by gentle inversion and add 1 drop of the selected Amp 4-FL to each well, place in the humidity control tray in the oven for 15 min. Caution: For the multiplexing protocol we used Amp 4-FL A.
17. Take slides out of the tray, inverse and wash twice for 2 min each in wash buffer.
18. Add 100 µL of 10% Roti™ImmunoBlock/PBS to each well and block for 1 h in the closed humidity control tray at room temperature.
19. Remove attached liquid by gentle inversion and wash once with PBS.
20. Add 50 µL 1:500 dilution of primary anti-histone H2A.X (phosphoS139) antibody [EP854(2)Y] (Abcam) in 1% Roti™ImmunoBlock/PBS per well and incubate in the closed humidity control tray in the fridge overnight.
21. Remove attached liquid by gentle inversion and wash twice with PBS.
22. Add 50 µL 1:1,000 dilution of secondary goat anti-rabbit IgG (H+L) Highly Cross-Adsorbed antibody, Alexa Fluor 555 (Invitrogen) in 1% Roti™ImmunoBlock/PBS per well and incubate in the closed humidity control tray at room temperature for 60 min.
23. Remove attached liquid by gentle inversion and wash twice with PBS.
24. Add 1 drop of 4′,6-diamidino-2-phenylindole (DAPI) per well and incubate for 1 min at room temperature (alternatively add 50 µL 1:2,000 Hoechst working solution and incubate for 5 min at room temperature).
25. Remove attached liquid by gentle inversion and wash once with PBS.
26. Add two drops of ProLong™ diamond antifade medium (Thermo Scientific) to each slide and gently apply the lid, make sure to gently remove all bubbles, and harden overnight in the fridge. Caution: The medium is highly viscose and can easily dry out. The cover slid is still moveable, even after drying. Be careful when cleaning the slide for imaging. Sealing the slide-lid combination with nail varnish can help in preventing the drying out and preserving the slides for later imaging.

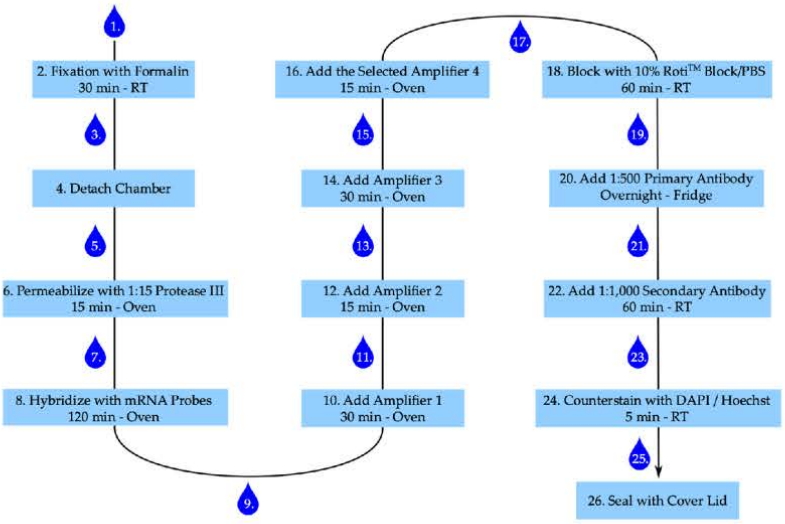

Figure 7. Staining procedure for RNAscope™ and senescence-associated heterochromatin foci. Numbering represents steps in staining procedure. Drop corresponds with washing step. RT: room temperature.

3.4. Imaging

For imaging any fluorescence microscope with appropriate filter setting or a confocal microscope is possible. We obtained the images while using a Zeiss Axiovert 200M inverted transmitted light microscope using the filter sets, as illustrated in Table 1. For image acquisition, the 40× F-Fluar objective with Immersol™ oil and the Zen software (Zeiss, Zen2 blue edition) was used. Each experiment was done in three independent experiments with duplicates for each stimulation drug. An acquisition of five images per well was done for analysis.

Table 1. Excitation/Emission Wavelength of the Dyes and Filters Used.

Dye	SPiDER SA-β-Gal	Hoechst 33342	Alexa 488	Alexa 555	Atto 647	DAPI
Beam Splitter	532	395	495	570	660	395
Filter Ex. Wavelength	500–530	335–383	450–490	538–562	625–665	335–383
Filter Em. Wavelength	545–605	420–470	500–550	570–640	665–715	420–470
Ex. Wavelength of Dye	528	348	493	553	644	348
Em. Wavelength of Dye	547	455	517	568	670	455

3.5. Quantification of Fluorescence Intensity

The fluorescence intensity per channel was quantified while using the Zen2 software (Zeiss, blue edition). Five images per well/stimulation were analyzed for three independent experiments.

3.6. Statistical Analysis

Mean ± SEM is given in the bar graph. Statistical significance between stimulation and respective control was analyzed using the Mann-Whitney-U Test. A p value < 0.05 was set as statistically significant.

4. Conclusions

In conclusion, the new experimental sets that are presented here allow for multiplexing and quantification of several markers of interest for calcification and senescence analysis in primary VSMC. This might not only help to reduce animal numbers for primary cell isolation and in vivo settings with regard to the 3R (Replacement, Reduction, and Refinement) thought of Russel and Burch [19], but also allow the visualization of markers of interest on a single cell basis.

Supplementary Materials: Supplementary materials can be found at http://www.mdpi.com/1422-0067/21/10/3475/s1.

Author Contributions: Conceptualization, M.S., J.H. and M.B.; methodology, J.H., M.S., M.B., and M.T.; experimental design and analysis, J.H., M.B. and M.S.; writing—original draft preparation, M.S., J.H. and M.B.; writing—review and editing, M.S., M.T., K.-U.E, and M.v.d.G.; visualization, J.H. and M.S.; project administration, M.S., K.-U.E. and M.v.d.G.; funding acquisition, M.S. and M.T. All authors have read and agreed to the published version of the manuscript.

Funding: The Sonnenfeld Stiftung (M.T., M.S.) the Berlin Institute of Health (M.S.) funded the research.

Acknowledgments: We thank Brigitte Egbers and Katharina Kuschfeldt for excellent technical assistance. We thank Manuel Herrmann-Fiechtner for support in figure creation.

Conflicts of Interest: The authors declare no conflict of interest. The funders had no role in the design of the study; in the collection, analyses, or interpretation of data; in the writing of the manuscript, or in the decision to publish the results.

Abbreviations

Amp-FL	Amplifier fluid
Ctrl	Control
DAPI	4′,6-diamidino-2-phenylindole
DMSO	Dimethylsulfoxide
DNA	Deoxyribonucleic acid
DMEM	Dulbeccos-modified Eagle medium
Dox	Doxorubicin
FCS	Fetal calf serum
mRNA	Messenger Ribonucleic acid
OPN	Osteopontin
PCR	Polymerase chain reaction
PBS	Phosphate-buffered saline
RT	Room temperature
rVSMC	Rat vascular smooth muscle cell
SA-β-Gal	Senescence-associated β-galactosidase
SAHF	Senescence-associated heterochromatin foci
SEM	Standard error of mean
Up_4A	Uridine adenosine tetraphosphate
VSMC	Vascular smooth muscle cell
X-Gal (BCIG)	5-bromo-4-chloro-3-indolyl-β-D-galactopyranoside

References

1. Jaminon, A.; Reesink, K.; Kroon, A.; Schurgers, L. The Role of Vascular Smooth Muscle Cells in Arterial Remodeling: Focus on Calcification-Related Processes. *Int. J. Mol. Sci.* **2019**, *20*, 5694. [CrossRef] [PubMed]
2. Nilsson, P.M.; Lurbe, E.; Laurent, S. The early life origins of vascular ageing and cardiovascular risk: The EVA syndrome. *J. Hypertens* **2008**, *26*, 1049–1057. [CrossRef] [PubMed]
3. Voelkl, J.; Lang, F.; Eckardt, K.-U.; Amann, K.; Kuro-O, M.; Pasch, A.; Pieske, B.; Alesutan, I. Signaling pathways involved in vascular smooth muscle cell calcification during hyperphosphatemia. *Cell Mol. Life Sci.* **2019**, *76*, 2077–2091. [CrossRef] [PubMed]
4. Henaut, L.; Mary, A.; Chillon, J.M.; Kamel, S.; Massy, Z.A. The Impact of Uremic Toxins on Vascular Smooth Muscle Cell Function. *Toxins* **2018**, *10*, 218. [CrossRef] [PubMed]
5. Tolle, M.; Reshetnik, A.; Schuchardt, M.; Hohne, M.; van der Giet, M. Arteriosclerosis and vascular calcification: Causes, clinical assessment and therapy. *Eur. J. Clin. Investig.* **2015**, *45*, 976–985. [CrossRef] [PubMed]
6. Sanchis, P.; Ho, C.Y.; Liu, Y.; Beltran, L.E.; Ahmad, S.; Jacob, A.P.; Furmanik, M.; Laycock, J.; Long, D.A.; Shroff, R.; et al. Arterial "inflammaging" drives vascular calcification in children on dialysis. *Kidney Int.* **2019**, *95*, 958–972. [CrossRef] [PubMed]
7. Herrmann, J.; Babic, M.; Tolle, M.; van der Giet, M.; Schuchardt, M. Research Models for Studying Vascular Calcification. *Int. J. Mol. Sci.* **2020**, *21*, 2204. [CrossRef] [PubMed]
8. Burton, D.G.; Matsubara, H.; Ikeda, K. Pathophysiology of vascular calcification: Pivotal role of cellular senescence in vascular smooth muscle cells. *Exp. Gerontol.* **2010**, *45*, 819–824. [CrossRef] [PubMed]
9. Muteliefu, G.; Shimizu, H.; Enomoto, A.; Nishijima, F.; Takahashi, M.; Niwa, T. Indoxyl sulfate promotes vascular smooth muscle cell senescence with upregulation of p53, p21, and prelamin A through oxidative stress. *Am. J. Physiol. Cell Physiol.* **2012**, *303*, C126–C134. [CrossRef] [PubMed]
10. Tuttle, C.S.L.; Waaijer, M.E.C.; Slee-Valentijn, M.S.; Stijnen, T.; Westendorp, R.; Maier, A.B. Cellular senescence and chronological age in various human tissues: A systematic review and meta-analysis. *Aging. Cell* **2020**, *19*, e13083. [CrossRef] [PubMed]
11. Carnero, A. Markers of cellular senescence. *Methods Mol. Biol. (Cliftonn. J.)* **2013**, *965*, 63–81.

12. Noren Hooten, N.; Evans, M.K. Techniques to Induce and Quantify Cellular Senescence. *J. Vis. Exp.* **2017**, *123*, 55533. [CrossRef] [PubMed]
13. Giachelli, C.M. Ectopic calcification: Gathering hard facts about soft tissue mineralization. *Am. J. Pathol.* **1999**, *154*, 671–675. [CrossRef]
14. Jensen, E. Technical review: In situ hybridization. *Anat. Rec. (Hoboken)* **2014**, *297*, 1349–1353. [CrossRef] [PubMed]
15. Wang, F.; Flanagan, J.; Su, N.; Wang, L.C.; Bui, S.; Nielson, A.; Wu, X.; Vo, H.T.; Ma, X.J.; Luo, Y. RNAscope: A novel in situ RNA analysis platform for formalin-fixed, paraffin-embedded tissues. *J. Mol. Diagn.* **2012**, *14*, 22–29. [CrossRef] [PubMed]
16. Cappetta, D.; De Angelis, A.; Sapio, L.; Prezioso, L.; Illiano, M.; Quaini, F.; Rossi, F.; Berrino, L.; Naviglio, S.; Urbanek, K. Oxidative Stress and Cellular Response to Doxorubicin: A Common Factor in the Complex Milieu of Anthracycline Cardiotoxicity. *Oxid. Med. Cell Longev.* **2017**, *2017*, 1521020. [CrossRef] [PubMed]
17. Schuchardt, M.; Tolle, M.; Prufer, J.; Prufer, N.; Huang, T.; Jankowski, V.; Jankowski, J.; Zidek, W.; van der Giet, M. Uridine adenosine tetraphosphate activation of the purinergic receptor P2Y enhances in vitro vascular calcification. *Kidney Int.* **2012**, *81*, 256–265. [CrossRef] [PubMed]
18. Yang, N.-C.; Hu, M.-L. The limitations and validities of senescence associated-β-galactosidase activity as an aging marker for human foreskin fibroblast Hs68 cells. *Exp. Gerontol.* **2005**, *40*, 813–819. [CrossRef] [PubMed]
19. Russell, W.M.S.; Burch, R.L. *The Principles of Humane Experimental Technique*; Methuen & Co Ltd.: London, UK, 1959.

IJMS
Herrmann et al.
"A novel protocol for detection of senescence and calcification markers by fluorescence microscopy"

Supplementary Material

1.1. Comparision of currently available detection methods

The suppl. Table 1 summarizes a comparison of the currently available detection methods for detection and measurement of mRNA or protein expression of mentioned senescence and osteoblastic markers during vascular calcification in cell culture experiments.

Table S1. Summary of pros and cons of currently available detection methods.

Methods	Disadvantages	Advantages
qPCR	– Bulk of cells are analyzed jointly, individual differences are not visible in this method – Quantification usually relative	– Multiple target genes can be analyzed – Analysis easily reproducible
Single Cell PCR	– Multistep, complex method – Difficult to train and error prone – Versatile hardware required	– Variety of target genes can be analyzed – Cluster analysis provides additional information
Immunohistochemistry	– Due to issues of specificity of antibodies often requires extensive protocol establishment – Monoclonal and polyclonal antibodies are of animal origin and can suffer from batch variances – Development of suitable protocol (blocking, pretreatment, etc.) often time and material consuming process – Only Semi-Quantification possible – Limited number of targets – Multiplexing can be complicated, especially if different secondary antibodies are employed	– Procedure with functioning protocol easily manageable, easy to teach and learn – Recombinant antibodies are animal free produced and have less issues with batch variances – Few hardware required – Multiplexing possible
RNA In Situ Hybridization	– Depending on the protocol, the number of targets is limited; in the presented protocol, the number of targets that can be analyzed parallelly is	– Different labeling and detection possible (radioactive, fluorescence and immunohisto-chemistry) – Huge variety of targets can

	limited to 3 – Extensive hardware required	be analyzed, as probes can be custom designed to targets – Single cell analysis in the tissue context is possible – Multiple target genes can be analyzed at once – Small growth area reduces necessary number of cells, working hours and material
X-Gal	– Long incubation time – Process of staining vulnerable to external influences (e.g., pH variation due to long staining times) – Semi-Quantification difficult – No Multiplexing	– Cheap – Frequently published protocol – Little hardware required –
SPiDER™ ß Gal Stain	– Multiplexing is difficult, as permeabilization of cells usually required for multiplexing facilitates washout of stain – Extensive hardware required	– Short and easy staining – Semi-Quantification possible, as image is easy to visualize – Multiplexing is possible

1.2. Reagents for cell stimulation

Table S2. Reagents for cell stimulation

Material	Company	Order Number
Doxorubicin hydrochloride	Thermo Fisher	BP2516-10
Up4A	Jena Bioscience	NU-528S

1.3. Kits and antibodies for fluorescence detection

Table S3. Kits and antibodies for fluorescence detection

Material	Company	Order Number
SPiDER™	Gerbu Biotechnologie	SG02-10
RNAscope™ Target Retrieval Reagents Containing: Protease III	ACD Bio	322000
RNAscope™ Fluorescent Multiplex Reagent Kit Containing: Amp 1-FL	ACD Bio	320850

Amp 2-FL Amp 3-FL Amp 4-FL DAPI		
RNAscope™ Wash Buffer Reagents	ACD Bio	310091
ImmEdge™ Hydrophobic Barrier Pen	ACD Bio	310018
RNAscope™ Probe - Rn-Cdkn1a	ACD Bio	423851-C3
RNAscope™ Probe - Rn-Spp1	ACD Bio	405441
RNAscope™ 3-plex Positive Control Probe - Rn	ACD Bio	320891
RNAscope™ 3-plex Negative Control Probe - Rn	ACD Bio	320871
Anti-Histone H2A.X (phospho S139) antibody [EP854(2)Y]	abcam	ab215967
Goat anti-Rabbit IgG (H+L) Highly Cross-Adsorbed Secondary Antibody, Alexa Fluor 555	Invitrogen	A-21429
ProLong™ Diamond antifade medium	Thermo Fisher Scientific	P10144

Manuscript 3: Stressor-Induced “Inflammaging” of Vascular Smooth Muscle Cells via Nlrp3-Mediated Pro-inflammatory Auto-Loop

This manuscript has been published in *Frontiers in Cardiovascular Medicine (IF: 6.050):*

Herrmann J, Xia M, Gummi MR, Greco A, Schacke A, van der Giet M, Tolle M, Schuchardt M. Stressor-Induced "Inflammaging" of Vascular Smooth Muscle Cells via Nlrp3-Mediated Pro-inflammatory Auto-Loop. *Front Cardiovasc Med.* 2021;8(1932):752305.

DOI: https://doi.org/10.3389/fcvm.2021.752305

The authors’ contributions are stated in the publication on page 12/13. My personal contribution to this article encompasses:

Laboratory work:

- Execution of experiments (including cell isolation, culture and stimulation):
  - RNA *in situ* staining, immunhistological staining, ROS staining and SA-ß-Gal staining; microscopic imaging, data analysis and quantification
  - Measurement and analysis of gene expression and cytokine secretion
  - Measurement of *in vitro* and *ex vivo* calcification

Manuscript preparation:

- Writing of the original draft, adaption after revision and final editing

frontiers in Cardiovascular Medicine

ORIGINAL RESEARCH
published: 20 December 2021
doi: 10.3389/fcvm.2021.752305

Stressor-Induced "Inflammaging" of Vascular Smooth Muscle Cells via Nlrp3-Mediated Pro-inflammatory Auto-Loop

Jaqueline Herrmann[1,2], *Mengdi Xia*[1,3], *Manasa Reddy Gummi*[1], *Anna Greco*[1], *Annika Schacke*[1], *Markus van der Giet*[1]*, *Markus Tölle*[1] *and Mirjam Schuchardt*[1]

[1] *Department of Nephrology and Medical Intensive Care, Charité – Universitätsmedizin Berlin, Cooperate Member of Freie Universität and Humboldt Universität, Berlin, Germany,* [2] *Department of Chemistry, Biochemistry and Pharmacy, Freie Universität Berlin, Berlin, Germany,* [3] *Department of Nephrology, Second Clinical Medical Institution of North Sichuan Medical College (Nanchong Central Hospital), Nanchong, China*

OPEN ACCESS

Edited by:
Masuko Ushio-Fukai,
Augusta University, United States

Reviewed by:
Delphine Gomez,
University of Pittsburgh, United States
David Anthony Tulis,
The Brody School of Medicine at East Carolina University, United States
Margreet R. De Vries,
Leiden University Medical Center, Netherlands

***Correspondence:**
Markus van der Giet
markus.vandergiet@charite.de

Specialty section:
This article was submitted to Atherosclerosis and Vascular Medicine, a section of the journal Frontiers in Cardiovascular Medicine

Received: *02 August 2021*
Accepted: *29 November 2021*
Published: *20 December 2021*

Citation:
Herrmann J, Xia M, Gummi MR, Greco A, Schacke A, van der Giet M, Tölle M and Schuchardt M (2021) Stressor-Induced "Inflammaging" of Vascular Smooth Muscle Cells via Nlrp3-Mediated Pro-inflammatory Auto-Loop. Front. Cardiovasc. Med. 8:752305. doi: 10.3389/fcvm.2021.752305

Calcification of the vessel wall as one structural pathology of aged vessels is associated with high cardiovascular mortality of elderly patients. Aging is linked to chronic sterile inflammation and high burden of reactive oxygen species (ROS), leading to activation of pattern recognition receptors (PRRs) such as Nlrp3 in vascular cells. The current study investigates the role of PRR activation in the calcification of vascular smooth muscle cells (VSMCs). Therefore, *in vitro* cell culture of primary rat VSMCs and *ex vivo* aortic stimulations were used to analyze osteogenic, senescence and inflammatory markers via real-time PCR, *in situ* RNA hybridization, Western Blot, photometric assays and histological staining. Induction of ROS and DNA-damage by doxorubicin induces a shift of VSMC phenotype toward the expression of osteogenic, senescence and inflammatory proteins. Induction of calcification is dependent on Nlrp3 activity. Il-1β as a downstream target of Nlrp3 induces the synthetic, pro-calcifying VSMC phenotype. Inhibition of PRR with subsequent reduction of chronic inflammation might be an interesting target for reduction of calcification of VSMCs, with subsequent reduction of cardiovascular mortality of patients suffering from vessel stiffness.

Keywords: calcification, senescence, inflammation, Nlrp3, smooth muscle cell

INTRODUCTION

Cardiovascular disease (CVD) is the most critical age-related cause of death. Almost 70% of patients with new CVD are over 75 years old, so that the age might be the most prominent cardiovascular risk factor (1). One sign of structural pathology of the vessel wall associated with vascular aging is medial calcification, leading to increased vessel stiffness and pulse-wave velocity (2, 3). Medial calcification is common in patients with other comorbidities as e.g., chronic kidney disease (CKD) (2, 4, 5). Until now, no therapy exists to effectively reduce the increased cardiovascular risk associated with vessel calcification (3).

In particular involved in calcification of the medial layer of the vessel wall is the accumulation of senescent vascular smooth muscle cells (VSMCs) with a senescence-associated secretory phenotype (SASP) (6). Senescent cells express typical senescence markers [e.g., p53/p21, lysosomal senescence-associated β-galactosidase activity (SA-β-Gal), γH2A.X], and show an increased

vulnerability to exogenous stressors (7–9). VSMCs physiologically have a contractile phenotype and express specific VSMC marker proteins (e.g., SM22α, Myh11, Cnn1, Acta2). Due to phenotype plasticity, VSMCs can adapt an osteoblast-like phenotype characterized by decreased expression of VSMC markers and increased expression of osteoblast markers e.g., core binding factor alpha-1 (Cbfa-1), tissue non-specific alkaline phosphatase (Alp), osteopontin (Opn), and bone morphogenetic protein-2 (Bmp-2) (9, 10). Recently, Shanahan's group pointed out that the DNA damage-induced calcification is dependent on activation of Cbfa1 in VSMCs (11). They found Cbfa1 to be involved in DNA damage response and therefore bridging osteogenic transition and apoptosis in the mineralization process (11).

During physiological aging, a chronic sterile inflammation, known as "inflammaging," develops. This "inflammaging" is primarily based on mechanisms of the innate immune system that involve activation of pattern recognition receptors (PRRs) (12, 13). PRRs are a link between inflammation and cellular senescence. PRRs are mainly transmembrane toll-like receptors (Tlrs) and cytoplasmic Nod-like receptor (Nlr) inflammasomes (14). The Nlrp3 is the best characterized inflammasome and is expressed in VSMCs (15). The activation of Nlr inflammasomes induces the secretion of Il-1 cytokines e.g., Il-1β (16). Il-1β has strong pro-inflammatory effects by activating different Il-1 receptors (Il-1Rs). It induces the expression of other pro-inflammatory cytokines, especially Il-6, and can increase its own expression by a positive feedback mechanism (17). Cytokines and chemokines as major pro-inflammatory mediators can contribute to chronic inflammation and senescence (18).

Doxorubicin (DOX) is an anthracycline antitumor drug (19). DOX is known to induce several kinds of DNA damages by intercalation, generation of free radicals, DNA-binding, alkylation and cross-linking, DNA strands separation, influenced helicase activity and inhibition of topoisomerase II (19). Previous studies have not only investigated effects of DOX on stress-induced senescence (20) but also, induction of Alp activity upon DOX treatment; however, only after seven days of treatment (20). In addition, recent studies have shown the important role of DNA-damage response and the Cbfa1-dependent link to the calcification process of VSMCs (9, 11). Cobb et al. pointed out that the DNA damage-induced calcification is dependent on activation of Cbfa1 in VSMCs (11). They found Cbfa1 to be involved in DNA damage response and therefore bridging osteogenic transition and apoptosis in the mineralization process (11).

However, there are no detailed studies on the relationship of stress-induced senescence as e.g., caused by DOX, subsequent activation of Nlrp3-dependent pro-inflammatory signaling and calcification in VSMCs. We aim to show that stressor-induced senescence in VSMCs results in a pro-inflammatory response and induction of calcification. Accordingly, we used DOX as stressor. We are aware that DOX might not reflect the whole spectrum of senescence induction in VSMCs; however, DNA damage, upregulated under treatment with DOX, is a known and well-documented inducer of cellular senescence (9, 11).

Therefore, the current study investigates the effects of the stressor DOX on the initiation of processes of acute "inflammaging" and vascular calcification. The increase in calcification upon DOX treatment was dependent on the activation of the Nlrp3 inflammasome. Il-1β as Nlrp3 downstream effector amplifies its own expression. The initial stressor-induced acute "inflammaging" process then can be continued via a Nlrp3 inflammasome-mediated auto-inflammatory loop resulting in SASP and calcification of VSMCs.

MATERIALS AND METHODS

All cell culture components were obtained from Biochrom AG and Bio and Sell. DOX was obtained from Thermo Fisher. Recombinant rat Il-6 and Il-1β were purchased from PeproTech. VAS2870 was obtained from Sigma Aldrich and MCC950 from Invivogen. Tiron was purchased from Biozol and TAK242 from Biomol.

Animals

All experiments with animals were done under minimal animal suffering and in accordance with the EU Directive 2010/63/EU. The experiments were approved by the Landesamt fuer Gesundheit und Soziales Berlin (T0211/02), Germany and the Charité - Universitätsmedizin Berlin, Germany.

Wistar rats were purchased from Janvier Labs. Nlrp3$^{-/-}$ and Nlrp3$^{+/+}$ (genetic background: C57BL/6) were bred at the Charité-Universitätsmedizin Berlin animal facility.

Euthanasia of animals was accomplished with intraperitoneal injection of sodium pentobarbital (rats: 400 mg/kg body weight, mice: 200 mg/kg body weight).

VSMCs Cell Culture

Primary rat VSMCs from aortic tissue (aortic arch and thoracic aorta) of Wistar rats (mean age 4 months, male/female) were cultured by the outgrowth technique described previously (21). VSMCs at passages 3 to 7 were used for experiments. Cells were cultured in a humidified incubator at 37°C with 5% carbon dioxide. If not stated otherwise, VSMCs were cultured in Dulbecco Modified Eagle Medium (DMEM) containing 1 g/l glucose, supplemented with 10% fetal calf serum (FCS), penicillin (100 U/ml) and streptomycin (0.1 mg/ml) (culture medium). For gene expression, ROS detection, protein secretion and immunohistology experiments, cells were serum-starved for

Abbreviations: Acta2, Actin alpha 2; Alp, Alkaline Phosphatase; Asc, Apoptosis-Associated Speck-like Protein Containing a Caspase-Recruitment Domain; ATM, Ataxia–Telangiectasia Mutated; BCA, Bicinchonic Acid; Bmp-2, Bone Morphogenetic Protein-2; Calc M, Calcification Medium; Cbfa-1, Core Binding Factor alpha 1; Cnn1, Calponin; Ctrl M, Control Medium; CVD, Cardiovascular Disease; DAMP, Damage Associated Molecular Pattern; DHE, Dihydroethidium; DMEM, Dulbecco's Modified Eagle Medium; DOX, Doxorubicin; FCS, Fetal Calf Serum; Il-1β, Interleukin 1 β; Il-6, Interleukin 6; Myh11, Myosin Heavy Chain 11; Nlr, Nod-like Receptor; Nlrp3, Nod-like receptor family pyrin domain containing 3; Opn, Osteopontin; PBS, Phosphate Buffered Saline; PRRs, Pattern Recognition Receptors; ROS, Reactive Oxygen Species; Tlr, Toll-like Receptor; SA-β-Gal, Senescence Associated β-Galactosidase; SASP, Senescence Associated Secretory Phentoype; Sm22α, Smooth Muscle Protein 22-alpha; VSMCs, Vascular Smooth Muscle Cells.

24 h and stimulated using DMEM with 4.5 g/l glucose (w/o phenol red), supplemented with 1% glutamine, penicillin (100 U/ml) and streptomycin (0.1 mg/ml).

Preparation of Aortic Rings for *ex vivo* Experiments

For *ex vivo* stimulation of aortic tissue, the adventitia was removed. Thoracic aortas of rats (mean age 4 months, male) or Nlrp3$^{-/-}$ and Nlrp3$^{+/+}$ mice (mean age 11 months, male/female) were dissected into aortic rings of equal size and incubated in a well-plate with the respective stimulation medium for 24 h or 14 days, respectively. Each stimulation contained several aortic rings from different aortic parts (aortic arch, different segments of descending aorta proximal to distal), which were equally distributed between stimulation and respective controls. The incubation procedure of the tissue took place in a humidified incubator at 37°C and 5% carbon dioxide.

In vitro and *ex vivo* Calcification

Calcification was induced by exposing VSMCs or aortic rings (rat and mice) to DMEM containing 4.5 g/l glucose, supplemented with 15% FCS, 284 μmol/l ascorbic acid and 5 mmol/l inorganic phosphate, penicillin (100 U/ml) and streptomycin (0,1 mg/ml) [Calcification Medium (Calc M)]. As Control Medium (Ctrl M) served DMEM containing 4.5 g/l glucose, supplemented with antibiotics. Calcification was induced over 14 days of stimulation with Ctrl M, Calc M and in co-stimulation with DOX (10 or 100 nmol/l), Il-6 (100 ng/ml), Il-β (100 ng/ml) and MCC950 (50 μmol/l). Medium was replaced every two to three days.

Gene Expression

VSMCs were serum-starved for 24 h prior to stimulation for 48 h. Cells were washed after stimulation with phosphate buffered saline (PBS) on ice and lysed with RLT^{TM} cell lysis buffer (Qiagen). RNA was isolated according to the RNeasy^{TM} Mini kit protocol (Qiagen). The RNA was reverse transcribed using the High-Capacity cDNA Reverse Transcription Kit^{TM} (Applied Biosystems) according to the manufacturer's instructions. For the quantitative determination of mRNA expression, the iQ^{TM} SYBR Green SuperMix and the CFX384 real-time PCR detection system (Biorad, CFX software version 3.1) were used. The oligonucleotides (**Supplementary Table 1**) were synthesized by TibMolBiol. Each sample was performed as technical duplicate for real-time PCR. β-actin and Gapdh were used as housekeeper genes for normalization. Analysis was performed with the ΔΔCT-method.

Measurement of Alp Activity

After stimulation, VSMCs were lysed and scraped in 0.2% Triton X/PBS lysis buffer. Alp activity was assessed using a p-nitrophenyl phosphate-based Alp Assay Kit (Abcam) according to the manufacturer's recommendations. Protein content was determined with the bicinchoninic acid (BCA) protein assay kit (Pierce) and was used for normalization. Photometric measurements were conducted with a Multiskan Spectrum (Thermo Electron Corporation).

Quantification of Calcium Content

For quantification of calcification, VSMCs or aortic rings were decalcified in 0.6 mol/l HCl overnight or for 24 h, respectively. After decalcification, cells were washed with PBS and lysed in 0.1 mol/l NaOH/0.1% SDS buffer. The protein content was quantified using BCA protein assay kit (Pierce). Aortic rings were dried and weighed. Calcium content was quantified using the colorimetrical o-cresolphthalein method (Colorimetric Calcium Assay, ScienCell) according to the manufacturer's recommendation. Photometric measurements were conducted with a Multiskan Spektrum (Thermo Electron Corporation). Protein content (*in vitro*) or aortic dry weight (*ex vivo*) was used for normalization, respectively.

Histological Staining of Calcium Deposits

Upon stimulation of VSMCs for 14 days, the cells were fixed with 4% buffered formaldehyde, washed with PBS and distilled deionized water and treated with Alizarin Red solution (2%, pH 4.2) for 20 min, then washed again and imaged.

Upon stimulation of aortic rings for 14 days, the tissue was fixed overnight, transferred to 70% ethanol, and embedded in paraffin via automatic procedure. The aortas were serially cut into 4 μm sections, stained with Alizarin Red solution (0.5%, pH 4.2) and imaged. For all histological imaging, the Axiovert 200M microscope (Zeiss) with Zen2 software (Blue edition, Zeiss) was used.

ROS Staining

VSMCs were seeded in 8-well slides (LabTec, Thermo Fisher, μ-slide, Ibidi), serum-starved for 24 h, and stimulated for 30 min as indicated. Afterwards, cells were washed and treated with 30 μmol/l dihydroethidium (DHE) (Molecular Probes) for 30 min. Cells were fixed with cold formalin (4%) for 5 min and subsequently washed with PBS. LabTec were mounted with ProLong^{TM} Gold antifade mount (Thermo Fisher) and stored in the dark until imaging. For μ-slides, wells were covered with PBS and immediately imaged. A more detailed description of the staining procedure and data analysis can be found in the **Supplementary Material**. For all imaging of fluorescence stainings, an Axiovert 200M microscope (Zeiss) with Zen2 software (Blue edition, Zeiss) was used.

Immunohistology and mRNA *in situ* Staining

VSMCs were stained for SA-β-Gal activity, histone γH2A.X, Bmp-2, Opn and p21 mRNA according to a previously published protocol (22) with some modifications. Briefly, cells were seeded in 8-well LabTec chamber slides (Thermo Fisher) or μ-slide (Ibidi), serum-starved for 24 h and stimulated for 48–72 h. Cells were stained for the desired target and imaged. A more detailed description of the staining procedure and data analysis can be found in the **Supplementary Material**. Quantification of fluorescence intensity was done with Zen2 (Blue edition, Zeiss) and Fiji/ImageJ.

Western Blot

VSMCs were stimulated with DOX (500 and 1,000 nmol/l) and Il-1β (100 ng/ml) in cell culture medium for 48 h. For protein extraction, cells were washed with ice-cold PBS and lysed in cold RIPA buffer (Thermo Fisher Scientific). Protein content was assessed with BCA protein assay kit (Pierce). 15–10 μg protein per lane (p21: 15 μg, all others 10 μg) was applied on the respective gel. Protein samples were mixed and dissolved in 4× Laemmli buffer (Biorad) and heated to 95°C for 15 min. The proteins were separated on 12% TGX Gels (Biorad) and transferred onto a polyvinylidene difluoride membrane. The membranes were immunoblotted overnight at 4°C with primary antibodies: rabbit anti-p21 (1:2,500, ab109199, Abcam), rabbit anti-Alp (1:500, 7H11L3, Invitrogen), rabbit anti-Cbfa1 (1:1,1000, sc-10758, Santa Cruz), and mouse anti-β-actin (1:5,000 8H10D10, Cell Signaling Technology). After washing five times for five min each with TBST, the membranes were incubated with conjugated fluorescent secondary antibodies [anti-rabbit-StarBright Blue700 (1:2,500, #12004162, Biorad) and anti-mouse-StarBright Blue520 (1:2,500, #12005867)]. The bands were visualized using a ChemiDoc MP Imaging System (Biorad).

Luminex™

VSMCs were serum-starved for 24 h prior to stimulation with Il-1β (100 ng/ml) and respective antagonists [VAS2870 (10 μM), MCC950 (50 μM), Tiron (10 mM), TAK242 (10 μM)] for 48 h. Rat aortic rings were stimulated with DOX (1000 nmol/l) and MCC950 (50 μM) for 24 h. After stimulation, supernatant was collected for cytokine quantification. Cytokine concentrations in the supernatant were determined using the Milliplex™ Cytokine Kit (Millipore) according to the manufacturer's instructions. Measurements were conducted using the Bio-Plex device and respective Bio-Plex software (version 6.1, Biorad). Cells were washed with cold PBS and lysed in NP40 buffer, followed by protein quantification using BCA protein assay kit (Pierce). Aortic rings were dried and weighed for normalization.

Statistical Analysis

Data are provided as mean ± SEM of at least 3 independent experiments. Statistical analysis was performed using GraphPad Prism software (version 6.0). The one-way Anova with multiple comparisons or Wilcoxon matched paired test were applied to evaluate differences between treatment groups. A p-value < 0.05 was considered as statistically significant.

RESULTS

Stressor-Induced Calcification With Osteogenic Transition

Stimulation with calcifying medium robustly induced calcification of VSMCs after 14 d (**Figure 1A**). Co-stimulation with DOX significantly and dose-dependently reinforced calcification of VSMCs *in vitro*: quantification (**Figure 1A**) shows a significant and dose-dependent induction of calcification under co-stimulation of calcification medium and DOX. This is also visualized by Alizarin Red staining (**Figure 1B**). To confirm these *in vitro* findings, an *ex vivo* setting using aortic rings was conducted. Calcium content of rat aortic rings was quantified upon 14 d of stimulation, and calcification was visualized via Alizarin Red staining (**Figures 1C,D**). DOX stimulation in calcifying medium dose-dependently increases calcium deposition *ex vivo*.

Further evidence for the pro-calcifying potential of DOX derives from mRNA detection of osteogenic markers as Bmp-2, Cbfa1 and Opn, all of them significantly increased upon DOX stimulation. VSMC marker as Acta2, Cnn1, Myh11, and SM22α slightly, but not significantly, decreased under stimulation with DOX (**Figure 2A**). The osteogenic transition is further confirmed by detection of Alp activity increase upon DOX treatment (**Figure 2B**). The induction of calcification markers after stimulation with DOX was confirmed by *in situ* hybridization analysis for Bmp-2 and Opn. Both markers were visualized via fluorescence staining and quantified by counting signal dots per whole image (**Figure 2C**). Although DOX influences cell behavior and growth, the cytotoxicity of DOX in our cell model did not reach statistical significance in the used setting (**Supplementary Figure 1**).

Stressor-Induced Induction of "Inflammaging"

Il-1β and Il-6 are known essential components of the SASP (23). Therefore, we investigated the effect of DOX on the expression of both cytokines. DOX induced Il-1β and Il-6 mRNA expression in VSMCs (**Figure 3A**). It is already known from the literature that the Nlrp3 inflammasome is involved in the phenotype switching of VSMCs and in Il-β production (15). Therefore, we measured the mRNA expression of Nlrp3, its cofactor Asc and the associated enzyme caspase-1 that cleaves the preform of Il-1β (pre-Il-1β) into active Il-1β. The mRNA expression of all three proteins was significantly increased upon DOX stimulation (**Figure 3A**). Also, the secretion of Il-1β was significantly upregulated after DOX stimulation, while no significant secretion of Il-6 was found upon DOX treatment. The DOX-induced Il-1β secretion was reduced by co-stimulation with Nlrp3 inhibitor MCC950 (**Figure 3B**). As Il-1β and Il-6 are both components of the SASP, we tested the pro-calcifying potential of both substances and found Il-1β to significantly induce calcification, whereas Il-6 did not exhibit calcifying potential in our model (**Figure 3C**). To validate the role of the Nlrp3 inflammasome for calcification, we used an *ex vivo* setting with aortic rings from Nlrp3$^{-/-}$ and respective control mice (Nlrp3$^{+/+}$). While DOX significantly induced aortic calcification in Nlrp3$^{+/+}$, the effect is lost in aortas from Nlrp3$^{-/-}$ mice (**Figure 3D**).

To further verify the involvement of Il-1β as effector molecule of the Nlrp3 inflammasome and of Il-6, we investigated their effect on mRNA expression of inflammation, senescence and calcification markers using real-time PCR and *in situ* hybridization. Il-1β significantly induces the expression of Il-6 and, in the context of a very potent pro-inflammatory auto-loop, Il-1β itself. In addition, Il-1β induces the expression of Nlrp3 (**Figure 4A**). Upon Il-1β treatment, VSMCs release

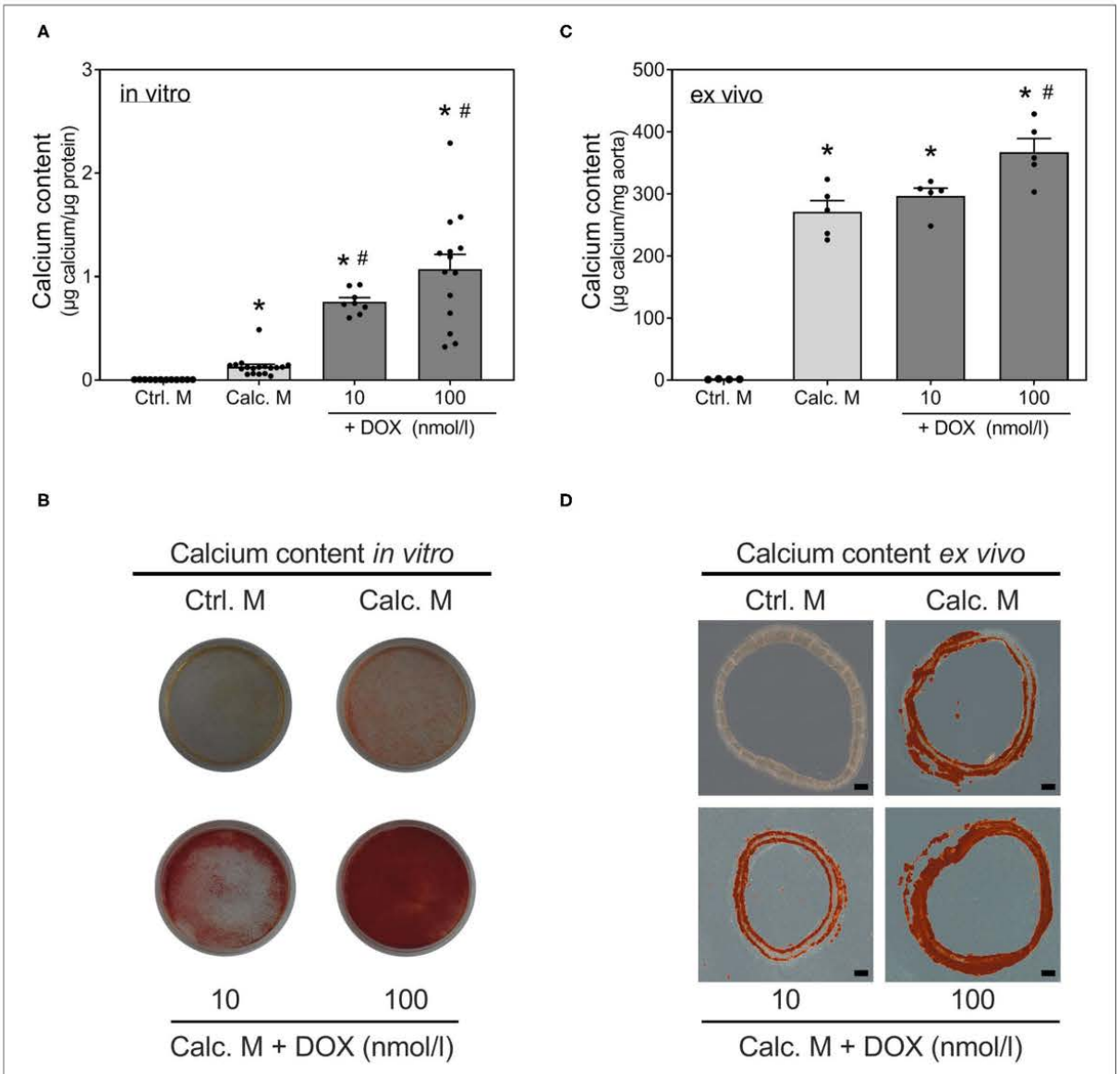

FIGURE 1 | Induction of calcification with doxorubicin. VSMCs **(A,B)** or rat aortic rings **(C,D)** were stimulated with control medium or calcification medium supplemented with DOX as indicated for 14 d. Calcium content was quantified with o-cresolphthalein **(A,C)** and normalized to protein content (µg) **(A)** or aortic weight (mg) **(C)**. Calcium deposits were stained with Alizarin Red **(B,D)**. Data represent mean ± SEM, $n \geq 3$, $^*p < 0.05$ vs. indicated control, $\#p < 0.05$ vs. calcification medium. Pictures show one representative experiment of $n \geq 3$ **(B,D)**, the scale bar indicates a 200 µm section **(D)**.

Il-6 (**Figure 4B**). While the Il-1β-induced expression of the osteogenic marker Bmp-2 increased, the VSMCs marker SM22α, Acta2, and Cnn1 decreased upon Il-1β (**Figure 4C**). The increased mRNA expression of Bmp-2 upon Il-1β stimulation was confirmed by *in situ* hybridization technique. While for Opn mRNA expression via real-time PCR no significant effect could be detected, the *in situ* hybridization found a slight induction (**Figure 4D**).

As already shown in **Figures 1–4**, both DOX and Il-1β induce several markers of calcification. In addition, the protein expression of Cbfa1 and Alp, detected via Western Blot, is increased upon DOX and Il-1β, respectively (**Figures 5A,B**). However, the effects of Il-1β and DOX on senescence markers differ in our experimental model. As shown in **Figure 5C**, ROS (superoxide production) is significantly increased by DOX and Il-1β. ROS are one inducer of DNA damage, which can

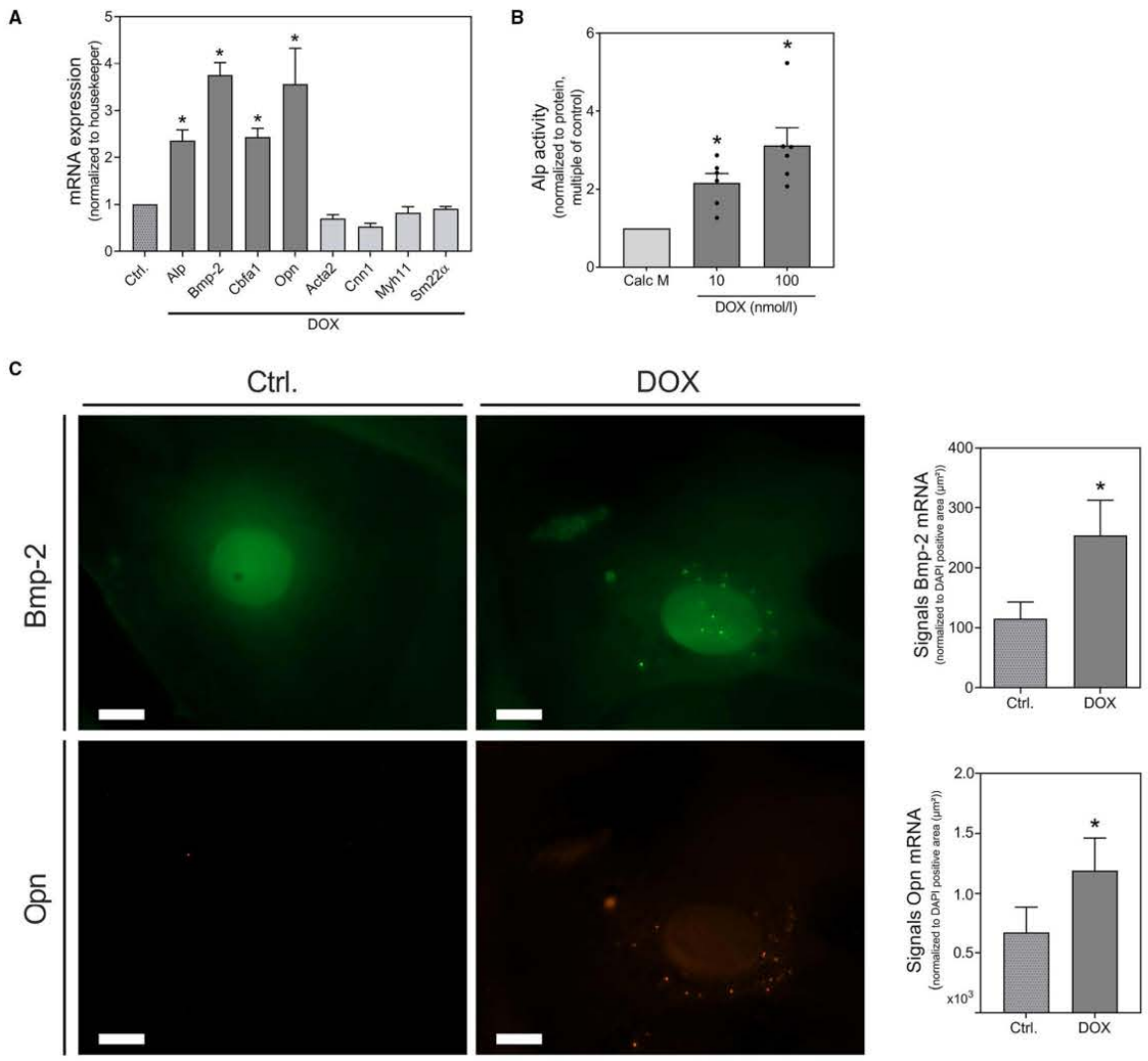

FIGURE 2 | Induction of osteoblastic trans-differentiation by doxorubicin. VSMCs were stimulated in quiescence medium **(A,C)** or calcification medium **(B)** with DOX as indicated or 1,000 nmol/l for 48 h **(A,C)** or 14 d **(B)**. mRNA expression was measured with quantitative real-time PCR **(A)**. Measured thresholds of the respective targets were normalized to the corresponding threshold of housekeeper gene actin before normalization to control **(A)**. Alp activity was measured with a p-nitrophenyl phosphate-based Alp Assay and normalized to protein content (µg/µl) before normalization to control **(B)**. mRNA expression of Bmp-2 and Opn were visualized with RNA *in situ* hybridization staining and were quantified by counting signal dots per whole image, normalized to the DAPI positive cell core area per image (μm^2) **(C)**. Data represent mean ± SEM, $n \geq 3$, $^*p < 0.05$ vs. control. Pictures show a section of a representative experiment of $n \geq 3$, the scale bar indicates a 10 µm section **(C)**. Full representative images are shown in **Supplementary Table 3**.

result in double-strand DNA breaks. A marker of double-strand DNA breaks, the formation of γH2A.X, was significantly increased upon DOX treatment, while it is not affected by Il-1β stimulation (**Figure 5C**). In line, while DOX stimulation results in upregulated expression of the senescence markers p21 and SA-β-Gal, both were not induced by Il-1β (**Figure 5C**). This could be confirmed by p21 protein detection via Western Blot (**Figure 5D**). mRNA detection via real-time PCR confirmed the findings of increased p21 mRNA expression upon DOX (**Figure 5E**) and no effect on p21 expression upon Il-1β treatment (**Figure 5F**). Neither DOX nor Il-1β induced p16 mRNA expression in our cell model (**Figures 5E,F**).

Involved Signaling Pathway

As Il-1β strongly stimulates its own expression, we tested possible mediators of the signaling pathway involved in Il-1β-induced

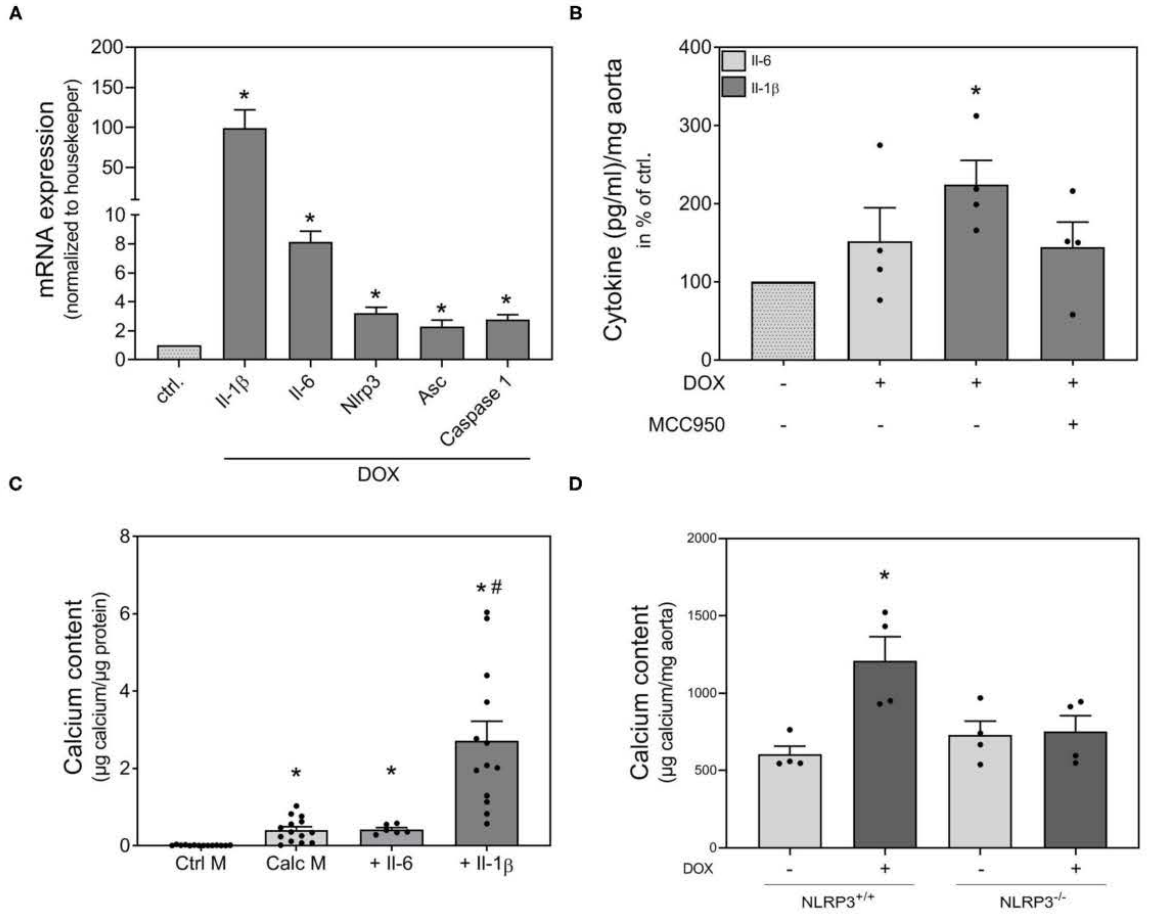

FIGURE 3 | Involvement of Nlrp3 in doxorubicin induced calcification. VSMCs **(A,C)** were stimulated as indicated with 1,000 nmol/l DOX **(A)**, 100 ng/ml Il-1β **(C)** and 100 ng/ml Il-6 **(C)** for 48 h **(A)** or 14 d **(C)** in quiescence medium **(A)**, control medium (Ctrl. M) **(C)** or calcification medium (Calc M) **(C)**. Aortic rings from rats were stimulated in quiescence medium with 1,000 nmol/l DOX and MCC950 (50 µM) as indicated for 24 h **(B)**. Aortic rings from Nlrp3$^{-/-}$ mice and respective controls were stimulated for 14 d in calcification medium with DOX (100 nmol/l) as indicated **(D)**. mRNA expression was measured with quantitative real time PCR **(A)**. Measured thresholds of the respective targets were normalized to the corresponding threshold of housekeeper gene actin before normalization to control **(A)**. Protein secretion was assessed with Luminex™ and normalized to aortic weight (mg) **(B)**. Calcium content was quantified with *o*-cresolphthalein **(C,D)** and normalized to protein content (µg) **(C)** or aortic weight **(D)**. Data represent mean ± SEM, $n \geq 3$, $^*p < 0.05$ vs. control, $\#p < 0.05$ vs. Calc M.

SASP activation. A schema of the Nlrp3 inflammasome activation and the therefore used antagonists is provided in **Figure 6A**. MCC950 was used as Nlrp3 inhibitor. It is already known from the literature that Tlrs work as one initial stimulus for Nlrp3 assembly and that the activation of Tlr2 and Tlr4 are involved in Il-1β release (24, 25). A previous study by our own working group has shown that the Tlr4 is constitutively active in our VSMCs cell model, whereas the Tlr2 is subsequently activated (26). Therefore, we tested the Tlr4 inhibitor TAK242. As increased ROS production serves as second stimulus for Nlrp3 activation (25), we also tested tiron as ROS scavenger. In VSMCs, the NADPH oxidase is one of the leading ROS producers (27). Therefore, the Nox1 inhibitor VAS2870 was also used. Both, Tlr2 as well as Tlr4 expression (first stimulus) and Nox1 expression (second stimulus), were induced in VSMCs upon Il-1β stimulation (**Figure 6B**). Both signals for Nlrp3 assembly could be significantly diminished by co-treatment with VAS2870 and tiron (**Figures 6C,D**). Nlrp3 mRNA expression itself was also diminished by tiron and MCC950 co-treatment, while VAS2870 and TAK242 have no significant effect (**Figure 6E**). Downstream, the Il-1β expression is significantly blocked by VAS2870, tiron, TAK242, and MCC950 (**Figure 6F**). The secretion of Il-6 could be significantly reduced by inhibition of ROS via tiron and Nlpr3 inhibition via MCC950 (**Figure 6G**). To verify the role of the Nlrp3-dependent pathway, we also tested Nlrp3 inhibition with MCC950 for calcification as endpoint. As shown in **Figure 6H**,

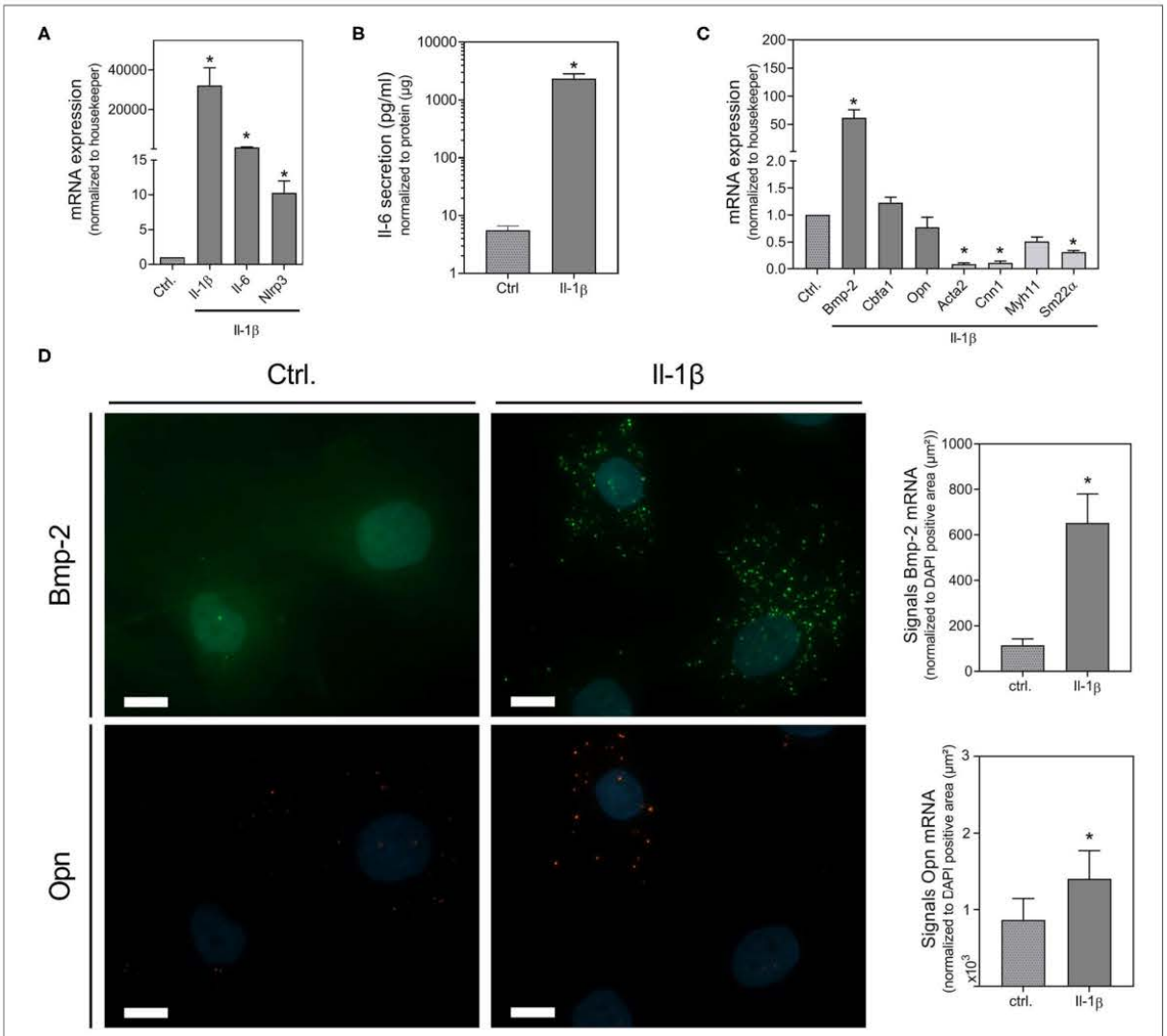

FIGURE 4 | Il-1β induced changes in osteoblastic and pro-inflammatory gene expression and protein secretion. VSMCs were stimulated for 48 h with 100 ng/ml Il-1β. mRNA expression was measured with quantitative real-time PCR **(A,C)**. Measured thresholds of the respective targets were normalized to the corresponding average threshold of housekeeper genes actin and Gapdh before normalization to control **(A,C)**. Secretion of Il-6 was measured with Luminex™ and normalized to protein content (µg) **(B)**. Expression of Bmp-2, Opn were visualized with RNA *in situ* hybridization staining and were quantified by counting signal dots per whole image, normalized to the DAPI positive cell core area per image (μm^2) **(D)**. Data represent mean ± SEM, $n \geq 3$, $^*p < 0.05$ vs. control, pictures show a section of a representative experiment of $n \geq 3$, the scale bar indicates a 10 µm section **(D)**. Full representative images are shown in **Supplementary Table 4**.

both the DOX-and Il-β-induced calcifications are significantly inhibited by MCC950 co-treatment.

DISCUSSION

In the current study, we investigated the effect of ROS induction, DNA damage, and inflammation on the process of cellular senescence and calcification in *in vitro* and *ex vivo* models using rat VSMCs and thoracic aortas from rats and mice. After induction of ROS and DNA-damage by the primary stressor, the Nlrp3 inflammasome is activated with a subsequent auto-inflammatory loop driven by its effector molecule Il-1β.

As primary stressor molecule for VSMCs the anthracycline DOX was used. It has already been shown in literature that DOX causes DNA damage via induction of double strand breaks and ROS and promotes cellular senescence (20). Bielak-Zmijewska et al. investigated several markers of senescence in VSMCs upon DOX treatment (20). Although DOX might not

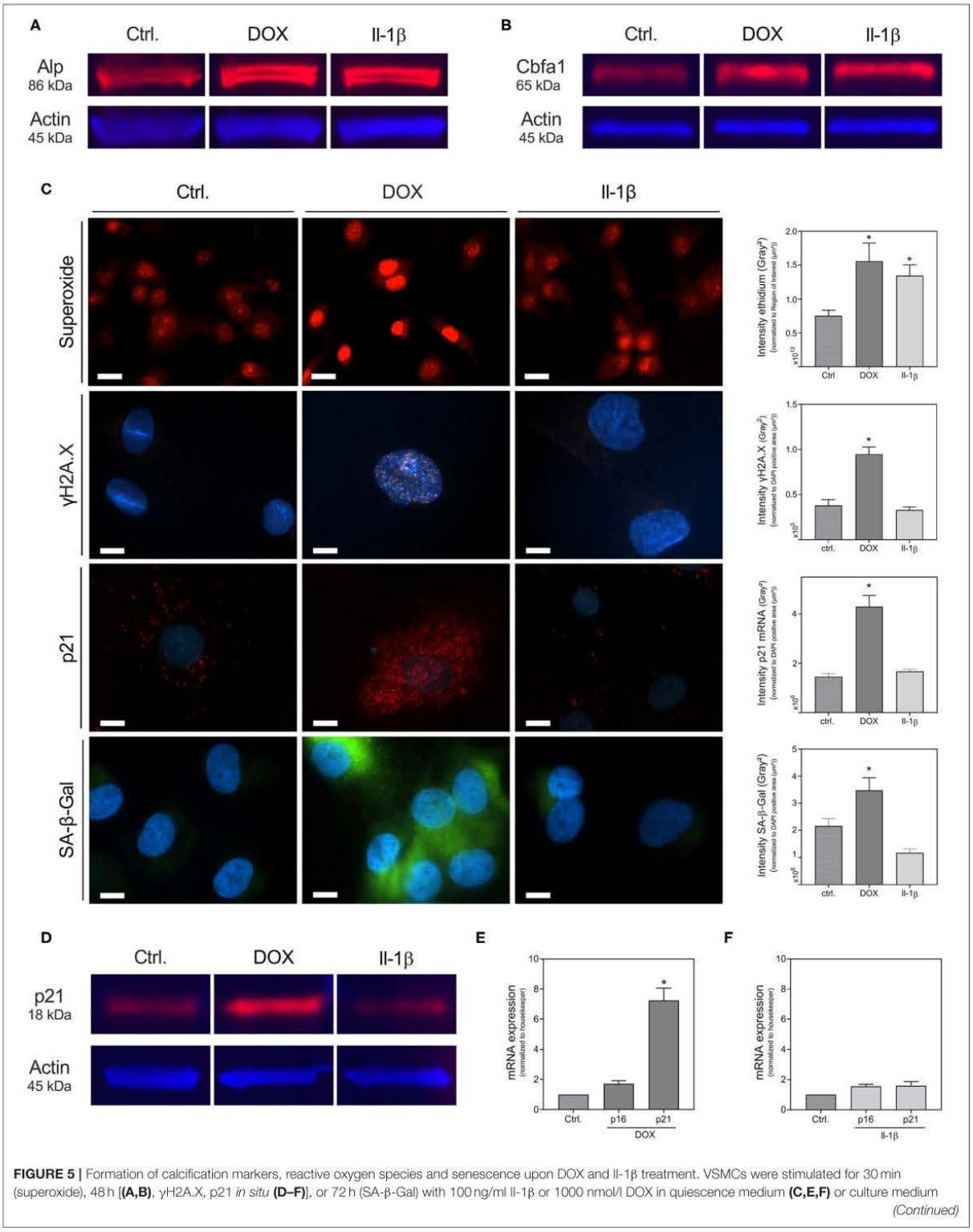

FIGURE 5 | Formation of calcification markers, reactive oxygen species and senescence upon DOX and Il-1β treatment. VSMCs were stimulated for 30 min (superoxide), 48 h [**(A,B)**, γH2A.X, p21 *in situ* **(D–F)**], or 72 h (SA-β-Gal) with 100 ng/ml Il-1β or 1000 nmol/l DOX in quiescence medium **(C,E,F)** or culture medium

(Continued)

FIGURE 5 | (A,B,D). Formation of superoxide was assessed with DHE, expression of γH2A.X was analyzed immunohistochemically, mRNA expression of p21 was assessed with RNA *in situ* hybridization and formation of SA-β-Gal was assessed with Spider staining **(C)**. For quantification of the expression of γH2A.X, mRNA expression of p21 and formation of SA-β-Gal, intensity of the respective fluorescence signal was measured after application of a threshold procedure as described in the supplement and the signal intensity then normalized to the DAPI positive cell core area per image (μm^2). For quantification of DHE, regions of interest were detected with a threshold procedure as described in the supplement and measured intensity was normalized to the area of interest detected by the threshold procedure. Alp protein, Cbfa1 protein and p21 protein were assessed with Western Blot **(A,B,D)**. mRNA expression was measured with quantitative real-time PCR **(E,F)**. Measured thresholds of the respective targets were normalized to actin **(E)** or the corresponding average threshold of housekeeper genes actin and Gapdh **(F)** before normalization to control. Data represent mean ± SEM, $n \geq 3$, $^*p < 0.05$ vs. Control. The Western Blots show a representative experiment of $n = 3$. Full blots are shown in **Supplementary Figures 3–5**. Pictures show a section of a representative experiment of $n \geq 3$, the scale bar indicates a 10 μm section (γH2A.X, p21, SA-β-Gal) or a 20 μm section (superoxide). Full representative images are shown in **Supplementary Tables 3–5**.

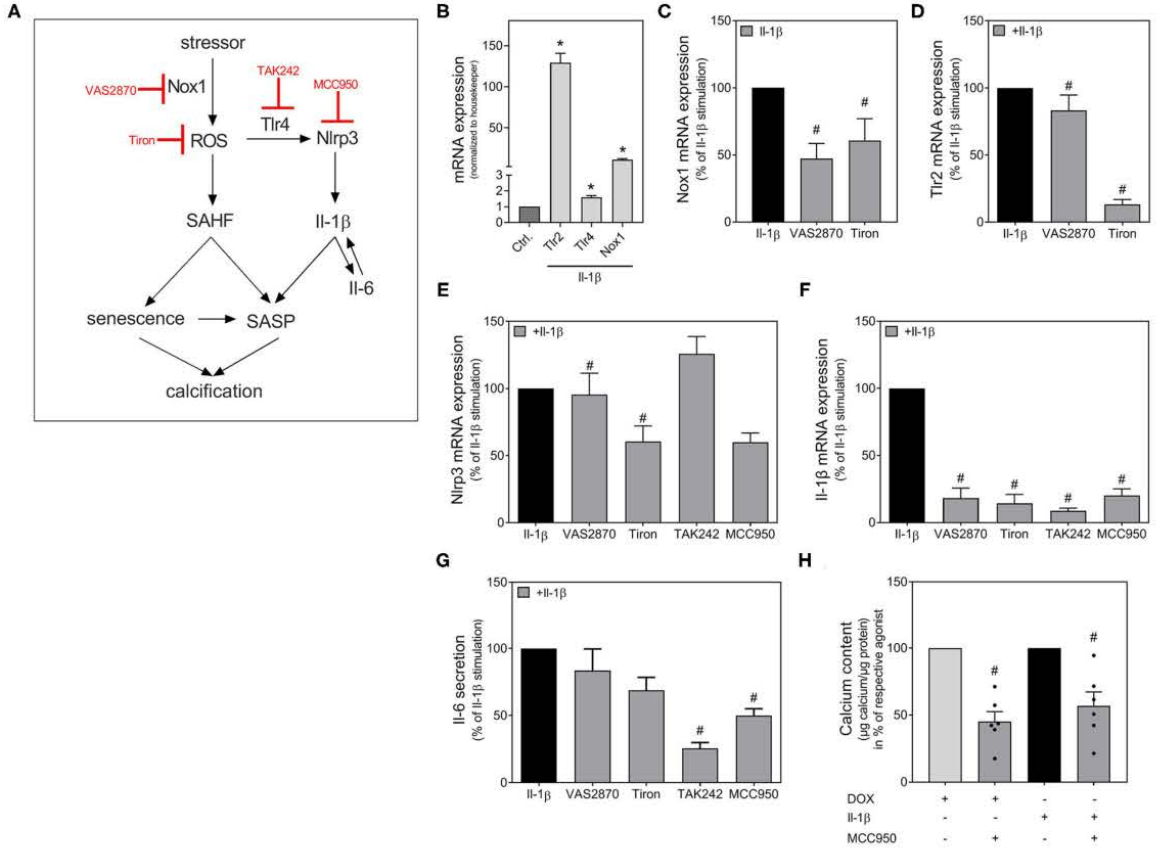

FIGURE 6 | Possible signaling pathways in Nlrp3 dependent calcification. Scheme with inhibitors used **(A)**. VSMC were stimulated for 48 h **(B–G)** or 14 d **(H)** with Il-1β (100 ng/ml), DOX (100 nmol/l), VAS2870 (10 μM), MCC950 (50 μM), TAK242 (10 μM) or Tiron (10 mM) as indicated. mRNA expression was measured with quantitative real-time PCR **(B–F)**. Measured thresholds of the respective targets were normalized to the corresponding average threshold of housekeeper genes actin and Gapdh before normalization to control **(B–F)**. Secretion of Il-6 was measured with Luminex™ and normalized to protein content (μg) **(G)**. Calcium content was quantified with *o*-cresolphthalein and normalized to protein content (μg) **(H)**. Data represent mean ± SEM, $n \geq 3$, $^*p < 0.05$ vs. Control, $^\#p < 0.05$ vs. Respective agonist (100 ng/ml Il-1β or 100 nmol/l DOX).

reflect the whole spectrum of senescence induction in VSMCs, DNA damage is a known and well-documented inducer of cellular senescence (9, 11). As shown recently by Shanahan's group, the formation of nuclei positive for γH2A.X and ATM in VSMCs is induced by calcium phosphate and correlates with the induction seen by other DNA damagers as DOX and hydrogen peroxide treatments (9). γH2A.X is a marker of double-strand DNA breaks, which are specific domains of facultative heterochromatin that contribute to silencing of genes promoting proliferation in senescent cells and are one known marker of senescence-associated heterochromatin foci (SAHF) (28). The phosphorylation of γH2A.X by ATM is a

key response mechanism to DNA damage, which can result in the activation of senescence pathways, including p21 (29). In line, in our experimental model treatment with DOX also induces DNA damage as γH2A.X and increases senescence markers p21 and SA-β-Gal. SA-β-Gal catalyzes the hydrolysis of β-galactosidase to monosaccharides in senescent cells. Cellular senescence is a dynamically regulated process, with activation of the p53/p21 and p16 pathways (30). In our experimental setting the p53/p21 pathway was upregulated by DOX, whereas p16 was not significantly affected (mRNA expression). While the senescence growth arrest via the p16 pathway seems not reversible, the p53-induced growth arrest is reversible upon p53 inactivation (31).

As in the previous study by Bielak-Zmijewska et al. only limited markers and only seven days of stimulation were investigated to study induction of calcification by DOX (20), we aimed to investigate DOX as primary stressor of DNA damage and senescence in order to analyze pro-inflammatory response and induction of calcification in VSMCs. In our experimental setting using primary VSMCs from rat thoracic aortas, DOX induces mineralization of VSMCs detected via calcium quantification and Alizarin Red staining after 14 days. The calcification induction was verified in an *ex vivo* setting using thoracic aortic rings. Analysis of the mRNA expression via real-time PCR and partly also *in situ* hybridization, enzyme activity and Western Blot confirmed the findings of osteogenic transformation of VSMCs; osteogenic markers as Cbfa1, Alp, Bmp-2, and Opn increase upon DOX treatment.

Senescent cells also have a metabolic active and pro-inflammatory phenotype termed as SASP. Cytokines of the Il-1 family and Il-6 are known to be part of this SASP (32). Furthermore, the induction of senescence by cytokines of the Il-1 family, e.g., Il-1β was investigated in cell culture and animal models (33). A microarray study has shown that senescent VSMCs reveal differential regulation of Matrix Gla Protein, Bmp-2, Osteoprotegerin, and Il-1β (34). In our own previous work, we demonstrated that plasma concentrations of Il-1β and Il-6 were significantly increased in rats treated with azathioprine, another known cellular stressor and ROS inducer, over a 24-weeks period of treatment (35). Increased expression of Il-1β and Il-6 was also detected in the aortas of treated rats, which were associated with increased expression of the osteogenic proteins Bmp-2, Alp and Cbfa1 (35). Therefore, we examined the effect of DOX on the expression of Il-1β and Il-6. The mRNA expression of Il-1β and Il-6 were significantly increased upon DOX stimulation, with higher induction for Il-1β. The Nlrp3 inflammasome, the most widely characterized inflammasome and known to be expressed in VSMCs (15), serves as most significant source of Il-1β production (16). Beside Nlr inflammasomes, transmembrane Tlrs are the main types of PRRs (14). The activation of PRRs mainly induces sterile inflammation associated with extensive transcriptional pro-inflammatory cellular reprogramming (36). This is temporarily useful in acute situations, while chronic activation is detrimental (37). Due to their potent pro-inflammatory potency, the Nlrp3 activation and assembly is a strictly controlled process with an initial stimulus e.g., activation of Tlr, and a second stimulus e.g., increased production of ROS (25). Subsequent activation of caspase-1 leads to cleavage and activation of pro-Il-1β into its active form Il-1β (25). PRRs are a link between the innate immune system, inflammation, and cellular senescence. VSMCs express small inflammasomes with low and slow onset, but long-lasting activity leading to a continuous release of Il-1 cytokines (15, 38). This mainly induces cellular hyperactivity and chronic sterile inflammation, which can maintain itself independently of the initial trigger (39). The cells retain their full viability and include Il-1 cytokines in the repertoire of their pro-inflammatory secretome (39). It was already shown that inflammasomes are involved in the calcification process and age-related diseases (40–42). In calcified VSMCs, Nlrp3, its cofactor Asc, and the cleavage enzyme caspase-1 are upregulated with subsequent Il-1β production, while Nlrp3 inhibition prevents *in vitro* calcification (38). In our experimental model, the expression of Nlrp3, Asc as well as caspase-1 is significantly upregulated upon DOX stimulation in VSMCs. Simultaneously, the expression of Tlr2 and Nox1 also increases. The NADPH oxidase, with Nox1 as one subunit, is one of the major sources for superoxide anion release in VSMCs (43). In VSMCs, the Tlr4 is constitutively active, while the Tlr2 is upregulated upon an inflammatory response (26).

As already known from a previous study by Wen et al., Il-1β can promote osteogenic differentiation and induction of calcification of VSMCs (38). In line, in our experimental setting, both Il-1β and DOX induce VSMC calcification. The DOX-induced mineralization could be significantly reduced by MCC950. This could be confirmed in the *ex vivo* setting with Nlrp3$^{-/-}$ mice, where the calcification induction by DOX is also inhibited compared to control mice. This finding is comparable to our previous results regarding the stressor azathioprine, whose calcifying effect could also no longer be seen in aortic rings from Nlrp3$^{-/-}$ mice (35). Therefore, Il-1β appears to be a very important effector cytokine, especially for the maintenance of a SASP after primary initiation of the SASP by the induction of "inflammaging" due to a cellular stressor. Thus, Il-1 cytokines might become an essential part of the respective pathogenesis by forming an auto-inflammatory loop, independent of the initial trigger.

Il-1β increases its own expression as well as the expression and secretion of Il-6. Moreover, Il-1β also enhances the expression of relevant components of the signaling pathway, particularly Tlr2, Nox1 and Nlrp3, also shown to be involved in DOX-mediated "inflammaging." Yet, in contrast to the DOX-induced effects in VSMCs, Il-1β does not affect the expression of senescence markers, such as p21 or SA-β-Gal, nor induces DNA breaks detected via γH2A.X in our model using primary rat VSMCs. In contrast, a recent study found induction of senescence in a co-treatment of Il-1β and phosphate in human umbilical cord VSMCs (42). Different effects on calcification were also seen for Il-6 when the origin of VSMCs differs: while pro-calcifying effects of Il-6 were found in human umbilical artery VSMCs in non-osteogenic medium (44), others found these effects only in co-stimulation with the soluble Il-6 receptor in osteogenic medium in human VSMCs (45). At least one explanation might be the different origin of VSMCs that differ in protein expression, as

demonstrated by proteomic analysis (46). Like Il-1β, processes of cellular senescence are not affected by Il-6 in our model (**Supplementary Material**), whereas an Il-6 production itself is a component of the SASP and therefore a sign of VSMCs senescence (32).

This study has some limitations that might hamper the direct translational aspects of the results: It was performed only in *in vitro* and *ex vivo* settings using cells and thoracic aortas from rats and mice. Further *in vivo* studies verifying the major role of Nlrp3 and Il-1β as a potential therapeutic target for the treatment of vessel "inflammaging" are necessary. In addition, the transferability in the current study is not shown for human aortic or other vessel beds.

In conclusion, the inhibition of PRRs could represent an essential approach for the therapy of systemic vascular diseases. The CANTOS study demonstrated for the first time in humans the importance of chronic vascular inflammation for CVD and the association of cardiovascular mortality with signs of systemic inflammation (47). The current study results provide further indications of a potential benefit of an interruption of the Nlrp3-associated auto-inflammatory loop.

DATA AVAILABILITY STATEMENT

The original contributions presented in the study are included in the article/**Supplementary Material**, further inquiries can be directed to the corresponding author/s.

ETHICS STATEMENT

The animal study was reviewed and approved by Landesamt für Gesundheit und Soziales Berlin, Germany.

AUTHOR CONTRIBUTIONS

MS, MT, and MvdG: conceptualization, supervision, and project administration. JH, MS, and MT: methodology, writing—original draft preparation, and visualization. JH, MS, MX, MG, AG, MS, and AS: investigation. JH, MS, MT, and MvdG: data curation. JH, MT, MG, MX, AG, AS, and MvdG: writing—review and editing. MT, JH, MX, and MS: funding acquisition. All authors contributed to the article and approved the submitted version.

FUNDING

This research was funded by a grant from the Bundesministerium für Bildung und Forschung (MT, MS), the Sonnenfeld Stiftung (MS, MT, JH) and the Berlin Institute of Health (MS). MX received a research scholarship of the Nanchong school science and technology strategic cooperation project (grant number: 20SXQT0117).

ACKNOWLEDGMENTS

The authors thank Katharina Kuschfeldt, Brigitte Egbers and Nadine Neitzel for excellent technical assistance and Raissa Stayzyk for her excellent work in the animal facility. We thank Marcus Maurer (Charité – Universitätsmedizin Berlin) for the release of the Nlrp3 knockout mice for breeding.

SUPPLEMENTARY MATERIAL

The Supplementary Material for this article can be found online at: https://www.frontiersin.org/articles/10.3389/fcvm.2021.752305/full#supplementary-material

REFERENCES

1. Virani SS, Alonso A, Aparicio HJ, Benjamin EJ, Bittencourt MS, Callaway CW, et al. Heart disease and stroke statistics-2021 update: a report from the American heart association. *Circulation.* (2021) 143:e254–743. doi: 10.1161/CIR0000000000000950
2. Tolle M, Reshetnik A, Schuchardt M, Hohne M, Van Der Giet M. Arteriosclerosis and vascular calcification: causes, clinical assessment and therapy. *Eur J Clin Invest.* (2015) 45:976–85. doi: 10.1111/eci.12493
3. Lanzer P, Hannan FM, Lanzer JD, Janzen J, Raggi P, Furniss D, et al. Medial arterial calcification: JACC state-of-the-art review. *J Am Coll Cardiol.* (2021) 78:1145–65. doi: 10.1016/j.jacc.2021.06.049
4. Iribarren C, Sidney S, Sternfeld B, Browner WS. Calcification of the aortic arch: risk factors and association with coronary heart disease, stroke, and peripheral vascular disease. *JAMA.* (2000) 283:2810–5. doi: 10.1001/jama.283.21.2810
5. Raggi P. Cardiovascular disease: coronary artery calcification predicts risk of CVD in patients with CKD. *Nat Rev Nephrol.* (2017) 13:324–6. doi: 10.1038/nrneph.2017.61
6. Childs BG, Durik M, Baker DJ, Van Deursen JM. Cellular senescence in aging and age-related disease: from mechanisms to therapy. *Nat Med.* (2015) 21:1424–35. doi: 10.1038/nm.4000
7. Kooman JP, Kotanko P, Schols AM, Shiels PG, Stenvinkel P. Chronic kidney disease and premature ageing. *Nat Rev Nephrol.* (2014) 10:732–42. doi: 10.1038/nrneph.2014.185
8. Munoz-Espin D, Serrano M. Cellular senescence: from physiology to pathology. *Nat Rev Mol Cell Biol.* (2014) 15:482–96. doi: 10.1038/nrm3823
9. Sanchis P, Ho CY, Liu Y, Beltran LE, Ahmad S, Jacob AP, et al. Arterial "inflammaging" drives vascular calcification in children on dialysis. *Kidney Int.* (2019) 95:958–72. doi: 10.1016/j.kint.2018.12.014
10. Herrmann J, Babic M, Tolle M, Van Der Giet M, Schuchardt M. Research models for studying vascular calcification. *Int J Mol Sci.* (2020) 21:2204. doi: 10.3390/ijms21062204
11. Cobb AM, Yusoff S, Hayward R, Ahmad S, Sun M, Verhulst A, et al. Runx2 (Runt-Related Transcription Factor 2) links the DNA damage response to osteogenic reprogramming and apoptosis of vascular smooth muscle cells. *Arterioscler Thromb Vasc Biol.* (2021) 41:1339–57. doi: 10.1161/ATVBAHA.120.315206
12. Childs BG, Li H, Van Deursen. J.M. Senescent cells: a therapeutic target for cardiovascular disease. *J Clin Invest.* (2018) 128:1217–28. doi: 10.1172/JCI95146
13. Krainer J, Siebenhandl S, Weinhausel A. Systemic autoinflammatory diseases. *J Autoimmun.* (2020) 109:102421. doi: 10.1016/j.jaut.2020.102421
14. Cao X. Self-regulation and cross-regulation of pattern-recognition receptor signalling in health and disease. *Nat Rev Immunol.* (2016) 16:35–50. doi: 10.1038/nri.2015.8
15. Sun HJ, Ren XS, Xiong XQ, Chen YZ, Zhao MX, Wang JJ, et al. NLRP3 inflammasome activation contributes to VSMC phenotypic transformation and proliferation in hypertension. *Cell Death Dis.* (2017) 8:e3074. doi: 10.1038/cddis.2017.470

16. Tangi TN, Elmabsout AA, Bengtsson T, Sirsjo A, Fransen K. Role of NLRP3 and CARD8 in the regulation of TNF-alpha induced IL-1beta release in vascular smooth muscle cells. *Int J Mol Med.* (2012) 30:697–702. doi: 10.3892/ijmm.2012.1026
17. Weber A, Wasiliew P, Kracht M. Interleukin-1 (IL-1) pathway. *Sci Signal.* (2010) 3:cm1. doi: 10.1126/scisignal.3105cm1
18. Kim DH, Bang E, Arulkumar R, Ha S, Chung KW, Park MH, et al. Senoinflammation: a major mediator underlying age-related metabolic dysregulation. *Exp Gerontol.* (2020) 134:110891. doi: 10.1016/j.exger.2020.110891
19. Cagel M, Grotz E, Bernabeu E, Moretton MA, Chiappetta DA. Doxorubicin: nanotechnological overviews from bench to bedside. *Drug Discov Today.* (2017) 22:270–81. doi: 10.1016/j.drudis.2016.11.005
20. Bielak-Zmijewska A, Wnuk M, Przybylska D, Grabowska W, Lewinska A, Alster O, et al. A comparison of replicative senescence and doxorubicin-induced premature senescence of vascular smooth muscle cells isolated from human aorta. *Biogerontology.* (2014) 15:47–64. doi: 10.1007/s10522-013-9477-9
21. Schuchardt M, Tolle M, Prufer J, Prufer N, Huang T, Jankowski V, et al. Uridine adenosine tetraphosphate activation of the purinergic receptor P2Y enhances in vitro vascular calcification. *Kidney Int.* (2012) 81:256–65. doi: 10.1038/ki.2011.326
22. Herrmann J, Babic M, Tolle M, Eckardt KU, Van Der Giet M, Schuchardt M. A novel protocol for detection of senescence and calcification markers by fluorescence microscopy. *Int J Mol Sci.* (2020) 21:3475. doi: 10.3390/ijms21103475
23. Lopes-Paciencia S, Saint-Germain E, Rowell MC, Ruiz AF, Kalegari P, Ferbeyre G. The senescence-associated secretory phenotype and its regulation. *Cytokine.* (2019) 117:15–22. doi: 10.1016/j.cyto.2019.01.013
24. Niemi K, Teirila L, Lappalainen J, Rajamaki K, Baumann MH, Oorni K, et al. Serum amyloid a activates the NLRP3 inflammasome via P2X7 receptor and a cathepsin B-sensitive pathway. *J Immunol.* (2011) 186:6119–28. doi: 10.4049/jimmunol.1002843
25. De Zoete MR, Palm NW, Zhu S, Flavell RA. Inflammasomes. *Cold Spring Harb Perspect Biol.* (2014) 6:a016287. doi: 10.1101/cshperspect.a016287
26. Schuchardt M, Prufer N, Tu Y, Herrmann J, Hu XP, Chebli S, et al. Dysfunctional high-density lipoprotein activates toll-like receptors via serum amyloid a in vascular smooth muscle cells. *Sci Rep.* (2019) 9:3421. doi: 10.1038/s41598-019-39846-3
27. Burtenshaw D, Hakimjavadi R, Redmond EM, Cahill PA. Nox, reactive oxygen species and regulation of vascular cell fate. *Antioxidants.* (2017) 6:90. doi: 10.3390/antiox6040090
28. Bernadotte A, Mikhelson VM, Spivak IM. Markers of cellular senescence. Telomere shortening as a marker of cellular senescence. *Aging.* (2016) 8:3–11. doi: 10.18632/aging.100871
29. Duer M, Cobb AM, Shanahan CM. DNA damage response: a molecular lynchpin in the pathobiology of arteriosclerotic calcification. *Arterioscler Thromb Vasc Biol.* (2020) 40:e193–202. doi: 10.1161/ATVBAHA.120.313792
30. Mijit M, Caracciolo V, Melillo A, Amicarelli F, Giordano A. Role of p53 in the regulation of cellular senescence. *Biomolecules.* (2020) 10:420. doi: 10.3390/biom10030420
31. Campisi J. Senescent cells, tumor suppression, and organismal aging: good citizens, bad neighbors. *Cell.* (2005) 120:513–22. doi: 10.1016/j.cell.2005.02.003
32. Orjalo AV, Bhaumik D, Gengler BK, Scott GK, Campisi J. Cell surface-bound IL-1alpha is an upstream regulator of the senescence-associated IL-6/IL-8 cytokine network. *Proc Natl Acad Sci USA.* (2009) 106:17031–36. doi: 10.1073/pnas.0905299106
33. Acosta JC, Banito A, Wuestefeld T, Georgilis A, Janich P, Morton JP, et al. A complex secretory program orchestrated by the inflammasome controls paracrine senescence. *Nat Cell Biol.* (2013) 15:978–90. doi: 10.1038/ncb2784
34. Burton DG, Giles PJ, Sheerin AN, Smith SK, Lawton JJ, Ostler EL, et al. Microarray analysis of senescent vascular smooth muscle cells: a link to atherosclerosis and vascular calcification. *Exp Gerontol.* (2009) 44:659–65. doi: 10.1016/j.exger.2009.07.004
35. Schuchardt M, Herrmann J, Henkel C, Babic M, Van Der Giet M, Tolle M. Long-term treatment of azathioprine in rats induces vessel mineralization. *Biomedicines.* (2021) 9:327. doi: 10.3390/biomedicines9030327
36. Chen GY, Nunez G. Sterile inflammation: sensing and reacting to damage. *Nat Rev Immunol.* (2010) 10:826–37. doi: 10.1038/nri2873
37. Roh JS, Sohn DH. Damage-associated molecular patterns in inflammatory diseases. *Immune Netw.* (2018) 18:e27. doi: 10.4110/in.2018.18.e27
38. Wen C, Yang X, Yan Z, Zhao M, Yue X, Cheng X, et al. Nalp3 inflammasome is activated and required for vascular smooth muscle cell calcification. *Int J Cardiol.* (2013) 168:2242–7. doi: 10.1016/j.ijcard.2013.01.211
39. Evavold CL, Ruan J, Tan Y, Xia S, Wu H, Kagan JC. The pore-forming protein gasdermin d regulates interleukin-1 secretion from living macrophages. *Immunity.* (2018) 48:35–44 e36. doi: 10.1016/j.immuni.2017.11.013
40. Rea IM, Gibson DS, Mcgilligan V, Mcnerlan SE, Alexander HD, Ross OA. Age and age-related diseases: role of inflammation triggers and cytokines. *Front Immunol.* (2018) 9:586. doi: 10.3389/fimmu.2018.00586
41. Xu D, Zeng F, Han L, Wang J, Yin Z, Lv L, et al. The synergistic action of phosphate and interleukin-6 enhances senescence-associated calcification in vascular smooth muscle cells depending on p53. *Mech Ageing Dev.* (2019) 182:111124. doi: 10.1016/j.mad.2019.111124
42. Han L, Zhang Y, Zhang M, Guo L, Wang J, Zeng F, et al. Interleukin-1beta-induced senescence promotes osteoblastic transition of vascular smooth muscle cells. *Kidney Blood Press Res.* (2020) 45:314–30. doi: 10.1159/000504298
43. Tsai IC, Pan ZC, Cheng HP, Liu CH, Lin BT, Jiang MJ. Reactive oxygen species derived from NADPH oxidase 1 and mitochondria mediate angiotensin II-induced smooth muscle cell senescence. *J Mol Cell Cardiol.* (2016) 98:18–27. doi: 10.1016/j.yjmcc.2016.07.001
44. Sun M, Chang Q, Xin M, Wang Q, Li H, Qian J. Endogenous bone morphogenetic protein 2 plays a role in vascular smooth muscle cell calcification induced by interleukin 6 in vitro. *Int J Immunopathol Pharmacol.* (2017) 30:227–37. doi: 10.1177/0394632016689571
45. Kurozumi A, Nakano K, Yamagata K, Okada Y, Nakayamada S, Tanaka Y. IL-6 and sIL-6R induces STAT3-dependent differentiation of human VSMCs into osteoblast-like cells through JMJD2B-mediated histone demethylation of RUNX2. *Bone.* (2019) 124:53–61. doi: 10.1016/j.bone.2019.04.006
46. Regent A, Ly KH, Lofek S, Clary G, Tamby M, Tamas N, et al. Proteomic analysis of vascular smooth muscle cells in physiological condition and in pulmonary arterial hypertension: toward contractile versus synthetic phenotypes. *Proteomics.* (2016) 16:2637–49. doi: 10.1002/pmic.201500006
47. Ridker PM, Everett BM, Thuren T, Macfadyen JG, Chang WH, Ballantyne C, et al. Antiinflammatory therapy with canakinumab for atherosclerotic disease. *N Engl J Med.* (2017) 377:1119–31. doi: 10.1056/NEJMoa1707914

Conflict of Interest: The authors declare that the research was conducted in the absence of any commercial or financial relationships that could be construed as a potential conflict of interest.

Publisher's Note: All claims expressed in this article are solely those of the authors and do not necessarily represent those of their affiliated organizations, or those of the publisher, the editors and the reviewers. Any product that may be evaluated in this article, or claim that may be made by its manufacturer, is not guaranteed or endorsed by the publisher.

Supplementary Material

1. Quantitative real-time PCR

The oligonucleotide sequences are summarized in Supplementary Table 1.

Supplementary Table 1. Oligonucleotide sequences (rat)

Gene	Fwd 5´-3´ Rev 5´-3´	Company	Reference
Acta2	ACC ATC GGG AAT GAA CGC TT CTG TCA GCA ATG CCT GGG TA	Tib Mol	(1)
β-Actin	TCG CTG ACA GGA TGC AGA AG CTC AGG AGG AGC AAT GAT CTT GAT	Tib Mol	Primer Blast
Bmp-2	ACT TCC CGA CGC TTC TTC TTC A GGC CAC TTC CAC CAC AAA CC	Tib Mol	(2)
Cbfa1	GCC GGG AAT GAT GAG AAC TA GGA CCG TCC ACT GTC ACT TT	Tib Mol	Primer Blast
Cnn1	GCC CAG AAA TAC GAC CAC CA CCG GCTGGA GCT TGT TGA TA	Tib Mol	(1)
Gapdh	TGC CAA GTA TGA CAT CAA GAA G AGC CCA GGA TGC CCT TTA GT	Tib Mol	Primer Blast
Il-1β	GCT ATG GCA ACT GTC CCT GA AAG GGC TTG GAA GCA ATC CTT A	Tib Mol	Primer Blast
Il-6	CTG GTC TTC TGG AGT TCC GT TGG TCC TTA GCC ACT CCT TCT	Tib Mol	Primer Blast
p16	GGC TTC ACC AAA CGC CCC GA GCT GCT TTG GGG GTT GGC CT	Tib Mol	Primer Blast
p21	TAT GTA CCA GCC ACA GGC AC ATC GGC GCT TGG AGT GAT AG	Tib Mol	Primer Blast
Myh11	CAC TGA GAG CAA TGA GGC CA TCT GAG TCC CGA GCA TCC AT	Tib Mol	(1)
Nlrp3	CCA GGG CTC TGT TCA TTG CCT TGG CTT TCA CTT CG	Tib Mol	(3)
Asc	TTA TGG AAG AGT CTG GAG CTG TG GCA ATG AGT GCT TGC CTG TG	Tib Mol	Primer Blast
Caspase-1	GGA GCT TCA GTC AGG TCC ATC CTT GAG GGA ACC ACT CGG TC	Tib Mol	Primer Blast
Tlr2	GGT CTC CAG GTC AAA TCT CAG AGG A CGG AGG TTC ACA CAG GCT CGC	Tib Mol	Primer Blast
Tlr4	GGC ATC ATC TTC ATT GTC CTT G AGC ATT GTC CTC CCA CTC G	Tib Mol	(4)
Nox1	CTG CTC TCC TTC CTG AGG GGC ACC TGC T GAC AAT CCC CCC CAG GCC ATG GAT CCC TA	Tib Mol	(5)

2. Cytotoxicity

Cytotoxicity was assessed with the CytoTox-Glo™ Cytotoxicity Assay (Promega) according to the manufacturer's instruction. VMSC were seeded in 96-well plates, serum starved for 24 h and stimulated for 48 h or 72 h. Luminescence was measured with the Mithras LB940 device and the MicroWin software (version 5.22, Berthold Technologies).

We found no statistically significant induction of cytotoxicity after stimulation with DOX, Il-6 and Il-1β. Nevertheless, although the effect does not reach statistical significance, the results indicate a dose-dependent cytotoxic effect of DOX after stimulation for 72 h that is also visible via light microscopy.

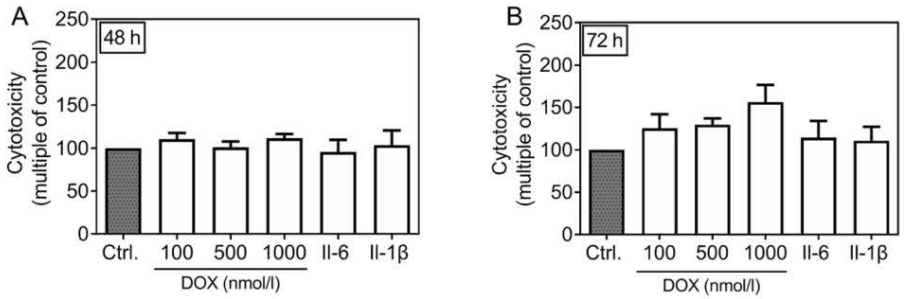

Supplementary Figure 1. Cytotoxicity upon stimulation with DOX, Il-6 and Il-1β

VSMCs were stimulated as indicated with DOX, 100 ng/ml Il-6 and 100 ng/ml Il-1β for 48 h (A) or 72 h (B). Cytotoxicity was determined using the CytoTox-Glo™ Cytotoxicity Assay. Data represent mean±SEM, n≥3.

3. Western Blots after stimulation with DOX and Il-1β

Suppl. Figure 2 shows the full representative multi-plex Western Blot for Figure 5D. Supplementary Figure 3 shows the full representative Western Blot for Cbfa1 from Figure 5A. Supplementary Figure 4 shows the full representative Western Blot for Actin from Figure 5B. The unspecific bands most likely comes from the secondary antibody.

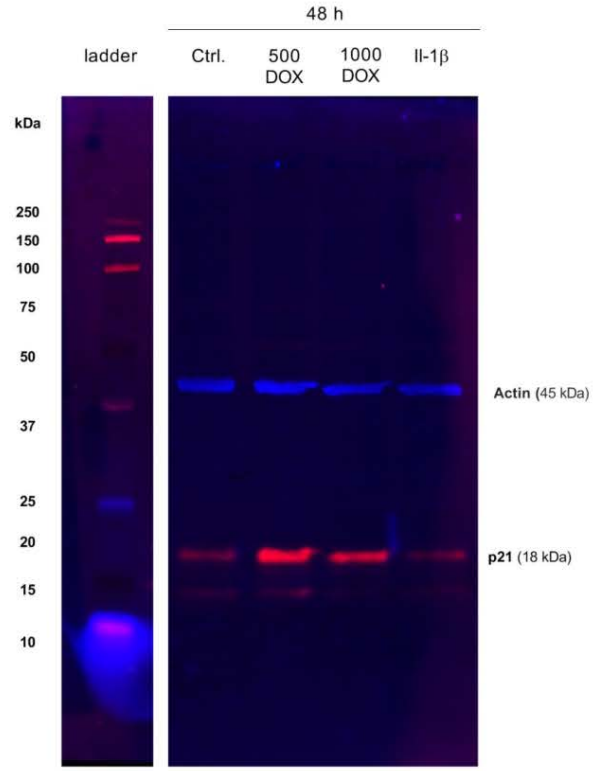

Supplementary Figure 2. p21 WB after stimulation with DOX and Il-1β
VSMCs were stimulated as indicated with 500 nmol/l or 1000 nmol/l DOX or 100 ng/ml Il-1β for 48 h as indicated. Protein content of p21 and Actin were identified with Western Blot. The Western Blot is a full representative image of n=3.

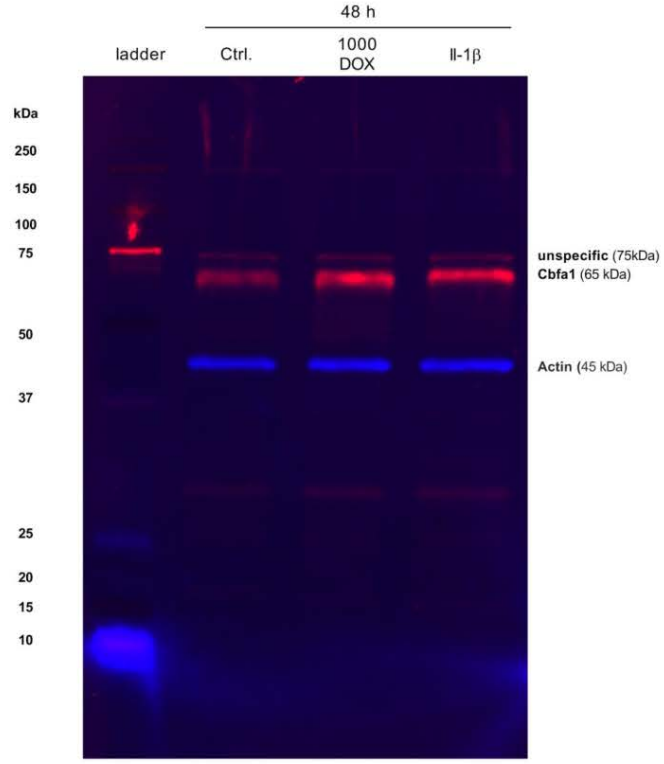

Supplementary Figure 3. Cbfa1 and Actin WB after stimulation with DOX and Il-1β
VSMCs were stimulated as indicated with 1000 nmol/l DOX or 100 ng/ml Il-1β for 48 h. Protein content of Cbfa1 and Actin were identified with Western Blot. The Western Blot is a full representative image of n=3.

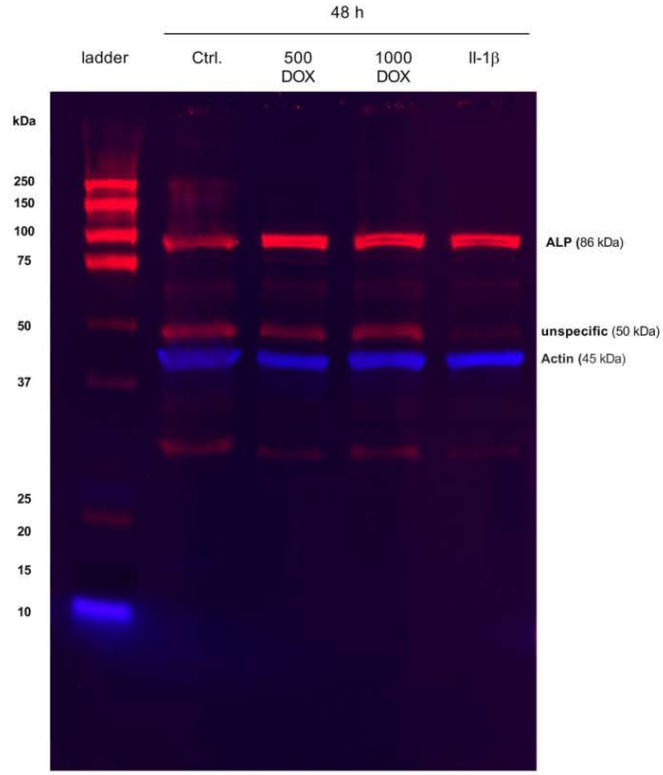

Supplementary Figure 4. Alp and Actin WB after stimulation with DOX and Il-1β
VSMCs were stimulated as indicated with 1000 nmol/l DOX or 100 ng/ml Il-1β for 48 h. Protein content of Alp and Actin were identified with Western Blot. The Western Blot is a full representative image of n=3.

4. Gene Expression after Il-6 Stimulation

Gene expression was measured after stimulation with Il-6 after 48h in quiescence medium.

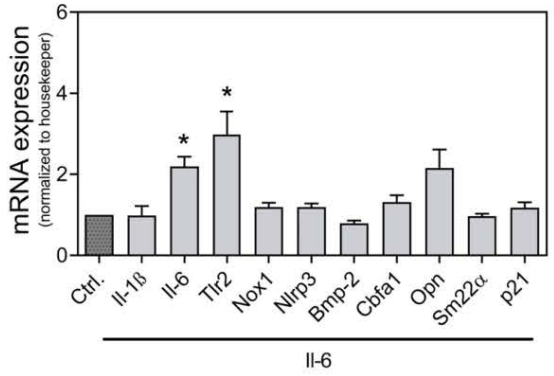

Supplementary Figure 5. Gene Expression upon stimulation with Il-6
VSMCs were stimulated as indicated with 100 ng/ml Il-6 for 48 h and mRNA expression was measured with quantitative real-time PCR. Measured thresholds of the respective targets were normalized to the corresponding

average threshold of housekeepers Actin and Gapdh before normalization to control. Data represent mean±SEM, n≥3.

5. RNA *in situ* hybridization

VSMCs were seeded in LabTec chamber slides (Thermo Fisher). Cells were serum starved for 24 h and stimulated for 48 h. Staining of mRNA was performed with the RNAscope® Fluorescent Multiplex Assay (ACD) according to the manufacturer's protocol. The materials used are given in suppl. Table 2.

Supplementary Table 2. Components for RNA *in situ* hybridization

Material	Company	Order Number
RNAscope™ Target Retrieval Reagents	ACD Bio	322000
RNAscope™ Fluorescent Multiplex Reagent Kit	ACD Bio	320850
RNAscope™ Wash Buffer Reagents	ACD Bio	310091
ImmEdge™ Hydrophobic Barrier Pen	ACD Bio	310018
RNAscope™ Probe - Rn-Cdkn1a	ACD Bio	423851-C3
RNAscope™ Probe - Rn-Spp1	ACD Bio	405441
RNAscope™ Probe - Rn-Bmp2	ACD Bio	581071
Prolong Diamond antifade medium	Thermo Fisher Scientific	P10144

Cells were imaged with an Axiovert 200M microscope. The channel Atto647 was quantified with Zen2 software (Blue edition, Zeiss) using a 3-Sigma-threshold approach. Nuclei area was calculated with Zen2 software (Zeiss) with manual threshold determination. Due to background and channel cross talk, the channels Alexa488 and Atto550 were analyzed manually with ImageJ. Briefly, pictures were exported from Zen in jpg-format, inverted and targets were identified, marked manually, and counted.

6. γH2A.X staining

VSMCs were seeded in LabTec chamber slides (Thermo Fisher). Cells were serum starved for 24 h and stimulated for 48 h. After permeabilization with Triton X (0,1%) cells were stained with (sc-101696) 1:500 in 10% RotiBlock/PBS for 1 h at RT, followed by incubation with the Alexa Fluor 555-coupled secondary antibody (Invitrogen, A-21429) 1:1,000 in 10% RotiBlock/PBS for 1 h at RT. Nuclei were counterstained with Hoechst33342 (Thermo Fisher) according to the manufacturer's protocol. Cells were imaged with an Axiovert 200M microscope. The channel "Alexa 555" was quantified with Zen2 software (Blue edition, Zeiss) using a 3 Sigma threshold approach. The cell core area was determined with Zen2 software with manual threshold determination.

7. SA-β-Gal Staining

VSMCs were seeded in μ-Slides slides (Ibidi). Cells were serum starved for 24 h and stimulated for 72 h. After stimulation, cells were washed with PBS, fixed for 3 min at room temperature with 4% Formalin and washed with PBS. A 2 μM working solution of SPiDER- β - Gal in 1:5 with ultrapure water diluted McIlvaine buffer was incubated for 30min at 37°C. Afterwards cells were washed, counterstained with Hoechst 33342 (Thermo Fisher) according to the manufacturer's protocol, covered with PBS and immediately imaged. The channel "BODIPY R6G" was quantified with Zen2 software (Blue edition, Zeiss) using a 3 Sigma threshold approach. The cell core area was determined with Zen2 software with manual threshold determination.

Supplementary Table 3. Representative Images of RNA *in situ* hybridization, γH2A.X staining and β-Gal staining upon DOX stimulation

VSMCs were stimulated with 1000 nmol/l DOX, for 48 h (RNA Scope and γH2A.X) staining or 72 h (SA-β-Gal). VSMCs were stained with RNA *in situ* hybridization technique for mRNA expression of Bmp-2, Opn and p21, for formation of γH2A.X immunohistochemically or for the formation of SA-β-Gal with Spider. Representative images are shown for n≥3 experiments. The scale bar indicates a 20 µm section.

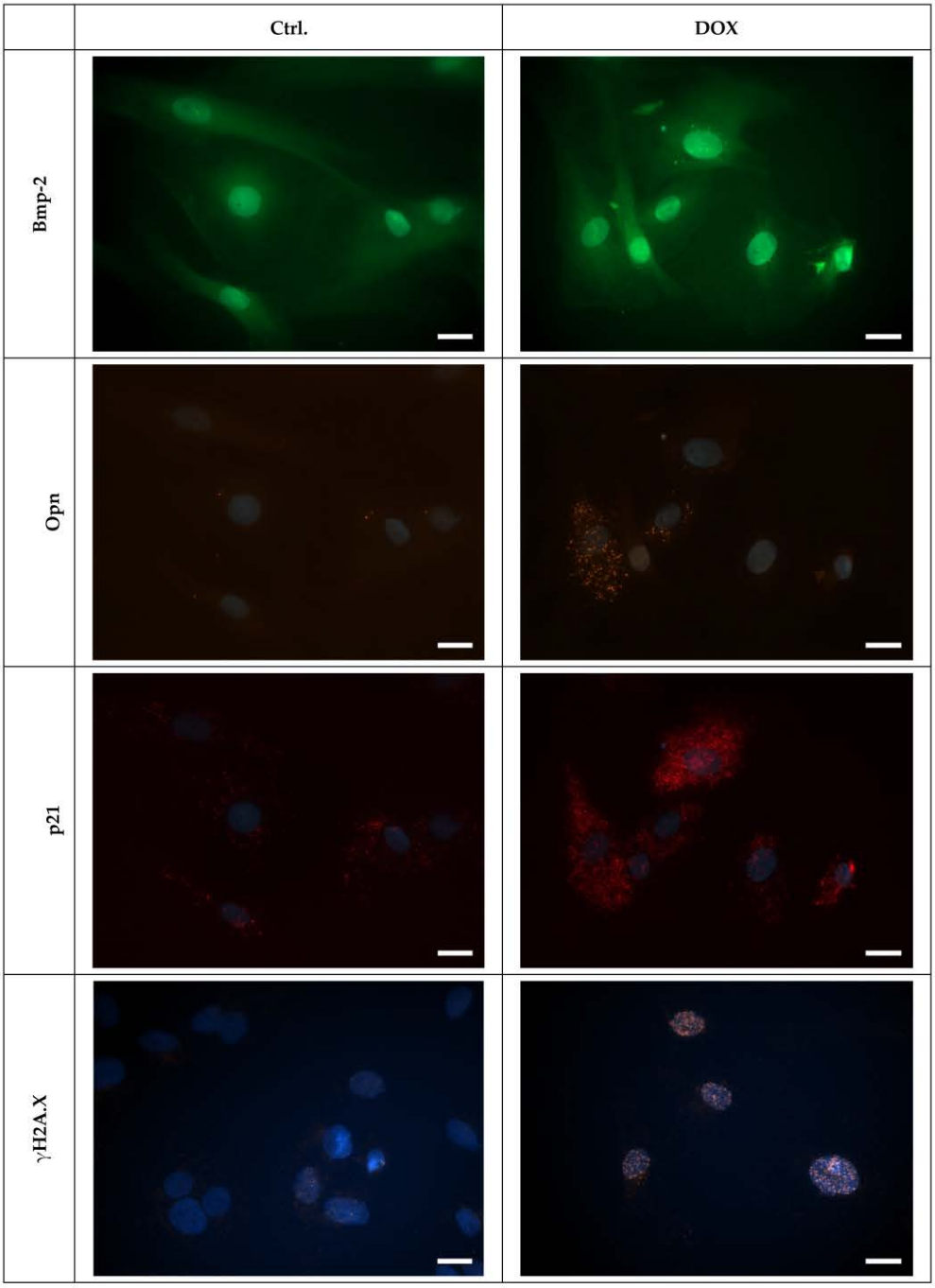

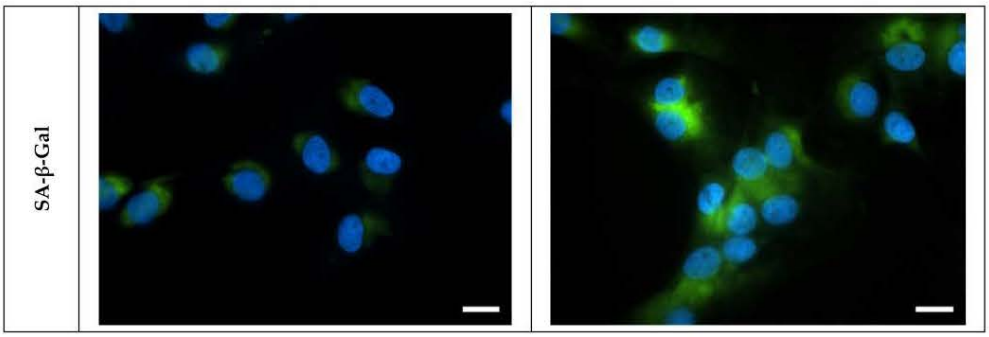
SA-β-Gal

Supplementary Table 4. Representative Images of RNA *in situ* hybridization, γH2A.X staining and SA-β-Gal staining upon Il-6 and Il-1β stimulation

VSMCs were stimulated with 100 ng/ml Il-1β or 100 ng/ml Il-6 for 48 h (RNA Scope and γH2A.X staining) or 72 h (SA-β-Gal). VSMCs were stained with RNA *in situ* hybridization technique for mRNA expression of Bmp-2, Opn and p21, for formation of γH2A.X immunohistochemically or for the formation of SA-β-Gal with Spider. Representative images are shown for n≥3 experiments. The scale bar indicates a 20 µm section.

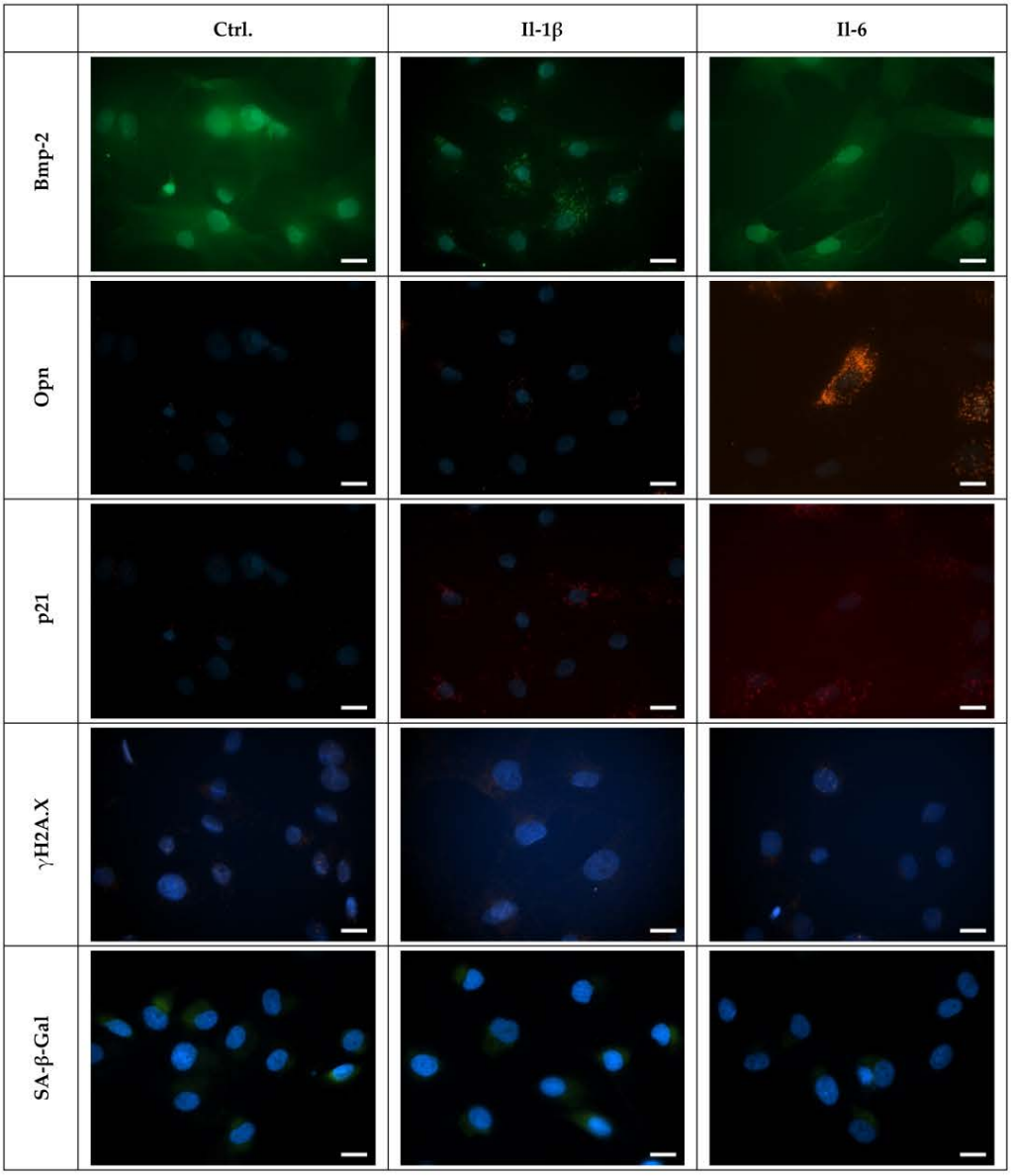

8. DHE staining

The detailed staining procedure is described in the main text. Cells were imaged with an Axiovert 200M microscope. The channel "ethidium homodimer" was quantified with Zen2 software (Blue edition, Zeiss) using an Otsu threshold approach. The detected intensity of the channel was normalized to area identified by the threshold procedure.

Supplementary Table 5. Representative Images of DHE staining

VSMCs were stimulated with 1000 nM DOX, 100 ng/ml Il-1β for 30 min. VSMCs were stained with DHE. Pictures show a representative experiment of n≥3.

Ctrl.	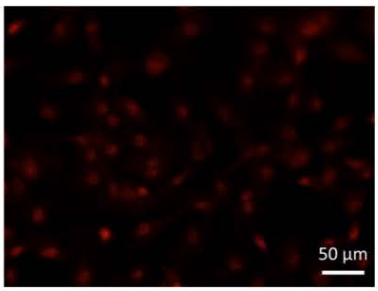	Ctrl.	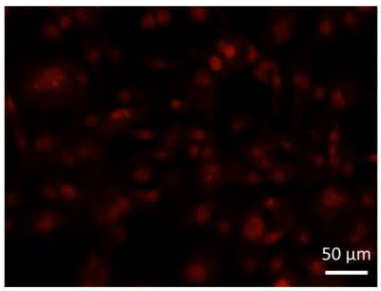
DOX	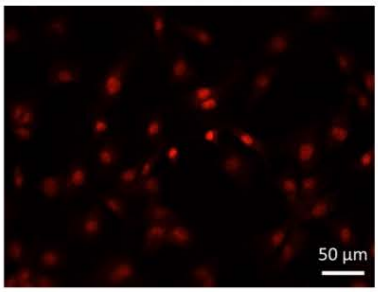	Il-1β	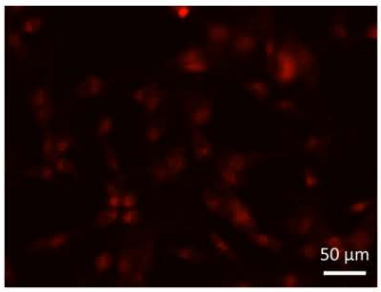

References

(1) Jung, Y., Lee, H.S., Ha, J.M., Jin, S.Y., Kum, H.J., Vafaeinik, F., Ha, H.K., Song, S.H., Kim, C.D., and Bae, S.S. (2021). Modulation of Vascular Smooth Muscle Cell Phenotype by High Mobility Group AT-Hook 1. *J Lipid Atheroscler* 10, 99-110.

(2) Maciel, T.T., Melo, R.S., and Campos, A.H. (2009). The bone morphogenetic protein antagonist gremlin promotes vascular smooth muscle cell apoptosis. *J Vasc Res* 46, 325-332.

(3) Liu, H.D., Li, W., Chen, Z.R., Hu, Y.C., Zhang, D.D., Shen, W., Zhou, M.L., Zhu, L., and Hang, C.H. (2013). Expression of the NLRP3 inflammasome in cerebral cortex after traumatic brain injury in a rat model. *Neurochem Res* 38, 2072-2083.

(4) Liu, N., Liu, J., Ji, Y., Lu, P., Wang, C., and Guo, F. (2010). C-Reactive Protein Induces TNF-alpha Secretion by p38 MAPK-TLR4 Signal Pathway in Rat Vascular Smooth Muscle Cells. *Inflammation*.

(5) San Martin, A., Foncea, R., Laurindo, F.R., Ebensperger, R., Griendling, K.K., and Leighton, F. (2007). Nox1-based NADPH oxidase-derived superoxide is required for VSMC activation by advanced glycation end-products. *Free Radic Biol Med* 42, 1671-1679.

Manuscript 4: Long-Term Treatment of Azathioprine in Rats Induces Vessel Mineralization

This manuscript has been published in *Biomedicines (IF:6.081)*:

Schuchardt M, **Herrmann J**, Henkel C, Babic M, van der Giet M, Tolle M. Long-Term Treatment of Azathioprine in Rats Induces Vessel Mineralization. *Biomedicines.* 2021;9(3):327.

DOI: 10.3390/biomedicines9030327

The authors' contributions are stated in the publication on page 11/14. My personal contribution to this article encompasses:

Laboratory work:

- Microscopic imaging of histological staining
- Quantification of gene expression (PCR)
- *Ex vivo* setting
- Luminex®

Manuscript preparation:

- Writing of the original draft. adaption after revision and final editing

biomedicines

MDPI

Article

Long-Term Treatment of Azathioprine in Rats Induces Vessel Mineralization

Mirjam Schuchardt [1], Jaqueline Herrmann [1,2], Cornelia Henkel [1], Milen Babic [1], Markus van der Giet [1,*] and Markus Tölle [1]

[1] Department of Nephrology and Medical Intensive Care, Charité–Universitätsmedizin Berlin, 12203 Berlin, Germany; mirjam.schuchardt@charite.de (M.S.); Jaqueline.Herrmann@charite.de (J.H.); Cornelia.Henkel@charite.de (C.H.); Milen.Babic@charite.de (M.B.); Markus.Toelle@charite.de (M.T.)
[2] Department of Biochemistry, Chemistry and Pharmacy, Freie Universität Berlin, 14195 Berlin, Germany
* Correspondence: Markus.vanderGiet@charite.de

Abstract: Medial vascular calcification (mVC) is closely related to cardiovascular disease, especially in patients suffering from chronic kidney disease (CKD). Even after successful kidney transplantation, cardiovascular mortality remains increased. There is evidence that immunosuppressive drugs might influence pathophysiological mechanisms in the vessel wall. Previously, we have shown in vitro that mVC is induced in vascular smooth muscle cells (VSMCs) upon treatment with azathioprine (AZA). This effect was confirmed in the current study in an in vivo rat model treated with AZA for 24 weeks. The calcium content increased in the aortic tissue upon AZA treatment. The pathophysiologic mechanisms involve AZA catabolism to 6-thiouracil via xanthine oxidase (XO) with subsequent induction of oxidative stress. Proinflammatory cytokines, such as interleukin (IL)-1ß and IL-6, increase upon AZA treatment, both systemically and in the aortic tissue. Further, VSMCs show an increased expression of core-binding factor α-1, alkaline phosphatase and osteopontin. As the AZA effect could be decreased in NLRP3$^{-/-}$ aortic rings in an ex vivo experiment, the signaling pathway might be, at least in part, dependent on the NLRP3 inflammasome. Although human studies are necessary to confirm the harmful effects of AZA on vascular stiffening, these results provide further evidence of induction of VSMC calcification under AZA treatment and its effects on vessel structure.

Keywords: aging; azathioprine; calcification; mineralization; senescence-associated secretory phenotype

Citation: Schuchardt, M.; Herrmann, J.; Henkel, C.; Babic, M.; van der Giet, M.; Tölle, M. Long-Term Treatment of Azathioprine in Rats Induces Vessel Mineralization. *Biomedicines* **2021**, *9*, 327. https://doi.org/10.3390/biomedicines9030327

Academic Editor: Andreas Weber

Received: 18 February 2021
Accepted: 17 March 2021
Published: 23 March 2021

1. Introduction

Vascular disease in general and arteriosclerosis in particular remain a major cause of cardiovascular morbidity and mortality, not only in patients suffering from chronic renal failure, but also in elderly patients. Up to now, convincing clinical therapy concepts are not available [1]. A longitudinal study with kidney transplant patients revealed substantial medial vascular calcification (mVC) within four years even when cardiovascular mortality decreases after transplantation [2,3]. Beside the influence of uremic toxins on vascular smooth muscle cell (VSMC) physiology [4] in patients with chronic kidney disease (CKD), evidence exists that immunosuppressive therapy can influence signaling pathways in vascular cells and thereby affect the progression of vascular alterations [5]. One of those potent immunosuppressive drugs is azathioprine (AZA) [6,7]. Even though AZA has been replaced in patients who have undergone solid organ transplantation [6], it is still routinely used as a treatment of several auto-immune diseases [7–9]. Several indications exist that AZA treatment has an impact on the cardiovascular risk and pathophysiology of the vessel wall [8,9]. In a previous study, we found an induction of mVC and oxidative stress upon treatment with the cleavage product of AZA, 6-mercaptopurine (6-MP), using an in vitro model with rat VSMCs [10]. Extensive research in the field of VSMC calcification revealed the involvement of several mechanisms including osteogenic, senescence and inflammatory signaling. VSMCs are characterized by a phenotype shift from a contractile

to a secreting cell called the senescence-associated secretory phenotype (SASP) [11–13]. Recently, Shanahan's group characterized the SASP of VSMCs by gene expression of several calcification markers, e.g., alkaline phosphatase (ALP), interleukin (IL)-1ß and p21 [13]. In the pathogenesis of CKD, inflammation and calcification are present in patients, even in early CKD stages [14]. A relevant role of NLRP3 inflammasome activation and IL-1ß production has been reported for the calcification process [15]. At least in vitro, IL-1ß stimulates VSMC calcification, while NLRP3 knockdown inhibits it [15]. Further, it has been shown that IL-6 induces calcification of human VSMCs in vitro [16]. In patients treated with AZA, the IL-6 plasma level and oxidative stress markers increase [17]. In the current study, the calcifying effect of AZA was investigated in an in vivo rat model treated with AZA for 24 weeks to support evidence of possible harmful effects on vessel stiffening in patients who underwent long-term AZA treatment over years.

2. Materials and Methods

2.1. Animals

Male Wistar rats ($n = 29$) were purchased from Janvier (Le Genest-Saint-Isle) at the age of 8 weeks. At the age of 14 weeks, rats were divided randomly into 2 groups. For 24 weeks, the treatment group ($n = 16$) received AZA (10 mg/kg body weight) orally via the drinking water and the control group ($n = 13$) received no therapy. The drinking solution for the animal treatment was prepared daily and the amount of drinking water per cage was monitored to determine the mean AZA uptake per animal and day. Health and body weight statuses were monitored in short intervals during the trial period. After 24 weeks, animals were sacrificed by intraperitoneal injection of pentobarbital (400 mg/kg body weight). Blood was obtained and organ specimens were prepared for cryofixation and formalin fixation. Heparin plasma was collected by centrifugation, aliquoted and frozen at −80 °C until use. NLRP3$^{+/+}$ and NLPR3$^{-/-}$ mice (C57/BL6 background) were sacrificed by intraperitoneal injection of pentobarbital (200 mg/kg body weight). Blood was obtained in heparinized tubes; heparin plasma was collected by centrifugation and aliquoted frozen at −80 °C until use. Rats and mice were kept on a 12 h light/dark cycle with chow and water ad libitum. The room temperature was around 22 °C. Chow was purchased from Ssniff (Soest).

2.2. Blood Parameters

Blood parameters were analyzed in heparin plasma by a blood dry chemistry analyzer (Fuji) for alkaline phosphatase (ALP), calcium (Ca) and inorganic phosphate (IP) according to the manufacture's recommendations. Parathyroid hormone (PTH) (Rat Biointact PTH ELISA, Immutopics), serum amyloid A (SAA, Rat SAA CLIA Kit, ElabScience), 8-oxo-2-deoxyguanosine (MyBioScource), Fetuin-A (LS Bio), Caspase-1 (Biorbyt) and MGP (LS Bio) plasma concentrations were measured via ELISA according to the manufacture's protocol. Plasma concentration of 23 cytokines was determined using Milliplex (Millipore) according to the manufacturer's instructions.

2.3. Histological Staining

Histological stains of the aorta were performed in 4 µm sections of paraffin-embedded tissue. Deparaffinized sections were subsequently stained using von Kossa staining. Images were acquired using a Zeiss AxioVert 200M light microscope with ZEN2 software (Zeiss, blue edition).

2.4. Quantification of the Tissue Calcium Content

Extracellular calcium content of different vascular beds was determined as previously published [10,18].

2.5. Ex Vivo Stimulation of Aortic Tissue

The thoracic aorta of NLRP3$^{+/+}$ and NLRP3$^{-/-}$ mice was stimulated with calcification medium: Dulbecco's modified Eagle medium (DMEM) 4.5 g/L glucose, supplemented with 15% fetal calf serum, 1% penicillin/streptomycin, 5 mmol/L sodium hydrogen phosphate and 0.284 mmol/L ascorbic acid. In co-stimulated samples, medium supplemented with 0.1 mmol/L AZA was used. The aortic tissue was stimulated for 14 days, and the medium was changed every three days. Afterwards, the aortic tissue was decalcified for 24 h with 0.6 mol/L hydrochloric acid (HCl). The tissue was dried, and dry weight was measured for normalization.

2.6. Gene Expression

Cryoconserved tissue was homogenized using the Tissue Ruptor with disposable probes (Qiagen). RNA was isolated using Trizol® (Fisher Scientific, Waltham, MA, USA) and afterwards reverse transcribed using the High-Capacity cDNA Reverse Transcription Kit™ (Applied Biosystems) according to the manufacture's protocol. Quantitative determination of mRNA expression was conducted using the iQ™ SYBR Green supermix and the CFX384 real-time PCR detection system (Biorad, CFX software version 3.1). The oligonucleotide sequences are given in Supplementary Table S1. GAPD, Ppia and Rpl13A were used as housekeeping normalization for each sample. The Ct average of the respective control mice was used for Ct normalization.

2.7. Statistical Analysis

Data are provided as mean ± SEM. Statistical analysis was performed using GraphPad Prism software (version 6.0). To evaluate differences between treatment groups, the Mann–Whitney U test or Wilcoxon matched pairs test was applied. A p-value < 0.05 was considered as statistically significant.

3. Results

3.1. In Vivo Model

The AZA treatment over 24 weeks was well tolerated by all rats. Both groups, the control and treatment groups, gained significantly in weight during the observation period without any significant difference between the two groups. Furthermore, there was no significant difference between the groups in organ weight of the heart and kidney (Table 1) and in the plasma concentration of the blood parameter IP. In contrast, Ca plasma levels and ALP plasma concentration increased significantly during long-term AZA treatment. However, the calcium phosphate product was not significantly different between both groups (Table 1). The PTH plasma concentration increased upon AZA treatment for 24 weeks but did not reach statistical significance.

Table 1. Body weight, blood parameters and organ weight of rats. Heart and kidney weights are given as wet tissue weight normalized to animal weight. Mean ± SEM.

Group	Rat N	Body Weight [g] Initial vs. Final	Heart Weight [mg/g]	Kidney Weight [mg/g]	ALP [U/L]	IP [mmol/L]	Ca [mmol/L]	Ca x IP	PTH [pg/mL]
Control	13	332.1 ± 6.2 504.2 ± 10.5 #	2.54 ± 0.06	5.09 ± 0.10	148.50 ± 18.49	2.03 ± 0.12	2.41 ± 0.07	4.9 ± 0.34	888.0 ± 155.4
AZA	16	344.9 ± 5.0 511.4 ± 11.9 #	2.60 ± 0.09	5.21 ± 0.13	204.30 [1] ± 23.54 *	2.10 ± 0.07	2.63 ± 0.08 *	5.5 ± 0.25	1.347.0 ± 387.7

AZA: azathioprine, ALP: alkaline phosphatase, IP: inorganic phosphate, Ca: calcium, PTH: parathyroid hormone. [1] Animal number 14, # $p < 0.05$ initial vs. final of the same group, * $p < 0.05$ control vs. AZA.

3.2. Effect of Azathioprine on Vessel Mineralization after 24 Weeks of Treatment

The degree of calcification of the Aorta (A.) thoracales and A. abdominales was determined by measurement of tissue calcium content and via von Kossa staining. The distribution and frequency of the calcium content of investigated vessels are given in Figure 1A. The majority of animals in the AZA-treated group (85%) had elevated tissue

calcium in both A. thoracales and A. abdominales. The calcium content was higher in the distal vessel part. The von Kossa-stained histological sections (Figure 1B) of AZA-treated rats demonstrate diffuse calcium deposits localized in the media of the vessel wall, indicating the progression of calcification. The plasma concentrations of the calcification inhibitors Fetuin A and MGP are not different between both groups (Table 2).

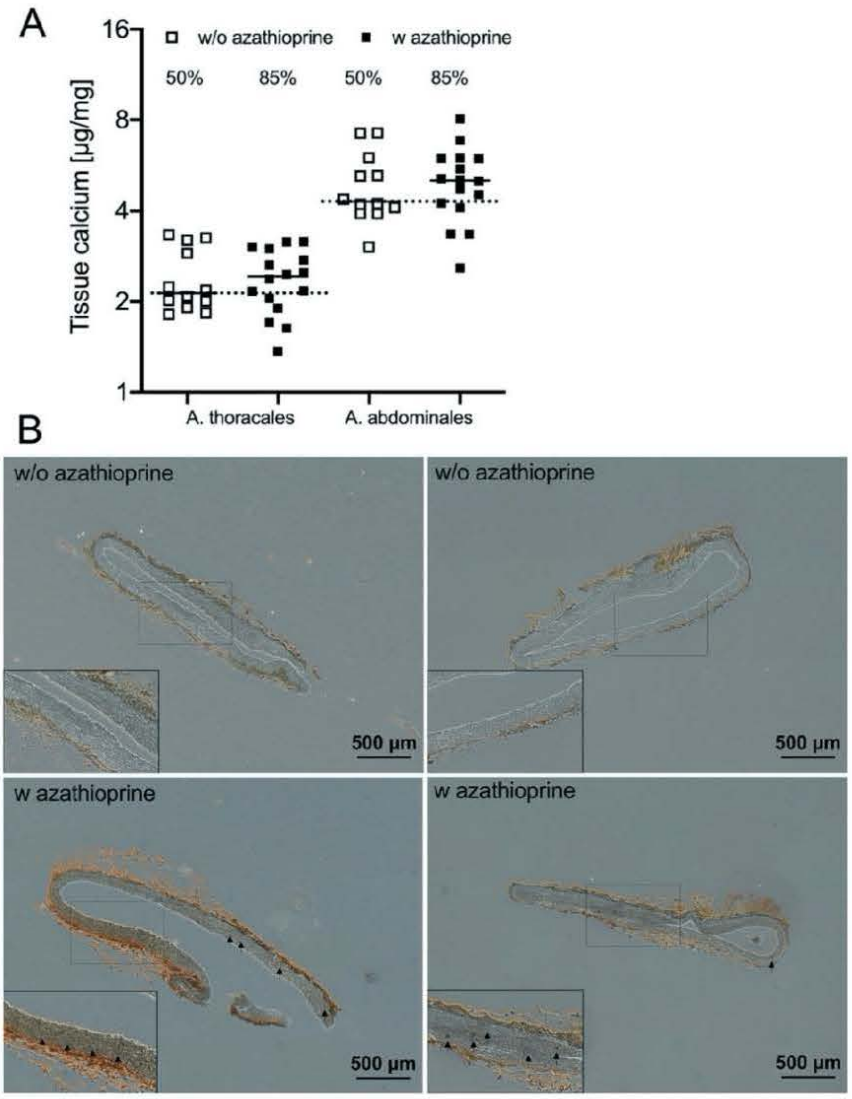

Figure 1. Quantification of mineralization of aortic tissue from rats. (**A**) Distribution and frequency of calcium content in different vessels (median). Each data point represents one animal; the dotted line represents the control median of azathioprine (AZA)-untreated animals; the % represents the number of animals above the control median (w/o AZA: $n = 12$, w AZA: $n = 16$). (**B**) Two representative images per group of von Kossa-stained aortic sections (A. abdominales). Arrow indicates vessel mineralization crystals.

Table 2. Plasma concentration of calcification inhibitors. Mean ± SEM.

Group	Rat Number	Fetuin-A [ng/mL]	MGP [ng/mL]
Control	13	89.22 ± 0.28	92.25 ± 4.17
AZA	16	89.21 ± 0.17	84.42 ± 2.81

AZA: azathioprine, MGP: matrix Gla protein.

3.3. Azathioprine Treatment Induces Oxidative Stress and Reduces Antioxidative Capacity in Aortic Tissue

A short schema of the AZA metabolism is given in Figure 2A. The prodrug AZA is cleaved non-enzymatically or by glutathione S-transferases (GST) to 6-MP, which is then further metabolized enzymatically by xanthine oxidase (XO) and hypoxanthine-guanine phosphoribosyl transferase (HRPT1) to 6-thiouracil or 6-thioionosine monophosphate. After AZA treatment, the HRPT1 mRNA in aortic tissue is significantly decreased (Figure 2B), while XO is significantly increased after AZA treatment (Figure 2C).

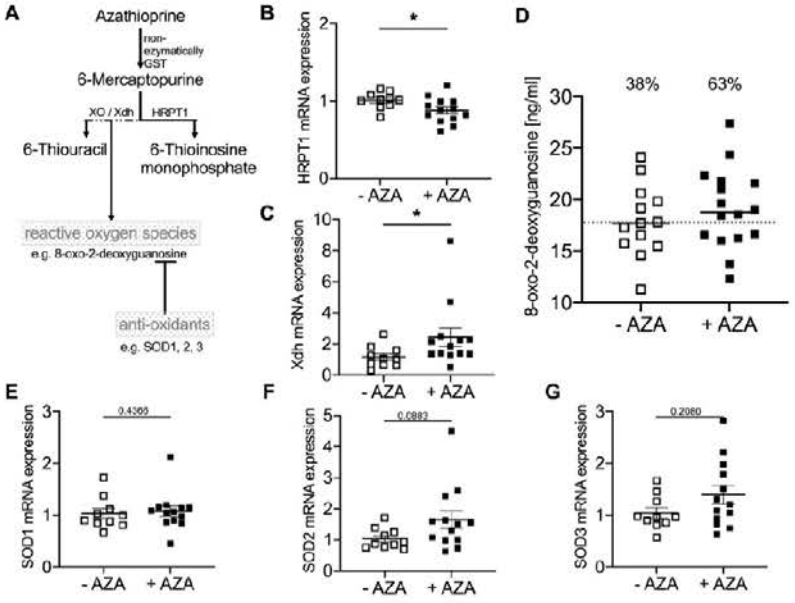

Figure 2. Oxidative and antioxidative capacity upon azathioprine (AZA) treatment. (**A**) Schema of AZA metabolism. (**B**,**C**,**E**–**G**) mRNA expression in aortic tissue from rats (w/o AZA: $n = 10$, w AZA: $n = 13$), Mean ± SEM. * $p < 0.05$ vs. control. (**D**) Reactive oxygen species (ROS) plasma level via detection of 8-oxo-2-deoxyguanosine. Each data point represents an animal (median, w/o AZA: $n = 13$, w AZA: $n = 16$); the dotted line represents the control median of AZA-untreated animals; the % represents the number of animals above the control median.

During AZA catabolism via XO, reactive oxygen species (ROS) are generated. Therefore, 8-oxo-2-desoxyguanosine plasma levels as a ROS marker were measured. The distribution and frequency of the ROS increase upon AZA treatment are shown in Figure 2D. To investigate the antioxidative capacity, SOD1, 2 and 3 mRNA expression was measured. SOD1 and SOD3 mRNA expression was not found to be different in the AZA-treated group compared to the untreated controls. For SOD2, the mRNA expression slightly increased upon AZA treatment; however, it did not reach statistical significance (Figure 2E–G).

3.4. Azathioprine Treatment Induces SASP: Cytokine Plasma Level

Secretion of proinflammatory cytokines is one sign of the SASP of cells [19]. Therefore, the plasma levels of different cytokines were measured as systemic markers of inflammation. Out of 23 investigated cytokines, plasma concentrations of six are increased (Figure 3A) and three are decreased (Figure 3B) upon AZA treatment compared to the control group. In the treatment group, the plasma concentration of IL-1ß, IL-6 and vascular endothelial growth factor (VEGF) significantly increased, whereas the concentration of IL-7, GM-CSF and MIP-1α only tends to be increased. Interestingly, the plasma concentration of IL-18, RANTES and serum amyloid A (SAA) significantly decreased in the treatment group.

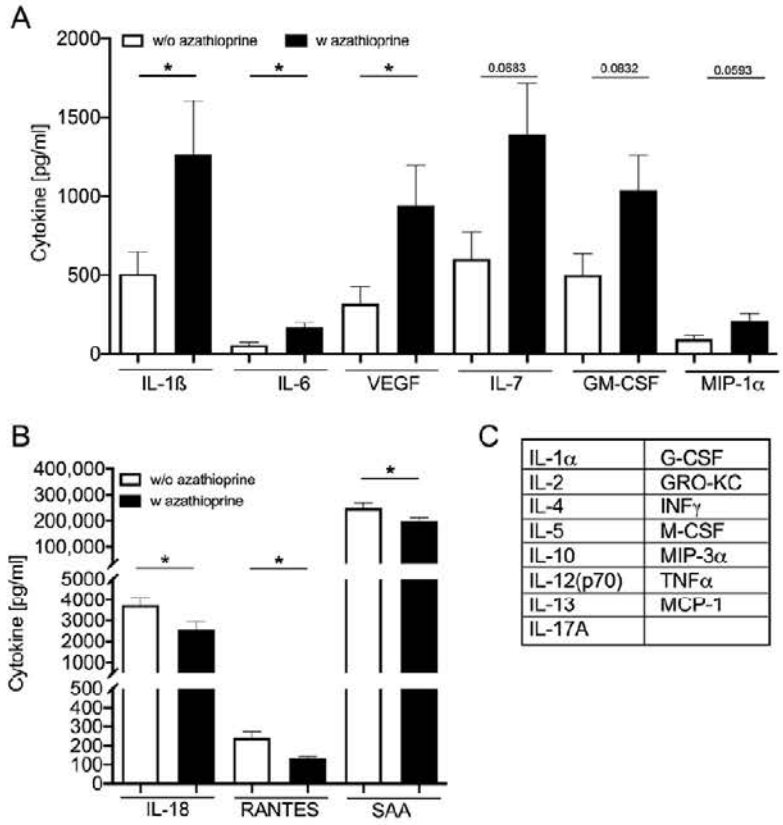

Figure 3. Cytokine plasma concentration in rats. (**A**) Cytokines that increase in plasma upon azathioprine (AZA) treatment and (**B**) that decrease compared to the untreated animals. Mean ± SEM, * $p < 0.05$. (**C**) Further measured cytokines without a significant difference between AZA-untreated and -treated groups.

3.5. Azathioprine Treatment Induces SASP and Mineralization in Aortic Tissue

Cells change their expression profile during SASP response [13]. Therefore, the mRNA expression of osteoblastic, inflammatory and senescence markers in aortic tissue was determined. In the treatment group, the expression of the osteoblastic marker protein core-binding factor α1 (Cbfa1), the tissue non-specific ALP and osteopontin (OPN) significantly increased, whereas the expression of the VSMC marker protein SM22α significantly decreased compared to the control group. In addition to the increased systemic expression of the proinflammatory cytokines IL-1ß and IL-6, their mRNA expression in aortic tissue was significantly upregulated after 24 weeks of AZA treatment. The expression of cell cycle proteins p16, p21 and p53 was not altered (Figure 4).

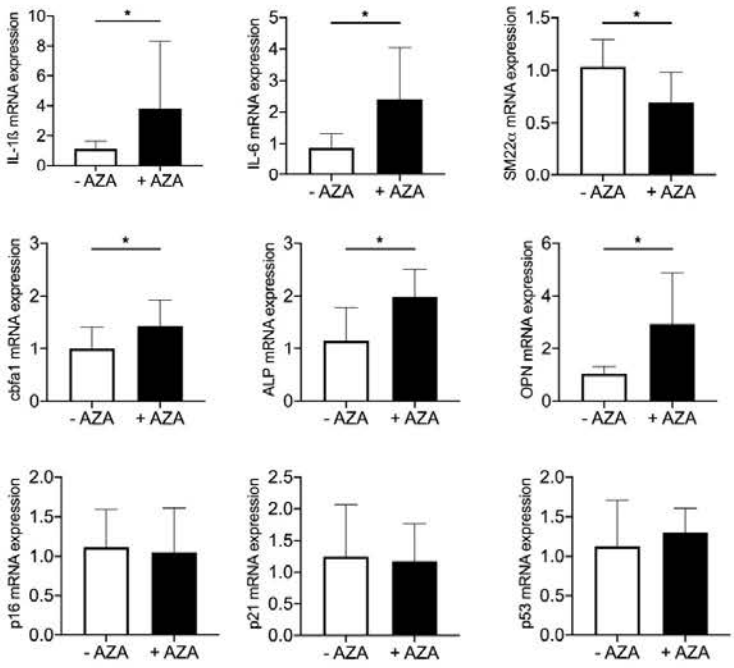

Figure 4. Expression of senescence-associated phenotype markers in aortic tissue from rats upon azathioprine treatment. mRNA expression in aortic tissue of azathioprine (AZA)-treated rats vs. control animals. Mean ± SEM, * $p < 0.05$.

3.6. SASP Induction Is NLRP3-Dependent

There is evidence that the NLRP3 inflammasome complex is involved in mVC [15]. Therefore, we tested the mRNA expression of ASC, NLRP3 and Caspase-1, in the aortic tissue of our model. In the treatment group, the expression of NLRP3, ASC and Caspase-1 is significantly increased in the aortic tissue (Figure 5A–C). The systemic plasma concentration of Caspase-1 is not significantly different between treated and untreated rats (Figure 5D). To further investigate the pathway via NLRP3 in the calcification process, aortic rings from the A. thoracales of $NLRP3^{-/-}$ mice and respective $NLRP3^{+/+}$ control animals were stimulated ex vivo for 14 days with calcification medium alone and with calcification medium supplemented with AZA. The plasma levels of ALP, IP and Ca do not significantly differ between knockout and control animals. However, in aortic rings of $NLRP3^{+/+}$ mice, calcification media significantly induce tissue calcium content, and co-stimulation with AZA further increases tissue calcium content in these animals. In $NLRP3^{-/-}$ mice, the induction effect of AZA is significantly reduced (Figure 5H).

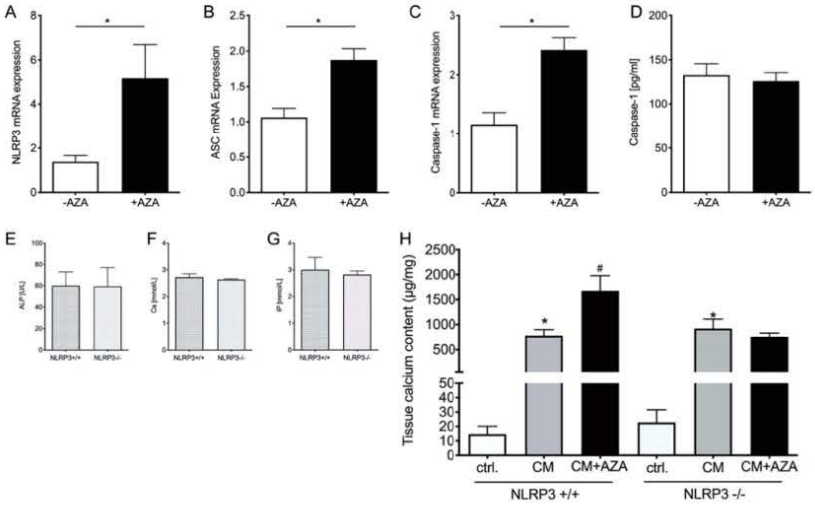

Figure 5. NLRP3-dependent induction of senescence-associated phenotype markers. (**A**–**C**) mRNA expression in aortic tissue from rats. (**D**) Caspase-1 plasma concentration in azathioprine (AZA)-treated and -untreated rats. (**E**–**G**) Plasma concentration of alkaline phosphatase (ALP), inorganic phosphate (IP) and calcium (Ca) in NLRP3$^{+/+}$ and NLRP3$^{-/-}$ mice. (**H**) Aortic tissue rings of NLRP3$^{+/+}$ and NLRP3$^{-/-}$ mice were treated for 14 days ex vivo using control and calcification media in the presence or absence of AZA (0.1 mmol/L) and tissue calcium contents were quantified. Arrows indicating calcification foci. (**E**–**H**) $n = 6$. (**A**–**H**) Mean ± SEM, * $p < 0.05$ vs. control, # $p < 0.05$ vs. CM.

4. Discussion

In the current study, we examined the in vivo long-term effect of AZA treatment on mVC in rats. In line with our in vitro data [10], we show that AZA treatment over 24 weeks induces vessel calcification and proinflammatory SASP activation in the aortic tissue. The effect is, at least in part, driven by the NLRP3 inflammasome (Figure 6).

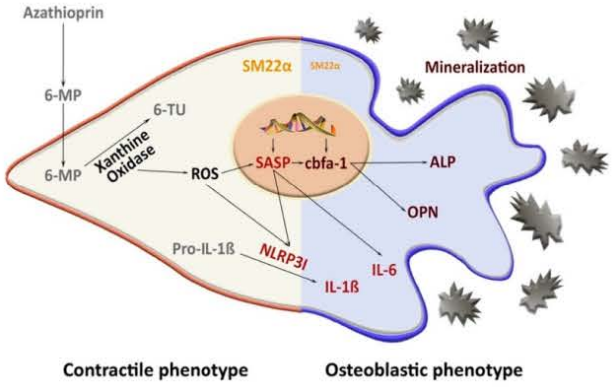

Figure 6. Proposed mechanism of azathioprine-induced vessel mineralization. 6-MP: 6-mercaptopurine, 6-TU: 6-thiouracil, ROS: reactive oxygen species, IL-ß: interleukin 1-ß, IL-6: interleukin 6, SASP: senescence-associated secretory phenotype, NLRP3I: NLRP3 inflammasome, SM22α: smooth muscle protein 22 α, cbfa1: core-binding factor alpha-1, OPN: osteopontin, ALP: alkaline phosphatase.

AZA is a potent immunosuppressive drug that it is still routinely used as a treatment of several auto-immune diseases [7–9]. Evidence exists that AZA treatment increases the cardiovascular risk of patients [8,9]. Arteriosclerosis and subsequent stiffening of the vessel wall are some of the risk factors for cardiovascular events, not only in patients with CKD or after organ transplantation [2,3].

In a recent in vitro study, we already observed an induction of VSMC calcification upon 6-MP treatment [10]. 6-MP is the active metabolite of AZA which is cleaved non-enzymatically or via GST [8,20]. In line with the in vitro data, the present study shows an increased mVC of the aortic tissue in the treatment group. However, even though the calcification was induced by AZA treatment, the effect was less robust than expected from the in vitro data. The animals in the current study were treated with 10 mg/kg body weight for 24 weeks.

For other animal studies, the drug dose of AZA or its active metabolite 6-MP differs between 2 and 60 mg/kg body weight depending on the research question and model [21–28]. The drug dose for humans is usually 1–4 mg/kg body weight and depends on the individual indication. As the dose in animals is mostly higher than in humans, the application time in the animal experiment is relatively short compared to the treatment period of often decades in humans. In line with previous studies for different treatment periods, we found no significant difference in rat body mass upon AZA treatment [24,29].

In contrast to the in vitro situation, where only one cell type is typically investigated in an artificial environment, the in vivo situation is influenced by multiple systemic factors [30] that might contribute to differences observed in vitro and in vivo. The mechanisms in mVC are multifactorial and in vivo triggered by an imbalance between mineralization inducers and inhibitors [11]. First, we looked at blood parameters typically associated with mVC. Plasma concentrations of IP, PTH and the calcium phosphate product do not significantly differ between the treatment and control groups in our rat model. Under pathophysiological conditions, calcium and phosphate concentrations typically exceed their solubility. Endogenous inhibitors such as Fetuin-A and MGP are required to prevent ectopic precipitation of calcium phosphate complexes. Fetuin-A has potent inhibitory effects on calcification by protecting crystal growth and deposition [31]. MGP is highly expressed in calcified VSMCs, acts via a vitamin K-dependent pathway and has a high binding affinity to calcium ions [32]. However, plasma concentrations of Fetuin-A and MPG are not significantly different between the treatment and control groups and therefore cannot explain the observed effects.

As shown in vitro, the induction of calcification upon 6-MP was, at least partially, dependent on ROS generation via XO [10]. Therefore, we investigated the mRNA gene expression of HPRT-1 and XO, the main catabolic enzymes of 6-MP, in the aortic tissue. The expression of HPRT-1 was reduced, whereas the expression of XO was significantly enhanced. The increased plasma level of 8-oxodehydrogenase supports the finding of an ROS-dependent effect of AZA treatment via XO, which is in accordance with our former in vitro results [10]. In vessels from children on dialysis [13], 8-oxodehydrogenase could also be detected in calcified medium-sized muscular arteries, which shows the relevance of ROS for the induction of mVC as discussed elsewhere [33]. In our rat model, the expression of SOD1, 2 and 3 in aortic tissue as a measure of antioxidant capacity was not significantly altered between the groups.

The enhanced production of inflammatory cytokines/chemokines, such as IL-1, IL-6 and VEGF, is associated with the prevalence of mVC and age-related diseases [34–37]. Therefore, we first measured the systemic plasma levels of 23 potentially relevant analytes from the class of cytokines/chemokines and growth factors with potentially proinflammatory properties in our rat model. Indeed, the known SASP cytokines IL-1ß, IL-6 and VEGF are significantly increased upon AZA treatment. The activation of those SASP cytokines is in line with further research that found an induction of "paracrine senescence" in cell culture as well as mouse models [38]. Furthermore, the plasma level of IL-7, GM-CSF and MIP-1α tends to be increased upon AZA treatment for 24 weeks. IL-7 has been shown to be

upregulated in some age-related diseases [34]. Although the main sources of origin of the cytokines are different, cells of the blood vessels such as macrophages, T cells, monocytes and platelets, as well as endothelial cells and VSMC, could also produce cytokines [39].

Beside upregulation of inflammatory cytokines, the plasma levels of IL-18, RANTES and SAA are significantly decreased in AZA-treated animals compared to their respective controls. SAA acts as a proinflammatory cytokine on VSMCs via activation of, among others, toll-like receptor (TLR) 2 and 4 to activate monocyte chemoattractant protein-1 production (MCP-1) [40]. MCP-1 and RANTES have chemoattractive properties on macrophages in the vessel wall [21]. Pols et al. found an inhibition of MCP-1 upon 6-MP treatment, whereas no significant effects could be shown on RANTES production [21]. The atheroprotective properties of 6-MP were observed in a mouse model of hypercholesterolemic apoE animals, whereby the inhibitory action was mainly triggered by a reduction in monocyte activation [21]. Beside the detection of systemic SASP markers, we investigated the SASP activation directly in aortic tissue. Here again, the mRNA expression of IL-1ß and IL-6 is significantly increased upon AZA treatment. IL-6 is known as an inducer of mineralization in VSMCs [16,41,42]. In part, IL-6 influences MPG's inhibitory action [43]. In addition, IL-6 induces bone morphogenetic protein (BMP)-2, ALP and OPN expression in VSMCs in vitro [42]. The neutralization of IL-6 reduced the osteogenic mRNA expression in an in vitro model [44]. For IL-1ß, a calcification induction in VSMCs was also shown [15]. Further, typical osteogenic markers such as the transcription factor Cbfa1 and its downstream genes ALP and OPN significantly increase in the aortic tissue of AZA-treated animals. Cbfa1, also known as Runx2, is not only a regulatory transcription factor of osteoblastic differentiation but also an initial osteoblastic differentiation factor of VSMCs that is required for medial calcification in mice [45,46]. OPN provides strong affinity for hydroxyapatite, due to its negatively charged phosphoserines, and therefore acts as an inhibitor of mVC by preventing crystal growth [47]. In healthy arteries, OPN is not detectable but was found increased in calcified tissue [48]. The inhibitory effect of OPN on mVC has been shown in vitro and in vivo [49–51]. As all of these proteins are upregulated in aortic tissue upon AZA treatment, this underlines the harmful effect on vessel physiology. Although the inductions of senescence markers such as p16, p21 and p53 are also described as SASP components, we found no significant induction of those in our model upon AZA treatment. The missing induction of the investigated senescence markers p21, p16 and p53 in the aortic tissue might be one explanation for the lesser calcification induction compared to our in vitro model [10]. Here, AZA induces p16, p21 and p53 (unpublished data). Induction of VSMC calcification by hyperphosphatemia also induces p21 [52]. However, IL-6 production itself is a sign of senescent VSMCs [53]. Furthermore, IL-1ß induces senescence of VSMCs and promotes osteogenic differentiation [35]. Several pieces of evidence exist of a vicious cycle of calcification and senescence in VMSCs; however, whether this is a conjoint or consecutive pathway is not clear up to now. Microarray analysis of senescent VSMCs reveals differential regulation of calcifying markers such as MGP, BMP2 and OPG as well as inflammation markers such as IL-1ß and tissue remodeling markers such as VEGF [36]. However, one has to keep in mind that some of the experimental settings investigate bulk cells and single-cell-based methods seem to be necessary to answer that question.

To further examine the intracellular signaling pathway of SASP induction in the aortic tissue, we investigated the NLRP3 inflammasome, which is believed to play a role in the mineralization process and contribute to age-related disease [15,34,54]. NLRP3, ASC and Caspase-1 are upregulated in calcified VSMCs and lead to a subsequent IL-ß production [15]. The inhibition of the NLRP3 prevents calcification in vitro [15]. In the aortic tissue of AZA-treated rats, we found a significant increase in NLRP3, ASC and Caspase-1 mRNA expression, which is in line with the detected aortic IL-1ß expression. However, the systemic Caspase-1 plasma levels were not found to be significantly induced upon AZA treatment. To further verify the critical role of NLRP3 activation in our model, we studied aortic tissue in an ex vivo setting for 14 days upon AZA incubation. Our

results confirm that NLRP3 inflammasome activation may be, at least, one crucial signaling pathway in AZA-induced mVC.

Limitations of the study: The current study investigated vessel alterations such as media calcification upon AZA treatment. We wanted to investigate the effect of AZA on adult rats and therefore started the six-month treatment at the age of 14 weeks. Although only slight mineralization foci were found in the aortic tissue, a more extended treatment period was not possible due to the 3R (Reduce, Replace, Refine) thought of Russel and Burch [55] due to the increased tumor risk in older rats [56]. The current study did not investigate vessel stiffness parameters upon treatment such as pulse wave velocity, pulse pressure and systolic/diastolic blood pressure. However, the mRNA expression profile in the aortic tissue shows changes in the expression pattern of typical marker proteins for stiffened, mineralized vessels. Here, bone remodeling was not investigated. However, from other studies, it is known that AZA treatment in rats induces bone remodeling disorders by inhibiting bone formation and bone mineralization [29].

5. Conclusions

In conclusion, the current study confirmed the possible harmful effect of AZA treatment on vessel structure that was previously found in vitro using rat VSMCs [10]. Beside mineralization foci in the media of the aortic vessel wall, several changes in the SASP profile could be detected in the aortic tissue. Even though the effect seems not to be as strong as expected from our in vitro results [10], one has to keep in mind that humans are treated over years with AZA, whereas in the current model, only a smaller period could be investigated. In addition, AZA-treated patients mostly suffer from several comorbidities that could further reduce the antioxidative capacity of the organism and therefore pronounce the AZA-induced oxidative stress effect on VSMCs. However, the hypothesis has to be confirmed in human studies.

Supplementary Materials: Supplementary materials are available online at https://www.mdpi.com/2227-9059/9/3/327/s1.

Author Contributions: Conceptualization, M.S., M.T. and M.v.d.G.; methodology, M.S., C.H., J.H., and M.B. All authors have read and agreed to the published version of the manuscript.

Funding: The Ernst-und-Berta Grimmke Stiftung (M.S.) and Sonnenfeld Stiftung (M.T.; J.H.) funded this research project.

Institutional Review Board Statement: The animal study was conducted according to the guidelines of the EU Directive 2010/63/EU and was approved by the Landesamt fuer Gesundheit und Soziales Berlin, Germany, and the Charité–Universitätsmedizin Berlin, Germany.

Informed Consent Statement: Not applicable.

Acknowledgments: We thank Nathalie Siegel and the student assistants in the laboratory for their help in animal caring, tissue collection and sample preparation. We are grateful to Raissa Stayzyk for her work in the animal facility and thank, Katharina Kuschfeldt, Brigitte Egbers and Nadine Neitzel for their excellent technical assistance during the project. We thank Marcus Maurer (Charité–Universitätsmedizin Berlin) for the release of the NLRP3 mice for breeding. We acknowledge support from the German Research Foundation (DFG) and the Open Access Publication Fund of Charité—Universitätsmedizin Berlin.

Conflicts of Interest: The authors declare no conflict of interest.

References

1. Tölle, M.; Reshetnik, A.; Schuchardt, M.; Höhne, M.; van der Giet, M. Arteriosclerosis and vascular calcification: Causes, clinical assessment and therapy. *Eur. J. Clin. Investig.* **2015**, *45*, 976–985. [CrossRef]
2. Bottomley, M.J.; Harden, P.N. Update on the long-term complications of renal transplantation. *Br. Med. Bull.* **2013**, *106*, 117–134. [CrossRef]

3. Maréchal, C.; Coche, E.; Goffin, E.; Dragean, A.; Schlieper, G.; Nguyen, P.; Floege, J.; Kanaan, N.; Devuyst, O.; Jadoul, M. Progression of Coronary Artery Calcification and Thoracic Aorta Calcification in Kidney Transplant Recipients. *Am. J. Kidney Dis.* **2012**, *59*, 258–269. [CrossRef]
4. Hénaut, L.; Mary, A.; Chillon, J.-M.; Kamel, S.; Massy, Z.A. The Impact of Uremic Toxins on Vascular Smooth Muscle Cell Function. *Toxins* **2018**, *10*, 218. [CrossRef] [PubMed]
5. Liefeldt, L.; Budde, K. Risk factors for cardiovascular disease in renal transplant recipients and strategies to minimize risk. *Transpl. Int.* **2010**, *23*, 1191–1204. [CrossRef] [PubMed]
6. Halloran, P.F. Immunosuppressive Drugs for Kidney Transplantation. *New Engl. J. Med.* **2004**, *351*, 2715–2729. [CrossRef] [PubMed]
7. Gearry, R.B.; Barclay, M.L. Azathioprine and 6-mercaptopurine pharmacogenetics and metabolite monitoring in inflammatory bowel disease. *J. Gastroenterol. Hepatol.* **2005**, *20*, 1149–1157. [CrossRef]
8. Solomon, D.H.; Avorn, J.; Katz, J.N.; Weinblatt, M.E.; Setoguchi, S.; Levin, R.; Schneeweiss, S. Immunosuppressive medications and hospitalization for cardiovascular events in patients with rheumatoid arthritis. *Arthritis Rheum.* **2006**, *54*, 3790–3798. [CrossRef]
9. Haque, S.; Gordon, C.; Isenberg, D.; Rahman, A.; Lanyon, P.; Bell, A.; Emery, P.; McHugh, N.; Teh, L.S.; Scott, D.G.; et al. Risk Factors for Clinical Coronary Heart Disease in Systemic *Lupus Erythematosus*: The Lupus and Atherosclerosis Evaluation of Risk (LASER) Study. *J. Rheumatol.* **2009**, *37*, 322–329. [CrossRef]
10. Prüfer, J.; Schuchardt, M.; Tolle, M.; Prüfer, N.; Höhne, M.; Zidek, W.; van der Giet, M. Harmful Effects of the Azathioprine Metabolite 6-Mercaptopurine in Vascular Cells: Induction of Mineralization. *PLoS ONE* **2014**, *9*, e101709. [CrossRef]
11. Lee, S.J.; Lee, I.-K.; Jeon, J.-H. Vascular Calcification—New Insights into Its Mechanism. *Int. J. Mol. Sci.* **2020**, *21*, 2685. [CrossRef] [PubMed]
12. Voelkl, J.; Lang, F.; Eckardt, K.-U.; Amann, K.; Kuro, O.M.; Pasch, A.; Pieske, B.; Alesutan, I. Signaling pathways involved in vascular smooth muscle cell calcification during hyperphosphatemia. *Cell. Mol. Life Sci.* **2019**, *76*, 2077–2091. [CrossRef] [PubMed]
13. Sanchis, P.; Ho, C.Y.; Liu, Y.; Beltran, L.E.; Ahmad, S.; Jacob, A.P.; Furmanik, M.; Laycock, J.; Long, D.A.; Shroff, R.; et al. Arterial "inflammaging" drives vascular calcification in children on dialysis. *Kidney Int.* **2019**, *95*, 958–972. [CrossRef] [PubMed]
14. Benz, K.; Varga, I.; Neureiter, D.; Campean, V.; Daniel, C.; Heim, C.; Reimann, A.; Weyand, M.; Hilgers, K.F.; Amann, K. Vascular inflammation and media calcification are already present in early stages of chronic kidney disease. *Cardiovasc. Pathol.* **2017**, *27*, 57–67. [CrossRef]
15. Wen, C.; Yang, X.; Yan, Z.; Zhao, M.; Yue, X.; Cheng, X.; Zheng, Z.; Guan, K.; Dou, J.; Xu, T.; et al. Nalp3 inflammasome is activated and required for vascular smooth muscle cell calcification. *Int. J. Cardiol.* **2013**, *168*, 2242–2247. [CrossRef] [PubMed]
16. Kurozumi, A.; Nakano, K.; Yamagata, K.; Okada, Y.; Nakayamada, S.; Tanaka, Y. IL-6 and sIL-6R induces STAT3-dependent differentiation of human VSMCs into osteoblast-like cells through JMJD2B-mediated histone demethylation of RUNX2. *Bone* **2019**, *124*, 53–61. [CrossRef]
17. Alvarez-Leite, J.I.; dos Santos, L.C.; Costa, A.V.; Lopes, L.G.; Leonel, A.J.; Aguilar, E.C.; Noviello, M.D.L.M.; Ferrari, M.D.L. Combination of Azathioprine and Aminosalicylate Treatment Prevent Risk of Cardiovascular Disease in Women with Ulcerative Colitis by Reducing Inflammation. *Med. Sci. Monit.* **2015**, *21*, 2305–2315. [CrossRef]
18. Schuchardt, M.; Tölle, M.; Prüfer, J.; Prüfer, N.; Huang, T.; Jankowski, V.; Jankowski, J.; Zidek, W.; van der Giet, M. Uridine adenosine tetraphosphate activation of the purinergic receptor P2Y enhances in vitro vascular calcification. *Kidney Int.* **2012**, *81*, 256–265. [CrossRef]
19. Kim, D.H.; Bang, E.; Arulkumar, R.; Ha, S.; Chung, K.W.; Park, M.H.; Choi, Y.J.; Yu, B.P.; Chung, H.Y. Senoinflammation: A major mediator underlying age-related metabolic dysregulation. *Exp. Gerontol.* **2020**, *134*, 110891. [CrossRef]
20. Polifka, J.E.; Friedman, J. Teratogen update: Azathioprine and 6-mercaptopurine. *Teratology* **2002**, *65*, 240–261. [CrossRef] [PubMed]
21. Pols, T.W.; Bonta, P.I.; Pires, N.M.; Otermin, I.; Vos, M.; de Vries, M.R.; van Eijk, M.; Roelofsen, J.; Havekes, L.M.; Quax, P.H.; et al. 6-Mercaptopurine Inhibits Atherosclerosis in Apolipoprotein E*3-Leiden Transgenic Mice Through Atheroprotective Actions on Monocytes and Macrophages. *Arter. Thromb. Vasc. Biol.* **2010**, *30*, 1591–1597. [CrossRef]
22. Ligumsky, M.; Badaan, S.; Lewis, H.; Meirow, D. Effects of 6-mercaptopurine treatment on sperm production and reproductive performance: A study in male mice. *Scand. J. Gastroenterol.* **2005**, *40*, 444–449. [CrossRef] [PubMed]
23. Kles, V.; Hyrien, O.; Poul, J.-M.; Sanders, P. Application of pharmacokinetic/pharmacodynamic and stochastic modelling to 6-mercaptopurine micronucleus induction in mouse bone marrow erythrocytes. *J. Appl. Toxicol.* **2003**, *23*, 59–70. [CrossRef] [PubMed]
24. Platzek, T.; Schwabe, R. Combined prenatal toxicity of 6-mercaptopurine riboside and hydroxyurea in mice. *Teratog. Carcinog. Mutagen.* **1999**, *19*, 223–232. [CrossRef]
25. Chang, C.-Z.; Lin, C.-L.; Kassel, N.F.; Kwan, A.-L.; Howng, S.-L. 6-Mercaptopurine attenuates adhesive molecules in experimental vasospasm. *Acta Neurochir.* **2010**, *152*, 861–867. [CrossRef]
26. Furukawa, S.; Hayashi, S.; Usuda, K.; Abe, M.; Ogawa, I. The relationship between fetal growth restriction and small placenta in 6-mercaptopurine exposed rat. *Exp. Toxicol. Pathol.* **2011**, *63*, 89–95. [CrossRef] [PubMed]

27. Kanemitsu, H.; Yamauchi, H.; Komatsu, M.; Yamamoto, S.; Okazaki, S.; Uchida, K.; Nakayama, H. 6-Mercaptopurine (6-MP) induces cell cycle arrest and apoptosis of neural progenitor cells in the developing fetal rat brain. *Neurotoxicol. Teratol.* **2009**, *31*, 104–109. [CrossRef] [PubMed]
28. Pires, N.M.; Pols, T.W.; de Vries, M.R.; van Tiel, C.M.; Bonta, P.I.; Vos, M.; Arkenbout, E.K.; Pannekoek, H.; Jukema, J.W.; Quax, P.H.; et al. Activation of Nuclear Receptor Nur77 by 6-Mercaptopurine Protects Against Neointima Formation. *Circulation* **2007**, *115*, 493–500. [CrossRef] [PubMed]
29. Cegiela, U.; Kaczmarczyk-Sedlak, I.; Pytlik, M.; Folwarczna, J.; Nowinska, B.; Fronczek-Sokol, J. Alendronate prevents development of the skeletal changes induced by azathioprine in rats. *Acta Pol. Pharm.* **2013**, *70*, 309–315. [PubMed]
30. Herrmann, J.; Babic, M.; Tölle, M.; van der Giet, M.; Schuchardt, M. Research Models for Studying Vascular Calcification. *Int. J. Mol. Sci.* **2020**, *21*, 2204. [CrossRef] [PubMed]
31. Heiss, A.; du Chesne, A.; Denecke, B.; Grötzinger, J.; Yamamoto, K.; Renné, T.; Jahnen-Dechent, W. Structural Basis of Calcification Inhibition by α2-HS Glycoprotein/Fetuin-A. *J. Biol. Chem.* **2003**, *278*, 13333–13341. [CrossRef]
32. Vassalle, C.; Iervasi, G. New insights for matrix Gla protein, vascular calcification and cardiovascular risk and outcome. *Atherosclerosis* **2014**, *235*, 236–238. [CrossRef]
33. Byon, C.H.; Heath, J.M.; Chen, Y. Redox signaling in cardiovascular pathophysiology: A focus on hydrogen peroxide and vascular smooth muscle cells. *Redox Biol.* **2016**, *9*, 244–253. [CrossRef] [PubMed]
34. Rea, I.M.; Gibson, D.S.; McGilligan, V.; McNerlan, S.E.; Alexander, H.D.; Ross, O.A. Age and Age-Related Diseases: Role of Inflammation Triggers and Cytokines. *Front. Immunol.* **2018**, *9*, 586. [CrossRef] [PubMed]
35. Han, L.; Zhang, Y.; Zhang, M.; Guo, L.; Wang, J.; Zeng, F.; Xu, D.; Yin, Z.; Xu, Y.; Wang, D.; et al. Interleukin-1β-Induced Senescence Promotes Osteoblastic Transition of Vascular Smooth Muscle Cells. *Kidney Blood Press. Res.* **2020**, *45*, 314–330. [CrossRef] [PubMed]
36. Burton, D.G.; Giles, P.J.; Sheerin, A.N.; Smith, S.K.; Lawton, J.J.; Ostler, E.L.; Rhys-Williams, W.; Kipling, D.; Faragher, R.G. Microarray analysis of senescent vascular smooth muscle cells: A link to atherosclerosis and vascular calcification. *Exp. Gerontol.* **2009**, *44*, 659–665. [CrossRef]
37. Xu, D.; Zeng, F.; Han, L.; Wang, J.; Yin, Z.; Lv, L.; Guo, L.; Wang, D.; Xu, Y.; Zhou, H. The synergistic action of phosphate and interleukin-6 enhances senescence-associated calcification in vascular smooth muscle cells depending on p53. *Mech. Ageing Dev.* **2019**, *182*, 111124. [CrossRef]
38. Acosta, J.C.; Banito, A.; Wuestefeld, T.; Georgilis, A.; Janich, P.; Morton, J.P.; Athineos, D.; Kang, T.-W.; Lasitschka, F.; Andrulis, M.; et al. A complex secretory program orchestrated by the inflammasome controls paracrine senescence. *Nat. Cell Biol.* **2013**, *15*, 978–990. [CrossRef]
39. Sprague, A.H.; Khalil, R.A. Inflammatory cytokines in vascular dysfunction and vascular disease. *Biochem. Pharmacol.* **2009**, *78*, 539–552. [CrossRef]
40. Schuchardt, M.; Prüfer, N.; Tu, Y.; Herrmann, J.; Hu, X.-P.; Chebli, S.; Dahlke, K.; Zidek, W.; van der Giet, M.; Tölle, M. Dysfunctional high-density lipoprotein activates toll-like receptors via serum amyloid A in vascular smooth muscle cells. *Sci. Rep.* **2019**, *9*, 3421. [CrossRef]
41. Hénaut, L.; Massy, Z.A. New insights into the key role of interleukin 6 in vascular calcification of chronic kidney disease. *Nephrol. Dial. Transplant.* **2018**, *33*, 543–548. [CrossRef] [PubMed]
42. Sun, M.; Chang, Q.; Xin, M.; Wang, Q.; Li, H.; Qian, J. Endogenous bone morphogenetic protein 2 plays a role in vascular smooth muscle cell calcification induced by interleukin 6 in vitro. *Int. J. Immunopathol. Pharmacol.* **2017**, *30*, 227–237. [CrossRef] [PubMed]
43. Yao, Y.; Watson, A.D.; Ji, S.; Boström, K.I. Heat Shock Protein 70 Enhances Vascular Bone Morphogenetic Protein-4 Signaling by Binding Matrix Gla Protein. *Circ. Res.* **2009**, *105*, 575–584. [CrossRef]
44. Callegari, A.; Coons, M.L.; Ricks, J.L.; Rosenfeld, M.E.; Scatena, M. Increased Calcification in Osteoprotegerin-Deficient Smooth Muscle Cells: Dependence on Receptor Activator of NF-κB Ligand and Interleukin 6. *J. Vasc. Res.* **2014**, *51*, 118–131. [CrossRef] [PubMed]
45. Tyson, K.L.; Reynolds, J.L.; McNair, R.; Zhang, Q.; Weissberg, P.L.; Shanahan, C.M. Osteo/Chondrocytic Transcription Factors and Their Target Genes Exhibit Distinct Patterns of Expression in Human Arterial Calcification. *Arter. Thromb. Vasc. Biol.* **2003**, *23*, 489–494. [CrossRef] [PubMed]
46. Lin, M.-E.; Chen, T.; Leaf, E.M.; Speer, M.Y.; Giachelli, C.M. Runx2 Expression in Smooth Muscle Cells Is Required for Arterial Medial Calcification in Mice. *Am. J. Pathol.* **2015**, *185*, 1958–1969. [CrossRef] [PubMed]
47. Scatena, M.; Liaw, L.; Giachelli, C.M. Osteopontin: A multifunctional molecule regulating chronic inflammation and vascular disease. *Arterioscler. Thromb. Vasc. Biol.* **2007**, *27*, 2302–2309. [CrossRef] [PubMed]
48. Giachelli, C.M.; Speer, M.Y.; Li, X.; Rajachar, R.M.; Yang, H. Regulation of Vascular Calcification. *Circ. Res.* **2005**, *96*, 717–722. [CrossRef]
49. Wada, T.; McKee, M.D.; Steitz, S.; Giachelli, C.M. Calcification of vascular smooth muscle cell cultures: Inhibition by osteo-pontin. *Circ. Res.* **1999**, *84*, 166–178. [CrossRef]
50. Speer, M.Y.; McKee, M.D.; Guldberg, R.E.; Liaw, L.; Yang, H.-Y.; Tung, E.; Karsenty, G.; Giachelli, C.M. Inactivation of the Osteopontin Gene Enhances Vascular Calcification of Matrix Gla Protein–deficient Mice. *J. Exp. Med.* **2002**, *196*, 1047–1055. [CrossRef]

51. Paloian, N.J.; Leaf, E.M.; Giachelli, C.M. Osteopontin protects against high phosphate-induced nephrocalcinosis and vascular calcification. *Kidney Int.* **2016**, *89*, 1027–1036. [CrossRef] [PubMed]
52. Takemura, A.; Iijima, K.; Ota, H.; Son, B.-K.; Ito, Y.; Ogawa, S.; Eto, M.; Akishita, M.; Ouchi, Y. Sirtuin 1 Retards Hyperphosphatemia-Induced Calcification of Vascular Smooth Muscle Cells. *Arterioscler. Thromb. Vasc. Biol.* **2011**, *31*, 2054–2062. [CrossRef]
53. Gardner, S.E.; Humphry, M.; Bennett, M.R.; Clarke, M.C. Senescent Vascular Smooth Muscle Cells Drive Inflammation Through an Interleukin-1α–Dependent Senescence-Associated Secretory Phenotype. *Arterioscler. Thromb. Vasc. Biol.* **2015**, *35*, 1963–1974. [CrossRef] [PubMed]
54. Zhang, X.; Li, Y.; Yang, P.; Liu, X.; Lu, L.; Chen, Y.; Zhong, X.; Li, Z.; Liu, H.; Ou, C.; et al. Trimethylamine-N-Oxide Promotes Vascular Calcification Through Activation of NLRP3 (Nucleotide-Binding Domain, Leucine-Rich-Containing Family, Pyrin Domain-Containing-3) Inflammasome and NF-κB (Nuclear Factor κB) Signals. *Arterioscler. Thromb. Vasc. Biol.* **2020**, *40*, 751–765. [CrossRef] [PubMed]
55. Russell, W.M.S.; Burch, R.L. *The Principles of Humane Experimental Technique*; Methuen & Co Ltd.: London, UK, 1959.
56. Otto, G.M.; Franklin, C.L.; Clifford, C.B. Biology and Diseases of Rats. *Lab. Anim. Med.* **2015**, 151–207. [CrossRef]

Supplementary Materials

Suppl. Table S1. Oligonucleotide sequences rat

Gene	Fwd 5′-3′ Rev 5′-3′	Company	Reference
HRPT-1	GAC TTT GCT TTC CTT GGT CA AGT CAA GGG CAT ATC CAA CA	Biozol, Eching	Order Nr. RHK-1
Xdh	TGG ACA AGT AGA GGG GGC AT ACA CAG GCG TTT CGG ATC TT	Tibmolbiol, Berlin	Primer Blast
SOD1	TTT TGC TCT CCC AGG TTC CG CCC ATG CTC GCC TTC ACT TA	Tibmolbiol, Berlin	Primer Blast
SOD2	CAC CGA GGA GAA GTA CCA CG TGG GTT CTC CAC CAC CCT TA	Tibmolbiol, Berlin	Primer Blast
SOD3	GAG AGC TTG TCA GGT GTG GA GTC AAG CCG GTC TGC TAA GT	Tibmolbiol, Berlin	Primer Blast
Cbfa1	GCC GGG AAT GAT GAG AAC TA GGA CCG TCC ACT GTC ACT TT	Tibmolbiol, Berlin	Primer Blast
ALP	TCC GTG GGT CGG ATT CCT GCC GGC CCA AGA GAG AAA	Tibmolbiol, Berlin	[48]
OPN	TGG TTT GCC TTT GCC TGT TC TCT CCT CTG AGC TGC CAA ACT C	Tibmolbiol, Berlin	Primer Blast
SM22α	AGA GGG GCC TCA CAG GCT GG ACA GCT GGG AAC AGG GGC CA	Tibmolbiol, Berlin	Primer Blast

p53	AGC TCC AGT TCA TTG GGA CTT CAG TTA TCC AGT CTT CAG GGG A	Tibmolbiol, Berlin	Primer Blast
NLRP3	TCT CTG CAT GCC GTA TCT GG ACG GCG TTA GCA GAA ATC CA	Tibmolbiol, Berlin	Primer Blast
Caspase-1	GGA GCT TCA GTC AGG TCC ATC CTT GAG GGA ACC ACT CGG TC	Tibmolbiol, Berlin	Primer Blast
ASC	TTA TGG AAG AGT CTG GAG CTG TG GCA ATG AGT GCT TGC CTG TG	Tibmolbiol, Berlin	Primer Blast
p16 (Cdkn2a)	CAG ATT CGA ACT GCG AGG AC CCC AGC GGA GGA GAG TAG AT	Biomol, Hamburg	Order Nr. VRPS-1014
p21 (Cdkn1a)	TGG TCC TTT CCC AGT ATT GA CAC GTG GGA GGT TTA CAA TC	Biomol, Hamburg	Order Nr. VRPS-1011
IL-1ß	AGA GTG TGG ATC CCA AAC AA AGT CAA CTA TGT CCC GAC CA	Biomol, Hamburg	Order Nr. VRPS-2929
IL-6	CTT CCT ACC CCA ACT TCC AA ACC ACA GTG AGG AAT GTC CA	Biomol, Hamburg	Order Nr. VRPS-2952
GAPD	AGA CAG CCG CAT CTT CTT GT CTT GCC GTG GGT AGA GTC AT	Biozol, Eching	Order Nr. RHK-1
Ppia	CTG GTG GCA AGT CCA TCT AC CCC GCA AGT CAA AGA AAT TA	Biozol, Eching	Order Nr. RHK-1
Rpl13A	GTG AGG GCA TCA ACA TTT CT CAT CCG CTT TTT CTT GTC AT	Biozol, Eching	Order Nr. RHK-1

5. Discussion

Even though VC is a known risk factor of cardiovascular morbidity and mortality, treatment options are scarce and to date mainly available for IVC [22]. For MVC, although risk factors for disease progression like age, DM and CKD are predicted to increase, no causal treatment is available [109]. This unmet clinical need arises in part from the fact that even though numerous inducers and participating pathways of VC are described in literature, the molecular pathogenesis is still incompletely understood [22].

5.1. Models and Detection Methods for Vascular Calcification

For the development of clinically effective treatment options, further insight into the pathogenesis of VC is necessary to unravel druggable targets [22]. But even though, or maybe because, basic research has already unravelled a multitude of different pathological pathways involved in VC and clinical research found a plurality of inducers, the development and selection of an encompassing model for VC, reflecting the human situation, is difficult [44]. One explanation is that different models and detection methods are often non-comparable and limited transferability from animal to human situation hinders translation from bench to bedside [110]. Apart from the development of more encompassing models and detection methods for VC, there is need for an assessment and contextualisation of currently available models and methods [110].

5.1.1 Heterogeneity of Models and Detection Methods Hinders Translation of Research Results

Several *in vivo*, *in vitro* and *ex vivo* models exist: Experimental heterogeneity in research of VC results from (1) the application of different models and (2) different methodologies for the detection and quantification of VC [44,110].

The variety in research models mirrors the different influencing factors of VC. But except for rare genetic disorders, like Pseudoxanthoma Elasticum and General Arterial Calcification in Infancy, these models only reflect one or few aspect(s) of the clinical picture of human VC [44]. Therefore, the available models of VC account only for parts of VC pathogenesis seen in the majority of the human patient population [44]. The assertion of the interconnection of underlying pathways and the interplay between different inducers is hindered by the fact that most models, *in vitro* as well as *in vivo*, require several stimuli for development of calcification [44,110]. Mice and rats, typical models for preclinical research, are not prone to VC [44]. Although in some models spontaneous calcification occurs, most models require a combination of different inducers to robustly induce calcification that resembles the human pathology [44,110]. These include (1) genetic manipulation (e.g., manipulation of cholesterol

metabolism or interruption of vascular protective mechanisms), (2) induction of disease state (e.g., CKD by adenine feeding or nephrectomy) and (3) application of additional calcification inducers (e.g., high phosphate or high fat diet) [44].

Besides variation in experimental models, the applied analysis methods vary over studies [110]. A basic problem is that VC as a heterogeneous disease can occur in different vessels as well as in different vessel layers (intimal, medial) and in different sizes (micro- and macro-calcification) [12]. There is no unifying marker for VC, but several methods are eligible for the detection of VC [110]. Both, in clinical and preclinical research, several detection methods for biomarkers of calcification, as well as for identification of calcium depositions in vessels and vessel stiffness as clinical endpoint are applied [110]. Yet, results from different assessment methods are often not comparable, thus hindering the comparability of different studies and the integration of results [22]. To facilitate navigating this massive quantity of different techniques, a recent review summarized and evaluated established and emerging methods for the detection and quantification of VC [110].

One promising opportunity to unravel the underlying mechanisms of VC derives from the recent progress and increased availability of single cell analysis methods, for example for analysis of genome, transcriptome, proteome, and metabolics [111,112]. These techniques include e.g., single cell sequencing or labelling of desired targets with chromophores or fluorophores, for example via RNA *in situ* hybridization [112]. Single cell protocols will further help to assess the influence and interconnection between different inducers of VC, like ROS, inflammation and senescence and will help to unravel signalling cascades and druggable targets in VSMCs calcification.

5.1.2. Detection of Calcification and Senescence Markers on Single Cell Level

In the context to VSMC calcification, one research objective is to monitor osteoblastic transdifferentiation of VSMCs. VSMCs are renowned for their phenotype plasticity [113]. Genetic reprogramming of VSMCs can result in various population subsets, which are known to have a decisive influence on disease progression [114]. Nevertheless, most of the research on interconnection between senescence and calcification in VSMCs has so far been conducted with protocols for bulk cell analysis, revealing that in VSMCs phenotype transition, markers of senescence, oxidative stress and calcification often appear conjointly [86]. Yet, also methods for analysis of bulk cells such as *Polymerase Chain Reaction* (PCR) are well established and extremely helpful to assess transcriptional changes, they are limited to showing the average expression profile of all constituent cells of the bulk. With standard PCR, it is not possible to assess, whether the cell bulks consist of uniformly transdifferentiated cells that are senescent and osteoblastic or whether the cells do differentiate into two or more distinctly different cell populations, with one subset being

senescent and one being osteoblastic. Individual cellular profiling is necessary to clarify the question, whether oxidative stress, inflammation and senescence, although clearly interconnected, are conjoint or consecutive processes.

Several technologies for analysing transcription changes in single cells become increasingly available, for example *single cell quantitative PCR* (scq PCR) and *single cell RNA sequencing* (sc-RNA-seq) [115]. Both, scq PCR and sc-RNA-seq permit the analysis of more transcriptionally altered targets than traditional *Fluorescence In Situ Hybridization* (FISH). For FISH, multiplexing has been limited in the number of available fluorescence channels e.g., due to channel crosstalk, but new technologies like for example sequencing FISH are evolving in the last years [116]. As a major disadvantage of these new and emerging technologies, they are expensive and work intensive [115]. Yet, for these technologies, high throughput measurements are essential to overcome the technological entailed problem of measurement noise and high variability [115]. We developed a protocol that had to enable single cell analysis under compliance with several restrictions, thus limiting the applicable protocols [117]: (1) detection of at least one marker of senescence and calcification in a multiplexed format, (2) no or low investment in additional hardware, (3) compact and robust workflow, (4) easy protocol alteration for additional targets and (5) possible modification for analysis of tissue. In accordance with these conditions, we developed a fluorescent microscopy-based protocol combining mRNA *in situ* hybridization and immunohistology [117]. For several alternative protocols, advantages and disadvantages of these techniques in comparison to the developed protocol are embodied in the supplement of manuscript 2 [117].

A drawback of the developed protocol and transcription analyses in general is their non-eligibility for longitudinal studies [117,118]. Each experiment can only present a snapshot at a single time point [118]. For RNA *in situ* analysis, fixation and permeabilization of cells is necessary, thus preventing an assessment of genotypic changes of one cell over time [117]. In the assessment, whether senescence and calcification are consecutive processes, longitudinal information would be highly relevant. One emerging possibility offering assessment at multiple time points is the establishment of a live cell reporting system, for example by tagging p53 and p21 with fluorescent protein tags [118].

5.2 Cellular Stressors as Inducers of Vascular Calcification

Even though research in the past years has detected an ever-growing number of different cellular stressors and signalling pathways inducing VSMC calcification, decisive questions remain unanswered: How are these different pathways interconnected and how does this interconnection integrate into possible druggable targets? Considering the broad range of possible cellular stress responses, both endogenous and exogenous [119], our work focused

on the formation of oxidative stress and DNA damage as inducers of senescence, inflammation and calcification of VSMCs.

5.2.1. Induction of Calcification and Senescence upon Treatment with Azathioprine

Several cellular stressors are considered possible inducers of cardiovascular risk and VC in CKD patients [60,120]. Next to the accumulation of uremic toxins as consequence of kidney insufficiency, oxidative cellular stress can also be drug-induced [121,122]. For example, immunosuppressive agents, which are applied for the prevention of draft rejections in kidney transplanted patients, can cause clinically relevant cardiovascular toxicity [123,124]. Even though the reasons for increased cardiovascular risk are certainly multi-factorial, induction of oxidative stress by the metabolism of xenobiotics is one possible source of cellular stress: E.g., the metabolism of 6-MP by XO can result in the formation of ROS [68]. Clinically, the application of AZA is associated with increased cardiovascular risk [125]. However, the cardiovascular risk associated with the application of AZA seems lower when compared to other available immunosuppressive agents [123]. AZA itself is a prodrug and cleaved to 6-MP [124]. 6-MP evokes multiple immunosuppressive properties after conversion to 6-thioinosine and 6-thioguanine: (A) inhibition of DNA synthesis, (B) inhibition of purine biosynthesis (reduction in leukocyte proliferation), and (C) induction of apoptosis of T-cells [124]. Previous results indicated that the application of 6-MP to rat VSMC *in vitro* and *ex vivo* induced oxidative stress and calcification [68]. To assess AZA induced ROS, senescence and VC in a more physiological setting, an *in vivo* rat model with repeated application of AZA over a time course of 24 weeks was established [126].

In rats, treatment with AZA over 24 weeks induced VC in the aorta thoracales and abdominales: The majority of AZA treated animals had increased calcium content and upregulated expression of osteogenic markers in the aortic tissue [126]. Yet, in contrast to the prior *in vitro* and *ex vivo* results, where a very potent induction of calcification upon treatment with 6-MP was found, the results were less pronounced in the *in vivo* model [68,126]. Treatment with AZA also resulted in slightly increased ROS and significantly increased serum concentrations of pro-inflammatory cytokines (Vascular Endothelial Growth Factor, IL-6 and IL-1ß) [126]. Interestingly, pro-inflammatory cytokines increased even though AZA's immunosuppressive properties might systemically inhibit leukocytes. With respect to transferability, it also has to be considered that in this model, AZA treatment was tested in healthy animals, which are not subject to disease associated increased inflammatory burden [126]. Patients with autoimmune diseases, such as rheumatic arthritis or psoriasis, on the other hand have a pathophysiological overactive immune system, resulting e.g., in higher baseline cytokine levels [127]. It might well be, that with regard to VC, these patients might benefit more from the reduction of systemic inflammation under AZA

treatment than they suffer from AZA metabolism associated ROS production and pro-inflammatory cytokine secretion.

Interestingly, even though in the *in vivo* AZA model SASP components (e.g., IL-1ß and IL-6) as markers of cellular senescence significantly increase, expression of senescence markers associated with cell cycle arrest (p16, p21 and p53) do not increase *in vivo* [126]. In total, even though ROS production, calcification and some markers of senescence were induced by AZA treatment *in vivo*, the effects were less pronounced than expected from the *in vitro* model [68,126] There are several possible explanations for the discrepancies: Counter regulatory mechanisms were found to take place *in vivo*, for example measurement of anti-oxidative SOD showed a slight increase in SOD2 and SOD3 in aortic tissue upon treatment with AZA [126]. In addition, it cannot be confirmed that regarding drug metabolism, distribution and the functional endothelium as possible barrier, the concentration of AZA in the aortic media was comparable to the *in vitro* model. Together with the relatively short treatment period in the *in vivo* model, the accumulation of DNA damage could be less pronounced in the aorta of our *in vivo* model than in the *in vitro* model, which could account for the discrepancies in finding between the two models.

5.2.2. Induction of Calcification and Senescence upon Treatment with Doxorubicin

DOX is a widely used, potent anti-neoplastic drug, employed in the treatment of hematopoietic cancer and solid tumours [128]. To date, doxorubicin's mechanisms of action are not fully unravelled: At least in part the mechanism of action is dependent on doxorubicin's ability to intercalate into the nuclear DNA, thereby inhibiting DNA replication and cellular proliferation [129]. In addition, DOX can intercalate into the mitochondrial DNA and can uncouple the mitochondrial oxygen chain, resulting in the formation of ROS [129,130]. Formation of ROS is one important aspect of the severe and dose limiting cardiotoxicity of DOX, observed also in the clinical usage [131]. ROS is also induced by modification of the anthracycline's quinone structure via an electron transfer into a semiquinone radical by several cellular oxidoreductases, including NADPH, XO and NOS [132]. We confirmed upregulation of superoxide formation upon DOX stimulation in VSMCs in our experimental setting [108].

DOX also inhibits topoisomerase II, resulting in double strand breaks of DNA [129]. The induction of DNA damage, both directly by DNA double strand breaks and as consequence of increased ROS, can result in overwhelmed and thus defective DNA repair mechanisms. As a major marker of DNA damage, we found γH2AX upregulated upon DOX stimulation [108]. As induction of persistent DNA damage can result in cellular senescence, we found stimulation with DOX to induce markers of cellular senescence: Stimulation with DOX induced the expression of p21, both on gene expression and on protein level, as well as SA-

ß-Gal and pro-inflammatory SASP components IL-6 and IL-1ß [108]. Our results on induction of oxidative stress, DNA damage and senescence are in line with the respective literature [84]. Especially the induction of senescence upon treatment with DOX is well recognized and considered a decisive effect in doxorubicin's mechanism of action as cancer treatment [133]. In addition to the induction of oxidative stress and senescence, we also found DOX to upregulate the osteogenic transdifferentiation of rat VSMCs: Expression of the master transcription factor RUNX2 as well as ALP, BMP2 and OPN increased significantly upon stimulation with DOX, while the VSMC markers SM22, MYH11 and *Calponin 1* (CNN1) decreased slightly, but not significantly [108]. Furthermore, stimulation with DOX upregulated protein content and activity of ALP and dose dependently increased the calcium content both *in vitro* and *ex vivo* [108]. Considering the therapeutic necessity of chemotherapy and the severe short-term adverse effects of DOX, possible long-term effects on VC have rarely been considered a clinically particular relevant side effect of DOX therapy so far. However, several recent studies highlight the long-term effects of DOX therapy on arterial stiffness in mice and humans [134-136]. Even though the induction of aortic stiffness upon chemotherapy is not limited to anthracyclines alone, a recent study acknowledges the need for specific vascular monitoring upon therapy with anthracyclines [135].

5.2.3. Stressor Induced Calcification is NLRP3 Dependent

Several pathways can link cellular stressors and vascular calcification, including the activation of the NLRP3 inflammasome, which becomes increasingly recognized as one pathway involved in vascular disease [93,137]. NLRP3, ASC and caspase 1 are upregulated in phosphate stimulated, calcifying VSMCs and inhibition of NLRP3 results in decreased calcification [93]. Considering the increased levels of IL-1ß we detected both in our AZA and in our DOX model we analysed the expression of NLRP3 components [108,126].

In the aortic tissue of the AZA rat model, the expression of NLRP3 components ASC, caspase 1 and NLRP3, as well as IL-1ß and IL-6 increased [126]. Upon treatment with DOX, we found upregulation in mRNA expression ASC, caspase 1 and NLRP3, as well as IL-1ß [108]. Treatment with DOX also resulted in an increased secretion of IL-1ß, strongly indicating an involvement of NLRP3 assembly and activation upon DOX treatment [108]. These results are in line with recent insights from the research on DOX induced cardiotoxicity: DOX was also found to NLRP3 dependently induce pyroptosis [138] and in cardiomyocytes, DOX upregulated NLRP3, ASC and caspase 1 expression and increased IL-1β secretion [139]. To verify the involvement of NLRP3 inflammasome in the calcification upon AZA treatment, the effect of AZA treatment was tested in an *ex vivo* aortic ring model in NLRP3$^{-/-}$ and *Wild Type* (WT) mice [126]. In WT mice, stimulation of aortic rings with calcifying medium induced calcification and this effect was significantly enhanced by co-

stimulation of calcifying medium with AZA [126]. The calcification inducing effect of AZA was abolished in NLRP3$^{-/-}$ mice, where no significant difference between culture in calcifying medium and a co-culture with calcifying medium and AZA was detectable [126]. Similar results were obtained from the *ex vivo* aortic ring model in NLRP3$^{-/-}$ and WT mice for stimulation of calcification medium with/without DOX: The calcification inducing effect of DOX was abolished in NLRP3$^{-/-}$ mice [108]. In addition, the DOX induced calcification of VSMCs *in vitro* was abolished by co-stimulation with the NLRP3 inhibitor MCC950 [108]. Noteworthy, while knockdown of NLRP3 significantly reduces calcification induced by AZA and DOX, it does not affect the baseline calcification induced by the applied calcification medium in our experimental setting [108,126].

IL-1ß is one of the NLRP3 inflammasome's effector molecules, cleaved from pro-IL-1ß by the NLRP3 inflammasome and considered a component of the cellular SASP [140]. IL-1ß has been implicated as an important inducer of VC and vascular disease both *in vitro* [98] and in the context of atherosclerosis in the *Canakinumab Anti-Inflammatory Thrombosis Outcome Study* (CANTOS) [141-143]. CANTOS investigated the use of a human, monoclonal antibody against IL-1ß in a study population with established atherosclerotic disease and prior *Myocardial Infarction* (MI) [142,144]. In the verum group, canakinumab was applied in addition to pharmacological secondary prevention regimes for MI, including lipid lowering therapies, anti-platelet therapies and pharmacological blood pressure control, e.g., by beta-adrenergic blockers and/or inhibitors of the renin-angiotensin system [141,143]. Treatment with canakinumab met the study's primary endpoints and reduced non-fatal stroke, non-fatal MI and cardiovascular death in the verum group, without significant alterations of LDL [141,143]. Therefore, the CANTOS study strongly confirmed the involvement of inflammatory processes in IVC. To date, no clinical trial for studying anti-inflammatory therapies for arteriosclerosis is under way, but recent research indicates an involvement of IL-1ß also in MVC [98].

As we detected upregulation and secretion of IL-1ß upon stimulation with the cellular stressors AZA and DOX, we analysed the pro-inflammatory and pro-calcific potential of IL-1ß in our *in vitro* model [108,126]. IL-1ß increased gene expression of markers of osteogenic transdifferentiation, including upregulation of ALP, BMP2 and RUNX2 and down-regulation of VSMC marker proteins such as SM22, MYH11 and CNN1, strongly indicating an osteogenic transition of VSMCs [108]. Stimulation with IL-1ß also increased calcification of VSMCs and we detected increased ROS production as well as induction of IL-6 expression and secretion [108]. In a potent auto-loop, IL-1ß increased its own expression [108]. The pro-calcifying effect of IL-1ß is NLRP3 dependent, as by co-stimulation with the NLRP3 inhibitor MCC950 the IL-1ß induced calcification is inhibited [108]. In line with our results, other researchers

found an inhibition of induced calcification upon co-treatment with MCC950 [145] as well as a reduction of DOX-induced myocardial dysfunction by inhibiting NLRP3-mediated pyroptosis with MCC950 [138]. Yet, considering potential off-target effects of NLRP3 inhibition, in an interesting study analysing DOX-induced cardiotoxicity, researchers found knockout of NLRP3 in mice to enhance the susceptibility to DOX-induced cardiotoxicity [146]. In this study, this effect was independent of IL-1ß but depended on a decreased Interleukin-10 production in macrophages in the mouse model, which was due to NLRP3 knockdown [146]. These differences clearly highlight the interconnection between different physiological pathways that make it so difficult to transfer potential druggable targets from bench to bedside. Our research findings on VSMCs calcification upon stimulation with cellular stressors and IL-1ß, as well as the effects of co-treatment with MCC950 is summarized in figure 5.

Interestingly, although we found an induction of calcification and inflammation in rat VSMCs treated with IL-1ß in our model, IL-1ß did not induce senescence markers (including p21, p16, SA-ß-Gal and γH2AX) [108]. Even though we found induction of superoxide and increased expression of pro-inflammatory cytokines upon stimulation with IL-1ß, we detected no IL-1ß induced DNA-damage [108]. This indicates that stimulation with IL-1ß in this experimental setting does not trigger the DDR and therefore does not induce senescence. Even though these results seem to be in opposition to recently published results by Han et al., who found an induction of senescence upon treatment with IL-1ß, it has to be considered, that their study analysed senescence upon co-treatment of IL-1ß with phosphate [98]. Overload with phosphate is a known inducer of senescence itself [29]. Potentially, synergistic effects of the co-treatment of phosphate and IL-1ß might account for the discrepancies in finding. A similar effect was found for co-stimulation of phosphate with IL-6, which was shown to synergistically induce senescence in VSMCs [147]. In our experimental setting, treatment with IL-6 did neither induce senescence nor calcification [108].

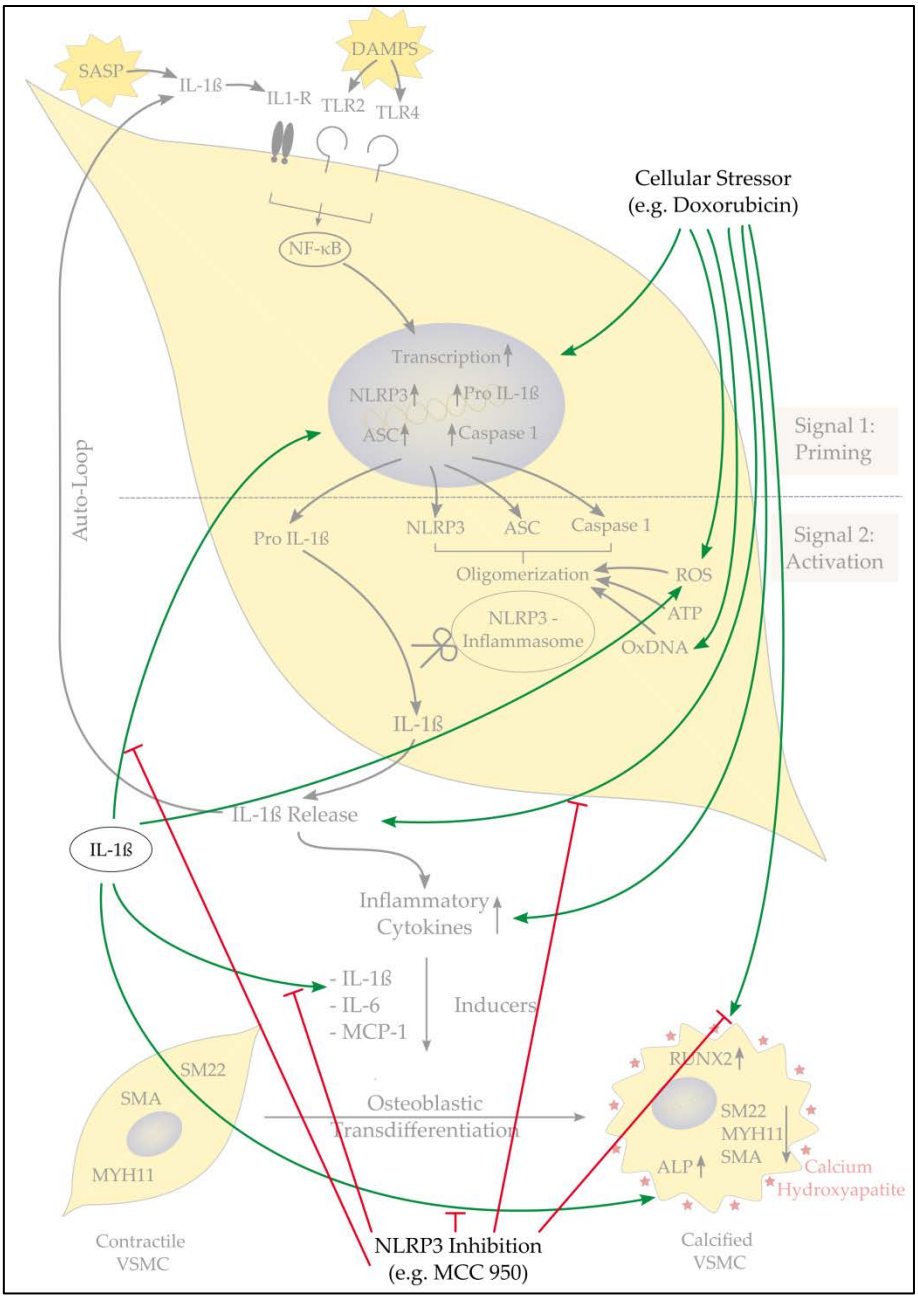

Fig. 5: NLRP3 Dependent Induction of VSMC Calcification by Cellular Stressors and IL-1ß

(Source: Own Illustration, based on [93,98,104,105,107,108]; green arrow: induction; red arrow: inhibition)

Cellular stressors (e.g., doxorubicin) and IL-1ß induce priming of the NLRP3 inflammasome (increased transcription of NLRP3 components) and provide signals (e.g., ROS) for the activation of the NLRP3 inflammasome. Subsequent there is release of IL-1ß, induction of VSMC osteoblastic transdifferentiation and VSMC calcification. IL-1ß induced transcription of NLRP3, doxorubicin induced secretion of IL-1ß and calcification of VSMCs can be inhibited by treatment with a NLRP3 inhibitor (MCC950).

Abbreviations: *ALP* - Alkaline Phosphatase; *ASC* – Apoptosis Associated Speck-like Protein Containing a Caspase Recruitment Domain; *DAMP* - Damage Associated Molecular Pattern; *IL-6* - Interleukin-6; *IL-1ß* - Interleukin-1ß; *IL-1R* - Interleukin 1 Receptor; *MCP-1* - Monocyte Chemoattractant Protein; *Myh11* - Myosin Heavy Chain 11; *NF-κB* - Nuclear Factor 'kappa-light-chain-enhancer' of Activated B-Cells; *NLRP3* - Nucleotide-Binding Oligomerization Domain-like Receptor family pyrin domain containing 3; *ROS* - Reactive Oxygen Species; *RUNX2* - Runt Related Transcription Factor 2; *SASP* - Senescence Associated Secretory Phenotype; *SMA* - Smooth Muscle Actin; *SM22* - Smooth Muscle 22alpha; *TLR* - Toll Like Receptor; *VMSC* - Vascular Smooth Muscle Cell

5.3. Interconnection between Senescence, Inflammation and VSMC Calcification – the Concept of Inflammaging

There is strong indication of interconnection between senescence, inflammation and calcification. Evidence derives from clinical observations as well as from basic research: In clinical observations, (1) patients suffering from specific aging diseases, resulting in high biological age, such a HGPS, (2) patients with increased oxidative and inflammatory burden, like patients on dialysis, or (3) patients with high chronological age all share an increased risk for VC [148-150]. In basic research, markers of calcification and senescence were found to conjointly occur in several studies, including stimulation of VSMCs with 6-MP [68], stimulation of VSMCs with DOX [108] and vessels from children with dialysis [86]. The mechanism of subsequent DNA damage, senescence and formation of the SASP has been proposed, among others, by Rodier et al., who found persistent DNA damage to induce the SASP [151]. As recently reviewed by Birch and Gil, components of the SASP do not only show a high association with age in human plasma, but levels of inflammatory factors are also reduced by removal of senescent cells, further highlighting the connection between inflammation and senescence [82].

Yet, results on the exact mechanism, linking DNA damage and induction of senescence with SASP formation and calcification, are scarce. This may be in part, because the complex orchestra of signalling involved in the SASP aggravates the identification of a specific signalling pathway. Several mechanisms were found to be linked in the induction, transcriptional control, epigenetic regulation and post-translational modulation of the SASP and in the induction of calcification [24]. Among those signalling pathways are (A) NFkB, (B) p38 Mitogen-Activated Protein Kinase, (C) *AKT/Mammalian Target of Rapamycin* (Akt/mTOR) and (D) ATM [24]. Although several separate studies link these pathways in different experimental settings to either induction of the SASP or VC, yet, for the exception of ATM, studies directly linking SASP and calcification to the underlying pathway in one joint experimental setting are warranted. For ATM, a kinase that phosphorylates the histone H2AX upon DNA damage, functioning as an essential component in DDR, the link between DNA damage, induction of the SASP and calcification has been recently established by several working groups: Liu et al. found in a model of HGPS associated calcification that inhibition of ATM with small interfering RNA or the ATM inhibitor Ku-55933 was successful in inhibition of calcification [85]. Sanchis et al. reported a successful inhibition of calcification and a reduction in expression of SASP markers in VSMC from children with dialysis upon treatment with Ku-55933 and inhibition of ATM with small interfering RNA [86]. Cobb et al. identified RUNX2 as a component of the DNA damage control, directly linking DDR and calcification: They found RUNX2 to be poly-ADP-ribosylated and located at the sites of DNA damage,

serving as a promotor for osteogenic targets, an effect that could be alleviated by application of an ATM or poly-ADP-ribose polymerase inhibitors [87].

Our results are in line with the proposed mechanism of primary induction of DNA damage and subsequent formation of pro-inflammatory SASP and calcification: In our models, we find primary stressors (DOX, AZA, 6-MP) to induce senescence, inflammation and calcification, while the pro-inflammatory cytokine (IL-1ß) that we consider one of the downstream signals, induces the formation of markers of inflammation and calcification, but not senescence [68,108,126]. Although IL-1ß further reinforced the expression of SASP components like IL-1ß, IL-6 and BMP2, for no other marker of cellular senescence an increase was detected [108]. Explicitly, we detected no DNA damage in form of γH2AX upon stimulation with IL-1ß, thus indicating that the DDR is not triggered by stimulation with IL-1ß [108]. Although senescence and formation of SASP can be the initial trigger, in our *in vitro* system the IL-1ß dependent autoinflammatory loop independently of cellular senescence forms a circulus vicious, resulting in significant calcification in the absence of senescence markers, apart from induction of the SASP [108]. Even though calcification in our model can also occur in the absence of a majority of common senescence markers [108], Budamagunta et al. found senescent cells to not only express higher basal levels of pro-inflammatory cytokines, but also reported senescent cells to react to pro-inflammatory stimuli (stimulation with IL-1ß, lipopolysaccharide and TNFα) with an exacerbated gene expression of pro-inflammatory cytokines, compared to non-senescent cells [152]. This is of special importance considering, that even though data on an increase in IL-1ß serum concentration in elderly is conflicting, research indicates that resident, non-circulatory cells might be critically involved in the pathology, fuelling release of cytokines, such as IL-1ß [153]. And indeed, the accumulation of senescent cells is related to a variety of age-associated diseases, with secretion of pro-inflammatory cytokines by the SASP of (senescent) cells accounting for at least parts of human pathology of CVD [74,154,155].

5.4. Inflammaging as Therapeutic Target in Prevention and Treatment of Vascular Calcification

Even though a variety of different treatment options for CVD became available in the last 3 decades, such as cholesterol lowering statins and angiotensin 1 receptor antagonists, CVD associated mortality continues to increase and patients suffering from MVC face an unmet clinical need [156]. Treatment options for MVC are particularly scarce, but desperately needed to improve patient outcome, especially for patients with high chronological age, but also for patient suffering from high biological age resulting from underlying diseases such as CKD and DM. Some pharmacological treatments are currently applied: Bisphosphonates as substances analogous to the endogenous calcification inhibitor pyrophosphate are applied

and treatment with etidronate has been shown effective in some clinical trials and case reports for the treatment of rare genetic calcification disorders [157,158]. Vitamin K supplementation has been shown in one study to have no significant effect on the progression of VC in hemodialysis patients [159]. Patients with CKD can profit from treatment with calcimimetics and phosphate binders [22,160,161] and inhibition of hydroxyapatite formation is currently researched for the treatment of MVC [162]. Targeting the diverse aspects of inflammaging emerges as a new and promising therapeutic avenue not only for MVC but also for several other age associated disorders [73,89,143,163].

Several concepts (summarized in figure 6) have been proposed to date and therapeutic options can include a reduction of oxidative stress, clearance of senescent cells (often referred to as senolytic therapy) and inhibition of the pro-inflammatory SASP (often called senomorphic therapy) [156,164].

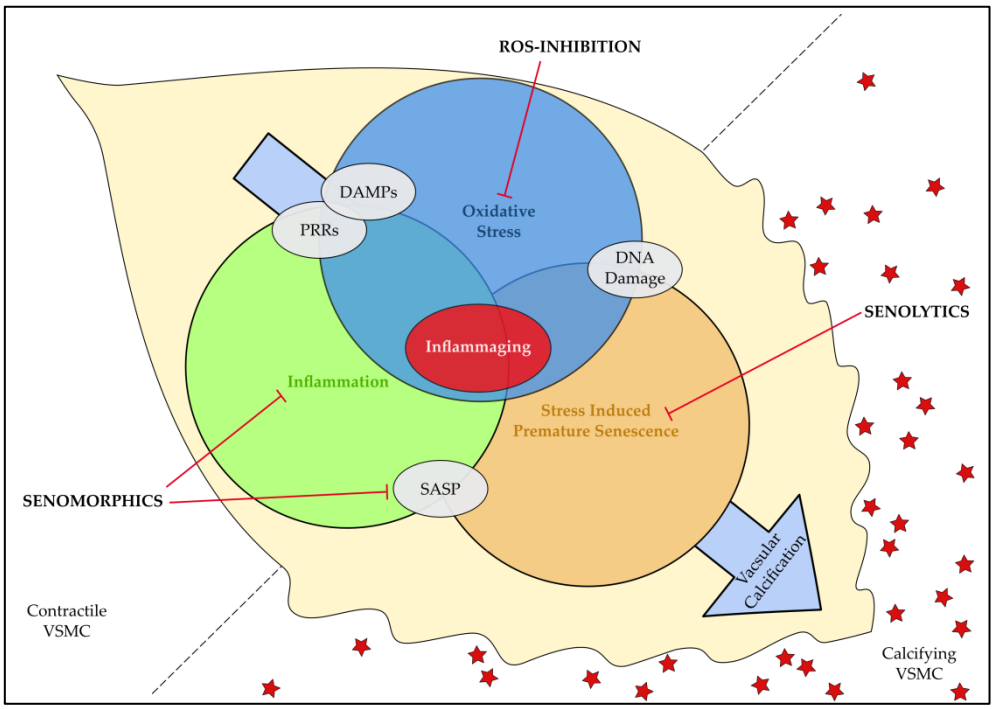

Fig. 6: Inflammaging as Decisive Process in VSMC Calcification and Evolving Therapeutic Strategies

(Source: Own Illustration, based on [66,73,156,164-167])

Merged in the concept of inflammaging, oxidative stress, inflammation and stress induced premature senescence are linked via several pathways. These include for example the oxidative stress induced formation of DAMPs, whose detection by PRR can activate pro-inflammatory signalling. Oxidative stress can also induce DNA damage, followed by activation of the DNA damage response and induction of senescence. The induction of the SASP upon senescence links senescence with pro-inflammatory signalling. Based on this concept several therapeutic approaches offer the possibility to interfere with inflammaging induced vascular calcification e.g., by targeting oxidative stress (ROS-inhibition), pro-inflammatory signalling (senomorphics) or clear senescent cells (senolytics).
Abbreviations: *DAMP* - Damage Associated Molecular Pattern; *PRR* - Pattern Recognition Receptors; *ROS* - Reactive Oxygen Species; *SASP* - Senescence Associated Secretory Phenotype; *VMSC* - Vascular Smooth Muscle Cell

5.4.1 Targeting Oxidative Stress

Oxidative Stress as cause of cellular damage is considered a major inducer of cellular senescence and VC and therefore an important therapeutic target [156]. Nevertheless, oxidative damage is only one form of damage that induces aging and senescence. Other cellular processes e.g., replication, transcription and translation, can also result in cellular damage and subsequent cellular senescence and organism aging [168]. Also, it must be considered that even though excessive ROS is clearly one inducer of cellular and organism aging, ROS also exerts decisive (beneficial) physiological effects and increased anti-oxidant protection can even decrease lifespan [168].

Due to the variety of different sources of ROS, therapeutic options for ROS decrease are manifold and include for example inhibition of ROS producing enzymes, such as NADPH and XO as well as direct inactivation of ROS e.g., by ROS scavenging [156]. Unfortunately, even though innumerable anti-oxidant components, often of natural origin and common dietary components like resveratrol or quercetin, are under research, clinical studies with sound sample sizes are warranted [156]. Therefore, a critical appraisal of the effectiveness of anti-oxidants for treatment of VC is difficult [156]. Some approved therapeutic drugs have anti-oxidant capacities, like e.g., metformin [169], statins [170] and XO inhibitors [171,172]. For example, different clinical studies indicate that inhibition of XO with allopurinol or febuxostat might have beneficial effects on arterial stiffness and cardiovascular outcome in hyperuricemic patients [172]. Considering the high costs of basic and clinical research and the difficulties to receive patents on biological substances it is prone to speculate, whether a therapeutic establishment is more likely to be successful for re-positioned pharmaceutical drugs that are already approved and established in clinical practice for other indications, as the clinical research necessary for development is less extensive and expensive.

5.4.2 Targeting Senescence and Inflammation – Senolytics and Senomorphics

Targeting cellular senescence to improve organismal outcome has been a huge research topic in the last years [173]. In theory it is possible to either (1) inhibit the induction of senescence, (2) eliminate cellular senescence directly e.g., by clearance of senescent cells, or (3) focus on modulation of the senescence induced secretome and the associated paracrine signalling [82,174]. But in a critical appraisal of emerging therapeutic options, the crucial physiological effects of senescence e.g., in tumour suppression and damage repair, must be considered [82,174]. For example, with reference to p53, accumulation of phosphorylated p53 in the cell is one elemental sign of cellular senescence, inducing cell cycle arrest [175]. But it is also an essential step in providing the cell with time for damage repair [175]. Damage in the gene encoding p53, for example by mutation, can lead to

functional loss of p53 [175,176]. Functional loss of p53 can result in a highly increased risk for cancer as early as in early adulthood, for example in the hereditary Li-Fraumeni syndrome, underlining the tight connection between senescence and tumour control [176]. It is therefore likely, that inhibition of senescence formation will hardly be a druggable target, but research will rather focus on the modulation of the SASP or the removal of senescent cells from the organism.

The SASP is heterogeneous and extensively regulated, depending for example on cell type and duration since senescence onset [155]. Thus a huge variety of different druggable targets emerge [155]. Potential processes that could be therapeutically targeted by senomorphics include (1) the induction of the SASP, (2) the transcriptional and epigenetic control of the SASP, (3) post-translational control of the SASP, and (4) effector molecules of the SASP [82]. Some therapeutic approaches interfering with SASP components are already approved, although for different indications [164]. These include for example antibodies against SASP components (like e.g. canakinumab), NF-κB inhibitors (e.g. metformin and resveratrol) and mTOR inhibitors (e.g. rapamycin) [164]. Although several pathways can be involved in the induction of the SASP, priming and activation of the NLRP3 inflammasome seem to play an essential role in the SASP induction [82]. Therefore, drugs inhibiting NLRP3 can be considered senomorphics. MCC950, a selective inhibitor of the NLRP3 inflammasome and a drug inhibiting cytokine release [177], can therefore be considered as a senomorphic drug. MCC950 is not an approved pharmaceutical drug, but shows very promising results *in vitro* and *in vivo*: Our research highlights the involvement of NLRP3 in VSMCs calcification and the effectiveness of NLRP3 inhibition by MCC950 treatment in decreasing calcification *in vitro* [108,126]. These results are in line with other research showing that targeting NLRP3-mediated inflammation with MCC950 (1) is anti-atherosclerotic, reducing plaque development and increasing plaque stability and (2) prolonging the life span of a mouse model of HGPS [178-181]. Several other potential inhibitors of NLRP3 exist to date, which have been extensively reviewed by Zahid et al. [182]. Also, activation of PRRs by DAMPs and subsequent PRR signalling emerge as therapeutic targets [183]. Next to prevention of DAMP formation, e.g., by inhibition of oxidative damage, also the PRR signalling e.g., via TLR2/4, can be targeted. In one of our studies, we showed an upregulation of *Monocyte Chemoattractant Protein-1* (MCP-1) production and secretion in rat VSMCs upon stimulation with *Serum Amyloid A* (SAA) and high density lipoprotein from septic patients [184]. MCP-1 is one component of the SASP of VSMCs [88]. SAA induced expression and secretion of MCP-1 was dependent on TLR2 and TLR4 [184]. Inhibition or knockdown of TLR2 and/or TLR4 as well as treatment with a NF-κB antagonist reduced the SAA induced MCP-1 secretion [184].

Yet, targeting components of the SASP also means, that the therapy is at the "*crossroad of inflammation and senescence*" [185] and aiming at inflammatory pathways involved in the SASP comes with the potential of immunosuppression [185]. Consistently, several pharmaceutical drugs, although functioning as senomorphics under appropriate conditions, can also be considered anti-inflammatory drugs and are already approved for the respective indications. For example, canakinumab as human monoclonal antibody against IL-1ß is applied for the treatment of systemic juvenile idiopathic arthritis [186] and in addition tested as treatment option for the prevention of cardiovascular events [141,143]. Even though treatment with canakinumab enhanced patient outcome in CVD, this therapy is highly priced in comparison to standard therapy and has to be applied by repeated injection, thus potentially limiting availability and adherence [187]. For senomorphic therapies in general, immunosuppression most likely will be an issue, potentially hindering applicability.

An alternative therapy concept involves the selective clearance of senescent cells from the organism by senolytics: Baker et al. provided first proof on the efficacy of clearance of senescent cells: In a transgene mouse model, elimination of $p16^{Ink4a}$ positive cells delayed the occurrence of age-associated dysfunctions, and Childs et al. demonstrated, that clearance of $p16^{Ink4a}$ positive cells reduced atherosclerotic lesions [188,189]. Next to targeting $p16^{Ink4a}$, several other approaches were developed with the objective to target senescent cells. The common therapeutic concept of senolytics is the induction of cell death in senescent cell with variations in (1) the mode of detection of senescent cells and (2) the mode of cell clearance [190-192]. Senolytics and chemotherapeutics share the same therapeutic objective: to selectively kill deleterious cells without negatively impacting or even killing "healthy" cells [191]. But, although senescent cells express features distinctly different from non-senescent cells, in an analogy to chemotherapeutics, therapeutic detection and elimination of senescent cells are often lacking specificity [192]. For example the senolytic drug ABT263 induced cell death by inhibiting the senescence feature anti-apoptotic protein B-cell Lymphoma 2 [193]. Childs et al. confirmed that ABT263 application to LDL $receptor^{-/-}$ mice on high fat diet can reduce atherogenesis onset [189]. Yet, in clinical trials, treatment in humans resulted in thrombocytopenia and neutropenia, thus raising questions about specificity [193]. Several other cellular features exist that could be used to target senescent cells [155,194] e.g., by aiming at increased SA-ß-Gal with cytotoxic drugs containing galacto-oligosaccharide encapsulated nanoparticles [195]. But, as senolytic therapy concept are mechanistically so very similar to anti-cancer treatments, in a realistic evaluation it has to be considered that even though in the last centuries tremendous financial, personal and technological resources were and still are invested in chemotherapeutics for cancer treatment, cancer treatments often continue to lack specificity and many cancers remain incurable [191]. It therefore seems illusive to expect senolytic therapies to evolve as large-

scale therapeutic options for treatment of age associated diseases such as VC in the near future [191]. Even if senescent cells can be specifically cleared, accumulating evidence indicates, that clearance of senescent cells can also have potentially harmful side effects, including for example defects in wound healing and regeneration of tissue, that will hinder applicability [173].

Considering all aspects of senotherapy together it becomes clear, that although this therapeutic avenue can potentially provide huge therapeutic benefit, much more basic and clinical research is warranted to fully determine the safety and efficacy of senotherapeutic compounds.

6. Conclusion

In line with several recent research results, our work on the effects of cellular stressors on VSMCs inflammatory response and calcification depict VC as a senescence driven, inflammatory disease. In our research, we observe the occurrence of SIPS with formation of elevated ROS and DNA damage upon challenge with cellular stressors, which fuel an inflammatory cellular secretory phenotype involving upregulation and activation of PRRs. IL-1ß, as one important inflammatory effector cytokine, induces a pro-inflammatory auto-loop and calcification of VSMCs. Even though we found both, cellular stressors and IL-1ß, effective in the induction of VC, in contrast to cellular stressors 6-MP/AZA and DOX, IL-1ß induces VC without induction of cellular senescence. Thus, our results on cellular stressors and IL-1ß point towards a subsequent induction of (1) senescence with SASP, (2) a senescence driven pro-inflammatory auto-loop, and (3) induction of osteoblastic transdifferentiation and calcification of VSMCs. In our models, an inhibition of NLRP3 was effective in reducing inflammatory response and calcification of VSMCs upon treatment with cellular stressors and IL-1ß.

The perception of VC as senescence driven, inflammatory disease discloses several new therapeutic approaches that might provide urgently needed therapeutic options for patients in the future: Druggable targets aiming at inflammaging can include (1) reduction of oxidative stress, (2) interference with cellular senescence, and (3) inhibition of senescence driven pro-inflammatory signalling. For all these therapeutic approaches possible drug candidates are currently under investigation. In addition to these several new therapeutic components under research, such as senolytics, repositioning of already established drugs might offer more rapidly implementable therapeutic options for the treatment of MVC. Therefore, there is room for hope, that new therapeutic approaches might finally result in a reduction of CKD and CVD associated mortality rates.

List of Publications

*authors contributed equally

1) Schuchardt M*, **Herrmann J***, Tolle M, van der Giet M. Xanthine Oxidase and its Role as Target in Cardiovascular Disease: Cardiovascular Protection by Enzyme Inhibition? *Curr Pharm Des.* 2017;23(23):3391-3404.
2) Schuchardt M, Prufer N, Tu Y, **Herrmann J**, Hu XP, Chebli S, Dahlke K, Zidek W, van der Giet M, Tolle M. Dysfunctional high-density lipoprotein activates toll-like receptors via serum amyloid A in vascular smooth muscle cells. *Sci Rep.* 2019;9(1):3421.
3) **Herrmann J**, Babic M, Tolle M, van der Giet M, Schuchardt M. Research Models for Studying Vascular Calcification. *Int J Mol Sci.* 2020;21(6):2204.
4) **Herrmann J***, Babic M*, Tolle M, Eckardt KU, van der Giet M, Schuchardt M. A Novel Protocol for Detection of Senescence and Calcification Markers by Fluorescence Microscopy. *Int J Mol Sci.* 2020;21(10):3475.
5) Schuchardt M, **Herrmann J**, Henkel C, Babic M, van der Giet M, Tolle M. Long-Term Treatment of Azathioprine in Rats Induces Vessel Mineralization. *Biomedicines.* 2021;9(3):327.
6) **Herrmann J**, Gummi MR, Xia M, van der Giet M, Tolle M, Schuchardt M. Vascular Calcification in Rodent Models-Keeping Track with an Extented Method Assortment. *Biology (Basel)*. 2021;10(6):459.
7) **Herrmann J**, Xia M, Gummi MR, Greco A, Schacke A, van der Giet M, Tolle M, Schuchardt M. Stressor-Induced "Inflammaging" of Vascular Smooth Muscle Cells via Nlrp3-Mediated Pro-inflammatory Auto-Loop. *Front Cardiovasc Med.* 2021;8(1932):752305.

Literature

1. Bikbov B, Purcell CA, Levey AS, Smith M, Abdoli A, Abebe M, Adebayo OM, Afarideh M, Agarwal SK, Agudelo-Botero M, Ahmadian E, Al-Aly Z, Alipour V, Almasi-Hashiani A, Al-Raddadi RM, Alvis-Guzman N, Amini S, Andrei T, Andrei CL, Andualem Z, Anjomshoa M, Arabloo J, Ashagre AF, Asmelash D, Ataro Z, Atout MMdW, Ayanore MA, Badawi A, Bakhtiari A, Ballew SH, Balouchi A, Banach M, Barquera S, Basu S, Bayih MT, Bedi N, Bello AK, Bensenor IM, Bijani A, Boloor A, Borzì AM, Cámera LA, Carrero JJ, Carvalho F, Castro F, Catalá-López F, Chang AR, Chin KL, Chung S-C, Cirillo M, Cousin E, Dandona L, Dandona R, Daryani A, Das Gupta R, Demeke FM, Demoz GT, Desta DM, Do HP, Duncan BB, Eftekhari A, Esteghamati A, Fatima SS, Fernandes JC, Fernandes E, Fischer F, Freitas M, Gad MM, Gebremeskel GG, Gebresillassie BM, Geta B, Ghafourifard M, Ghajar A, Ghith N, Gill PS, Ginawi IA, Gupta R, Hafezi-Nejad N, Haj-Mirzaian A, Haj-Mirzaian A, Hariyani N, Hasan M, Hasankhani M, Hasanzadeh A, Hassen HY, Hay SI, Heidari B, Herteliu C, Hoang CL, Hosseini M, Hostiuc M, Irvani SSN, Islam SMS, Jafari Balalami N, James SL, Jassal SK, Jha V, Jonas JB, Joukar F, Jozwiak JJ, Kabir A, Kahsay A, Kasaeian A, Kassa TD, Kassaye HG, Khader YS, Khalilov R, Khan EA, Khan MS, Khang Y-H, Kisa A, Kovesdy CP, Kuate Defo B, Kumar GA, Larsson AO, Lim L-L, Lopez AD, Lotufo PA, Majeed A, Malekzadeh R, März W, Masaka A, Meheretu HAA, Miazgowski T, Mirica A, Mirrakhimov EM, Mithra P, Moazen B, Mohammad DK, Mohammadpourhodki R, Mohammed S, Mokdad AH, Morales L, Moreno Velasquez I, Mousavi SM, Mukhopadhyay S, Nachega JB, Nadkarni GN, Nansseu JR, Natarajan G, Nazari J, Neal B, Negoi RI, Nguyen CT, Nikbakhsh R, Noubiap JJ, Nowak C, Olagunju AT, Ortiz A, Owolabi MO, Palladino R, Pathak M, Poustchi H, Prakash S, Prasad N, Rafiei A, Raju SB, Ramezanzadeh K, Rawaf S, Rawaf DL, Rawal L, Reiner RC, Rezapour A, Ribeiro DC, Roever L, Rothenbacher D, Rwegerera GM, Saadatagah S, Safari S, Sahle BW, Salem H, Sanabria J, Santos IS, Sarveazad A, Sawhney M, Schaeffner E, Schmidt MI, Schutte AE, Sepanlou SG, Shaikh MA, Sharafi Z, Sharif M, Sharifi A, Silva DAS, Singh JA, Singh NP, Sisay MMM, Soheili A, Sutradhar I, Teklehaimanot BF, Tesfay Be, Teshome GF, Thakur JS, Tonelli M, Tran KB, Tran BX, Tran Ngoc C, Ullah I, Valdez PR, Varughese S, Vos T, Vu LG, Waheed Y, Werdecker A, Wolde HF, Wondmieneh AB, Wulf Hanson S, Yamada T, Yeshaw Y, Yonemoto N, Yusefzadeh H, Zaidi Z, Zaki L, Zaman SB, Zamora N, Zarghi A, Zewdie KA, Ärnlöv J, Coresh J, Perico N, Remuzzi G, Murray CJL, Vos T. Global, regional, and national burden of chronic kidney disease, 1990–2017: a systematic analysis for the Global Burden of Disease Study 2017. *The Lancet.* 2020;395(10225):709-733.
2. van Walraven C, Manuel DG, Knoll G. Survival trends in ESRD patients compared with the general population in the United States. *Am J Kidney Dis.* 2014;63(3):491-499.
3. Nelson AJ, Raggi P, Wolf M, Gold AM, Chertow GM, Roe MT. Targeting Vascular Calcification in Chronic Kidney Disease. *JACC Basic Transl Sci.* 2020;5(4):398-412.
4. World Health Organization. Cardiovascular diseases (CVDs). https://www.who.int/news-room/fact-sheets/detail/cardiovascular-diseases-(cvds). Published 2021. Accessed 25.02.2022.
5. Villa-Bellosta R, Rivera-Torres J, Osorio FG, Acin-Perez R, Enriquez JA, Lopez-Otin C, Andres V. Defective extracellular pyrophosphate metabolism promotes vascular calcification in a mouse model of Hutchinson-Gilford progeria syndrome that is ameliorated on pyrophosphate treatment. *Circulation.* 2013;127(24):2442-2451.
6. Leftheriotis G, Omarjee L, Le Saux O, Henrion D, Abraham P, Prunier F, Willoteaux S, Martin L. The vascular phenotype in Pseudoxanthoma elasticum and related disorders: contribution of a genetic disease to the understanding of vascular calcification. *Front Genet.* 2013;4(4):4.
7. Lanzer P, Boehm M, Sorribas V, Thiriet M, Janzen J, Zeller T, St Hilaire C, Shanahan C. Medial vascular calcification revisited: review and perspectives. *Eur Heart J.* 2014;35(23):1515-1525.
8. Olive M, Harten I, Mitchell R, Beers JK, Djabali K, Cao K, Erdos MR, Blair C, Funke B, Smoot L, Gerhard-Herman M, Machan JT, Kutys R, Virmani R, Collins FS, Wight TN, Nabel EG, Gordon LB. Cardiovascular pathology in Hutchinson-Gilford progeria: correlation with the vascular pathology of aging. *Arterioscler Thromb Vasc Biol.* 2010;30(11):2301-2309.
9. Mizobuchi M, Towler D, Slatopolsky E. Vascular calcification: the killer of patients with chronic kidney disease. *J Am Soc Nephrol.* 2009;20(7):1453-1464.
10. Tolle M, Reshetnik A, Schuchardt M, Hohne M, van der Giet M. Arteriosclerosis and vascular calcification: causes, clinical assessment and therapy. *Eur J Clin Invest.* 2015;45(9):976-985.

11. Salhotra A, Shah HN, Levi B, Longaker MT. Mechanisms of bone development and repair. *Nat Rev Mol Cell Biol.* 2020;21(11):696-711.
12. Lee SJ, Lee IK, Jeon JH. Vascular Calcification-New Insights Into Its Mechanism. *Int J Mol Sci.* 2020;21(8):2685.
13. Giachelli CM. Vascular calcification mechanisms. *J Am Soc Nephrol.* 2004;15(12):2959-2964.
14. Castling B, Bhatia S, Ahsan F. Monckeberg's arteriosclerosis: vascular calcification complicating microvascular surgery. *Int J Oral Maxillofac Surg.* 2015;44(1):34-36.
15. Dos Santos VP, Pozzan G, Castelli V, Caffaro RA. Arteriosclerosis, atherosclerosis, arteriolosclerosis, and Monckeberg medial calcific sclerosis: what is the difference? *J Vasc Bras.* 2021;20:e20200211.
16. Virchow R. Die Cellularpathologie in ihrer Begründung auf physiologische und pathologische Gewebelehre : Zwanzig Vorlesungen, gehalten während der Monate Februar, März und April 1858 im pathologischen Institute zu Berlin. 1858.
17. Zhu D, Mackenzie NC, Farquharson C, Macrae VE. Mechanisms and clinical consequences of vascular calcification. *Front Endocrinol (Lausanne).* 2012;3:95.
18. Virchow R. Cellular pathology. As based upon physiological and pathological histology. Lecture XVI--Atheromatous affection of arteries. 1858. *Nutr Rev.* 1989;47(1):23-25.
19. Mönckeberg JG. VIII. Über die reine Mediaverkalkung der Extremitätenarterien und ihr Verhalten zur Arteriosklerose. (Aus dem Pathologisch-anatomischen Institut des Allgem. Krankenhauses Hainburg-Eppendorf.). In: *Virchows Archiv.*1903:141-167.
20. Micheletti RG, Fishbein GA, Currier JS, Fishbein MC. Monckeberg sclerosis revisited: a clarification of the histologic definition of Monckeberg sclerosis. *Arch Pathol Lab Med.* 2008;132(1):43-47.
21. Millan A, Lanzer P, Sorribas V. The Thermodynamics of Medial Vascular Calcification. *Front Cell Dev Biol.* 2021;9:633465.
22. Lanzer P, Hannan FM, Lanzer JD, Janzen J, Raggi P, Furniss D, Schuchardt M, Thakker R, Fok PW, Saez-Rodriguez J, Millan A, Sato Y, Ferraresi R, Virmani R, St Hilaire C. Medial Arterial Calcification: JACC State-of-the-Art Review. *J Am Coll Cardiol.* 2021;78(11):1145-1165.
23. Amann K. Media calcification and intima calcification are distinct entities in chronic kidney disease. *Clin J Am Soc Nephrol.* 2008;3(6):1599-1605.
24. Duer M, Cobb AM, Shanahan CM. DNA Damage Response: A Molecular Lynchpin in the Pathobiology of Arteriosclerotic Calcification. *Arterioscler Thromb Vasc Biol.* 2020;40(7):e193-e202.
25. Durham AL, Speer MY, Scatena M, Giachelli CM, Shanahan CM. Role of smooth muscle cells in vascular calcification: implications in atherosclerosis and arterial stiffness. *Cardiovasc Res.* 2018;114(4):590-600.
26. Bostrom K, Watson KE, Horn S, Wortham C, Herman IM, Demer LL. Bone morphogenetic protein expression in human atherosclerotic lesions. *J Clin Invest.* 1993;91(4):1800-1809.
27. James AW. Review of Signaling Pathways Governing MSC Osteogenic and Adipogenic Differentiation. *Scientifica (Cairo).* 2013;2013:684736.
28. Jaminon A, Reesink K, Kroon A, Schurgers L. The Role of Vascular Smooth Muscle Cells in Arterial Remodeling: Focus on Calcification-Related Processes. *Int J Mol Sci.* 2019;20(22).
29. Abbasian N. Vascular Calcification Mechanisms: Updates and Renewed Insight into Signaling Pathways Involved in High Phosphate-Mediated Vascular Smooth Muscle Cell Calcification. *Biomedicines.* 2021;9(7):804.
30. Liu Y, Shanahan CM. Signalling pathways and vascular calcification. *Front Biosci (Landmark Ed).* 2011;16(4):1302-1314.
31. Yang P, Troncone L, Augur ZM, Kim SSJ, McNeil ME, Yu PB. The role of bone morphogenetic protein signaling in vascular calcification. *Bone.* 2020;141:115542.
32. Wu M, Chen G, Li YP. TGF-beta and BMP signaling in osteoblast, skeletal development, and bone formation, homeostasis and disease. *Bone Res.* 2016;4(1):16009.
33. Sun Y, Byon CH, Yuan K, Chen J, Mao X, Heath JM, Javed A, Zhang K, Anderson PG, Chen Y. Smooth muscle cell-specific runx2 deficiency inhibits vascular calcification. *Circ Res.* 2012;111(5):543-552.
34. Voelkl J, Lang F, Eckardt KU, Amann K, Kuro OM, Pasch A, Pieske B, Alesutan I. Signaling pathways involved in vascular smooth muscle cell calcification during hyperphosphatemia. *Cell Mol Life Sci.* 2019;76(11):2077-2091.
35. Alves RD, Eijken M, van de Peppel J, van Leeuwen JP. Calcifying vascular smooth muscle cells and osteoblasts: independent cell types exhibiting extracellular matrix and biomineralization-related mimicries. *BMC Genomics.* 2014;15(1):965.

36. Karwowski W, Naumnik B, Szczepanski M, Mysliwiec M. The mechanism of vascular calcification - a systematic review. *Med Sci Monit.* 2012;18(1):RA1-11.
37. Sage AP, Tintut Y, Demer LL. Regulatory mechanisms in vascular calcification. *Nat Rev Cardiol.* 2010;7(9):528-536.
38. Back M, Aranyi T, Cancela ML, Carracedo M, Conceicao N, Leftheriotis G, Macrae V, Martin L, Nitschke Y, Pasch A, Quaglino D, Rutsch F, Shanahan C, Sorribas V, Szeri F, Valdivielso P, Vanakker O, Kempf H. Endogenous Calcification Inhibitors in the Prevention of Vascular Calcification: A Consensus Statement From the COST Action EuroSoftCalcNet. *Front Cardiovasc Med.* 2018;5(196):196.
39. Proudfoot D, Shanahan CM. Molecular mechanisms mediating vascular calcification: role of matrix Gla protein. *Nephrology (Carlton).* 2006;11(5):455-461.
40. Lee D. Vascular calcification: Inducers and inhibitors. *Materials Science and Engineering: B.* 2011;176(15):1133-1141.
41. Murshed M, Harmey D, Millan JL, McKee MD, Karsenty G. Unique coexpression in osteoblasts of broadly expressed genes accounts for the spatial restriction of ECM mineralization to bone. *Genes Dev.* 2005;19(9):1093-1104.
42. Proudfoot D, Skepper JN, Hegyi L, Bennett MR, Shanahan CM, Weissberg PL. Apoptosis regulates human vascular calcification in vitro: evidence for initiation of vascular calcification by apoptotic bodies. *Circ Res.* 2000;87(11):1055-1062.
43. Shi X, Gao J, Lv Q, Cai H, Wang F, Ye R, Liu X. Calcification in Atherosclerotic Plaque Vulnerability: Friend or Foe? *Front Physiol.* 2020;11:56.
44. Herrmann J, Babic M, Tolle M, van der Giet M, Schuchardt M. Research Models for Studying Vascular Calcification. *Int J Mol Sci.* 2020;21(6):2204.
45. Zhou C, Shi Z, Ouyang N, Ruan X. Hyperphosphatemia and Cardiovascular Disease. *Front Cell Dev Biol.* 2021;9(370):644363.
46. Trion A, Schutte-Bart C, Bax WH, Jukema JW, van der Laarse A. Modulation of calcification of vascular smooth muscle cells in culture by calcium antagonists, statins, and their combination. *Mol Cell Biochem.* 2008;308(1-2):25-33.
47. Zhang D, Bi X, Liu Y, Huang Y, Xiong J, Xu X, Xiao T, Yu Y, Jiang W, Huang Y, Zhang J, Zhang B, Zhao J. High Phosphate-Induced Calcification of Vascular Smooth Muscle Cells is Associated with the TLR4/NF-kappab Signaling Pathway. *Kidney Blood Press Res.* 2017;42(6):1205-1215.
48. Shioi A, Nishizawa Y, Jono S, Koyama H, Hosoi M, Morii H. Beta-glycerophosphate accelerates calcification in cultured bovine vascular smooth muscle cells. *Arterioscler Thromb Vasc Biol.* 1995;15(11):2003-2009.
49. Gayrard N, Muyor K, Notarnicola C, Duranton F, Jover B, Argiles A. Optimisation of cell and ex vivo culture conditions to study vascular calcification. *PLoS One.* 2020;15(3):e0230201.
50. Wei R, Enaka M, Muragaki Y. Activation of KEAP1/NRF2/P62 signaling alleviates high phosphate-induced calcification of vascular smooth muscle cells by suppressing reactive oxygen species production. *Sci Rep.* 2019;9(1):10366.
51. Chen NX, Duan D, O'Neill KD, Moe SM. High glucose increases the expression of Cbfa1 and BMP-2 and enhances the calcification of vascular smooth muscle cells. *Nephrol Dial Transplant.* 2006;21(12):3435-3442.
52. Schuchardt M, Tolle M, Prufer J, Prufer N, Huang T, Jankowski V, Jankowski J, Zidek W, van der Giet M. Uridine adenosine tetraphosphate activation of the purinergic receptor P2Y enhances in vitro vascular calcification. *Kidney Int.* 2012;81(3):256-265.
53. Lau WL, Pai A, Moe SM, Giachelli CM. Direct effects of phosphate on vascular cell function. *Adv Chronic Kidney Dis.* 2011;18(2):105-112.
54. Henaut L, Sanz AB, Martin-Sanchez D, Carrasco S, Villa-Bellosta R, Aldamiz-Echevarria G, Massy ZA, Sanchez-Nino MD, Ortiz A. TWEAK favors phosphate-induced calcification of vascular smooth muscle cells through canonical and non-canonical activation of NFkappaB. *Cell Death Dis.* 2016;7(7):e2305.
55. Giachelli CM. The emerging role of phosphate in vascular calcification. *Kidney Int.* 2009;75(9):890-897.
56. Troyano N, Nogal MD, Mora I, Diaz-Naves M, Lopez-Carrillo N, Sosa P, Rodriguez-Puyol D, Olmos G, Ruiz-Torres MP. Hyperphosphatemia induces cellular senescence in human aorta smooth muscle cells through integrin linked kinase (ILK) up-regulation. *Mech Ageing Dev.* 2015;152:43-55.
57. Mittal M, Siddiqui MR, Tran K, Reddy SP, Malik AB. Reactive oxygen species in inflammation and tissue injury. *Antioxid Redox Signal.* 2014;20(7):1126-1167.

58. Sena CM, Leandro A, Azul L, Seica R, Perry G. Vascular Oxidative Stress: Impact and Therapeutic Approaches. *Front Physiol.* 2018;9(1668):1668.
59. Nowak WN, Deng J, Ruan XZ, Xu Q. Reactive Oxygen Species Generation and Atherosclerosis. *Arterioscler Thromb Vasc Biol.* 2017;37(5):e41-e52.
60. Toth A, Balogh E, Jeney V. Regulation of Vascular Calcification by Reactive Oxygen Species. *Antioxidants (Basel).* 2020;9(10):963.
61. Thanan R, Oikawa S, Hiraku Y, Ohnishi S, Ma N, Pinlaor S, Yongvanit P, Kawanishi S, Murata M. Oxidative stress and its significant roles in neurodegenerative diseases and cancer. *Int J Mol Sci.* 2014;16(1):193-217.
62. Lassegue B, Griendling KK. NADPH oxidases: functions and pathologies in the vasculature. *Arterioscler Thromb Vasc Biol.* 2010;30(4):653-661.
63. Konior A, Schramm A, Czesnikiewicz-Guzik M, Guzik TJ. NADPH oxidases in vascular pathology. *Antioxid Redox Signal.* 2014;20(17):2794-2814.
64. Gimenez M, Schickling BM, Lopes LR, Miller FJ, Jr. Nox1 in cardiovascular diseases: regulation and pathophysiology. *Clin Sci (Lond).* 2016;130(3):151-165.
65. Touyz RM, Montezano AC. Vascular Nox4: a multifarious NADPH oxidase. *Circ Res.* 2012;110(9):1159-1161.
66. Hu CT, Shao YD, Liu YZ, Xiao X, Cheng ZB, Qu SL, Huang L, Zhang C. Oxidative stress in vascular calcification. *Clin Chim Acta.* 2021;519:101-110.
67. Byon CH, Javed A, Dai Q, Kappes JC, Clemens TL, Darley-Usmar VM, McDonald JM, Chen Y. Oxidative stress induces vascular calcification through modulation of the osteogenic transcription factor Runx2 by AKT signaling. *J Biol Chem.* 2008;283(22):15319-15327.
68. Prufer J, Schuchardt M, Tolle M, Prufer N, Hohne M, Zidek W, van der Giet M. Harmful effects of the azathioprine metabolite 6-mercaptopurine in vascular cells: induction of mineralization. *PLoS One.* 2014;9(7):e101709.
69. Sutra T, Morena M, Bargnoux AS, Caporiccio B, Canaud B, Cristol JP. Superoxide production: a procalcifying cell signalling event in osteoblastic differentiation of vascular smooth muscle cells exposed to calcification media. *Free Radic Res.* 2008;42(9):789-797.
70. Zhao MM, Xu MJ, Cai Y, Zhao G, Guan Y, Kong W, Tang C, Wang X. Mitochondrial reactive oxygen species promote p65 nuclear translocation mediating high-phosphate-induced vascular calcification in vitro and in vivo. *Kidney Int.* 2011;79(10):1071-1079.
71. Herranz N, Gil J. Mechanisms and functions of cellular senescence. *J Clin Invest.* 2018;128(4):1238-1246.
72. Miller YI, Choi SH, Wiesner P, Fang L, Harkewicz R, Hartvigsen K, Boullier A, Gonen A, Diehl CJ, Que X, Montano E, Shaw PX, Tsimikas S, Binder CJ, Witztum JL. Oxidation-specific epitopes are danger-associated molecular patterns recognized by pattern recognition receptors of innate immunity. *Circ Res.* 2011;108(2):235-248.
73. Shanahan CM. Mechanisms of vascular calcification in CKD-evidence for premature ageing? *Nat Rev Nephrol.* 2013;9(11):661-670.
74. Childs BG, Durik M, Baker DJ, van Deursen JM. Cellular senescence in aging and age-related disease: from mechanisms to therapy. *Nat Med.* 2015;21(12):1424-1435.
75. Hayflick L, Moorhead PS. The serial cultivation of human diploid cell strains. *Exp Cell Res.* 1961;25(3):585-621.
76. Kumari R, Jat P. Mechanisms of Cellular Senescence: Cell Cycle Arrest and Senescence Associated Secretory Phenotype. *Front Cell Dev Biol.* 2021;9:645593.
77. Toussaint O, Royer V, Salmon M, Remacle J. Stress-induced premature senescence and tissue ageing. *Biochem Pharmacol.* 2002;64(5-6):1007-1009.
78. Shiloh Y. ATM and related protein kinases: safeguarding genome integrity. *Nat Rev Cancer.* 2003;3(3):155-168.
79. Bernadotte A, Mikhelson VM, Spivak IM. Markers of cellular senescence. Telomere shortening as a marker of cellular senescence. *Aging (Albany NY).* 2016;8(1):3-11.
80. Campisi J. Senescent cells, tumor suppression, and organismal aging: good citizens, bad neighbors. *Cell.* 2005;120(4):513-522.
81. Campisi J, d'Adda di Fagagna F. Cellular senescence: when bad things happen to good cells. *Nat Rev Mol Cell Biol.* 2007;8(9):729-740.
82. Birch J, Gil J. Senescence and the SASP: many therapeutic avenues. *Genes Dev.* 2020;34(23-24):1565-1576.
83. Nakano-Kurimoto R, Ikeda K, Uraoka M, Nakagawa Y, Yutaka K, Koide M, Takahashi T, Matoba S, Yamada H, Okigaki M, Matsubara H. Replicative senescence of vascular smooth muscle cells enhances the calcification through initiating the osteoblastic transition. *Am J Physiol Heart Circ Physiol.* 2009;297(5):H1673-1684.

84. Bielak-Zmijewska A, Wnuk M, Przybylska D, Grabowska W, Lewinska A, Alster O, Korwek Z, Cmoch A, Myszka A, Pikula S, Mosieniak G, Sikora E. A comparison of replicative senescence and doxorubicin-induced premature senescence of vascular smooth muscle cells isolated from human aorta. *Biogerontology.* 2014;15(1):47-64.
85. Liu Y, Drozdov I, Shroff R, Beltran LE, Shanahan CM. Prelamin A accelerates vascular calcification via activation of the DNA damage response and senescence-associated secretory phenotype in vascular smooth muscle cells. *Circ Res.* 2013;112(10):e99-109.
86. Sanchis P, Ho CY, Liu Y, Beltran LE, Ahmad S, Jacob AP, Furmanik M, Laycock J, Long DA, Shroff R, Shanahan CM. Arterial "inflammaging" drives vascular calcification in children on dialysis. *Kidney Int.* 2019;95(4):958-972.
87. Cobb AM, Yusoff S, Hayward R, Ahmad S, Sun M, Verhulst A, D'Haese PC, Shanahan CM. Runx2 (Runt-Related Transcription Factor 2) Links the DNA Damage Response to Osteogenic Reprogramming and Apoptosis of Vascular Smooth Muscle Cells. *Arterioscler Thromb Vasc Biol.* 2021;41(4):1339-1357.
88. Gardner SE, Humphry M, Bennett MR, Clarke MC. Senescent Vascular Smooth Muscle Cells Drive Inflammation Through an Interleukin-1alpha-Dependent Senescence-Associated Secretory Phenotype. *Arterioscler Thromb Vasc Biol.* 2015;35(9):1963-1974.
89. Franceschi C, Campisi J. Chronic inflammation (inflammaging) and its potential contribution to age-associated diseases. *J Gerontol A Biol Sci Med Sci.* 2014;69 Suppl 1:S4-9.
90. Zhao H, Wu L, Yan G, Chen Y, Zhou M, Wu Y, Li Y. Inflammation and tumor progression: signaling pathways and targeted intervention. *Signal Transduct Target Ther.* 2021;6(1):263.
91. Rapa SF, Di Iorio BR, Campiglia P, Heidland A, Marzocco S. Inflammation and Oxidative Stress in Chronic Kidney Disease-Potential Therapeutic Role of Minerals, Vitamins and Plant-Derived Metabolites. *Int J Mol Sci.* 2019;21(1):263.
92. Wang S, Tong M, Hu S, Chen X. The Bioactive Substance Secreted by MSC Retards Mouse Aortic Vascular Smooth Muscle Cells Calcification. *Biomed Res Int.* 2018;2018:6053567.
93. Wen C, Yang X, Yan Z, Zhao M, Yue X, Cheng X, Zheng Z, Guan K, Dou J, Xu T, Zhang Y, Song T, Wei C, Zhong H. Nalp3 inflammasome is activated and required for vascular smooth muscle cell calcification. *Int J Cardiol.* 2013;168(3):2242-2247.
94. Henaut L, Mary A, Chillon JM, Kamel S, Massy ZA. The Impact of Uremic Toxins on Vascular Smooth Muscle Cell Function. *Toxins (Basel).* 2018;10(6):218.
95. Castillo-Rodriguez E, Pizarro-Sanchez S, Sanz AB, Ramos AM, Sanchez-Nino MD, Martin-Cleary C, Fernandez-Fernandez B, Ortiz A. Inflammatory Cytokines as Uremic Toxins: "Ni Son Todos Los Que Estan, Ni Estan Todos Los Que Son". *Toxins (Basel).* 2017;9(4):114.
96. Lee HL, Woo KM, Ryoo HM, Baek JH. Tumor necrosis factor-alpha increases alkaline phosphatase expression in vascular smooth muscle cells via MSX2 induction. *Biochem Biophys Res Commun.* 2010;391(1):1087-1092.
97. Tintut Y, Patel J, Parhami F, Demer LL. Tumor necrosis factor-alpha promotes in vitro calcification of vascular cells via the cAMP pathway. *Circulation.* 2000;102(21):2636-2642.
98. Han L, Zhang Y, Zhang M, Guo L, Wang J, Zeng F, Xu D, Yin Z, Xu Y, Wang D, Zhou H. Interleukin-1beta-Induced Senescence Promotes Osteoblastic Transition of Vascular Smooth Muscle Cells. *Kidney Blood Press Res.* 2020;45(2):314-330.
99. Sun M, Chang Q, Xin M, Wang Q, Li H, Qian J. Endogenous bone morphogenetic protein 2 plays a role in vascular smooth muscle cell calcification induced by interleukin 6 in vitro. *Int J Immunopathol Pharmacol.* 2017;30(3):227-237.
100. Kurozumi A, Nakano K, Yamagata K, Okada Y, Nakayamada S, Tanaka Y. IL-6 and sIL-6R induces STAT3-dependent differentiation of human VSMCs into osteoblast-like cells through JMJD2B-mediated histone demethylation of RUNX2. *Bone.* 2019;124:53-61.
101. Roh JS, Sohn DH. Damage-Associated Molecular Patterns in Inflammatory Diseases. *Immune Netw.* 2018;18(4):e27.
102. El-Zayat SR, Sibaii H, Mannaa FA. Toll-like receptors activation, signaling, and targeting: an overview. *Bulletin of the National Research Centre.* 2019;43(1):187.
103. Goulopoulou S, McCarthy CG, Webb RC. Toll-like Receptors in the Vascular System: Sensing the Dangers Within. *Pharmacol Rev.* 2016;68(1):142-167.
104. Swanson KV, Deng M, Ting JP. The NLRP3 inflammasome: molecular activation and regulation to therapeutics. *Nat Rev Immunol.* 2019;19(8):477-489.
105. Vilaysane A, Chun J, Seamone ME, Wang W, Chin R, Hirota S, Li Y, Clark SA, Tschopp J, Trpkov K, Hemmelgarn BR, Beck PL, Muruve DA. The NLRP3 inflammasome promotes renal inflammation and contributes to CKD. *J Am Soc Nephrol.* 2010;21(10):1732-1744.
106. Tong Y, Wang Z, Cai L, Lin L, Liu J, Cheng J. NLRP3 Inflammasome and Its Central Role in the Cardiovascular Diseases. *Oxid Med Cell Longev.* 2020;2020:4293206.

107. Kelley N, Jeltema D, Duan Y, He Y. The NLRP3 Inflammasome: An Overview of Mechanisms of Activation and Regulation. *Int J Mol Sci.* 2019;20(13).
108. Herrmann J, Xia M, Gummi MR, Greco A, Schacke A, van der Giet M, Tolle M, Schuchardt M. Stressor-Induced "Inflammaging" of Vascular Smooth Muscle Cells via Nlrp3-Mediated Pro-inflammatory Auto-Loop. *Front Cardiovasc Med.* 2021;8(1932):752305.
109. Schantl AE, Ivarsson ME, Leroux J-C. Investigational Pharmacological Treatments for Vascular Calcification. *Advanced Therapeutics.* 2019;2(1):1800094.
110. Herrmann J, Gummi MR, Xia M, van der Giet M, Tolle M, Schuchardt M. Vascular Calcification in Rodent Models-Keeping Track with an Extented Method Assortment. *Biology (Basel).* 2021;10(6):459.
111. Alsaigh T, Di Bartolo BA, Mulangala J, Figtree GA, Leeper NJ. Bench-to-Bedside in Vascular Medicine: Optimizing the Translational Pipeline for Patients With Peripheral Artery Disease. *Circ Res.* 2021;128(12):1927-1943.
112. Yuan GC, Cai L, Elowitz M, Enver T, Fan G, Guo G, Irizarry R, Kharchenko P, Kim J, Orkin S, Quackenbush J, Saadatpour A, Schroeder T, Shivdasani R, Tirosh I. Challenges and emerging directions in single-cell analysis. *Genome Biol.* 2017;18(1):84.
113. Iyemere VP, Proudfoot D, Weissberg PL, Shanahan CM. Vascular smooth muscle cell phenotypic plasticity and the regulation of vascular calcification. *J Intern Med.* 2006;260(3):192-210.
114. Miano JM, Fisher EA, Majesky MW. Fate and State of Vascular Smooth Muscle Cells in Atherosclerosis. *Circulation.* 2021;143(21):2110-2116.
115. Kanter I, Kalisky T. Single cell transcriptomics: methods and applications. *Front Oncol.* 2015;5(53):53.
116. Aldridge S, Teichmann SA. Single cell transcriptomics comes of age. *Nat Commun.* 2020;11(1):4307.
117. Herrmann J, Babic M, Tolle M, Eckardt KU, van der Giet M, Schuchardt M. A Novel Protocol for Detection of Senescence and Calcification Markers by Fluorescence Microscopy. *Int J Mol Sci.* 2020;21(10):3475.
118. Hafner A, Reyes J, Stewart-Ornstein J, Tsabar M, Jambhekar A, Lahav G. Quantifying the Central Dogma in the p53 Pathway in Live Single Cells. *Cell Syst.* 2020;10(6):495-505 e494.
119. Fulda S, Gorman AM, Hori O, Samali A. Cellular stress responses: cell survival and cell death. *Int J Cell Biol.* 2010;2010:214074.
120. Huang M, Zheng L, Xu H, Tang D, Lin L, Zhang J, Li C, Wang W, Yuan Q, Tao L, Ye Z. Oxidative stress contributes to vascular calcification in patients with chronic kidney disease. *J Mol Cell Cardiol.* 2020;138:256-268.
121. Deavall DG, Martin EA, Horner JM, Roberts R. Drug-induced oxidative stress and toxicity. *J Toxicol.* 2012;2012:645460.
122. Lim YJ, Sidor NA, Tonial NC, Che A, Urquhart BL. Uremic Toxins in the Progression of Chronic Kidney Disease and Cardiovascular Disease: Mechanisms and Therapeutic Targets. *Toxins (Basel).* 2021;13(2).
123. Miller LW. Cardiovascular toxicities of immunosuppressive agents. *Am J Transplant.* 2002;2(9):807-818.
124. Broen JCA, van Laar JM. Mycophenolate mofetil, azathioprine and tacrolimus: mechanisms in rheumatology. *Nat Rev Rheumatol.* 2020;16(3):167-178.
125. Teixeira V, Tam LS. Novel Insights in Systemic Lupus Erythematosus and Atherosclerosis. *Front Med (Lausanne).* 2017;4:262.
126. Schuchardt M, Herrmann J, Henkel C, Babic M, van der Giet M, Tolle M. Long-Term Treatment of Azathioprine in Rats Induces Vessel Mineralization. *Biomedicines.* 2021;9(3):327.
127. Lai Y, Dong C. Therapeutic antibodies that target inflammatory cytokines in autoimmune diseases. *Int Immunol.* 2016;28(4):181-188.
128. Carvalho C, Santos RX, Cardoso S, Correia S, Oliveira PJ, Santos MS, Moreira PI. Doxorubicin: the good, the bad and the ugly effect. *Curr Med Chem.* 2009;16(25):3267-3285.
129. Tacar O, Sriamornsak P, Dass CR. Doxorubicin: an update on anticancer molecular action, toxicity and novel drug delivery systems. *J Pharm Pharmacol.* 2013;65(2):157-170.
130. Zhu H, Sarkar S, Scott L, Danelisen I, Trush MA, Jia Z, Li YR. Doxorubicin Redox Biology: Redox Cycling, Topoisomerase Inhibition, and Oxidative Stress. *React Oxyg Species (Apex).* 2016;1(3):189-198.
131. Cappetta D, Rossi F, Piegari E, Quaini F, Berrino L, Urbanek K, De Angelis A. Doxorubicin targets multiple players: A new view of an old problem. *Pharmacol Res.* 2018;127:4-14.

132. Kostrzewa-Nowak D, Paine MJ, Wolf CR, Tarasiuk J. The role of bioreductive activation of doxorubicin in cytotoxic activity against leukaemia HL60-sensitive cell line and its multidrug-resistant sublines. *Br J Cancer.* 2005;93(1):89-97.
133. Ewald JA, Desotelle JA, Wilding G, Jarrard DF. Therapy-induced senescence in cancer. *J Natl Cancer Inst.* 2010;102(20):1536-1546.
134. Bosman M, Favere K, Neutel CHG, Jacobs G, De Meyer GRY, Martinet W, Van Craenenbroeck EM, Guns PDF. Doxorubicin induces arterial stiffness: A comprehensive in vivo and ex vivo evaluation of vascular toxicity in mice. *Toxicol Lett.* 2021;346:23-33.
135. Parr SK, Liang J, Schadler KL, Gilchrist SC, Steele CC, Ade CJ. Anticancer Therapy-Related Increases in Arterial Stiffness: A Systematic Review and Meta-Analysis. *J Am Heart Assoc.* 2020;9(14):e015598.
136. Mozos I, Borzak G, Caraba A, Mihaescu R. Arterial stiffness in hematologic malignancies. *Onco Targets Ther.* 2017;10:1381-1388.
137. Takahashi M. NLRP3 inflammasome as a key driver of vascular disease. *Cardiovasc Res.* 2022;118(2):372-385.
138. Zhang L, Jiang YH, Fan C, Zhang Q, Jiang YH, Li Y, Xue YT. MCC950 attenuates doxorubicin-induced myocardial injury in vivo and in vitro by inhibiting NLRP3-mediated pyroptosis. *Biomed Pharmacother.* 2021;143:112133.
139. Wei S, Ma W, Li X, Jiang C, Sun T, Li Y, Zhang B, Li W. Involvement of ROS/NLRP3 Inflammasome Signaling Pathway in Doxorubicin-Induced Cardiotoxicity. *Cardiovasc Toxicol.* 2020;20(5):507-519.
140. Coppe JP, Patil CK, Rodier F, Sun Y, Munoz DP, Goldstein J, Nelson PS, Desprez PY, Campisi J. Senescence-associated secretory phenotypes reveal cell-nonautonomous functions of oncogenic RAS and the p53 tumor suppressor. *PLoS Biol.* 2008;6(12):2853-2868.
141. Ridker PM, Everett BM, Thuren T, MacFadyen JG, Chang WH, Ballantyne C, Fonseca F, Nicolau J, Koenig W, Anker SD, Kastelein JJP, Cornel JH, Pais P, Pella D, Genest J, Cifkova R, Lorenzatti A, Forster T, Kobalava Z, Vida-Simiti L, Flather M, Shimokawa H, Ogawa H, Dellborg M, Rossi PRF, Troquay RPT, Libby P, Glynn RJ, Group CT. Antiinflammatory Therapy with Canakinumab for Atherosclerotic Disease. *N Engl J Med.* 2017;377(12):1119-1131.
142. Ridker PM, Thuren T, Zalewski A, Libby P. Interleukin-1beta inhibition and the prevention of recurrent cardiovascular events: rationale and design of the Canakinumab Anti-inflammatory Thrombosis Outcomes Study (CANTOS). *Am Heart J.* 2011;162(4):597-605.
143. Libby P. Interleukin-1 Beta as a Target for Atherosclerosis Therapy: Biological Basis of CANTOS and Beyond. *J Am Coll Cardiol.* 2017;70(18):2278-2289.
144. Baylis RA, Gomez D, Mallat Z, Pasterkamp G, Owens GK. The CANTOS Trial: One Important Step for Clinical Cardiology but a Giant Leap for Vascular Biology. *Arterioscler Thromb Vasc Biol.* 2017;37(11):e174-e177.
145. Zhang X, Li Y, Yang P, Liu X, Lu L, Chen Y, Zhong X, Li Z, Liu H, Ou C, Yan J, Chen M. Trimethylamine-N-Oxide Promotes Vascular Calcification Through Activation of NLRP3 (Nucleotide-Binding Domain, Leucine-Rich-Containing Family, Pyrin Domain-Containing-3) Inflammasome and NF-kappaB (Nuclear Factor kappaB) Signals. *Arterioscler Thromb Vasc Biol.* 2020;40(3):751-765.
146. Kobayashi M, Usui F, Karasawa T, Kawashima A, Kimura H, Mizushina Y, Shirasuna K, Mizukami H, Kasahara T, Hasebe N, Takahashi M. NLRP3 Deficiency Reduces Macrophage Interleukin-10 Production and Enhances the Susceptibility to Doxorubicin-induced Cardiotoxicity. *Sci Rep.* 2016;6(1):26489.
147. Xu D, Zeng F, Han L, Wang J, Yin Z, Lv L, Guo L, Wang D, Xu Y, Zhou H. The synergistic action of phosphate and interleukin-6 enhances senescence-associated calcification in vascular smooth muscle cells depending on p53. *Mech Ageing Dev.* 2019;182:111124.
148. Ebert T, Pawelzik SC, Witasp A, Arefin S, Hobson S, Kublickiene K, Shiels PG, Back M, Stenvinkel P. Inflammation and Premature Ageing in Chronic Kidney Disease. *Toxins (Basel).* 2020;12(4):227.
149. Dai L, Qureshi AR, Witasp A, Lindholm B, Stenvinkel P. Early Vascular Ageing and Cellular Senescence in Chronic Kidney Disease. *Comput Struct Biotechnol J.* 2019;17:721-729.
150. Pescatore LA, Gamarra LF, Liberman M. Multifaceted Mechanisms of Vascular Calcification in Aging. *Arterioscler Thromb Vasc Biol.* 2019;39(7):1307-1316.
151. Rodier F, Coppe JP, Patil CK, Hoeijmakers WA, Munoz DP, Raza SR, Freund A, Campeau E, Davalos AR, Campisi J. Persistent DNA damage signalling triggers senescence-associated inflammatory cytokine secretion. *Nat Cell Biol.* 2009;11(8):973-979.

152. Budamagunta V, Manohar-Sindhu S, Yang Y, He Y, Traktuev DO, Foster TC, Zhou D. Senescence-associated hyper-activation to inflammatory stimuli in vitro. *Aging (Albany NY).* 2021;13(15):19088-19107.
153. Di Iorio A. Serum IL-1β levels in health and disease: a population-based study. 'The InCHIANTI study'. *Cytokine.* 2003;22(6):198-205.
154. Childs BG, Li H, van Deursen JM. Senescent cells: a therapeutic target for cardiovascular disease. *J Clin Invest.* 2018;128(4):1217-1228.
155. Childs BG, Gluscevic M, Baker DJ, Laberge RM, Marquess D, Dananberg J, van Deursen JM. Senescent cells: an emerging target for diseases of ageing. *Nat Rev Drug Discov.* 2017;16(10):718-735.
156. Chao CT, Yeh HY, Tsai YT, Chuang PH, Yuan TH, Huang JW, Chen HW. Natural and non-natural antioxidative compounds: potential candidates for treatment of vascular calcification. *Cell Death Discov.* 2019;5(1):145.
157. Rutsch F, Boyer P, Nitschke Y, Ruf N, Lorenz-Depierieux B, Wittkampf T, Weissen-Plenz G, Fischer RJ, Mughal Z, Gregory JW, Davies JH, Loirat C, Strom TM, Schnabel D, Nurnberg P, Terkeltaub R, Group GS. Hypophosphatemia, hyperphosphaturia, and bisphosphonate treatment are associated with survival beyond infancy in generalized arterial calcification of infancy. *Circ Cardiovasc Genet.* 2008;1(2):133-140.
158. Kranenburg G, de Jong PA, Bartstra JW, Lagerweij SJ, Lam MG, Ossewaarde-van Norel J, Risseeuw S, van Leeuwen R, Imhof SM, Verhaar HJ, de Vries JJ, Slart R, Luurtsema G, den Harder AM, Visseren FLJ, Mali WP, Spiering W. Etidronate for Prevention of Ectopic Mineralization in Patients With Pseudoxanthoma Elasticum. *J Am Coll Cardiol.* 2018;71(10):1117-1126.
159. De Vriese AS, Caluwe R, Pyfferoen L, De Bacquer D, De Boeck K, Delanote J, De Surgeloose D, Van Hoenacker P, Van Vlem B, Verbeke F. Multicenter Randomized Controlled Trial of Vitamin K Antagonist Replacement by Rivaroxaban with or without Vitamin K2 in Hemodialysis Patients with Atrial Fibrillation: the Valkyrie Study. *J Am Soc Nephrol.* 2020;31(1):186-196.
160. Raggi P, Chertow GM, Torres PU, Csiky B, Naso A, Nossuli K, Moustafa M, Goodman WG, Lopez N, Downey G, Dehmel B, Floege J, Group AS. The ADVANCE study: a randomized study to evaluate the effects of cinacalcet plus low-dose vitamin D on vascular calcification in patients on hemodialysis. *Nephrol Dial Transplant.* 2011;26(4):1327-1339.
161. Jamal SA, Vandermeer B, Raggi P, Mendelssohn DC, Chatterley T, Dorgan M, Lok CE, Fitchett D, Tsuyuki RT. Effect of calcium-based versus non-calcium-based phosphate binders on mortality in patients with chronic kidney disease: an updated systematic review and meta-analysis. *Lancet.* 2013;382(9900):1268-1277.
162. Raggi P, Bellasi A, Bushinsky D, Bover J, Rodriguez M, Ketteler M, Sinha S, Salcedo C, Gillotti K, Padgett C, Garg R, Gold A, Perelló J, Chertow GM. Slowing Progression of Cardiovascular Calcification With SNF472 in Patients on Hemodialysis. *Circulation.* 2020;141(9):728-739.
163. Zuo L, Prather ER, Stetskiv M, Garrison DE, Meade JR, Peace TI, Zhou T. Inflammaging and Oxidative Stress in Human Diseases: From Molecular Mechanisms to Novel Treatments. *Int J Mol Sci.* 2019;20(18).
164. Lagoumtzi SM, Chondrogianni N. Senolytics and senomorphics: Natural and synthetic therapeutics in the treatment of aging and chronic diseases. *Free Radic Biol Med.* 2021;171:169-190.
165. Bostrom KI. DNA Damage Response, Runx2 (Runt-Related Transcription Factor 2), and Vascular Calcification. *Arterioscler Thromb Vasc Biol.* 2021;41(4):1358-1359.
166. Hedayati SS. A Novel Treatment for Vascular Calcification in Patients With Dialysis-Dependent Chronic Kidney Disease: Are We There Yet? *Circulation.* 2020;141(9):740-742.
167. Balistreri CR, Madonna R, Ferdinandy P. Is it the time of seno-therapeutics application in cardiovascular pathological conditions related to ageing? *Curr Res Pharmacol Drug Discov.* 2021;2:100027.
168. Gladyshev VN. The free radical theory of aging is dead. Long live the damage theory! *Antioxid Redox Signal.* 2014;20(4):727-731.
169. Apostolova N, Iannantuoni F, Gruevska A, Muntane J, Rocha M, Victor VM. Mechanisms of action of metformin in type 2 diabetes: Effects on mitochondria and leukocyte-endothelium interactions. *Redox Biol.* 2020;34:101517.
170. Moon GJ, Kim SJ, Cho YH, Ryoo S, Bang OY. Antioxidant effects of statins in patients with atherosclerotic cerebrovascular disease. *J Clin Neurol.* 2014;10(2):140-147.
171. Battelli MG, Bortolotti M, Bolognesi A, Polito L. Pro-Aging Effects of Xanthine Oxidoreductase Products. *Antioxidants (Basel).* 2020;9(9).

172. Schuchardt M, Herrmann J, Tolle M, van der Giet M. Xanthine Oxidase and its Role as Target in Cardiovascular Disease: Cardiovascular Protection by Enzyme Inhibition? *Curr Pharm Des.* 2017;23(23):3391-3404.
173. Kang C. Senolytics and Senostatics: A Two-Pronged Approach to Target Cellular Senescence for Delaying Aging and Age-Related Diseases. *Mol Cells.* 2019;42(12):821-827.
174. Amaya-Montoya M, Perez-Londono A, Guatibonza-Garcia V, Vargas-Villanueva A, Mendivil CO. Cellular Senescence as a Therapeutic Target for Age-Related Diseases: A Review. *Adv Ther.* 2020;37(4):1407-1424.
175. Mijit M, Caracciolo V, Melillo A, Amicarelli F, Giordano A. Role of p53 in the Regulation of Cellular Senescence. *Biomolecules.* 2020;10(3):420.
176. Guha T, Malkin D. Inherited TP53 Mutations and the Li-Fraumeni Syndrome. *Cold Spring Harb Perspect Med.* 2017;7(4):a026187.
177. Wu D, Chen Y, Sun Y, Gao Q, Li H, Yang Z, Wang Y, Jiang X, Yu B. Target of MCC950 in Inhibition of NLRP3 Inflammasome Activation: a Literature Review. *Inflammation.* 2020;43(1):17-23.
178. Zeng W, Wu D, Sun Y, Suo Y, Yu Q, Zeng M, Gao Q, Yu B, Jiang X, Wang Y. The selective NLRP3 inhibitor MCC950 hinders atherosclerosis development by attenuating inflammation and pyroptosis in macrophages. *Sci Rep.* 2021;11(1):19305.
179. El Hadri K, Smith R, Duplus E, El Amri C. Inflammation, Oxidative Stress, Senescence in Atherosclerosis: Thioredoxine-1 as an Emerging Therapeutic Target. *Int J Mol Sci.* 2022;23(1):77.
180. Sharma A, Choi JSY, Stefanovic N, Al-Sharea A, Simpson DS, Mukhamedova N, Jandeleit-Dahm K, Murphy AJ, Sviridov D, Vince JE, Ritchie RH, de Haan JB. Specific NLRP3 Inhibition Protects Against Diabetes-Associated Atherosclerosis. *Diabetes.* 2021;70(3):772-787.
181. Gonzalez-Dominguez A, Montanez R, Castejon-Vega B, Nunez-Vasco J, Lendines-Cordero D, Wang C, Mbalaviele G, Navarro-Pando JM, Alcocer-Gomez E, Cordero MD. Inhibition of the NLRP3 inflammasome improves lifespan in animal murine model of Hutchinson-Gilford Progeria. *EMBO Mol Med.* 2021;13(10):e14012.
182. Zahid A, Li B, Kombe AJK, Jin T, Tao J. Pharmacological Inhibitors of the NLRP3 Inflammasome. *Front Immunol.* 2019;10(2538):2538.
183. Prata L, Ovsyannikova IG, Tchkonia T, Kirkland JL. Senescent cell clearance by the immune system: Emerging therapeutic opportunities. *Semin Immunol.* 2018;40:101275.
184. Schuchardt M, Prufer N, Tu Y, Herrmann J, Hu XP, Chebli S, Dahlke K, Zidek W, van der Giet M, Tolle M. Dysfunctional high-density lipoprotein activates toll-like receptors via serum amyloid A in vascular smooth muscle cells. *Sci Rep.* 2019;9(1):3421.
185. Stojanovic SD, Fiedler J, Bauersachs J, Thum T, Sedding DG. Senescence-induced inflammation: an important player and key therapeutic target in atherosclerosis. *Eur Heart J.* 2020;41(31):2983-2996.
186. Ruperto N, Brunner HI, Quartier P, Constantin T, Wulffraat N, Horneff G, Brik R, McCann L, Kasapcopur O, Rutkowska-Sak L, Schneider R, Berkun Y, Calvo I, Erguven M, Goffin L, Hofer M, Kallinich T, Oliveira SK, Uziel Y, Viola S, Nistala K, Wouters C, Cimaz R, Ferrandiz MA, Flato B, Gamir ML, Kone-Paut I, Grom A, Magnusson B, Ozen S, Sztajnbok F, Lheritier K, Abrams K, Kim D, Martini A, Lovell DJ, Printo, Prcsg. Two randomized trials of canakinumab in systemic juvenile idiopathic arthritis. *N Engl J Med.* 2012;367(25):2396-2406.
187. Sehested TSG, Bjerre J, Ku S, Chang A, Jahansouz A, Owens DK, Hlatky MA, Goldhaber-Fiebert JD. Cost-effectiveness of Canakinumab for Prevention of Recurrent Cardiovascular Events. *JAMA Cardiol.* 2019;4(2):128-135.
188. Baker DJ, Wijshake T, Tchkonia T, LeBrasseur NK, Childs BG, van de Sluis B, Kirkland JL, van Deursen JM. Clearance of p16Ink4a-positive senescent cells delays ageing-associated disorders. *Nature.* 2011;479(7372):232-236.
189. Childs BG, Baker DJ, Wijshake T, Conover CA, Campisi J, van Deursen JM. Senescent intimal foam cells are deleterious at all stages of atherosclerosis. *Science.* 2016;354(6311):472-477.
190. Kirkland JL, Tchkonia T. Clinical strategies and animal models for developing senolytic agents. *Exp Gerontol.* 2015;68:19-25.
191. Blagosklonny MV. Anti-aging: senolytics or gerostatics (unconventional view). *Oncotarget.* 2021;12(18):1821-1835.
192. Kirkland JL, Tchkonia T. Senolytic drugs: from discovery to translation. *J Intern Med.* 2020;288(5):518-536.
193. Chang J, Wang Y, Shao L, Laberge RM, Demaria M, Campisi J, Janakiraman K, Sharpless NE, Ding S, Feng W, Luo Y, Wang X, Aykin-Burns N, Krager K, Ponnappan U, Hauer-Jensen

M, Meng A, Zhou D. Clearance of senescent cells by ABT263 rejuvenates aged hematopoietic stem cells in mice. *Nat Med.* 2016;22(1):78-83.

194. Gasek NS, Kuchel GA, Kirkland JL, Xu M. Strategies for Targeting Senescent Cells in Human Disease. *Nat Aging.* 2021;1(10):870-879.

195. Munoz-Espin D, Rovira M, Galiana I, Gimenez C, Lozano-Torres B, Paez-Ribes M, Llanos S, Chaib S, Munoz-Martin M, Ucero AC, Garaulet G, Mulero F, Dann SG, VanArsdale T, Shields DJ, Bernardos A, Murguia JR, Martinez-Manez R, Serrano M. A versatile drug delivery system targeting senescent cells. *EMBO Mol Med.* 2018;10(9):e9355.